Chapter 3

The Influence of Physical and Chemical Processes on Contaminant Transport into and within the Arctic

Contents

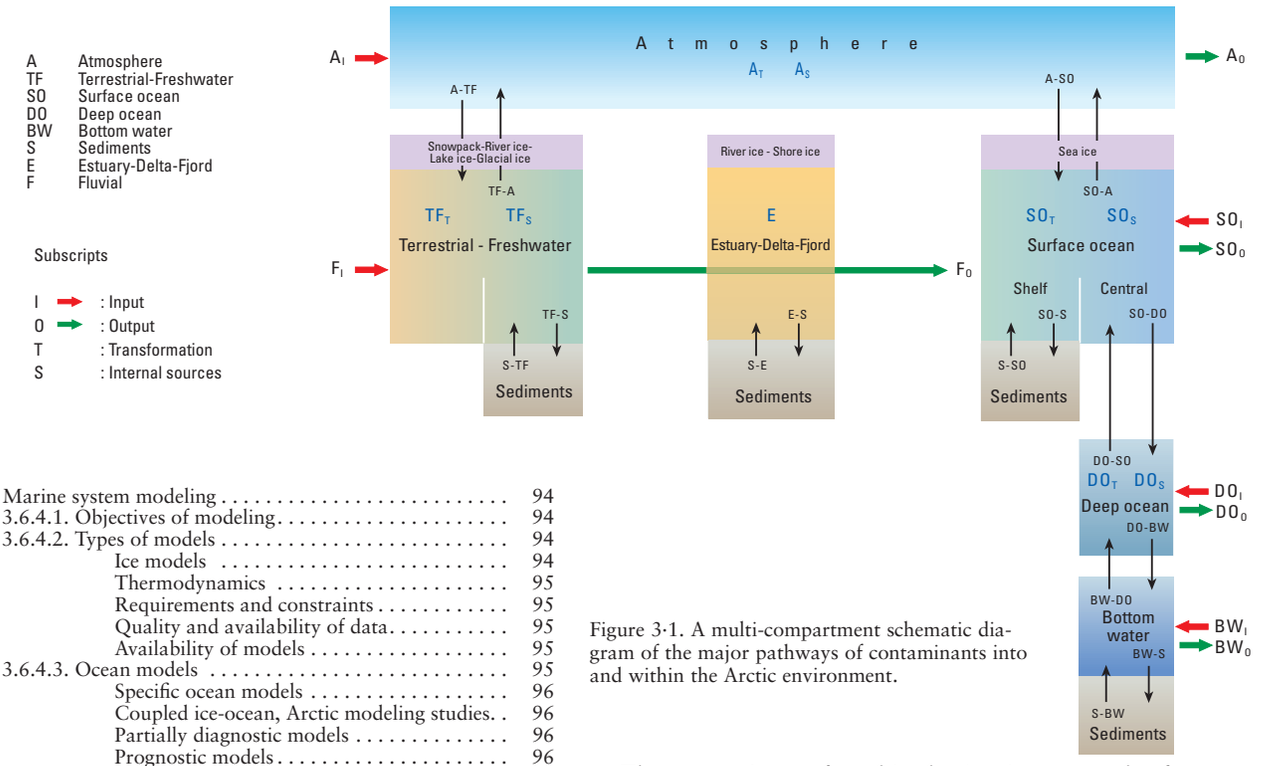

Figure 3·1. A multi-compartment schematic diagram of the major pathways of contaminants into and within the Arctic environment.

3.1. Introduction

The Arctic region is a seemingly pristine, remote environment, yet there is increasing evidence that it is greatly impacted by global pollution. It is a highly sensitive ecosystem. Compounds found in the Arctic are of concern not just because they are transported long distances, but also because they are bioaccumulated and biomagnified in the food chain. Consequently, an understanding of pollution pathways to and within the Arctic is of special concern.

The sources of most contaminants of interest to AMAP generally lie outside of the Arctic region; however, there are some internal regional sources, especially from mineral extraction and related activities. Pathways within the three major environmental compartments, specifically the atmosphere, terrestrial/freshwater, and marine compartments, all contribute to the delivery of contaminants to the Arctic (Barrie 1986, Ottar 1989, Barrie *et al.* 1992). Both the physical processes and the general nature of the main pathways within these three compartments are reviewed in this chapter. This complements the next chapter on biological systems and processes and subsequent chapters on specific contaminant groups.

The objective of this chapter is to provide a general understanding of the physical processes and pathways, both within and between the main environmental compartments, which determine the fate of contaminants in the Arctic environment. General consideration is given to sources and emissions, transport mechanisms, and the processes affecting the inter- and intra-compartmental interactions of contaminants of concern.

The contaminants found in the Arctic as a result of transport over long distances are those that have been produced in large quantities and are environmentally stable. Properties which promote the long-range transport of pollutants into the Arctic via the atmosphere are: large-scale and geographically widespread emissions; low water solubility; the presence of the chemical in the gas phase, or on small particles with atmospheric residence times of several days or longer; and, chemical stability. These properties are also important with respect to long-range riverine and marine transport, with the additional requirement that these compounds must be biologically stable.

The phenomenon of Arctic haze was the first indication of long-range transport to the Arctic, occurring from December through April each year. Arctic haze was reported as early as 1956 (Mitchell 1956), and was later shown to be a manifestation of the atmospheric long-range transport of acid sulfur pollution (Rahn and Shaw 1982, Barrie 1986, Shaw 1995). This was followed by convincing evidence of the atmospheric transport of persistent organic pollutants (POPs) to the Arctic (Oehme 1991, Barrie *et al.* 1992).

The Arctic region, as defined in chapter 2, encompasses a total of 13.4×10^6 km^2 of land and 20×10^6 km^2 of ocean (Gloersen *et al.* 1992). Clearly, there is a large degree of variability across this huge area. To provide a framework for this discussion, therefore, a simple box model has been used to illustrate the dominant processes and pathways of contaminants for the Arctic region. The principal physical contaminant pathways into and within the region are described schematically in Figure 3·1. This figure represents a simplification of the complex transport pathways and reservoirs operating in the Arctic system. The main compartments are the atmosphere, terrestrial/freshwater, and ocean. The ocean compartment is separated into three components, specifically, the surface ocean (0-200 m), the deep ocean (>200 m depth), and the bottom water. The surface ocean can be further subdivided into a stable upper layer of 50-60 m depth and characterized by low salinity, on top of a pycnocline layer which extends down to approximately 150 m depth and is located above the shelf and central ocean waters. Both the shelf and bottom waters are connected to the

marine sediments. The terrestrial/freshwater compartment also contains a sediment subcompartment associated with rivers, lakes, and reservoirs. The main interfaces between the compartments are indicated by arrows.

Both the terrestrial/freshwater and ocean compartments have seasonally variable subcompartments, i.e., snowpack, river/lake ice, and glacial ice for terrestrial/freshwater systems, and sea ice in oceans. Deltas, estuaries, and fjords are much smaller spatially than the three main compartments, but have been identified as a key interface between the terrestrial/freshwater and ocean compartments. Large amounts of sediment transported by rivers are deposited in deltas and estuaries, and thus, sediments are also identified here. In all cases, water transfers include, by definition, organic and inorganic particulate matter.

The pathways shown in Figure 3·1 illustrate transport by air ('A') or water ('F' for freshwater, including suspended sediments; 'SO' for surface ocean; and, 'DO' for deep ocean, with the 'I' or 'O' subscript indicating input to and output from the system). Chemical and biological transformations resulting in removal of material from the compartment are indicated by a 'T' subscript, while source terms ('S' subscript) represent anthropogenic or natural sources within the compartment and exchange processes between the compartments. The exchange processes involve transport, as well as chemical and physical reactions, as contaminants move across the interface. Note that the relative size of the boxes is not of significance in this figure. In most cases of inter-compartmental transfer, double arrows are used to indicate two-way movement. This model is a useful tool in the quantitative assessment of pathways. For instance, it has been applied to a group of pesticides that are commonly found in air in the Arctic (hexachlorocyclohexanes or HCHs) in order to understand the sources of this POP to the surface ocean (see chapter 6).

Following this brief introduction, section 3.2 explores the atmospheric compartment and its direct exchange with snowpack, lake ice, sea ice, and the surface ocean. Also considered are the indirect exchanges between the atmosphere and the terrestrial/freshwater compartments through the delivery of contaminants via precipitation (rain, fog, and snow) and dry deposition, as well as direct atmospheric exchange with rivers, lakes, soil, and vegetation. Section 3.3 is concerned more specifically with the transport and fate of contaminants in the terrestrial/freshwater compartment, with emphasis on the role of freshwater in transporting these contaminants. Discussion includes the delivery of pollutants from the land to the aquatic system, and sedimentation and sediment recycling in fluvial and limnic systems. Section 3.4 reviews processes in deltas, estuaries, and fjords, as these environments serve as an interface between rivers and lakes in the case of freshwater deltas, and between the terrestrial/freshwater and ocean compartments for marine deltas, estuaries, and fjords. Section 3.5 explores various components of the ocean system, including the surface and deep ocean compartments, sea ice, and the major intra- and inter-compartmental exchange processes. Lastly, the role of modeling as a pivotal tool in developing our understanding of the complex pathways into and within the Arctic is briefly reviewed in section 3.6.

3.2. Atmosphere

The occurrence of contaminants in the Arctic is influenced by the nature and rate of emissions from sources, the processes by which these compounds are transported to the Arctic, removal processes, and the exchange of compounds between the different compartments. Generally, the atmosphere contains a relatively small amount of a contaminant compared to the total amount in other environmental compartments (e.g., for HCH, see Strand and Hov 1996). The importance of the atmosphere is that it provides a significant mode of rapid transport of contaminants from source areas to the Arctic region. Transport times of contaminants via air currents are rapid compared to those in the oceans. The time for an air parcel to completely mix in the troposphere of the northern hemisphere is of the order of six months. Mixing in the region north of 30°N is of the order of three months (Plumb and Mahlman 1987). In contrast, transport times of water parcels in northern marine systems are measured in years and decades.

Atmospheric contaminants that are transported to the Arctic can be introduced from point, area, and regionally-distributed sources. Point sources include power generating stations, smelters, incinerators, and dump sites. This is the predominant source type in the northern regions of Eurasia and North America. Dump sites are of greatest concern for semi-volatile contaminants which volatilize once they are exposed to the air. Area sources consist of urban-industrial complexes. In heavily populated regions, a number of urban-industrial complexes mixed with point sources constitute a regionally-distributed source.

In the following sections, the sources, processes and factors affecting atmospheric transport, as well as the exchange processes between the atmosphere and other media (ice, land, ocean) are described.

3.2.1. Single and multi-hop pathways

Atmospheric transport pathways can be subdivided into two types: one-hop pathways and multi-hop pathways. One-hop pathways describe the movement of compounds that are emitted to the atmosphere, transported, and then deposited to the surface, never to return to the atmosphere. In such cases, the source region of an Arctic contaminant is simply defined by its source distribution, its lifetime in the atmosphere (governed by removal processes), and atmospheric circulation. This applies to acids, heavy metals with the exception of mercury, and nonvolatile, particle-bound organics, such as benzo(a)pyrene [B(a)P], black carbon particles, and radionuclides. The pathways of these constituents follow that of Arctic haze from mid-latitudinal sources into the Arctic (Barrie 1986, Barrie 1995, Barrie 1996b). Single-hop compounds are marked by longer atmospheric residence times in winter (≈20-30 days) compared to summer (≈3-7 days), as well as stronger south to north transport into the Arctic from Eurasia in winter than in summer. With multi-hop pathways, a compound re-enters the atmosphere after initial deposition to the Earth's surface, and continues over time to move through the environment in multiple hops. Processes by which this can occur include volatilization from the Earth's surface under temperatures warmer than during initial deposition; sudden exposure to the atmosphere of ocean water saturated with a volatile contaminant after being covered by ice; and, resuspension by wind, dust or snow. For multi-hop compounds, the source region affecting the Arctic is not only defined by atmospheric transport, removal and circulation, but also by surface processes that control its re-entry into the atmosphere. Mercury, most organochlorines (OCs), and many PAHs fall into the multi-hop group.

3.2.2. Atmospheric transport

Barrie (1992) and Iversen (1989a, 1989b, 1996) have discussed the role of atmospheric circulation in the transport of contaminants from mid-latitudes to the Arctic region. At-

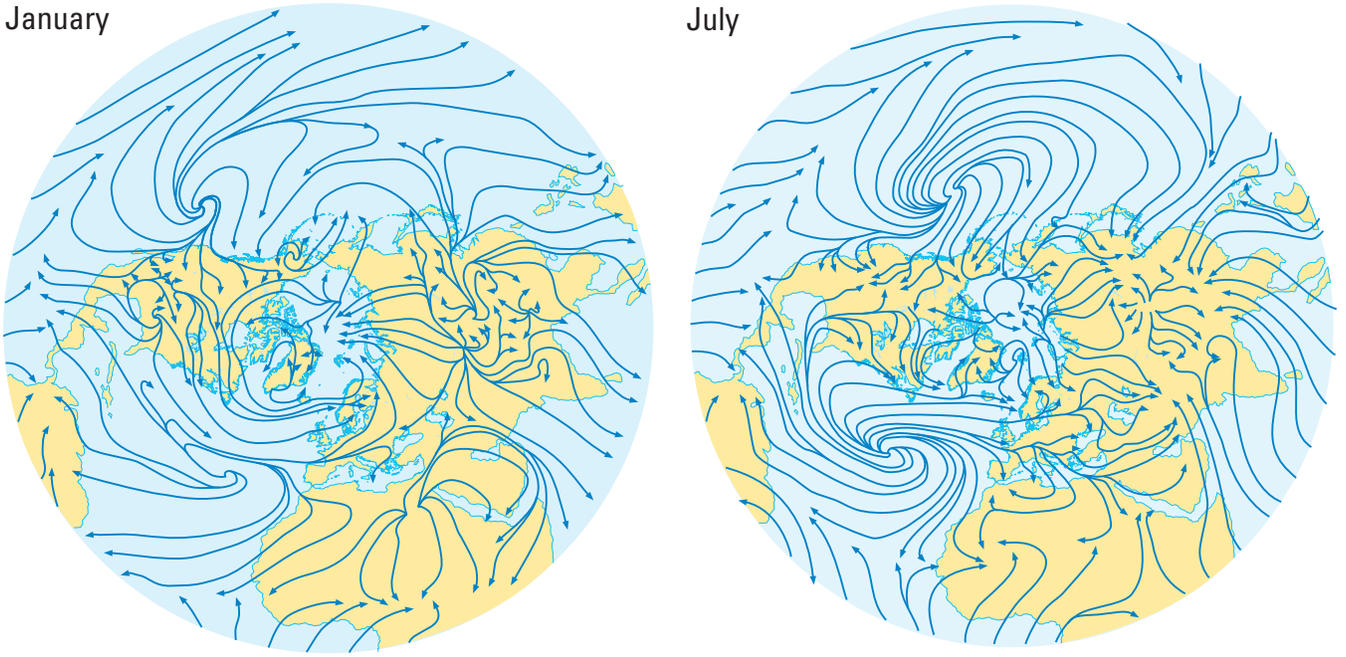

Figure 3·2. The mean circulation of the lower atmosphere during January and July as depicted by mean streamlines of the resultant winds (Source: Wendland and Bryson 1981).

mospheric winds deliver contaminants to the north. This is illustrated by streamlines of average winds in the northern hemisphere in January and July (Figure 3·2). In winter, the lower tropospheric circulation of the northern polar region is dominated by high pressures over the continents and low pressures over the northern Pacific and Atlantic Oceans. In particular, the intense Siberian high pressure cell tends to force air on its western side northward into the Arctic. The high pressure ridge over North America generally drives air out of the Arctic southward. The mean flow in winter is out of Eurasia into the Arctic, and out of the Arctic into North America. Some air is also exchanged with the south when low pressure vortices along the Arctic front mix warm southern air with cold northern air in a large-scale turbulent eddy.

In summer (Figure 3·2), the continental high pressure cells disappear, and the oceanic low pressure cells weaken, particularly in the north Pacific. Northward transport from mid-latitudes decreases accordingly. Mean circulation in the lower atmosphere gives way to a more circular clockwise flow around the pole at a higher altitude prompted by polar low pressures prominent in both summer and winter. The winter Siberian high pressure cell at the lower elevations disappears at an altitude of 3 km.

The mean flow maps in Figure 3·2 present a simplified picture of the circulation. Three types of flow regimes are involved in the exchange of mass or heat between polar regions and extra-polar regions: 1) mean meridional circulation (MMC), 2) standing eddies (SE), and 3) transient eddies (TE). To illustrate that these can all contribute substantially to north-south mass exchange, consider the seasonal distribution of energy exchange for each flow regime calculated by Nakamura and Oort (1988) for the Arctic and Antarctic (Figure 3·3). Heat exchange is least in summer and greatest in winter. Quantitative parallels between heat and mass exchange are erroneous, since the exchange depends on the lifetime and spatial distribution of the sources of a contaminant. Nevertheless, this analogy is valid qualitatively, and hence instructive.

Standing eddies, such as the Siberian high pressure cell (marked by a source of surface winds in Figure 3·3), tend to play a more prominent role in the northern hemispheric winter than in summer, or than in the Antarctic at any time

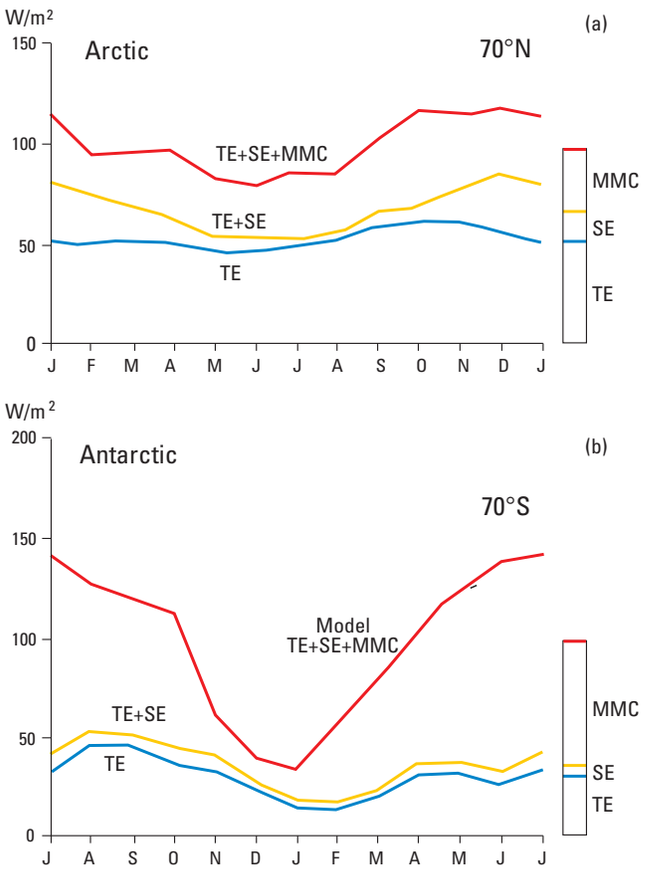

Figure 3·3. Modeled annual variation in poleward energy flux through latitude 70°, as effected by transient eddies (TE), standing eddies (SE), and mean meridional circulation (MMC) for the atmosphere from the surface to 25 hPa, for a) the Arctic and b) the Antarctic (adapted from Nakamura and Oort 1988).

of year. The difference between the Arctic and Antarctic is due to the very different distribution of continents and oceans, as well as the major mountain ranges between the two hemispheres. These cause an almost rotational symmetric gyre around Antarctica, while long planetary waves forced by the ground surface influence the circulation pattern around the

Figure 3·4. The mean position of the Arctic air mass in winter (January) and summer (July) from Li *et al.* (1993), superimposed on the (summer value % (orange) – winter value % (blue)) frequency of major south-to-north air transport routes into the Arctic (Source: Iversen 1996).

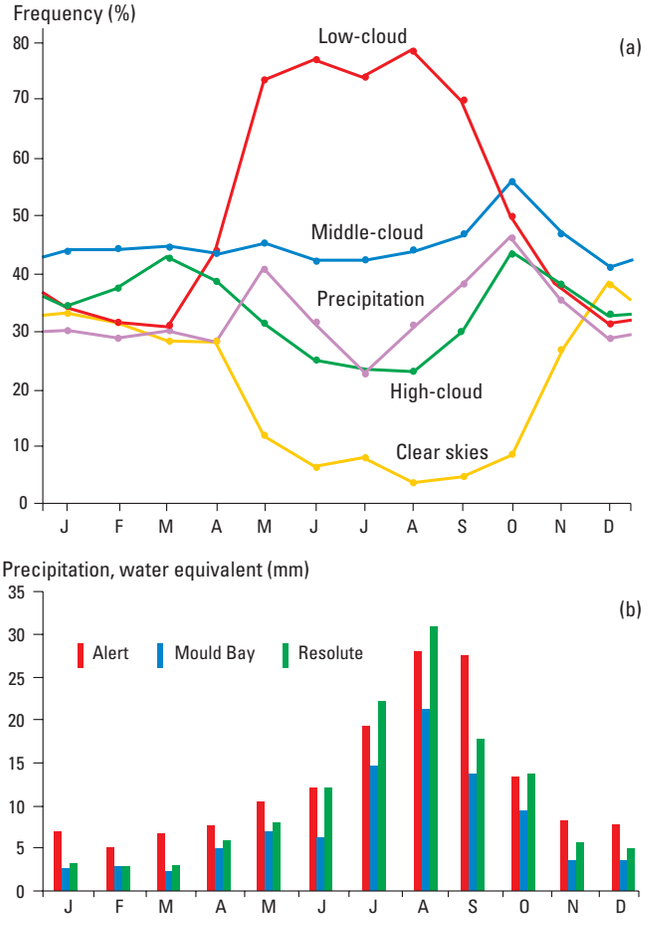

Figure 3·5. Seasonal variation in a) cloud cover and precipitation occurrence and b) precipitation amount in the Canadian High Arctic, 1951-1980 norms (Source: Barrie 1986).

Arctic. The stationary planetary wave pattern in the northern hemisphere is more pronounced during winter, when the temperature contrast between the tropics and the polar regions, and the strength of the jet streams are at their maximum. Furthermore, the total eddy exchange (SE+TE) is stronger than MMC at all times in the northern hemisphere, while in the southern hemispheric winter, the exchange is dominated by MMC. The thermal contrast between oceans and continents during the northern hemispheric winter is believed to be the major cause of stationary eddy features in the lower atmosphere close to the ground, where the main part of the transport of anthropogenic contaminants takes place. These features include the Aleutian and Icelandic lows, as well as large northern continental anticyclones. In connection with transport to the Arctic, the occurrence of the Siberian winter high pressure over large portions of Eurasia is of particular importance, as it causes a deep extension of the very stable Arctic boundary layer to parts of Eurasia which contain a large number of anthropogenic sources.

Winter flow patterns are markedly different from those in the summer. In winter in the lower atmosphere, air movement is driven by both the strong quasi-stationary cyclones over the Aleutians and near Iceland, and anticyclones residing over the North American and Eurasian continents, resulting in the transport of air over Siberia into the High Arctic, and south over North America. Consequently, contaminants which are introduced into the atmosphere in Siberia or Eastern Europe (in either vapor form or bound to small particles which have a low deposition velocity) are frequently transported into the Arctic region. Anticyclones are also characterized by relatively low wind speed, and thus stagnant conditions. Near the surface, the relative lack of cloud cover and low incident solar radiation during the Arctic winter can produce extended periods of surface radiation inversions. These factors reduce the effectiveness of vertical mixing and removal at the surface, resulting in the accumulation of contaminants in the lower Arctic atmosphere.

Contaminants having ground-level sources at mid- and low latitudes will, on average, experience rising air motions during their atmospheric transport to Arctic areas. This is a consequence of the temperature distribution in the atmosphere and the energy conversions driving the air motions. With few exceptions, atmospheric flow systems convert potential energy to kinetic energy through rising flows of relatively warm and light air and sinking flows of relatively cold and heavy air. The reservoir of potential energy remains unchanged as the tropics are warmed by solar radiation, while the polar areas are cooled by terrestrial outgoing radiation. As a consequence, contamination at higher altitudes (2-8 km) in the Arctic generally originates from lower latitudes than contamination in the lower Arctic atmosphere (0-2 km), the latter originating in colder and more northerly regions (Carlson 1981, Iversen 1984). Since many contaminants are water-soluble, and rising motions frequently are connected with precipitation release, upper level atmospheric Arctic contamination is generally less concentrated than in the lower atmosphere. Nevertheless, it is characteristic of the Arctic that the vertical extent of anthropogenic aerosol particles is greater than at mid-latitudes (Hansen and Rosen 1984, Radke *et al.* 1984, Schnell and Raatz 1984, Barrie 1986, Pacyna and Ottar 1988). In summer and autumn, when temperature contrasts between major pollution source areas and the Arctic are smaller, dispersion of contaminants in the vertical is less pronounced than at other times of the year.

Figure 3·4 illustrates the mean position of the Arctic air mass and the frequency of south-to-north transport in both summer and winter at various points on the Arctic Circle. In contrast to the winter period, in the summer, south-to-north transport from Eurasia is much weaker as the Siberian high dissipates. Marked variation in cloud cover and precipitation accompanies this seasonal variation (Figure 3·5). In

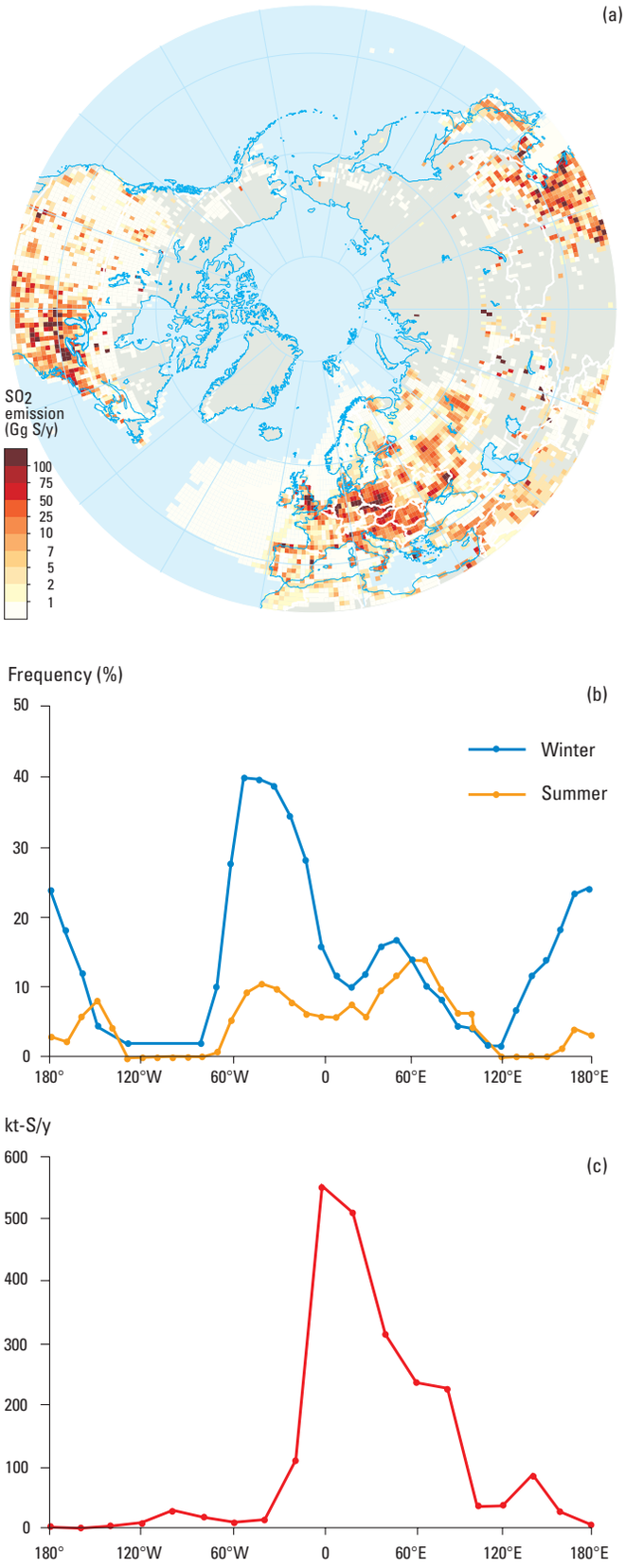

Figure 3·6. An illustration of the interplay between a) contaminant emissions distribution for sulfur dioxide and b) frequency of atmospheric south-to-north transport, yielding c) a net annual input of sulfur to the Arctic as a function of longitude that favors Eurasian sources in the winter half of the year. This contaminant has a one-hop pathway in contrast to more volatile persistent organochlorines, PAHs, and mercury. a) Gridded global emissions inventory of sulfur dioxide for 1985 as compiled on a 1°× 1° grid by the Global Emissions Inventory Activity (GEIA) of the International Global Atmospheric Chemistry Program (IGACP); b) the frequency of south-to-north transport of air in summer and in winter as a function of longitude (from Iversen 1989a); and, c) the annual input of anthropogenic sulfur to the Arctic at the Arctic Circle as a function of longitude as calculated for July 1978 to June 1979 (Source: Barrie *et al.* 1989b).

summer, temperatures in the High Arctic are near 0°C, allowing much more drizzling marine stratus than in winter, when temperatures between –25 and –45°C prevent build-up of moisture in the atmosphere. Photochemical activity during summer months is also higher, and provides an additional loss mechanism for some contaminants. Thus, during summer, transport from mid-latitudes to the Arctic is least for soluble, cloud-reactive or particle-bound compounds that are more easily removed by precipitation scavenging than insoluble or cloud-unreactive gases.

To illustrate the interplay between atmospheric circulation and the spatial distribution of contaminant emissions to the atmosphere, consider the case of anthropogenic sulfur transport to the Arctic. In Figure 3·6, three panels are shown. The top one (a) is the spatial distribution of annual anthropogenic sulfur dioxide emissions to the atmosphere, the center one (b) is the frequency of south-to-north flow of air as a function of longitude in summer and winter (Iversen 1989a), and the bottom panel (c) is the flux of anthropogenic sulfur into the Arctic for a one-year period (July 1978 to June 1979), as a function of longitude, modeled by Barrie *et al.* (1989b). The greatest inputs of these one-hop compounds occur in the Eurasian longitude sector (0-70°E) in winter. North American sources are not well connected to the Arctic by winds. Air tends to move eastward from North America over the stormy north Atlantic Ocean, where contaminants tend to be lost to the North Atlantic Ocean rather than northward into the Arctic air mass (Figure 3·4).

3.2.3. Atmosphere–surface exchange

Figure 3·7 summarizes schematically the major contaminant pathways between the atmosphere and the surface, as well as our current ability to calculate exchanges using flux equations. Transfers from the atmosphere to the Earth's surface in the polar regions are complicated by the presence of a seasonally varying intermediate media, namely, snowpack and ice. In the Arctic Ocean, the marginal seas undergo the greatest variations in percentage of ice cover.

The snowpack plays an important role in atmosphere–surface exchange. During the winter, as snow accumulates on the surface as snowpack, it stores contaminants gained during its formation in addition to those delivered by particle dry deposition and gaseous exchange. The latter component may be negative (surface loss), or positive (surface gain). At present, there is no way of measuring it directly. However, there are indirect means which can be used to infer gas exchange (see below). The net exchange between the atmosphere and the Earth is the result of all these processes.

3.2.3.1. Particle deposition (processes 2 and 7 in Figure 3·7)

Turbulent transport and/or sedimentation bring airborne particulate contaminants to the near-surface layer from the free atmosphere. Then processes of convection, diffusion, or inertial impaction carry them across a viscous sublayer where chemical and physical processes trap them on or in the surface (Voldner *et al.* 1986). The rate of particle transfer depends on the type of surface, the physical/chemical characteristics of the contaminant, and the state of the atmosphere.

The flux of contaminants from the atmosphere to the Earth's surface via particle dry deposition (F) is calculated as the product of a particle dry deposition velocity (V_d) and the contaminant concentration on particles in air (C_p) at some reference height above the surface (usually 10 m). V_d depends on particle size and physical properties such as water vapor

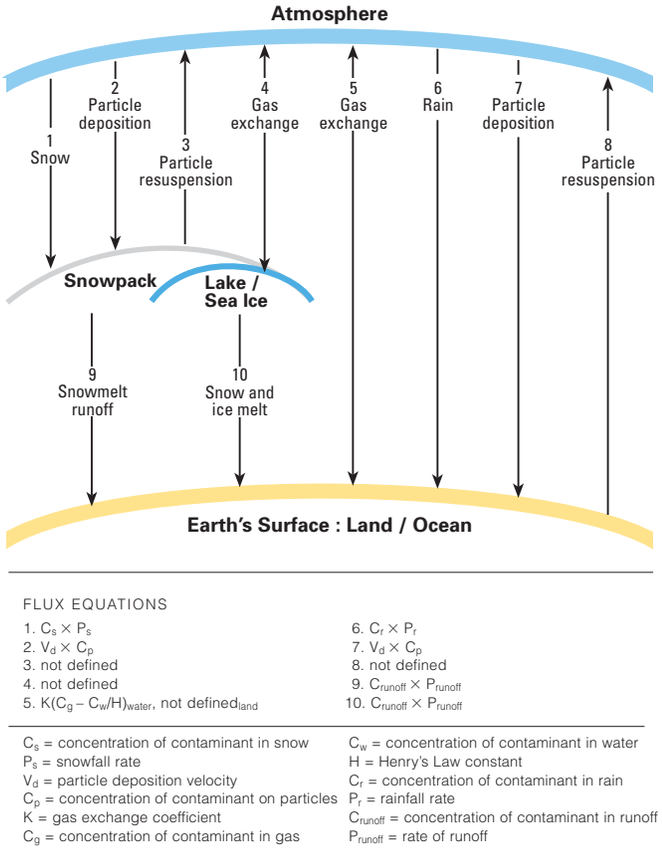

Figure 3·7. Schematic diagram of processes of atmosphere-surface exchange (Source: Barrie *et al.* 1997).

sorption (hygroscopicity). The flux of contaminants is being studied intensively in many research programs, including European and North American acid rain research programs. A rigorous treatment requires a knowledge of C_p and V_d for each particle size. However, in practice, a knowledge of the size distribution of particulate matter measured in the north can be used to obtain an average V_d to estimate dry deposition. For the Arctic, most anthropogenic aerosols that reach the region are smaller than 1 μm in diameter (Barrie 1986, Barrie 1996b). In this case for snow, a V_d for submicrometer particles, typical of those carrying most contaminants, of 0.05-0.1 cm/s has been determined in field studies (Ibrahim *et al.* 1983, Davidson 1989) and applied to estimate contaminant deposition (Giorgi 1986, McVeety and Hites 1988, Jantunen and Bidleman 1995).

3.2.3.2. Particle resuspension (processes 3 and 8 in Figure 3·7)

It is well established that desert soils can be suspended to great heights in the atmosphere and then transported long distances. For instance, Gobi desert dust is observed in Hawaii in the central Pacific, and occasionally in the Canadian Arctic (Welch *et al.* 1991, Barrie 1995, Barrie 1996). Considerable quantities of snow can be suspended in the atmospheric boundary layer together with suspended soil. However, little is known quantitatively about the resuspension of snowbound contaminants during blowing snow conditions (Pomeroy and Jones 1996) when surface wind speeds exceed 3 m/s in the Arctic. Surface soil is not covered by snow in many regions of the High Arctic which receives little precipitation during the winter (see Figure 3·5). These exposed soils commonly exist throughout the year allowing soil dust to be mobilized and mixed with surface snow during wind events (see also section 3.3.3.1). Air concentrations of soil aluminum measured at Alert during a blizzard in April 1986 were 5-7 times higher than during low wind conditions (Barrie *et al.* 1989a). Thirteen years of routine aerosol aluminum observations at Alert show much higher concentrations of suspended soil during windy periods than during low-wind weeks (Barrie 1995).

The erosion of surface snow occurs when the shear force at the air/snow interface exceeds inter-particle cohesive forces and particle inertia. The two primary modes of snow transport are saltation and suspension. Saltation is a near-surface phenomenon which occurs at low wind speeds, while suspension can disperse snow to heights of tens of meters and dominates as wind speed increases. Both are important phenomena in the Arctic, especially in the tundra and barren lands. Blowing snow grains become fragmented during collision with other snow particles or surface snow, resulting in a change to a more amorphous particle shape (Pomeroy *et al.* 1991, Pomeroy and Gray 1995) and an associated decrease in surface area.

The effect of surface area changes during blowing snow events on contaminant concentrations is not well understood. Pomeroy and Gray (1995) have shown that wind velocity, temperature, and relative humidity are important factors in snow sublimation, which can cause increased concentrations of major ions and the loss of volatile organochlorines (VOCs). More research is needed on the resuspension of contaminants during high winds.

3.2.3.3. Wet deposition (processes 1 and 6 of Figure 3·7)

Wet deposition of contaminants occurs when contaminants are incorporated into rain or snow which subsequently falls to the ground. The process, which is highly complex (Barrie 1991), includes in-cloud removal and below-cloud removal. In clouds, nucleation scavenging of particles is followed by uptake of soluble and reactive gases, as well as Brownian diffusion of particles to form liquid cloud droplets. Then cloud water is converted to precipitation (rain or snow) in complex ways that may be either efficient or inefficient in removing contaminants, depending on the process of precipitation formation. During unstable atmospheric conditions, below-cloud scavenging is generally thought to be of less importance than in-cloud scavenging (Murakami *et al.* 1983, Schumann *et al.* 1988). However, when stable atmospheric stratification causes contaminants to accumulate within the surface boundary layer, below-cloud scavenging may contribute significantly to wet deposition, especially of the larger particles (>2 μm) (Zinder *et al.* 1988). The processes of diffusion and interception may be of greater significance for precipitation in the form of snow, since snowflakes have a larger surface area than rain droplets.

The concentration of condensation nuclei collected in precipitation may be significantly reduced if conversion from liquid to solid phase dominates the aggregation of cloud droplets during the growth of snowflakes. Relatively large sedimenting hydrometeors (e.g., raindrops, snowflakes) can intercept cloud droplets as they sweep through the cloud, an accretion process known as 'riming' when associated with snowflakes. Since cloud droplets contain most of the aerosol mass within the cloud, riming can yield concentrations in precipitation that are similar to cloud droplet concentrations (Barrie 1985, Parungo *et al.* 1987, Borys *et al.* 1988, Collett *et al.* 1993). The accretional sweep out of cloud droplets (riming) is considered to be the dominant process controlling atmospheric removal by precipitation (Scott 1981, Borys *et al.* 1988, Barrie 1991). In Greenland, rimed snow has been

estimated to contribute about 5% of the annual snow mass, while accounting for approximately 30% of the annual deposition of atmospheric contaminants (Borys *et al.* 1993).

In northern regions, in-cloud scavenging is thought to be more important than below-cloud scavenging (Scott 1981, Murakami *et al.* 1983, Rehkopf *et al.* 1984, Schumann *et al.* 1988). Generally, in-cloud scavenging incorporates submicron particles into cloud droplets and precipitation elements, while below-cloud scavenging captures supermicron particles (>2 μm) and submicron particles (diameters <0.01 μm) (Slinn *et al.* 1978). However, field observations show that below-cloud rain scavenging coefficients for submicron particles are about an order of magnitude larger than predicted by theory (Volken and Schumann 1993). Additional factors encountered in the ambient atmosphere, such as phoretic and electrostatic forces and turbulent diffusion, may enhance particle scavenging by snow over theoretical predictions which neglect these mechanisms (Martin *et al.* 1980, Murakami *et al.* 1985a, Murakami *et al.* 1985b).

The efficiency of the particle scavenging process depends on a number of meteorological and physical factors, such as the hygroscopic nature of the particles, the size distribution of both the hydrometeors and atmospheric particles, precipitation intensity and cloud base height (Doskey and Andren 1981, Pruppacher 1981, Slinn 1983, Sauter and Wang 1989, Mitra *et al.* 1990, Sparmacher *et al.* 1993). The ratio of pollutant concentration in precipitation to that in air feeding the cloud is the scavenging ratio (W_p). Use of this is fraught with difficulties (Barrie 1992). However, as a rough measure of relative scavenging efficiencies, it is useful. It has been estimated that the coalescence of cloud droplets to rain drops produces particle scavenging ratios (W_p) of about 10^6 (on an equivalent volume basis), while W_p values of $\leq 10^5$ are indicative of unrimed snow, or scavenging of either insoluble particles or particles with diameters of 0.1-1.0 μm (Scott 1981). These latter ratios reflect the inefficiency of unrimed snow to scavenged particles within cloud droplets, or the inefficiency of accumulation-mode particles to be removed below the cloud base. By comparison, W_p values for rain, based on field measurements, range from $\approx 10^3$ to 10^6 (Bidleman 1988).

Snow is likely more efficient than rain at below-cloud scavenging of particles because of the larger size and surface area of the snowflakes (Redkin 1973, Graedel and Franey 1975, Murakami *et al.* 1983, Raynor and Hayes 1983, Parungo *et al.* 1987, Leuenberger *et al.* 1988, Schumann *et al.* 1988, Nicholson *et al.* 1991). Particle scavenging at low temperatures, typical of the early fall and late spring Arctic seasons (0 to –30°C), may be more effective than dry snowfall during the winter, as water film on the crystal surface enhances the probability that particles contacting the surface will stick (Mitra *et al.* 1990). In addition, the particle scavenging efficiency of snow depends on the crystalline shape, with needles and columns being less effective than stellar plates, dendrites and snowflakes (Takahashi 1963, Miller and Wang 1991). Both snowflakes, which are aggregates of individual crystals, and dendritic crystals tend to have a 'filtering effect' on atmospheric particles during sedimentation as a result of the passage of air through the crystal pores. This ventilation increases the scavenging efficiencies, especially for small particles (0.2-2 μm) which would otherwise follow the streamlines around a nonporous hydrometeor, thereby reducing the probability of being scavenged (Redkin 1973, Mitra *et al.* 1990). Field studies have demonstrated that snow may be five times more efficient than rain at below-cloud scavenging (Murakami *et al.* 1983, Sparmacher *et al.* 1993).

It may be that both adsorption and dissolution mechanisms operate in rimed snow. Interfacial adsorption to the surface water film of snow crystals occurs as does Henry's Law dissolution into cloud droplets scavenged by rimed snowflakes. Because droplets rimed to snowflakes, freeze on contact with the snowflake, Henry's Law partitioning behavior may be important only if there is negligible loss of contaminants during freezing of the droplet. Some fraction of both soluble and particulate contaminants may be excluded from the crystalline lattice upon freezing (Uhlmann *et al.* 1964, Hoekstra and Miller 1967, Gross *et al.* 1975, Iribarne *et al.* 1983, Lamb and Blumenstein 1987, Iribarne and Pyshnov 1990, Iribarne and Barrie 1995).

Another atmosphere-surface exchange pathway is fog water deposition (Barrie and Schemenauer 1986, 1989). It is a hybrid of precipitation scavenging and dry deposition processes. Fogs are essentially clouds at the ground. In some cases, this is literally true, for example when a layer of cloud passes over a mountain. In other cases, the fog is formed by processes (different than those of cloud formation) that take place near the Earth's surface. If air is cooled sufficiently, the water vapor in it will condense into liquid drops. The cooling can be produced by several different meteorological situations leading to different types of fogs. At night, the Earth's surface loses heat through the transmission of terrestrial infrared radiation to the atmosphere above. Sufficient surface cooling leads to saturation of the near-surface layer and 'radiation fog'. Light winds (<10 km/hr) promote fog development by mixing cool, moist surface air in the vertical. At higher wind speeds, mixing with drier air aloft is so great that fog formation is inhibited.

'Advection fog' is produced when warm, moist air is transported over a colder surface. Most coastal fogs are of this type. 'Upslope fog' is produced when air is forced to rise over a topographical barrier decreasing atmospheric pressure that produces expansion and cooling of the air. Other types of fogs are less important vehicles of deposition. 'Steam fog' or 'Arctic sea smoke' is produced by the condensation of water vapor from a relatively warm sea surface in much colder air aloft. When Arctic Ocean ice cracks to form open leads in winter and the atmospheric temperature is much below 0°C, this type of fog is observed. 'Ice fog' is produced at temperatures below about –30°C when water vapor sublimes directly onto atmospheric ice nuclei (particles) thus forming tiny ice crystals. This illustrates a characteristic of fogs (and clouds) that is important in the scavenging of contaminants from the atmosphere, namely that fogs remain liquid (containing supercooled water drops) down to temperatures as low as –20°C, and occasionally to much lower temperatures.

The means by which particles and gases are incorporated into fog droplets of 1-20 micrometer diameter are the same as for cloud droplets. They are then deposited to the Earth by processes similar to that of dry deposition of particles: sedimentation for droplets larger than 5 micrometers and impaction on surface roughness elements for smaller particles. The microstructure of fogs is strongly influenced by the characteristics of atmospheric cloud condensation nuclei (i.e., hygroscopic aerosol particles dominated by sulfates and sea salt). Polluted air masses with high aerosol concentrations generally produce fogs with high fog droplet number concentrations and smaller drop sizes. Sea fogs generally have lower total droplet concentrations and larger droplets. Knowledge of the chemical composition of fogwater as a function of droplet diameter is important in calculating the deposition of contaminants in fogs. Unfortunately, reliable size-dependent chemical composition data are not available for fogs in the polar regions.

3.2.3.4. **Gas exchange between atmosphere and snowpack/ice (process 4 in Figure 3·7)**

Material can be added to the snowpack by snowfall and by particle dry deposition, while gas exchange can both add and remove it. The partial vapor pressure gradient of an organochlorine (OC) between ambient air and interstitial air in snowpack or ice determines the potential for exchange. This is strongly dependent on temperature. In general, compounds with relatively high vapor pressures, such as hexachlorobenzene (HCB) and α- and γ-HCH, can volatilize substantially from the snowpack, while polyaromatic hydrocarbons (PAHs) and many of the polychlorinated biphenyl (PCB) congeners with lower vapor pressures may not. Supporting evidence for volatilization from snow is drawn from past and present studies in the Arctic. For instance, at the Canadian Ice Island, HCB and chlordane were detected in snow collected from May-June, 1986 (33 and 91 pg/L, respectively), though not found in snow (< 1 pg/L) from the same area several months later in August-September (Hargrave *et al.* 1988).

Several observational studies in the Canadian Northern Contaminants Program (Barrie *et al.* 1997) indicate that the process of post-depositional gas exchange between the snowpack and atmosphere is a significant pathway for many of the relatively volatile OCs. These include: 1) Agassiz Icecap studies (Gregor 1990, Gregor 1991, Franz *et al.* 1997), 2) Amituk Lake basin studies (Semkin 1996), and 3) snowpack–snowfall chemistry surveys.

3.2.3.5. **Gas exchange between the atmosphere and soil, water, and vegetation (process 5 in Figure 3·7)**

Gas exchange between the atmosphere and liquid water (fresh or salt water), vegetation, or soil is commonly a reversible process. Most is known about the exchange to water, that is usually described by the two-film model (Liss and Slater 1974), in which the rate of transfer is assumed to be limited by molecular diffusion across thin air and water films at the interface. The net gas flux can be estimated by:

$$F = K[C_w - C_a RT/H] \quad (1)$$

$$1/K = 1/k_w + RT/Hk_a \quad (2)$$

In these equations, C_w and C_a are the concentrations of dissolved and gaseous chemicals in water and air, k_w and k_a are the mass transfer coefficients for the individual water and air films, H is the Henry's Law constant at the water temperature, R is the ideal gas constant, and T is the air temperature (°K). K is the overall mass transfer coefficient that takes into account the resistance to transfer offered by both the air and water films.

These relationships have been applied to the exchange of OCs by Bidleman and McConnell (1995) and Cotham and Bidleman (1991) as well as to the calculation of Arctic Ocean HCH budgets (Barrie *et al.* 1992, 1997). It is important to recognize that gas exchange takes place even under equilibrium conditions when invasion and evasion are balanced and the net flux is zero. Thus, the mass of material transferred by gas exchange is much larger than is apparent from the net flux. For this reason, Murphy (1995) suggested that gas exchange be calculated as two separate terms, one for volatilization and the other for deposition.

The oceans represent a large reservoir of some contaminants, with total burdens thousands of times greater than those found in air. Given this, and the fact that the Arctic Ocean covers the majority of the area considered to be within the Arctic region, the air/water exchange represents a significant potential source for the Arctic atmosphere. The air–water partition coefficient decreases with decreasing temperatures, and thus, the highest equilibrium concentrations of OCs in surface waters are expected to occur at cold water temperatures (Wania and Mackay 1993).

Gas exchange to soils depends on the sorption of contaminant vapors on soil surfaces. It is poorly understood and is being studied in other programs focused on the movement of contaminants in agricultural areas, though usually not at Arctic temperatures (Eitzer and Hites 1989, Hart *et al.* 1993, Staehelin *et al.* 1993, Leister and Baker 1995). Models for such exchange are available, but are very uncertain. In forested areas (leaf:ground area ratios of 3-19), leaves or needles may represent the primary terrestrial contact for airborne chemicals (Schulze, 1982) and thus for gas-phase transfers. Uptake and loss of OCs by Arctic plants, such as lichens, and by frozen soils are poorly understood, necessitating further research if the air-plant-terrestrial food chain pathway is to be better quantified.

3.2.3.6. **Snow and ice melt (processes 9 and 10 in Figure 3·7)**

Runoff from snowpack melt and lake- and sea-ice melt delivers water, particulate matter, and dissolved and particle-associated contaminants from their winter storage reservoirs to terrestrial, freshwater, and ocean environments. While atmospheric processes are still important (e.g., temperature, precipitation), terrestrial and fluvial processes (e.g., runoff, hydrology, infiltration, permafrost) tend to predominate with respect to the delivery of contaminants between compartments. Consequently, these processes will be considered in section 3.3.

3.3. Terrestrial/Freshwater

3.3.1. Introduction and scope

The Arctic land mass, which includes freshwater lakes and river systems as well as the islands of the Arctic Ocean and adjacent seas, measures a full 13.4×10^6 km^2 or about 40% of the total AMAP area. This compartment, referred to as the 'terrestrial/freshwater' compartment in Figure 3·1, is important in its own right in that it supports terrestrial and freshwater ecosystems, but also because its large surface area serves as a receptor for atmospherically transported contaminants. The emphasis of this section is on the general features of the sources of contaminants to this compartment and the processes that determine their fate, including the connective function that the terrestrial/freshwater compartment provides between the atmosphere and the oceans. For example, while surficial geology generally determines infiltration rates and groundwater conductivity, permafrost is an overriding factor with respect to groundwater in cold regions. Similarly, ice and snow play a dominant role in the physical and chemical processes influencing contaminant transport and fate.

Different types of development associated with urbanization and industrialization, including construction of roads and pipelines, directly contribute to erosion (Claridge and Mirza 1981). Where the ground cover has been disturbed or removed, subsidence and trapping of water may follow, resulting in an accelerated degradation of permafrost. If water begins to flow, hydraulic erosion may follow and result in the formation of erosion gullies (Claridge and Mirza 1981) and export of particulate matter from the area. Deforestation is often the cause of increased erosion and in tem-

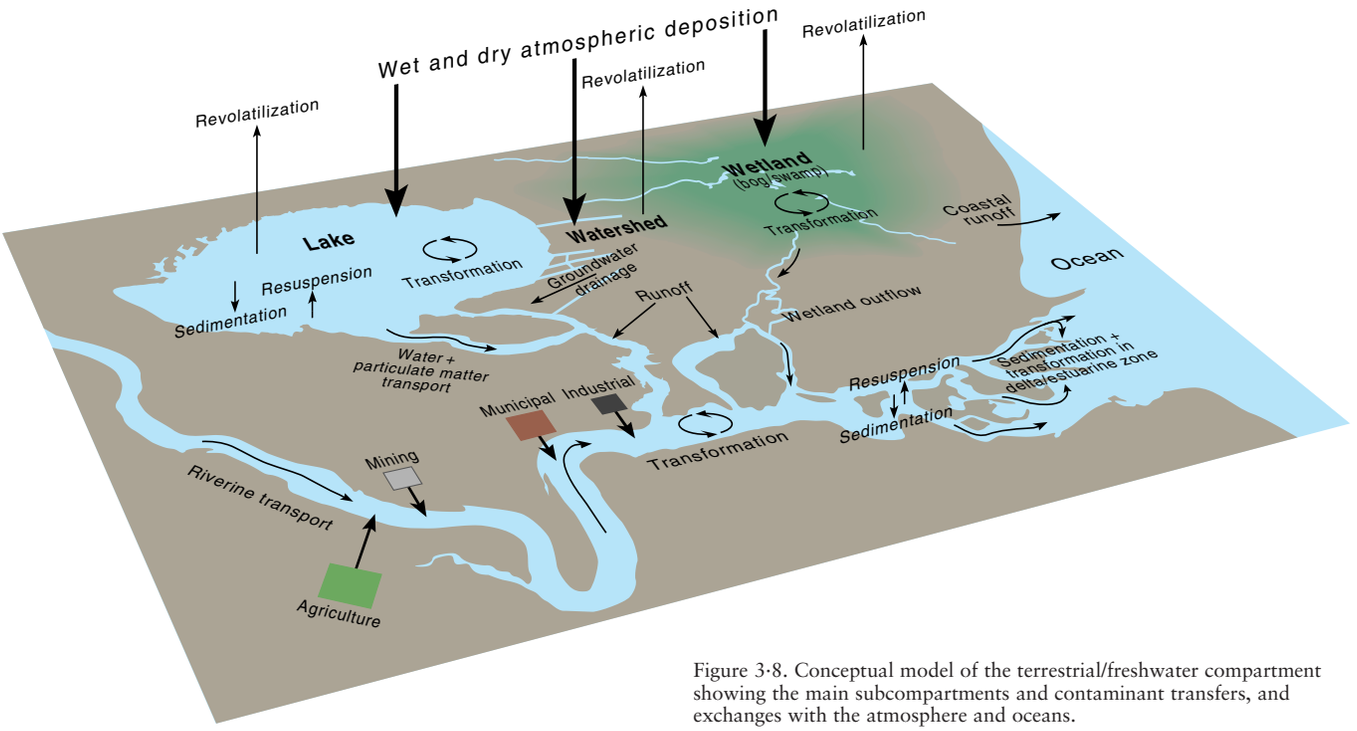

Figure 3·8. Conceptual model of the terrestrial/freshwater compartment showing the main subcompartments and contaminant transfers, and exchanges with the atmosphere and oceans.

perate areas can result in an increase in sedimentation of between 20 and 50 times.

Rather than considering each and every process and its role with respect to contaminant transport, this discussion will emphasize the processes that are unique or specific to the Arctic. In addition, the mass transport of water, sediment, and organic matter, which are important determinants for the transfer of contaminants in fluvial systems are quantified where possible. This will set the stage for discussions on the delivery and fate of these contaminants to the marine system including deltas, estuaries, and fjords which provide an interface between the terrestrial/freshwater compartment and the ocean compartment.

The terrestrial/freshwater compartment is multi-faceted and Figure 3·8 provides an overview of the components of this compartment, the transfers and processes that will be considered, and the main sources of contaminants. Note that precipitation, including snowfall, is part of the atmospheric compartment discussed in section 3.2, whereas snow on the ground (snowpack and ice) and snowmelt are included here. The other main components of the terrestrial/freshwater system are the land surface and subsurface, wetlands, rivers, and lakes/reservoirs. Both water and suspended and bottom sediments are considered. These components are reviewed below, presenting their unique character and magnitude in the context of the Arctic system.

As illustrated in Figure 3·8, contaminants are delivered to the terrestrial/freshwater environment by the atmosphere and from direct discharges of wastes to land and water. Large river systems that drain to the Arctic, but that have a major portion of their drainage basin outside of the Arctic, including many of the rivers of Russia (e.g., Yenisey, Lena, Ob) as well as several Canadian Rivers (e.g., Mackenzie, Churchill and Nelson), are important conduits to the northern marine environment. While details of specific contaminant loadings from point and diffuse sources will be considered in subsequent chapters, general features of sources relevant to their interaction with physical processes in a cold environment will be provided in this section.

3.3.2. Sources of contaminants

3.3.2.1. Atmospheric deposition

The most important, large-scale contaminant delivery process to the terrestrial/freshwater compartment is deposition from the atmosphere through wet and dry particle scavenging as discussed in section 3.2. The influence of atmospheric contaminants on Arctic freshwater systems starts with their deposition onto surface waters (lakes, rivers, wetlands) or land surfaces in their catchment area. While the total surface area of some lakes, reservoirs, and rivers is large, it remains small relative to the total land surface area (<1%), and thus, deposition directly to the water/ice surface will not be considered separately from the land mass. Reports describing the input of contaminants to remote freshwater systems by long-range atmospheric transport include Gregor and Gummer (1989), Barrie *et al.* (1992), Mackay and Wania (1995), Oehme *et al.* (1995), and Barrie *et al.* (1997).

Land and freshwater can also be contaminated via the atmosphere by sources within the Arctic. These contaminants are often of the single-hop variety as defined in section 3.2, although the heavier, multi-hop contaminants could also initially be deposited close to the emission source (e.g., higher chlorinated PCB congeners and PAHs), especially during the colder winter months, and then selected, more volatile compounds could be remobilized and transferred over greater distances during warmer periods. This is most important in the vicinity of large urban and industrial complexes and consequently, this pathway will be dealt with as part of the point source discussion below.

3.3.2.2. Direct wastewater discharges

Development has a direct influence on water quality. In addition to the effects on the environment from land clearing, construction, and decreased permeability, the quality of water returned to the basin is usually diminished even after treatment. The disposal of industrial and municipal waste waters is always a concern. Storm and meltwater runoff,

which is usually routed directly to receiving water bodies without treatment, may be highly contaminated due to spills and localized atmospheric fallout. These factors can exacerbate the problems of providing clean water to basin residents. This and the subsequent section provide some examples of the industrial and municipal sources of contamination within the Arctic.

Russia

The large Arctic drainage basin within Russia has been developed, especially along the major rivers which have provided a transportation corridor. Information on discharges from many of the industrial sources was not available.

Oil and gas extraction activities have led to significant contamination of vast areas of adjacent land containing wetlands. For instance, in northwest Siberia, a wide range of contaminants have been discharged, both from natural seeps which are typical for oil and gas deposits, and from anthropogenic sources. The anthropogenic contaminants are typically used in the processes of extraction, pre-treatment and transportation of raw products (e.g., petroleum hydrocarbons (PHC), phenols, nitrogen compounds, heavy, alkaline and alkaline-earth metals, diethylenglycol (DEG), and methanol). These waste waters are usually discharged in an untreated condition into landscape depressions. Under northern temperature and light conditions, the degradation rates for many organic contaminants are likely lower than farther south. Horizontal and vertical drainage rates are also low in these areas due to the low relief and presence of permafrost. Hence, it is expected that in the areas surrounding oil and gas extraction activities, polluted wetlands can represent long-term sources of secondary contamination of surface waters, particularly during seasonal and rain floods, even after cessation of the extraction activities (NEFCO 1995). These releases and their effect on the environment will be considered further in chapter 10.

Forests destroyed by air pollution primarily from large metal smelters in Pechenga and Monchegorsk, have become typical of the Kola Peninsula (Igamberdiev *et al.* 1995, NEFCO 1995). This impact on forests extends into the northern areas of Lapland and Finnmark, Norway. The deforestation results in more runoff and reduced infiltration. In turn, this increases the amount of erosion in the basin, increasing the sediment load and any associated contaminants to the fluvial systems. Within the river channel, higher flows result in greater erosion and transport of sediments. Investigations of the effects on water quality and contaminant transport in these areas are scarce.

The problem of poor drinking water supply in Monchegorsk City on the Kola Peninsula is one example of significant local industrial impact on water bodies. The tap water supply of this city is taken from Lake Moncha, which is located a few kilometers from the city, where a large nickel smelter, Severonickel, is located. Channeled waste waters are not discharged into the lake. However, contaminants are transported into the lake either by direct atmospheric deposition or with meltwaters and surface runoff. As a result, nickel concentrations in this lake reach 0.05 mg/L or five times the maximum allowable concentration (NEFCO 1995).

Wetlands are known as efficient scavengers of many types of wastes, and, indeed, have been used under various circumstances as surface water quality cleansers. In areas with strong anthropogenic impact, wetlands can serve as accumulators of contaminants, but subsequently may serve as sources of significant secondary contamination of river waters. Based on a study of more than 250 wetlands in the Russian sector of the Arctic, it has been shown that the levels of heavy metals in wetland ecosystems are generally low, with the exception of areas with intensive heavy industrial development (Zhulidov *et al.* 1977). (See chapter 7 for additional details regarding heavy metals).

Alaska

Large volumes of used drilling fluids have been released into Arctic wetlands during exploration. Increased concentrations of common and trace metals and organic hydrocarbons have been found in ponds both near and at a distance from drill site sumps (Garland *et al.* 1988). In addition, there are mining activities which are potential sources to the environment of acid mine drainage and trace elements.

Canada

Over 1200 oil and gas exploratory wells have been drilled on land in the Yukon and NWT (COGLA 1989), mostly in the western portion of the NWT and adjacent portion of the Yukon, from the 60th parallel to the Arctic Islands. Drilling fluids, containing a range of contaminants from common metal salts, surfactants, and petroleum hydrocarbons, have commonly been disposed of in sumps adjacent to the rigs. French (1978) observed that approximately one-third of the sumps had problems, including:

- non-containment of fluids during drilling;
- melt-out problems during summer operations;
- sump subsidence and collapse;
- non-containment of fluids during in-filling of sumps; and,
- subsurface leakage of fluids.

Nonetheless, detailed studies of abandoned sumps in the NWT by Smith and James (1979) indicated that contaminants in soils and plants were localized to within 100 m of the sump.

As of 1986, 14 mines were producing lead, zinc, silver, gold, copper, tungsten, cadmium, or arsenic. Prior to this time, 68 mines had been developed and abandoned (Thomas *et al.* 1991). The concern with these abandoned mine sites is primarily the refuse that has been left behind, including fuels and waste oils. The main active mines in the Northwest Territories (NWT) are the base metal mines at Polaris on Little Cornwallis Island and at Nanisivik on Baffin Island, and gold mines at Contwoyto Lake and Yellowknife. Perhaps the largest single source of anthropogenic contaminants are the gold mines in the vicinity of Yellowknife, where the presence of sulfides requires roasting prior to the cyanide process. The fumes produced from the roasting process can contain significant amounts of arsenic trioxide, and sulfur dioxide, some of which are released to the atmosphere (Thomas *et al.* 1991). Processing of the ores often results in the pollution of both land and water with heavy metals, but this has been relatively small in magnitude (see also chapter 7) (Allan 1979, Mudroch *et al.* 1989, Mudroch *et al.* 1992).

Base metal mines commonly involve the processing of sulfide rocks. The resultant acid mine drainage from the tailings can often solubilize and consequently mobilize metals. To date, more than 10^{11} kg of tailings have been produced (Thomas *et al.* 1991). Mine tailings can become a long-term source of metals to surface waters, while the acid drainage in and of itself can be a concern in poorly buffered aquatic systems. For example, acid mine drainage is not a major concern in the vicinity of Nanisivik on Baffin Island due to presence of dolomite bedrock, whereas acid mine drainage and the mobilization of metals (especially Zn) are a definite and ongoing concern at the Faro mine in the Yukon, which began production in the 1970s (R. Nicholson, pers. comm., Department of Earth Sciences, University of Waterloo, 1996).

3.3.2.3. **Municipal wastewater sources**

Rivers draining to the Arctic Ocean receive contaminants from different sources within and outside their catchment areas. Direct discharges of industrial, mining, and urban wastes into water bodies are the main sources of surface water contamination, unless stringent discharge regulations are in effect and enforced. The Arctic rivers with vast basins may receive contaminants discharged in heavily industrialized zones and large cities located far to the south of the Arctic region. For example, in the territory of Russia, southern reaches of the large Arctic rivers include large industrial complexes and cities with populations often exceeding a million inhabitants.

The Barents region of the Russian Arctic is the most highly populated and industrially developed part of the circumpolar Arctic. The province of Murmansk has over one million inhabitants with many in major industrial cities, including Murmansk, Apatity, Kirovsk, Kandalaksha, and Monchegorsk. To the east of Murmansk is the province of Archangel, which, including the Nenets autonomous area, in 1993 had a total population of 1561 000 inhabitants with over 70% in major cities (including the cities of Archangel and Severodvinsk). In highly urbanized areas, surface runoff waters, including organized industrial and communal wastewater discharges, can contribute up to 40-50% of total pollution entering the water bodies (WHO/UNEP in press).

In contrast, the large drainage basins of North America have relatively small populations with limited industrial development and relatively stringent environmental controls. The largest cities in the Canadian Arctic are Yellowknife and Iqaluit in the NWT, with populations of approximately 12 000 and 3000, respectively, and Whitehorse in the Yukon, with about 15 000 inhabitants.

Russia

Arctic rivers in Russia are affected by untreated or partially treated waste water (Table 3·1) due to the high level of industrial development in their basins, especially in the European part and in western and central Siberia. It is only recently that attempts have been made to quantify the most hazardous sources in the Arctic region of Russia (Igamberdiev *et al.* 1995).

Table 3·1. Range of annual discharges of waste waters to the river basins of the Russian Arctic between 1988 and 1993 (10^6 m^3/y) (Source: CIP 1995).

Territory	Range
Northwest Region	
Republic of Karelia[a]	206.1-288.1
Komi Republic	168.7-193.7
Archangel Province	642.5-696.7
Vologda Province	240.5-325.6
Murmansk Province	260.3-382.1
Urals	
Chalyabinsk Province[a]	608.9-707.9
Sverdlovsk Province[a]	728.3-864.1
Kurgan Province	13.1-25.5
Western Siberia	
Republic of Altai[b]	0.1-0.3
Altai Territory	61.2-117.8
Kemerovo Province	567.4-768.3
Novosibirsk Province	326.0-360.6
Omsk Province	136.7-291.1
Tomsk Province	47.3-68.3
Tyumen Province	69.1-183.8
Eastern Siberia	
Republic of Tuva	6.1-13.4
Republic of Khakassia[b]	71.5-78.1
Krasnoyarsk Territory	785.4-1405.5
Irkutsk Province	1353.7-2056.8
Far East	
Republic of Sakha (Yakutia)	44.8-95.4
Chukchi Autonomous Area[a,b]	10.2-11.0
Magadan Province[a]	31.4-53.4

a. Only a portion of the Territory belongs to the Arctic basin.
b. Data available only from 1988-1990.

The impact of anthropogenic contamination on Arctic waterways can be illustrated by the condition of waste water discharged to waterbodies in Murmansk province (Kola Peninsula), which is the most industrialized area of the whole Arctic region. In 1994, only 4.7% of the waste water in the province was treated to specified standards. Approximately 6.1% of the waste water (103.5×10^6 m^3) was discharged into waterbodies without any treatment and 13.6% (229.1×10^6 m^3) was considered insufficiently treated. The remaining 75.6% (1269.8×10^6 m^3) was classified as 'conditionally clean' and allowed to be discharged without treatment. Most of this latter group is generated by cooling waters of the Kola nuclear power plant (NEFCO 1995). The distribution of wastewater discharge rates in Russia are summarized in Table 3·1. Amounts of contaminated waters and releases of selected contaminants in the Murmansk province are given in Table 3·2. Murmansk city discharges its waste waters partly into the Kola Fjord and partly into freshwater bodies. The Kola River, which serves as a source of drinking water for Murmansk, receives discharges of municipal and agricultural waste, significantly affecting the quality of this supply.

There are also the so-called fugitive discharges of unknown content and size. These include dump sites and spills and require further investigation to determine the scale of potential and real emissions.

Canada

There are only five major cities in Canada that discharge effluents into rivers which drain to the AMAP region. All of these, identified in Table 3·3, are within the Nelson River system, with the closest, Winnipeg, being more than 1000 km from the outlet to Hudson Bay. It should be noted that all industries in these cities are required to discharge through the sewage treatment plants, except for uncontaminated wastes, such as cooling waters. As mentioned above, within the Arctic, the cities of Whitehorse, Yukon and Yellowknife, NWT are relatively small in population and have little industry.

POPs and radioactive material are thought to reach the Arctic areas of North America mainly through atmospheric long-range transport. However, a few local sources of OCs have been disclosed. Military 'DEW Line' (Distant Early Warning Line radar) installations deployed between 1950 and 1970, used DDT mixtures, as well PCB-containing devices (electrical transformers and capacitors) widely. Following disposal, vandalism and natural processes resulted in the release of some of the PCBs to the environment (see chapter 6 for additional details).

Greenland

Apart from mining, there are no other major industrial enterprises in Greenland. A few mines are known to discharge heavy metals directly into the marine environment. However, according to available sources, there is only an insignificant level of discharge into rivers (M. Holm, pers. comm., Greenland Hjemmestyre, 1996).

Iceland

Only a very limited amount of heavy metals, POPs, and PAHs are suspected to be directly discharged into lakes and rivers of Iceland. There are no major mining activities involving metals, and hence the risk of heavy metal discharge into freshwater is low.

Table 3·2. Annual wastewater discharges in the cities and counties in Murmansk province in 1994 (Source: ECMP 1995).

City, district	Annual wastewater volume, 10^6 m^3	Amount of contaminants discharged (tonnes/y)										
		BOD	Petrol hydro-carbon	Sus-pended matter	$N\text{-}NH_4$	$N\text{-}NO_3$	Al	Fe, total	SO_4	$P\text{-}PO_4$	F	Cl^-
Murmansk	65.2	7429	56.4	5347	871	45.9		27.5	1531	116		4960
Kirovsk and Apatity area	1356	872	41.7	1637	416	4051		15.0	8191	87	297	2357
(Kola nuclear power plant)	(1172)	(8.6)	(1.3)	(9.3)	(4.6)				(110)	(0.3)		(22)
Kandalaksha	41.5	438	5.5	436	30.9	28.6	0.03	3.0	0.8	12.1	313	
Monchegorsk	24.6	139	3.0	721	53.0	11.3		0.02	34679	14.4		7344
Olenegorsk	14.7	80	3.4	97.2	47.5	77.1		1.6	122	6.2		235
Polyarny	16.1	430	8.2	445	167	18.8		0.04	377	22.6		1088
Severomorsk	17.6	903	6.1	512	146	15.7		0.1	236	18.5		373
Kovdor County	39.5	251	2.4	265	26.7	107	0.27	14.0	4543	32.4		876
Kola County	44.8	246	1.7	202	72.5	46.8	0.48	1.4	80.5	16.6	1.3	222
Lovozero County	17.7	103	2.3	317	25.4	7.3		0.2	103	4.6	115.6	131
Pechenga Country	37.7	279	31.3	249	80.7	101	0	0.8	2252	0.1	0	377
Murmansk Province (total[a])	1680	11487	162	10387	1955	841	0.78	63.9	52170	332	415	18343

a. This total includes additional discharge areas to those listed in the table.

Table 3·3. Wastewater treatment plant effluent discharge data for major Canadian cities discharging into rivers draining to the AMAP region. (Data sources: Gold Bar Waste Water Treatment Plant (Edmonton); City of Calgary Engineering and Environmental Services Department (Calgary); Pollution Control Plant (Saskatoon); Treatment Plant and Public Works Department (Regina); City of Winnipeg and Wastewater Department (Winnipeg).

City	Population served	Treated wastewater 10^6 m^3/yr	Amount of contaminants discharged (tonnes/y)									
			$N\text{-}NH_4$	$P\text{-}PO_4$	$N\text{-}NO_3$	Al	Cl	Fe, total	SO_4	Mn^{2+}	Ni^2+	BOD
Edmonton	740000	940	n.r.	n.r.	n.r.	n.r.	n.r.	n.r.	n.r.	n.r.	n.r.	8460
Calgary[a]	767059	146	461.0	104.0	1055.4	51.6	n.r.	12.9	17245.4	n.r.	2.7	699.3
Regina	183000	26	641.3	71.8	2.6	20.5	5900	10.3	7952.1	4	<0.5	359.1
Saskatoon	200000	33	n.r.	2404	n.r.	n.r.	n.r.	n.r.	n.r.	n.r.	n.r.	2800
Winnipeg[a]	607000	122	2708	n.r.	219.8	n.r.	n.r.	n.r.	n.r.	n.r.	n.r.	2629.6

n.r..: not reported
a. Since Calgary and Winnipeg both have more than one wastewater treatment facility (two and three plants, respectively), the contaminant level totals from the different plants are summed.

Norway

The few sources of direct discharges of contaminants by industrial and mining wastes in northern Norway are listed in Table 3·4. The production and use of POPs are negligible, and most of the emissions are not discharged into freshwater systems, but directly into the marine environment or the atmosphere. Mines represent the main local sources of heavy metal pollution. Although most mines have been closed down, many of the abandoned sites are still a source of contamination. The Pasvik River on the Russian-Norwegian border is contaminated with heavy metals originating in the nickel plants of the Kola Peninsula. However, the actual amount of heavy metals discharged directly to the river system is unknown.

Contaminated effluent from coal mines and fuel tanks on Spitsbergen represent the major hazardous discharges into aquatic media. There are no other Norwegian industrial activities in the area, except for a thermal electric plant using local coal and a waste incineration plant. All of these discharges are directly to the ocean. Russia operates mines and related facilities on Spitsbergen, but no information has been provided with respect to discharges.

3.3.2.4. **Agricultural sources**

The potential for agricultural activities to act as sources for pesticides to the Arctic environment is real. The global cultivation intensity, as a percent of the total land area within each zone, is shown in Figure 3·9. Soil can serve as both a long-term and short-term storage reservoir of, for example, pesticides, if they are not degraded. There are two pathways for agricultural pesticides to be transported long distances.

Table 3·4. Large industrial plants and mines in northern Norway with emissions of hazardous substances. Estimated total yearly releases (1985 and 1993) to freshwater courses from mining areas (Source: Arnesen and Iversen 1995) and amounts discharged yearly by industries (1989 and 1993) (Source: Industrial Database, Norwegian State Pollution Control Authority).

Company	Place	Plant/mine	Operating status	Discharges, tonnes/y[a] 1985[b]/1989[c]	1993	Receiving water body
Løkken Gruber	Trondheim	Mines	Closed down 1987	48 Cu 60 Zn	18 Cu 64 Zn	Orkla watercourse
Skorovas Gruber	Namsos	Mines	Closed down 1984	12 Cu 35 Zn	5 Cu 26 Zn	Local freshwater (to Namsen River)
Elkem	Mosjøen	Aluminum plant		1 PAH	0.2 PAH 6.1 PAH	Vefsnafjord (marine) Air
Elkem	Rana	Smelting works		0.1 Cr 0.2 kg PAH Pb, Cu, Zn	<0.003 Cr^{6+}, <0.1 Cr-T, 0.05 PAH, Pb, Cu, Zn	Ranafjord (marine)
Koks-verket	Rana	Chemical industry	Closed down	18 PAH		
Sulitjelma Gruber	Sulitjelma (Fauske)	Mines	Closed down 1991	40 Cu 54 Zn	28 Cu 25 Zn	Sulitjelma watercourse

a. Unless otherwise indicated.
b. Data for mines are from 1985.
c. Data for industries are from 1989.

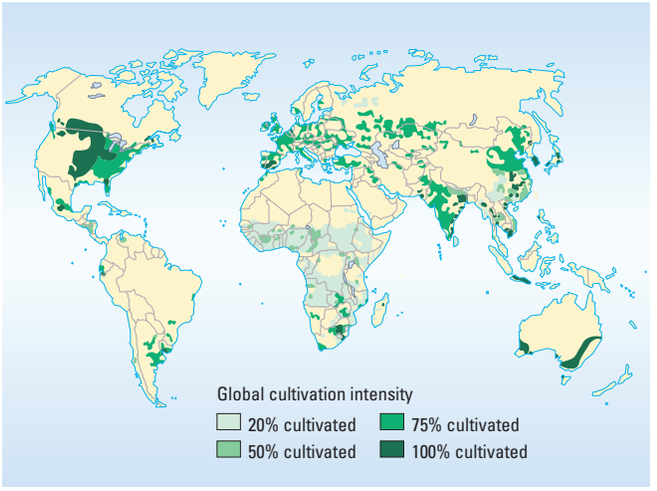

Figure 3·9. Global distribution of cultivation intensity based on a 1°×1° latitude/longitude grid (Source: Canadian Global Emissions Interpretation Center (CGEIC) 1996).

The first is via the atmosphere. Transport can occur during application and for extended periods thereafter, especially following precipitation and cultivation. The second pathway is riverine. This pathway tends to be slower, often with transport only in the spring.

While there is little agricultural activity within the boundary of the Arctic as defined for this report, the agricultural lands of the entire northern hemisphere are potential sources for atmospheric delivery of contaminants. As well, the large rivers in Canada and Russia which drain to the Arctic, often have drainage basins extending far outside of the Arctic that contain extensive agricultural activities, which represent a potential source of contaminants.

Especially noticeable in Figure 3·9 is the intense agriculture in the southern midwest of Canada which lies within the drainage basins of the Nelson River system. This river system is routinely monitored for agricultural contaminants by Environment Canada, but there has been no intensive study of the Nelson River with respect to the delivery of agricultural chemicals. Although the agricultural activity of the Mackenzie River basin is not as intensive as in the Nelson, there has been some investigation of the transfer of contaminants from the southern part of the watershed into the Arctic as part of the Slave River study. While this is considered further in chapter 6, there is little evidence of significant transport of selected current-use pesticides to the north from agricultural use areas upstream in the drainage basin (McCarthy *et al.* 1997).

Another indirect agricultural effect is the impact of reindeer farming on vegetation and erosion. Overgrazing by reindeer is an increasing problem in Norway, Sweden, Finland, and Russia. Locally, overgrazing has resulted in a total disappearance of the lichen cover (Johansen and Tømmervik 1992). This can lead to soil erosion in those areas where re-establishment of the vegetation is slow, causing mobilization of particle-bound contaminants. Quantitative data on the impacts of agricultural activity on the chemistry of the Russian Arctic rivers were not available. There are also indications that areas in North America might be overgrazed by caribou (Bergerud 1990, CAFF 1994).

3.3.3. Terrestrial processes

3.3.3.1. Snowpack and snowmelt

Although snow is just one form of precipitation in the Arctic, it merits separate discussion for a number of reasons. First, snow is an important medium for the wet deposition of contaminants in the Arctic, not only because winters are long and snow is the main form of precipitation, but also because snowflakes are effective scavengers (Gregor 1996). Nonetheless, concentrations of contaminants in the atmosphere are, on average, higher in summer than in winter (Barrie 1995 and 1996b, Pacyna 1995, Fellin *et al.* 1996, Oehme 1996). Second, the snowpack is a major storage variable in the overall water budget of Arctic systems, and contaminants accumulated in the snowpack during the winter are released to the underlying land and water during a short period of snowmelt in spring. Third, snowfall is to a large extent decoupled from the entire terrestrial compartment throughout the winter season because of frozen soil.

The measurement of snowfall quantity is difficult. Consequently, snowfall data should be used with caution as a result of problems related to the wind-induced under-catch of various instruments, the sparseness and location of the sampling network, the redistribution of snow by wind, and the effect of sublimation (Kane 1994, and see also, for example, Larson and Peck 1974, Woo and Marsh 1977, Benson 1982, Woo *et al.* 1983, Sturgess 1986, Clagett 1988, Thomsen 1994). Difficulties in snowfall measurement are illustrated for Alert, Canada in Figure 3·10. Using standard Canadian snow gauges, a large number of the days when snow did fall without wind would have actually been reported as trace quantities and not quantified, because the

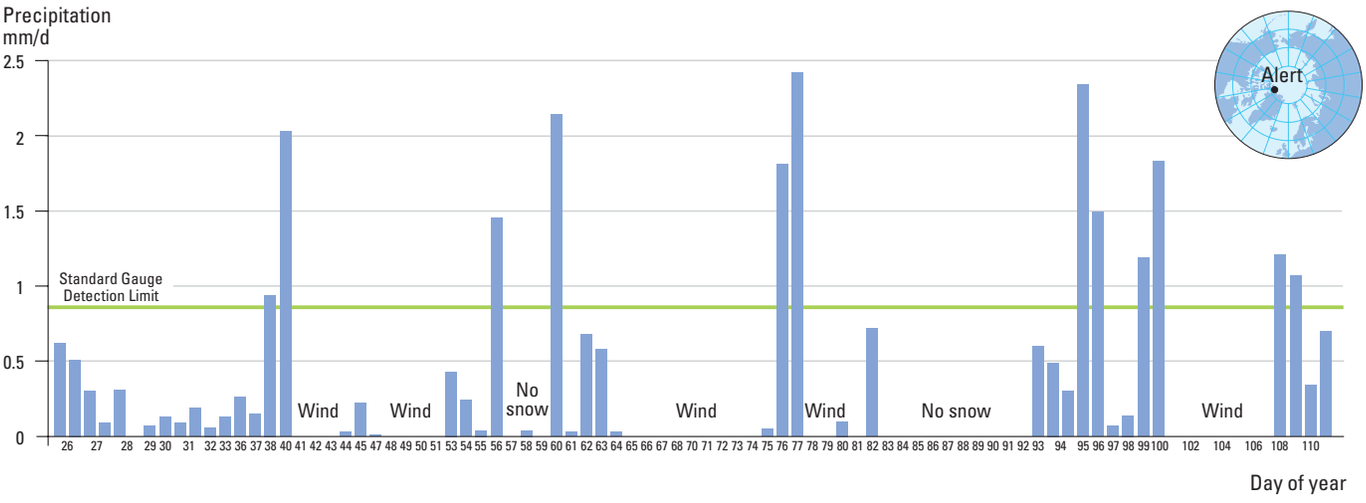

Figure 3·10. Precipitation rate measurements at Alert from January through April 1992 showing periods of no snow, periods of no snow measured due to wind events, and the relatively large quantities of precipitation on days during which precipitation rates were less than the detection limit of the standard gauge and which would normally be unreported. During periods marked 'wind', no measurements were possible due to the blowing snow (Source: Barrie 1996a).

accumulated snowfall was less than the standard gauge detection limit.

Snowpack measurements, pioneered extensively in Scandinavia and in Finland in particular, where records of snow accumulation extend back to the early and mid-18th century (Kuusisto 1994), tend to be more reliable for determining snow accumulation. Extensive research and development work into measurement techniques have been undertaken in Norway and Sweden (Bengtsson 1994, Killingtveit 1994), including the development and calibration of snow pillows (an automated system for measuring snow water equivalents), snow measurements by means of gamma radiation, and airborne surveys using surface and airborne radar and remote sensing (Kuusisto 1994).

In general, annual snowpack depths range from 20 to 40 cm in the Canadian eastern Arctic and Arctic islands and in central Siberia to several meters in Iceland, the coastal regions of Norway, and the west coast of North America (including parts of Alaska and the Yukon). This regional variability is mainly determined by large-scale meteorological patterns, proximity to relatively warm oceans, and topographical extremes (Killingtveit and Sand 1991).

Snowpack accumulation is also susceptible to mesoscale variability. Wind drift of snow is the most important process at this scale, causing scouring at exposed locations and deposition of densely packed snow at sheltered sites. Density of snow redistributed by wind ranges between 0.25 and 0.50 g/cm^3, prior to the onset of melting (Grigoriev and Sokolov 1994). The resultant snow distribution is largely related to local variation in topography (Killingtveit and Sand 1991), with the bulk of the snow accumulating in ravines and river valleys, frequently to depths of many meters, while ridges are snow free, and intermediate areas have relatively shallow snowpacks. This redistribution of the snowpack is important, because the net result is that much of the land surface area has little snowcover, which frequently sublimates, generating little or no runoff. On the other hand, deep snowpacks within the depressions and watercourses serve to retain surface meltwater, thus increasing the water content of this snowpack during the ripening stage. At spring melt, the Arctic snowpack disappears, releasing large quantities of water in a period of only a few weeks. Melt rates and total runoff are enhanced if spring melt coincides with rainfall (Woo and Sauriol 1980). In addition to the direct impacts on the hydrograph of Arctic river systems, this phenomenon influences the quantity of specific contaminants released to surface waters (see chapter 6).

The most extreme manifestation of snowpack accumulation is the development of polar and alpine icecaps and glaciers (see chapter 2). Icecaps can provide a long-term sink for snow-scavenged contaminants, while glaciers influence the hydrologic regime of rivers and can deliver snowmelt contaminants to surface waters, including oceans.

In addition to the physical weathering of snow crystals by wind transport, fresh snow crystals metamorphose as they mature. The intricate crystalline structure changes into a more compact structure because of the instability caused by large surface-to-volume ratios (LaChapelle 1969). The surface free energy of the snow crystal is reduced by transferring water molecules through the vapor phase to achieve a structure that is rounded and more compact. This process, referred to as destructive metamorphism, occurs in the absence of any temperature gradient within the snowpack and is most rapid near the freezing point. The rate diminishes with temperature, and below –40°C, it does not occur (LaChapelle 1969).

The erosion of surface snow occurs when the shear force at the air/snow interface exceeds the inter-particle cohesive forces and particle inertia. The two primary modes of snow transport are saltation and suspension. Saltation is a near-surface phenomenon that occurs at low wind speeds, while suspension can disperse snow to heights of tens of meters and dominates as wind speed increases. Blowing snow grains become fragmented during collision with other particles or surface snow and may experience sublimation during suspension (Pomeroy *et al.* 1991). Franz *et al.* (1996) noted that to their knowledge the effect of wind transport on retention or, conversely, volatilization of contaminants, has not been investigated. As noted by Pomeroy *et al.* (1991), sublimation may increase the chemical concentration of the blowing snow if the contaminants do not volatilize while being blown about as has been observed for conservative substances including acids. Volatilization of semivolatile OCs may be attributable to the reduction in crystalline surface area that begins to occur immediately upon deposition of contaminants (Gregor 1996). While additional scavenging may occur during suspension as the snow grains encounter atmospheric vapors and particles, it is not likely to offset the loss resulting from the reduction of surface area.

During spring melt, percolation of meltwater through the snowpack preferentially elutes soluble compounds from the snowpack. Volatilization to the atmosphere may occur at this time due to both the continued metamorphosis of the snowpack reducing surface area and the warming temperatures. However, it has been suggested that deep snowpacks are able to retain volatile contaminants, such as HCHs, more effectively than shallow snowpacks (Semkin 1996). In addition, degradation of compounds, such as PAHs, may occur in the snowpack as a result of photolysis or through liquid phase reactions with hydroxyl radicals (Jaffrezo *et al.* 1994).

Chromatographic fractionation of contaminants in the snowpack occurs by meltwater percolation that preferentially elutes soluble compounds, leaving residues that are less soluble or bound to solid surfaces within the snowpack. For inorganic ions, the initial 20-30% of meltwater may remove 40-80% of the snowpack chemical burden (Johanessen and Henriksen 1978, Davies *et al.* 1982, Cadle *et al.* 1984a, Cadle *et al.* 1984b, Brimblecombe *et al.* 1985, Tranter *et al.* 1986, Brimblecombe *et al.* 1987, Williams and Melack 1991). The scavenging processes responsible for incorporating atmospheric contaminants into snow influences their elution from snowpack (Tsiouris *et al.* 1995). Soluble contaminants scavenged during snowfall by attachment to the surface of the crystal are more available for removal during the initial melting period than soluble contaminants within the crystal.

Fractionation of organic compounds (such as PAHs, OCs, etc.) depends upon their solubility and dissolved particle partitioning behavior. Relatively soluble compounds (e.g., HCHs) may be enriched in initial meltwaters, whereas those that are adsorbed to particles (e.g., PCBs, PAHs) may remain in the snowpack (Schöndorf and Herrmann 1987). The Amituk Lake study in the Canadian Arctic Archipelago (Semkin 1996, Barrie *et al.* 1997) has shown that most OCs left in the snowpack immediately prior to melt enter the lake in streams experiencing little snowmelt-soil interaction, and leave in the river outflow. The exception was PCB which showed 40% retention in Amituk Lake. Mercury cycling was similar to that of a volatile OC. Post-depositional and snowmelt processes of semivolatile contaminants in snowpacks require extensive and careful experimental design and interpretation of results to adequately quantify contaminant loads to surface waters (Franz *et al.* 1996, Barrie *et al.* 1997).

The transport and migration of compounds through the snowpack is highly dependent on the 'premelt' condition of the snow. Shallow snowpacks exposed to above freezing

temperatures may show extensive fractionation of contaminants by meltwater elution. Deep snowcovers, however, may retain most of the meltwater either within the snowpack or within ice lenses that form at depth, thus delaying the meltwater wave front from exiting the snowpack until extensive melting has occurred (Franz *et al.* 1996). Arctic snowmelt chemistry is further complicated by the presence of permafrost which can refreeze meltwaters, creating a basal ice layer. Refreezing of early meltwater can delay the release of the more water-soluble compounds to surface flow until late in the melting cycle. Particulate matter may also accumulate in the lower portions of the snowpack by filtration through less permeable bottom snow. Permafrost also channels more snowpack contaminants into runoff, preventing interaction with soil.

The snowpack also has a direct influence on the biological cycle of Arctic freshwater systems. The combination of accumulated snowpack and the reduced sunlight during the winter season combine to make light the limiting factor for biological productivity. Even with increased light in the spring, the snowpack on the river and lake ice surface effectively reduces light penetration (Prowse and Stephenson 1986). Light remains limiting until the surface snow melts after which biological productivity increases and frequently reaches a maximum while the ice surface is still intact.

In summary, snowpacks reflect the net influence of deposition (wet and dry) and post-deposition processes; consequently, for semivolatile substances, snowpack measurements cannot be employed to monitor atmospheric deposition. Nevertheless, snowpacks can be useful to assess net deposition. Snowpack chemistry surveys can also be used to examine regional variations in deposition, provided that diagenetic processes (i.e., post-depositional chemical changes) are assumed to be similar in magnitude among regions. Such surveys may yield information on atmospheric transport and help determine the relative source strength of atmospheric contaminants to which an area is exposed (Franz *et al.* 1996).

3.3.3.2. **Terrestrial drainage systems**

Snowmelt and rainfall, and any associated contaminants, are delivered to the surface waters directly or become part of the terrestrial drainage system. Terrestrial drainage introduces a significant lag time into the transfer of the water and depending upon the nature of the subsurface material, can greatly influence the water chemistry. As well, transport through the porous subsurface media can result in losses and/or gains of contaminants. This discussion will consider the influence of bedrock geology, surficial geology, soils, and permafrost on groundwater and drainage water. Drainage water is defined here as the part of the groundwater which drains to a river.

Geology influences natural water chemistry and runoff yield principally through the magnitude of storage potential and related water transmission properties. In the Arctic, subsurface storage and transmission properties are further complicated by the presence of permafrost. Permafrost can influence infiltration, surface and subsurface storage, and transmission of water.

With respect to surficial geology, which includes the soils that have developed on the parent material, the infiltration rate into unfrozen, unconsolidated surface layers is complex and dependent on a number of variables, including vegetation cover, particle size distribution, porosity, layering, soil packing properties, and organic matter content (Gray *et al.* 1973). Thus, while generalized maps showing topography and surficial geology of the entire Arctic region are provided in chapter 2, it is not possible to generalize the impact of surficial and bedrock geology on runoff and infiltration, due to the heterogeneous nature and complex interaction of variables that determine these processes in large Arctic watersheds. The integrated effect of physical controls on runoff in large watersheds is illustrated by a comparison of hydrographs for northern rivers (see section 3.3.4.1).

Just as unconsolidated material has different infiltration and transport coefficients, so does bedrock. Generally, bedrock aquifers are found in sedimentary sandstone formations and in limestone and dolomite. Limestone and dolomite may be especially important due to the dissolution of the rock by water, which opens up joints and fractures, thus increasing the permeability and storage capacity. Sandstone, which is either interbedded with shale or highly cemented, has low hydraulic conductivity, and is thus less important as a groundwater aquifer. Similarly, most igneous and metamorphic rocks have low hydraulic conductivities and limited storage potential except along fracture zones. Bedrock aquifers have generally not been well documented in the Arctic region, since surface aquifers have been adequate to meet water demands. The exception is Iceland where aquifers form in highly permeable lava (Elíasson 1994).

The amount of water available for groundwater movement is restricted by low precipitation over large areas of the Arctic. Active layer (i.e., the upper soil layer which seasonally melts) thawing and water drainage may only occur during as little as two months of the year. The base flow in streams without lake storage in their drainage basins consists primarily of the discharge of groundwater. In the zone of discontinuous permafrost, the contribution of groundwater to base flow ranges between 2 and 5 L/s/km^2 (van Everdingen 1990). In the zone of continuous permafrost the winter base flow approaches zero. Only 10-19% of the snowpack volume adds to the moisture of the underlying soil (Kane *et al.* 1991), and may, under the right geomorphological circumstances, be transported as drainage water. Horizontal and vertical drainage intensities are low in areas with low relief and permafrost layers close to the surface.

The role of lakes in influencing groundwater is important due to the suppression of permafrost beneath the lake (i.e., talik). Based on a study of a small watershed in the northeastern Canadian Arctic (62°41'N, 97°03'W), which is underlain by continuous permafrost, it has been estimated that snowmelt runoff accounts for 45% of the total annual runoff, which is largely the proportion of annual precipitation represented by snow. This is a result of the restricted infiltration of snowmelt into the frozen active layer (Bursey *et al.* 1991). Depending on the saturation state at freezing the previous fall, some snowmelt will penetrate the frozen ground, and remain in temporary storage. Groundwater flow becomes progressively more important as the frost table declines, releasing stored water and increasing the capacity to accept recharge from summer rain. Peak groundwater flow is probably attained by late August and slowly diminishes through September. Bursey *et al.* (1991) estimated that groundwater comprises 55% or more of the average annual water balance for this site. These subsurface waters are a mixture of ground-ice melt derived from late season rain of the previous year, rainfall from the current year, and local recharge from streams and ponds. Farther north, the role of groundwater in lake water budgets decreases, while larger lakes may have a greater contribution from groundwater due to the larger talik beneath the lake.

The physical and chemical characteristics of groundwater in the permafrost region of the Yukon and NWT (van Ever-

dingen 1990) are similar to those in non-permafrost areas. Limited data from Russia (Runnells *et al.* 1992) support this. The chemical composition of suprapermafrost water (drainage water in the active layer, undergoing seasonal freezing) reflects the influence of rainfall, snowmelt, and surface runoff. This water is often characterized by a high organic content (humic acid) derived from the peat substrate. Where there is a strong influence of intra- and subpermafrost water, the concentration of dissolved solids can be extremely high (van Everdingen 1990). In areas rich in mineral deposits, natural concentrations of metals in the characteristic acidic stream waters and shallow groundwater may be naturally high (Runnells *et al.* 1992).

The ion chemistry of Arctic rivers is strongly influenced seasonally through the proportional increase in the contribution of groundwater. Groundwaters have a different hydrochemical composition to that of surface waters. For example, during the greater part of the year, bicarbonates and calcium ions predominate in the lower reaches of the Lena River. However, during the winter period, when the concentration of dissolved solids exceeds 250 mg/L, Lena River waters are transformed to a chloride class, with sodium and potassium ions dominating calcium. This is due to the increasing influence of groundwater input. The chemical composition of the groundwater is controlled mainly by the widespread limestone and dolomite deposits in the upper and middle reaches of the river (Gordeev and Sidorov 1993).

Contaminants originating from rainfall, snowmelt, and surface runoff might be present in the active layer (suprapermafrost water). The transport of contaminants by drainage water is probably very limited, owing both to the strong association of many of these compounds with organic matter or particles, as well as to the seasonally short and restricted water flow through an often thin active layer. Hardisty *et al.* (1991) reported no known cases of groundwater contamination in the Canadian Arctic.

In summary, processes and levels of contamination of drainage waters and their discharge to Arctic rivers have rarely been studied. The variables controlling the transport and fate of contaminants in surface waters (such as pH, organic matter, ions, etc.) also influence drainage waters, but these processes and the overall extent or potential for contamination of Arctic groundwater have apparently not been investigated. This is not surprising, at least for the Canadian Arctic, due to the sparse population and limited industrial development in the region, although this may not be the case in some parts of Scandinavia and Russia.

3.3.3.3. **Wetlands**

The term 'wetland' is commonly used for a large variety of biotopes, including freshwater meadows, salt marshes, reed swamps, bogs, ponds, shallow lakes (depth below 2 m), and tidal and some other coastal zones (Cowardin *et al.* 1979). Their nature and distribution in the Arctic have been discussed in chapter 2.

Deposition of contaminants from the atmosphere, along with direct discharges from mining, oil and gas extraction, and other industry and urban wastes in the Arctic may contribute to the accumulation of significant amounts of contaminants in wetlands. Wetlands may serve as sinks for contaminants, and in turn, become sources of secondary contamination through indirect discharges to river systems. Contaminants can be carried into wetlands by flooding waters. The frequency and velocity of flooding is important in determining the total amount of contaminants in wetlands and their availability for flora and fauna (Gosselink and Turner 1978).

The flows of melt and rain water from palsas and polygons are mainly filtered through the active layer. Swamp water flows down inter-polygonal cracks and discharges to rivers and lakes. Wetland runoff is characterized by permafrost, a prolonged seasonal frost, a shallow active layer, rapid and considerable release of snowmelt water, limited groundwater capacity, and the prevalence of surface flow on wetlands. The frozen condition of wetlands during the spring impedes infiltration of snowmelt water, resulting in a rapid increase to maximum surface flow across the wetlands. Later, when the active layer thaws and water recedes, the water-retention capacity increases and summer flows are leveled out (Woo 1992). There is no water discharge from swamps during the winter period.

Ombrotrophic bogs receive water only from rainfall and snowfall, there being no exchange of material with groundwater. The water is nutrient poor, contains low levels of dissolved solids and becomes acidic in contact with peat (Lockhart *et al.* 1992). Hence, cores or samples from ombrotrophic bogs can be very appropriate for the measurement of the deposition trends of organic contaminants from the atmosphere, though little work has been completed using this natural archive.

Minerotrophic bogs, receiving water both from rain and from surface runoff, contain mineral-rich waters, and the water is less prone to acidification in contact with peat (Gosselink and Turner 1978). In general, however, Arctic wetlands are characterized by a very low pH value (3-5.5). There does not seem to be any information available on the overall effect of these natural water quality attributes on the degradation and transformation of contaminants.

The volatilization of hydrophobic contaminants is probably limited from wetlands, compared with clear water lakes under similar climatic conditions, because wetlands are rich in organic matter, which binds hydrophobic contaminants. On the other hand, Bursey *et al.* (1991) have shown that wetlands can have high evaporation losses, of the order of 40% of the total runoff from the area, which may result in revolatilization of more water-soluble compounds.

In addition to the input of contaminants from the atmosphere, wetlands are also subject to local activities with associated contamination risks, such as mining, pipeline operations, and facilities for petroleum exploration. Some examples are outlined below.

Oil and gas extraction activities have led to significant contamination of vast areas of adjacent land containing wetlands, as is the case in northwest Siberia. In this area, a wide range of contaminants are discharged, both through natural seeps (typical for oil and gas deposits) and through extraction, processing, and transportation activities. These wastes are usually discharged in an untreated condition into natural depressions in the landscape. Under northern temperature conditions, the decay rates for many organic contaminants are likely low. Horizontal and vertical drainage rates are also low in these areas due to the relatively flat land and the closeness of permafrost to the surface. This is probably a positive situation, as the contaminants would tend to remain concentrated in a localized area rather than being spread horizontally and vertically. However, it is expected that in the areas surrounding oil and gas extraction activities, polluted wetlands can represent long-term sources of secondary contamination of surface waters, even after cessation of the extraction activities, particularly during seasonal and rain-induced floods.

Large areas in northeast Canada and Alaska are dominated by lakes and rivers surrounded by land saturated with water, forming different types of wetlands. The small amount

of industrial development in the Canadian Arctic is likely indicative of minor anthropogenic input to wetlands except in the local vicinity of DEW Line military sites (see chapter 6).

In Alaska, more than 40 placer gold operations exist, mainly on previously mined tailings in and along the wetlands and riparian habitat areas. Aside from the obvious physical disturbance of the surficial material, there is no information on significant emissions.

3.3.4. Aquatic processes

3.3.4.1. Hydrology

River systems are a major pathway for contaminants from the Arctic terrestrial compartment to the oceans, as a result of snowmelt runoff in addition to contaminants from local sources. In general, the quality of river waters is highly dependent on the water flow regime. Many dissolved components tend to be diluted during high flows, whereas particulate matter and associated contaminants tend to increase with water discharge. Discharge is a major factor in assessing environmental quality, as the load of contaminants to a receiving water body will increase with discharge even for chemical constituents that are diluted (Meybeck *et al.* 1989). Consequently, it is necessary to consider the hydrology of Arctic river systems in some detail. Throughout most of this chapter, the emphasis is on large rivers. However, as it is the large land area and the strong influence of snowmelt that feeds these rivers and dominates the hydrologic cycle, it is also necessary to consider the hydrology of smaller rivers and headwater systems as part of the total hydrologic regime.

Rivers in the AMAP region can be classified into those that originate in the Arctic region (referred to here as Arctic rivers) and those that have headwaters in the subarctic, boreal, or temperate zones (e.g., Mackenzie River in Canada and the large Russian rivers including the Ob, Yenisey, Lena, etc.). These large rivers, which originate outside of the Arctic and which are referred to here as Arctic drainage basins, have different flow regimes than Arctic rivers and have often been significantly modified by impoundments and diversions. Arctic rivers, on the other hand, tend to have a short flow season, concentrated within the brief spring and summer periods and with little or no flow during the long, cold winters. These rivers are very responsive to snow and ice melt events and rainfall due to the presence of relatively impervious permafrost and a shallow active zone (Woo 1992), resulting in highly episodic flow regimes.

The discharge of a river system depends upon the water gains and losses within the basin and can be summarized by the water balance relationship:

$$Q = P - E + \Delta S$$

which partitions precipitation (P) into runoff (Q), evaporation (E), and a change in basin storage (ΔS) be it in the form of snow and ice, soil moisture and groundwater storage, or retention in lakes and wetlands. Annual snow storage changes are particularly significant in the Arctic, with snow accumulations in winter causing an increase in basin storage followed by storage depletion in spring and summer (Woo 1992). Arctic rivers are likely to have a higher unit area yield of runoff, relative to the amount of precipitation, than do the Arctic drainage basins, due to the limited infiltration capacity of frozen soil. In general, the surface runoff in Arctic river basins is relatively low compared to the mean global surface runoff. For example, the mean runoff in the Russian Arctic is 7 L/s/km^2, versus 10 L/s/km^2 on a worldwide basis (WHO/UNEP in press).

Little is known about the rate of snow sublimation which can cause a moderate amount of snow loss relative to the total snowpack (Woo 1992). Evapotranspiration can be significant in the summer, ranging from about 150 mm/y in the northeastern Canadian Arctic to >200 mm/y in the Mackenzie Valley and the Yukon. In a single watershed in the eastern Canadian Arctic, it has been demonstrated that there can be a wide variation in the degree of evaporation from various levels of the drainage system. For example, evaporation can account for 40% or more of the discharge from shallow tundra ponds, whereas the average annual vapor discharge from the entire watershed is likely about 10%. Evaporative losses are minimized in part by the relative importance of subsurface storage and flow within the active layer (Bursey *et al.* 1991). Evaporation is greatest in the early summer, immediately following the spring snowmelt, during the period with maximum radiation, but not necessarily the maximum air or soil temperatures (Kane *et al.* 1990). Analysis of stable hydrogen and oxygen isotope composition in northern Alaska revealed that evaporation from soil, vegetation, stream flow, permafrost, and snowcover is also a critical factor in the hydrological cycle (Cooper *et al.* 1993). Studies carried out over a five year period indicated that of the original snowpack water volume in the catchment, snowmelt runoff amounted to 50-66%, 20-34% evaporated directly, and only 10-19% remained in the soil (Kane *et al.* 1991).

The measurement of precipitation, especially during the winter season, is believed to be the most significant source of error in applying the water balance equation to Arctic sites, requiring positive adjustment by up to 100% (Haas 1991) (see also section 3.3.3.1).

Headwater systems

Streamflow regime is defined by the average seasonal pattern of runoff, as determined by the timing and quantity of water supplied to, or lost from the basin, as well as by the storages which modify water delivery from the basin to its channels. Streamflow is also affected by in-channel attributes, including the formation and dissipation of river ice, flow blockages by deep snow accumulation in the channels, or transit across wetlands and lakes (Woo 1992).

Most rivers in areas of continuous permafrost exhibit an Arctic nival regime (Church 1974) with pronounced spring high flow generated by snowmelt. During this period, streamflow in headwater streams follows prominent diurnal cycles, which lag the daily pattern of incoming solar radiation. This pattern is illustrated in Figure 3·11. Spring floods are accentuated by snow dams along the channels formed by the redistribution of the snowpack by wind (Woo and Sauriol 1980). These dams temporarily block the flow of water until the dams are breached, resulting in a high flow pulse. After a major flood, generally of several weeks duration, runoff recedes rapidly, being sustained by melting of the deepest snow accumulations and ground ice in the active layer. Rainfall during this time can result in significant peak flows due to the limited infiltration capacity of the active layer. Flow ceases in most small rivers by early fall as a result of the lack of available groundwater to maintain base flow as the active layer begins to freeze and precipitation changes to snow. Small and many medium-sized rivers freeze to the bottom during the winter season, resulting in no flow for several months.

Basins draining glaciated regions display a proglacial flow regime (Church 1974). As illustrated in Figure 3·11, spring snowmelt in the basin is superseded by high flows from glacier melt, with the discharge often related again to the energy input to the glacier. Melt runoff can be considerably reduced

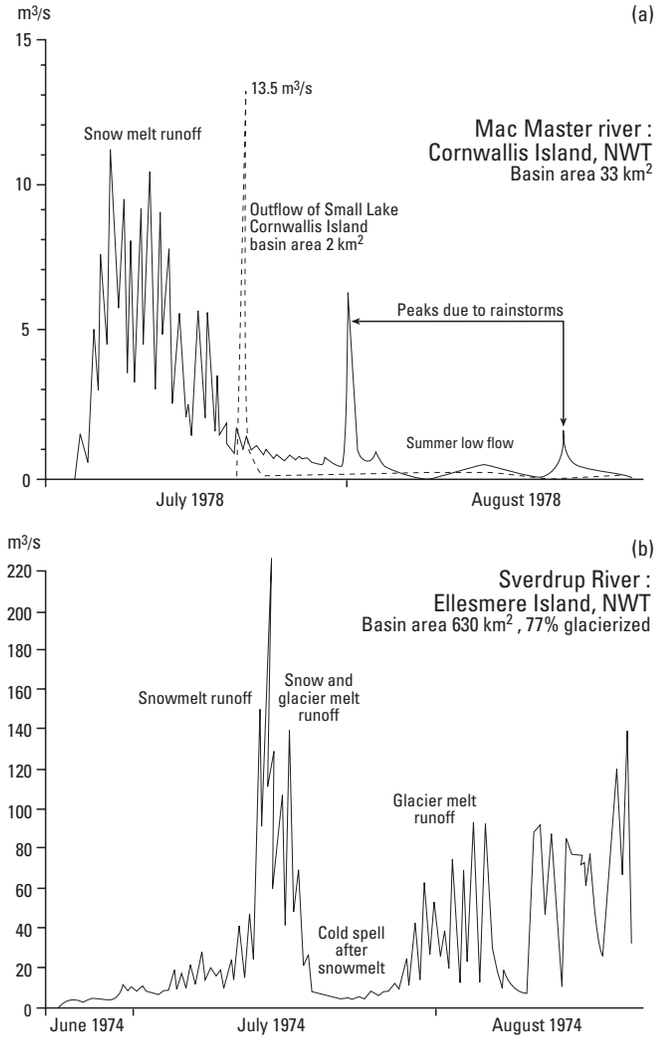

Figure 3·11. Hydrographs showing two types of streamflow regimes for Arctic rivers: a) Arctic nival regime and b) proglacial regime (Source: Woo 1992).

by overcast conditions or periods of cold weather. From time to time, small glacial lakes may be breached, causing periodic high flows.

Streams flowing through wetlands acquire a wetland or muskeg regime, which is typified by little or no winter flow, followed by a spring snowmelt freshet when surface runoff sweeps across the frozen ground with little infiltration (Woo 1992). Once the wetland starts to thaw, the uneven ground contains a high degree of storage, and thus, even the response to rainfall is attenuated by poor drainage and by water retention in ponds and peaty soils. Normally, the shallow thawed layer does not yield much drainage water, thus restricting the amount of summer flow (Woo 1992).

Large river systems

The hydrologic regimes of large river systems reflect the climate and physiography of the total watershed, as well as the nature of the river (i.e., reservoirs and lakes). As a result, large river systems tend to have a less well-defined hydrograph pattern. A unique feature of some of these large rivers is that because they flow north, their headwaters generally melt first. Thus, the peak flow is transferred downstream often resulting in a hydrograph significantly dominated by snowmelt, which will have taken several weeks to progress from the upstream areas, during which time downstream snowmelt will have supplemented the flood crest. This is well illustrated for the Mackenzie River in Figure 3·12.

Examples of annual hydrographs are provided in Figure 3·13 (next page) for a number of Arctic rivers. Rivers having a characteristic Arctic hydrograph, that is, very low flows during the winter and a spring snowmelt dominated by a peak discharge include: the North Dvina, Mezen, Pechora, Ob, Yenisey, and Lena Rivers in Russia; and, the Back and Caniapiscau Rivers in Canada. The Khatanga, Olenyok, and Indigirka Rivers in Russia form a special subset of this group, as they freeze entirely during the winter, resulting in negligible flow. During the flood period, which usually happens in June-July, these rivers discharge more than a half of their annual water flow. For example, average June discharge of the Olenyok River (Laptev Sea basin) is 60% of the annual discharge (see Figure 3·13).

Many of the Canadian rivers retain relatively higher flows during the winter season than do the Russian Arctic rivers, and thus, the spring peak is less dramatic. This is due to the large storage capacity of lakes within these systems. These rivers include the Mackenzie, Coppermine, Kasan, and Hayes Rivers. The remaining group, which includes the Churchill, Nelson (see Figure 3·13), Rupert, and Grande Baleine Rivers are indicative of systems which: 1) have largely temperate and/or subarctic watersheds; 2) have a large natural storage capacity; and, 3) demonstrate the additional influence of flow regulation by controlled releases from reservoirs.

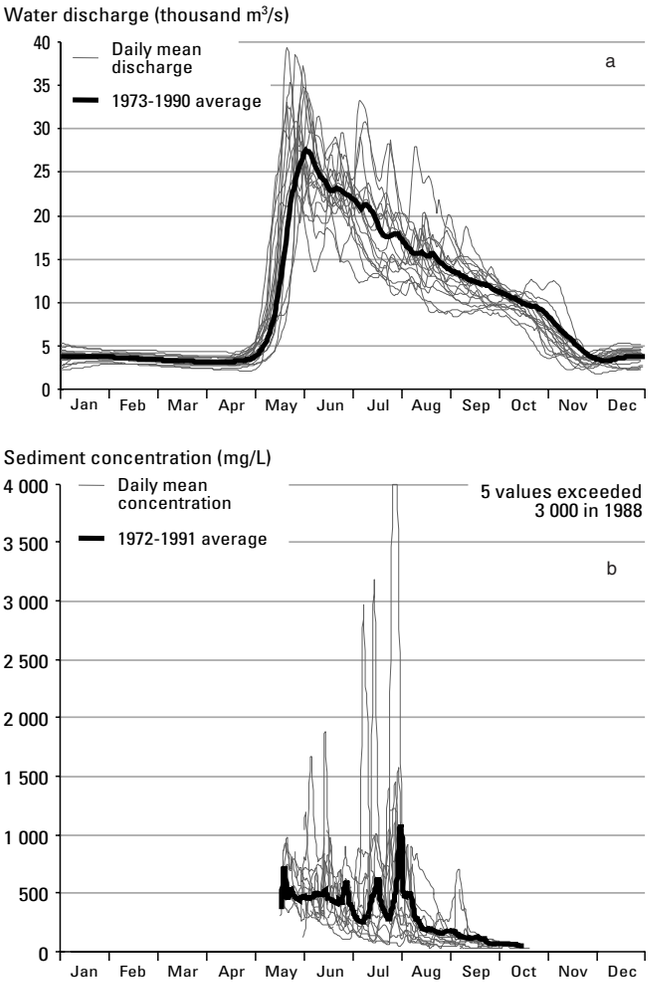

Figure 3·12. a) The annual (1973-1990) and mean annual hydrographs for the Mackenzie River above the Arctic Red River, NWT, Canada, indicating the dominance of the spring freshet in May. b) Daily suspended sediment concentrations (mg/L) and mean annual suspended sediment concentrations (1972-1991) for periods of high flow and high sediment concentration in the Mackenzie River above the Arctic Red River (Source: HYDAT 1994).

Hydrographs of Russian Arctic rivers

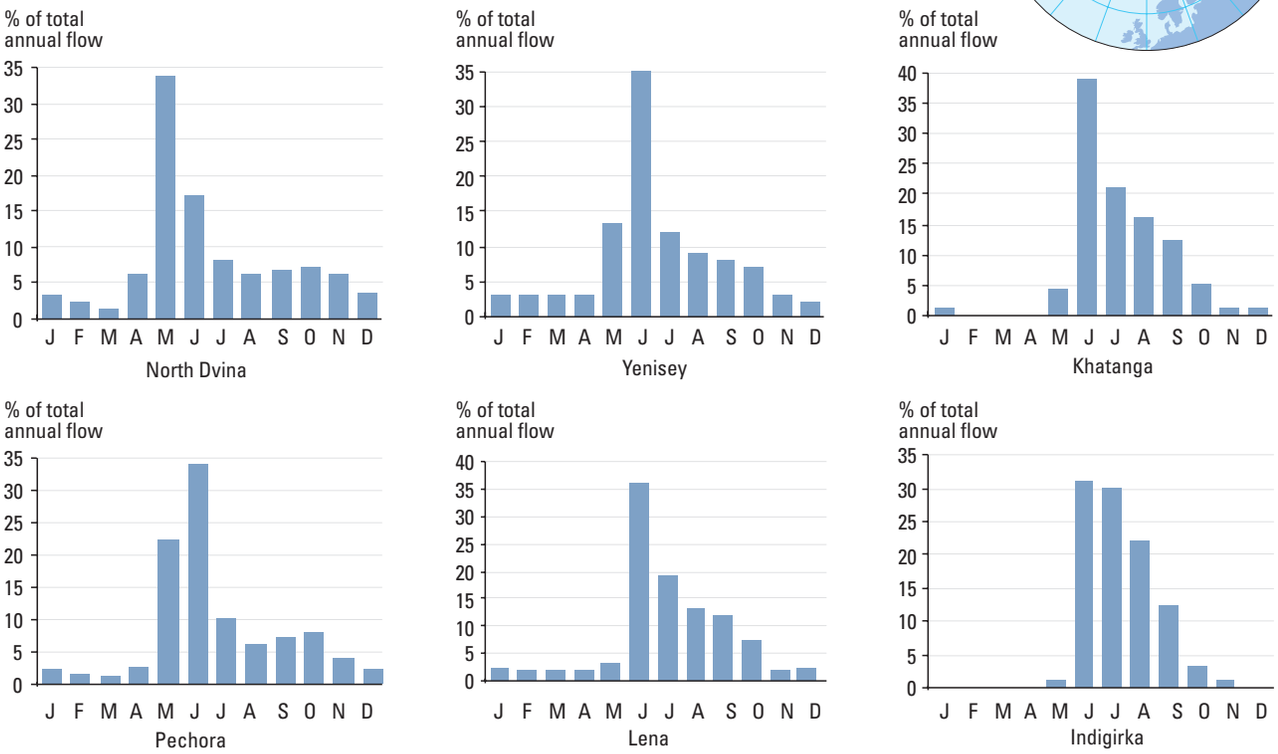

Hydrographs of Canadian Arctic rivers

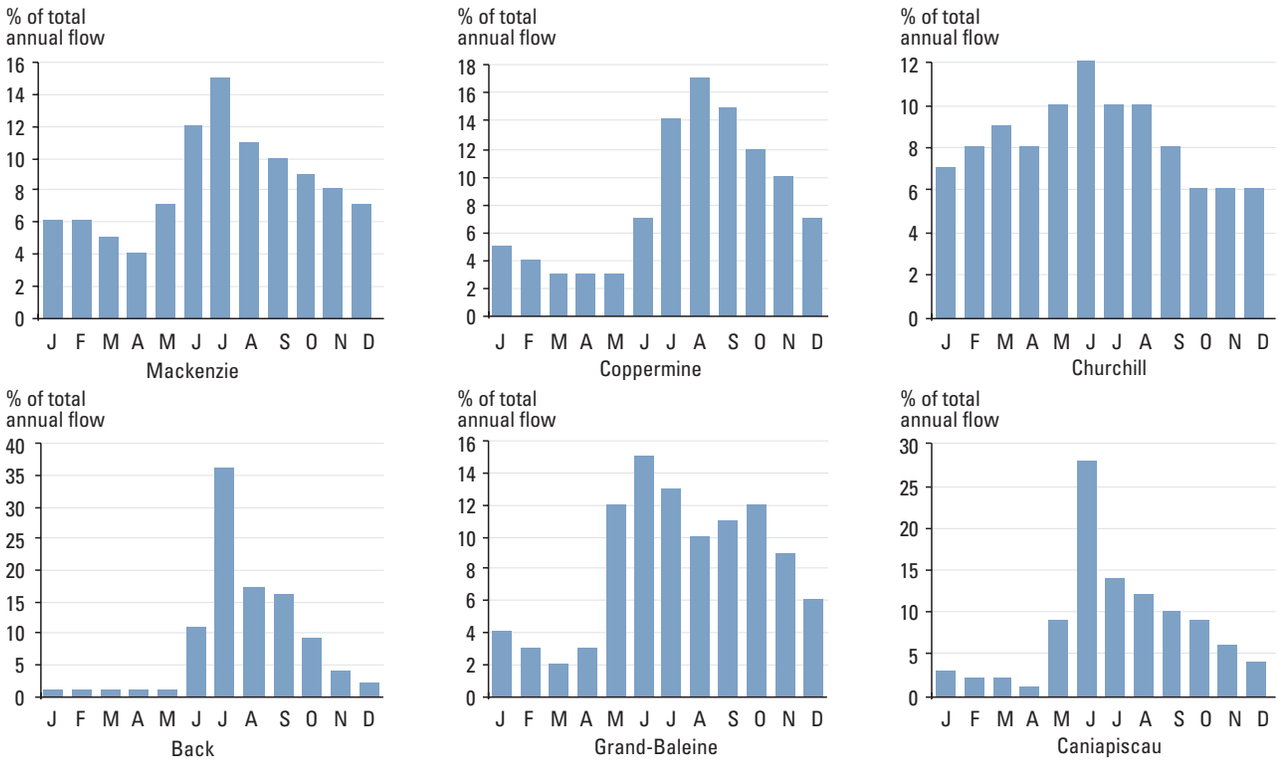

Figure 3·13. Monthly mean discharge expressed as a percent of annual discharge from available data for selected Russian and Canadian rivers draining to the Arctic (Source for Canadian river data: HYDAT 1994).

Table 3·5. Summary of selected physical and chemical characteristics of major lakes and reservoirs.

Lake (L.) /Reservoir (Res.)	Surface area, km^2	Volume, km^3	Maximum depth, m	Mean depth, m	Drainage area, 10^3 km^2	Residence time, y	Transparency, m	DO, mg/L	pH	TDS, mg/L	Suspended solids, mg/L
Russia											
L. Baikal[a]	31500	23000	1741	740	560	–	~5-23	9.6-13	6.8-8.5	–	–
Krasnoyarskoye Res.[a]	2000	73.3	105	37	28700	0.81	1.2-6.0	7.7-14.2	7.2-8.4	–	–
Uste-Ilimskoye Res.[a]	1920	58.9	97	30.7	785080	0.58	2.3-4.1	2.7-16.4	7.8-7.5	–	–
Bratskoye Res.[a]	5478	169.3	150	31.1	757200	1.8	2.6-11.0	9.2-14.2	7.1-8.9	–	–
Canada (within Arctic)											
Great Bear L.[b]	31153	2236	446	71.7	114717	124	20-30	Saturation	7.8-7.9	78-81	–
Great Slave L.[c]	28600	–	614	41	–	–	<1.0-17	Saturation	6.6-6.9	22-150	–
Hazen L.[e]	541.8	–	280	–	–	–	–	10.41-15.11	–	–	–
Dubawnt L.	3830	–	–	–	–	–	–	–	–	–	–
Laberge L.[d]	201	10.8	146	54	3500	1	4-11	9.7-11.6	7.7	–	–
Atlin L.[f]	588	–	283	85.6	–	–	10	9.7-9.9	7.5	–	–
Marsh L.[f]	64.5	53	–	–	–	–	5	–	–	–	–
Tagish L.[f]	340.8	214	–	–	–	–	1.0-6.1	–	–	–	–
Canada (within drainage basins draining into Arctic)											
Winnipeg L.[e]	23750	284	36	12	953250	2.9-4.3	0.35-2.0	–	8.1-8.4	–	–
Reindeer L.	6650	–	–	–	–	–	–	–	–	–	–
L. Winnipegosis	5370	–	–	–	–	–	–	–	–	–	–
L. Athabasca	7940	–	–	–	–	–	–	–	–	–	–
S Indian Res.[g] (Churchill)	2391	23.4	–	9.8	242	0.72	–	–	–	–	1.2-11.0

Data sources: a. ILEC 1993; b. Johnson 1975a; c. Rawson 1947, 1950; d. Gray *et al.* 1992; e. Allan *et al.* 1994; f. Lindsey *et al.* 1981; g. Newbury *et al.* 1984.

3.3.4.2. **Lakes and reservoirs**

Arctic lakes and reservoirs, like those in temperate climates, reflect loadings of contaminants supplied by the rivers and streams flowing into them, as well as exchanges of contaminants directly with the atmosphere at the lake surface, the bottom sediments, biota, and subsurface drainage. Most Arctic lakes were formed recently following the retreat of glacial ice, and, in contrast to temperate lakes, permafrost plays an important role, in that it controls the depth of the active layer and thus, the groundwater in the vicinity of lakes.

Few large Arctic lakes have been studied in detail. Johnson (1975a, 1975b) described the physical and biochemical limnology of Great Bear Lake in the Mackenzie River basin in Canada (see Table 3·5) between 1963 and 1965. Great Slave Lake (also in the Mackenzie River system) was studied extensively by Rawson during the summers of 1944 and 1945 (Rawson 1947, Rawson 1950), but has not been studied since. The characteristics of Great Slave Lake are more complex than Great Bear Lake, as the former receives turbid water from the Slave River, which mixes into the western part of the lake to a distance of about 40 km from the delta (Mudroch *et al.* 1992). In 1994/95, an investigation of the biomagnification of POPs in the Great Slave Lake system was initiated by Evans (1996) (see chapter 6). Lastly, Lake Hazen on Ellesmere Island in the Canadian Arctic, the largest and most northern Arctic lake, was studied in the 1960s and 1970s (Hunter 1960, McLaren 1964, Johnson 1994b).

Several studies have investigated the limnology of Yukon Territory lakes (Lindsey *et al.* 1981). Four of these lakes, Atlin, Laberge, Marsh, and Tagish, were investigated in greater detail in 1982 and 1983, in an effort to understand better the processes controlling the limnology of these lakes, and to assess the effect of potential developments within the basin (Kirkland and Gray 1986, Gray 1994). These authors concluded that the biological productivity in these lakes is nutrient limited, the optimal time for algal uptake of nitrate being between snowmelt and ice-out, when there is adequate light and an absence of wind-induced mixing. As an example of this, Shortreed and Stockner (1986) observed that chlorophyll levels under ice were higher than average summer chlorophyll in 5 of 10 Yukon lakes sampled. Production under ice has also been indirectly measured by dissolved oxygen (DO) concentrations in both Arctic rivers and lakes (Albright *et al.* 1980, Schreier *et al.* 1980, Prowse and Stephenson 1986, Whitfield and McNaughton 1986). The phenomenon of biological productivity in Arctic lakes occurring in the spring and being controlled by the light penetrating a stable ice cover after snowmelt is likely typical of many Arctic lakes. Recently, the biomagnification and fate of POPs in Yukon lakes have been investigated for Lake Laberge and other Yukon River system lakes (Kidd *et al.* 1996, Lockhart and Muir 1996) (see chapter 6), but whether or not the timing and physical processes associated with the period of maximum productivity plays an important role in the fate of contaminants delivered to these lakes has not been considered.

Hydroelectric power production on Arctic rivers and within Arctic drainage basins has produced large reservoirs in both Canada and Russia (see Table 3·5). Reservoirs significantly change the hydrologic regime of rivers, intercept the sediment load, and can affect the river ecology through interrupting species migration and increasing contaminant concentration (e.g., mercury). Also, the loss of waterfalls and rapids can greatly reduce the natural aeration of the waters and increase ice coverage. In turn, this could result in increased contaminant concentrations under the ice due to reduced exchange with the air (Dynesius and Nilsson 1994).

Reservoirs can have a significant effect on downstream temperatures. The storage and release of large quantities of water at about 4°C throughout the winter can keep the reaches immediately downstream of the reservoir free of ice and retard the formation of ice cover farther downstream. Even ice cover type and the nature of its hydraulic effects can be modified. Further, the dam virtually eliminates the supply of ice to the downstream river reaches from the reservoir and upstream. Fluctuating flows caused by releases from the reservoir can result in increased ice thicknesses as a result of surface ice overflows or they can induce premature ice break-up during the winter. The magnitude of the effect of regulation on spring break-up varies according to the ratio of the regulated flow to the total river discharge. Depending on this ratio, break-ups and associated ice-jam flooding could be more or less severe compared to unregulated conditions (Prowse and Conly 1996).

The generation of hydroelectricity from the Churchill-Nelson River systems (in Manitoba, Canada) began in the 1950s. The first reservoir on the Nelson River was com-

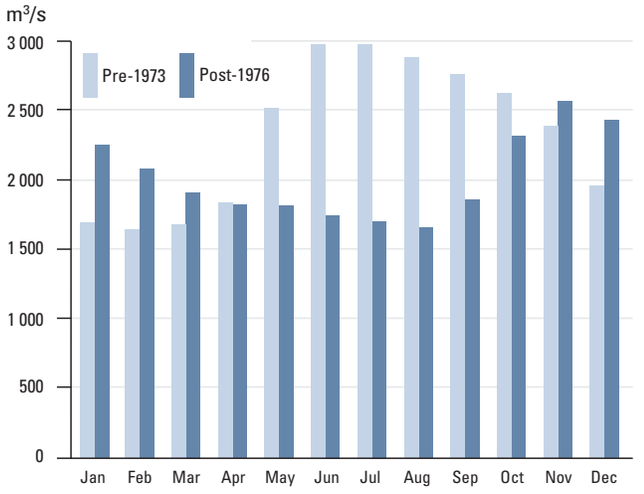

Figure 3·14. Monthly mean discharges for the Nelson River, Canada for the period 1960 to regulation in 1973, compared to post-regulation discharges from 1976 to 1990 (Source: HYDAT 1994).

pleted in 1961, and in 1976 most of the flow of the Churchill River was diverted into the Nelson River basin through the enlargement of South Indian Lake (1977 km^2). The combined annual mean flow of the Churchill and Nelson Rivers amounts to 3500 m^3/s (Rosenberg *et al.* 1987) and the effect of this regulation on hydrology is illustrated in Figure 3·14. The effect has been a change to peak flows in November, December, and January (corresponding to peak hydroelectric demand) as opposed to the natural peak flows in June, July, and August. These developments have been studied for their environmental impacts, and have been considered elsewhere (e.g., Hecky *et al.* 1984, Rosenberg *et al.* 1985) and will be discussed further in chapter 7 in the context of the fate of mercury in reservoirs.

The James Bay project is Canada's largest hydroelectric development, and it affects rivers flowing both into James Bay and southeastern Hudson Bay. The first phase of the La Grande River development included three main diversions, specifically, of the Caniapiscau, Eastmain, and Opinaca Rivers into the La Grande River. The limnology of La Grande 2 reservoir, filled in 1978 and 1979, is reviewed in Kislalioglu and Berkes (1994).

In Russia, the Kransnoyarskoye Reservoir on the Yenisey River is one of the largest man-made lakes in Siberia (Table 3·5). Construction began in 1967 and the reservoir was filled in 1970 (Data Book of World Lake Environments 1994). Also within the Yenisey River basin, are the Ust-Ilimskoye and Bratskoye Reservoirs which were filled in 1974 and 1967 respectively. The Lena River has dams in only one large and one very small tributary and as such retains a natural hydrologic regime (Dynesius and Nilsson 1994).

Small lakes

There are innumerable small lakes in the Arctic, as described in chapter 2. Unfortunately, to date there has been little attempt to characterize these large numbers of lakes regionally, in order to provide a rational basis for a systematic investigation of the operation of Arctic lakes and the fate of contaminants within them. The exceptions to this are in Alaska, where regional characterization has commenced, and in Norway, where this is being considered (D. Landers, pers. comm., US Environmental Protection Agency, Environmental Research Laboratory, Corvallis, Oregon, 1996). Some of the major studies are described below.

Early investigations into northern limnology were undertaken in Alaska (e.g., Hobbie 1973) and at Char Lake, in the vicinity of Resolute, NWT, Canada. Char Lake was studied intensively between 1969 and 1973, with the aim of describing for the first time the complete annual cycle of physical and chemical events in a High Arctic lake (Schindler *et al.* 1974, Welch 1994). In most years, Char Lake is a typical polar lake never rising above 4°C, and having a brief summer overturn period of up to six weeks duration. The lake is extremely oligotrophic, with soluble reactive phosphorus measurements (SRP) consistently lower than the detection level (<0.7 mg/L); nevertheless, winter oxygen depletion at the sediment/water interface was considerable, probably reflecting respiration by the benthic community. Dissolved oxygen concentrations were greatest just under the ice when it was thickest in late May (Schindler *et al.* 1974). This probably reflects increased photosynthesis in the surface waters in association with increased light penetration (24 hours of sunlight and melting snow) at this time of year (Albright *et al.* 1980, Prowse and Stephenson 1986, Whitfield and McNaughton 1986). Schindler *et al.* (1974) also noted that mixing continues after the lake is frozen over, as evidenced by the general uniformity of specific conductance with depth. This mixing delays reduced oxygen levels at depth.

There was evidence at Char Lake of a freeze out of solute-rich water which concentrates gases and dissolved solids in the deepest part of the lake over the course of the winter. This cryoconcentration can be quite substantial in Arctic lakes. For example, a lake 5.2 m deep at 64°N was 77% frozen with 2 m of ice cover, and even a lake 34.2 m deep had 23% of its volume frozen (Welch *et al.* 1987). Cryoconcentration likely affects the fate of contaminants in the water column of these lakes. However, the cryoconcentration of contaminants and the effect of anoxia at the sediment/water interface on contaminant recycling has not been considered for this environment.

Limnological research into the effect of anthropogenic activities on water quality in northern Canada has also been undertaken as part of a multidisciplinary research project at Sagvagjuac, near Chesterfield Inlet on the west coast of Hudson Bay. This work began in 1976 to parallel a project at the Experimental Lakes Area in southern Manitoba (Welch 1985). Sagvagjuac is an area of numerous glacial ice-scoured lakes, most of which are small (<50 ha). The lakes are cold and monomictic, circulating once annually during the summer with temporary thermal stratification in midsummer. The water is generally soft, with total dissolved solid concentrations between 15 and 30 mg/L, and oligotrophic and clear. Water circulation and winter respiration of these lakes has been discussed by Welch and Bergmann (1985a, 1985b), while the chemical limnology has been reviewed in Welch and Legault (1986). This was the first detailed investigation of element input/output on continuous permafrost watersheds. The year-to-year variability in solute output from these permafrost watersheds was high, and shown to be determined by the timing and magnitude of the snowmelt runoff. Welch and Legault (1986) concluded that the solute output was low in years with little mid- to late-summer rainfall, causing the runoff into the lake to consist mostly of snowmelt, which occurred before the active layer was well developed. The importance of mid- to late-summer rainfall was demonstrated by its coincidence with high solute outputs from the basin into the lake. This was also an important factor with respect to lake element loading and retention. If most of the runoff occurred prior to ice-off, the inflowing water and solutes flowed out from the surface of the lake prior to mixing with the bulk of the lake water where biological removal could take place (Welch 1974).

Rivers draining into a lake tend to flow before the ice of the lake has begun to melt and before there is any outflow

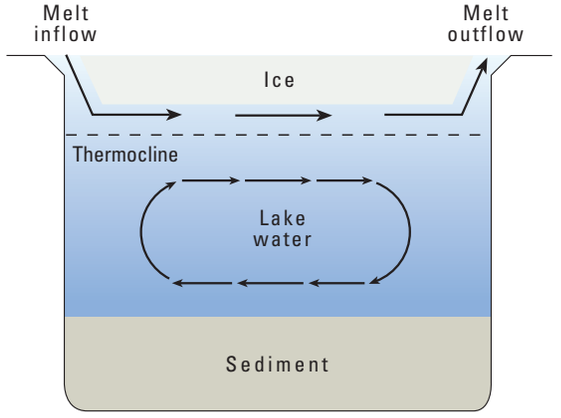

Figure 3·15. Illustration of the movement of less dense spring freshet water moving through a small Arctic lake underneath the surface ice cover, but not mixing with the water column.

from the lake. As a result, the lake temporarily stores this water, causing the water level of the lake to rise, and eventually float the ice clear of the lakeshore, creating a moat around the lake. The lake level will continue to rise until the level of the outflow is exceeded. Because the incoming meltwater is relatively warm, compared to the lake water which is stratified under the ice, this first flush of meltwater tends to pass through the lake with little or no mixing with the lake water, as illustrated in Figure 3·15. Thus, contaminants transported by early snowmelt probably move through a lake without mixing with the water that has been stored there from the previous fall (Welch 1974, Barrie *et al.* 1997, Freitas *et al.* 1997). This suggests that: 1) rivers will tend to transport the main load of soluble contaminants from snowmelt beyond headwater lakes; and, 2) lake water chemistry will generally reflect that of summer rain and ground-ice melt, as modified by movement through the active layer and mixing with the perennial lake waters.

Recently, a contaminant mass balance study of Amituk Lake (75°02'57''N, 93°45'51''W) in the Canadian Arctic Archipelago was initiated by Environment Canada. This is the first integrated study of contaminants in freshwater systems in the Arctic (Semkin 1996). While work is still progressing on this study (the contaminant details are reported in chapter 6), it is appropriate to note here that even in such a small study area (drainage area ≈26 km^2), considerable variability occurs with respect to stream delivery of water and sediments due to the basin geography and surficial geology. In this case, the importance of a particular stream to the delivery of atmospheric-derived contaminants seems to be primarily determined by the presence of depressions where wind-blown snow is trapped, which in turn delivers contaminants to the system at snowmelt (Semkin 1996).

A number of other lakes in the Canadian Arctic have been investigated in less detail than Amituk Lake to determine depositional trends of contaminants by means of dated sediment cores. In 1994/95, a number of Russian Lakes were added to this spatial/temporal study (Lockhart 1996). A comparable study has been reported on two lakes in Alaska (Gubala *et al.* 1995). Sedimentation in small Arctic lakes is considered further in section 3.3.4.3, while contaminant studies are synthesized in chapters 6 and 7.

Many Arctic water bodies are very shallow (frequently less than 2-3 m maximum depth) and are characterized by being unstratified during the summer. These lakes tend to be warmer in summer due to their shallow depth and early loss of ice, but are also likely to be totally frozen during the winter. Lakes of this type have not been investigated to any great extent in the Arctic.

3.3.4.3. **Suspended sediments, sedimentation, and resuspension**

Many contaminants are hydrophobic and consequently tend to be adsorbed to and transported with sediments in rivers. Sedimentation processes in lakes, deltas, and other quiescent zones can remove contaminants from the water column and store them temporarily or permanently. The resuspension of these sediments can result in the reentrainment of the associated contaminants and ongoing transport. These processes will be considered in the context of Arctic river systems.

Suspended sediments

The particulate matter transported by a river is commonly divided into wash and suspended load and bed load. The latter is the coarse material (sand size >63 mm particle diameter) moving on or near the stream bed, whereas the former is continuously suspended in the water and is carried with approximately the same velocity as the water (Meybeck *et al.* 1989).

Particulate matter, or suspended solids, originate from soil and bank erosion in the watershed and by the resuspension of particles deposited in the river bed. A general relationship can often be seen between water discharge and the concentration of suspended solids (Meybeck *et al.* 1992). Resuspension of fine-grained bottom sediment with increasing discharge is often a major cause of increased suspended solids (Thomas and Meybeck 1992). Particle size and organic carbon content are acknowledged as playing key roles in the adsorption of chemical compounds to particulate matter (Knezovich *et al.* 1987). It is the surface area of the particles and the amount of organic carbon present that controls adsorption capacity. This capacity is inversely proportional to grain size. Thus, the finest clays are generally those with the highest concentrations of contaminants (Thomas and Meybeck 1992). Also important is the fact that these finer-grained particles settle less quickly, and thus, there is potential for riverine transport over long distances.

Contaminants also bind to suspended organic particulate matter as well as aggregates of various origins and chemical characteristics. These carrier particles may consist of the following fractions/phases: organic, carbonate, Mn and Fe, detrital/non-detrital, adsorption, and cation exchange phases (Håkanson and Jansson 1983). Humic matter is known to be an important carrier for contaminants in freshwater systems (Håkanson and Jansson 1983).

Pulp mill effluents have been shown to affect the physical transport characteristics of sediment. The effects are most pronounced during low-flow periods (i.e., winter) when the ratio of the effluent discharge to the flow discharge is greatest. The effluent contains organic fibers and bacteria that have affinity for ambient inorganic sediment resulting in sedimenting particles larger in size than the ambient material (Krishnappan *et al.* 1995). The nature of this material may result in its subsequent remobilization during periods of high flow. This interaction can have important consequences for contaminant transport.

The most important stream characteristics which determine the input of contaminants to the river, their transport down the river system, and their concentration in the water include the rate of water flow from slopes and in channels, as well as the capacity of the flow to transport suspended particles. The concentration of suspended matter in the flow depends on the nature of the soils and sub-soils of the watershed, vegetative cover, slope, infiltration capacity, depth of active layer, etc. Land runoff reflects the geology and physiography of the drainage basin. In Canada, for example,

Table 3·6. Contributions of suspended sediments from rivers draining the three physiographic regions of the Northwest Territories, Canada. (Source: Brunskill 1986).

Drainage region	Average suspended sediment load, 10^3 kg/km^2/y
Precambrian Shield	<3
Interior Plains	56
Cordillera	101

rivers draining the Precambrian Shield, the Interior Plains, and the Cordillera can be distinguished by their suspended sediment burdens (Table 3·6) (Brunskill 1986).

The highest concentrations of suspended matter generally occur near the bottom, and are related to the presence of coarser grains in suspension (Eisma 1993). The conditions for generating high sediment loads are usually maximized in the spring. For example, the amount of sediment transported during the 10 days/year with the highest water discharges was on average 47% of the total annual sediment load transported in a mountainous river course in northern Norway (Calles 1977). In the Mackenzie River, approximately 65% of the total annual sediment load is delivered in two months (July and August), representing about 36% of the annual flow (Figure 3·16).

Most POPs are hydrophobic (and lipophilic) and adsorb and partition (dissolve in a polar phase) to particles. The amount of contaminants adsorbed on particles depends on the sorption potential (number of surface sites) of the particles, the binding energy and the hydrophobicity (expressed as K_{OW} – see chapter 6 for details) of the compound, plus its chain length and its molecular configuration (Means *et al.* 1979). The hydrophobicity of most organic compounds is such that the mass transport in the dissolved phase (water concentration) tends to be less than that of the particulate

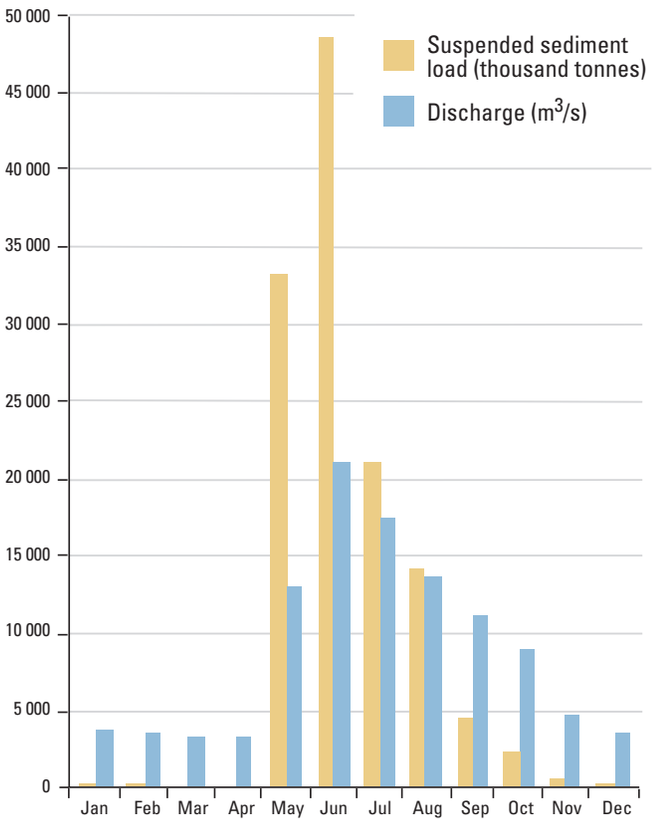

Figure 3·16. Comparison of monthly water and suspended sediment loads to the Mackenzie Delta plain for the period 1974-1983 (Source: Lewis 1988).

phase determined by concentrations on the suspended matter. Nevertheless, if the concentration of particulate matter in rivers, for example headwater systems, is low, contaminants will be transported in the dissolved phase. Field studies in two Canadian rivers have shown that, under the majority of flow conditions, the main transport medium for most hydrophobic contaminants is in the dissolved phase (Carey 1995).

Most metals have low water solubilities, but high natural concentrations of metals can occur as a result of suspension and of the transport of fine-grained sediments as part of the natural weathering process. In addition, factors such as the pH, redox, alkalinity, salinity, and trophic level are also important in the spread and fate of metals (Means *et al.* 1979).

Regardless of the hydrophobicity of many of the contaminants, hydrological measurements of snowmelt runoff indicate a poor mixing of meltwater with underlying ice-rich soils, and only minor amounts of this water remain in the watershed (Cooper *et al.* 1991, Cooper *et al.* 1993). Simultaneously, substances scavenged from the atmosphere and deposited in the snowpack are often strongly retained by sorption or chemical interaction with vegetation and soil during snowmelt (Cooper *et al.* 1991). It has, for instance, been shown that over 90% of the atmospheric load of the isotope ^{7}Be and about 70% of the isotope ^{35}S, were adsorbed onto the surficial 2-3 cm of frozen organic soils and tundra vegetation in Alaska. In contrast, in the Canadian Arctic, little loss to soil was observed in the Amituk Lake basin for OCs and mercury (Semkin 1996), probably because these contaminants are being sourced from deep snowpacks within stream valleys, allowing little opportunity for loss to soils following snowmelt.

Sediment deposition and resuspension

In general, the processes of transport and deposition of sediment are governed by the water flow rate and the size of the particles. In a turbulent water stream, upward forces are responsible for the transport of the fine fractions in suspension. Quartz-density solids with a diameter less than approximately 0.015 cm are mainly transported as a suspended load (Allen 1970). Erosion and deposition are results of the varying ability of stream water to carry sedimentary particles. The flow force and the sediment transport rate are proportional to the mean water flow velocity (Allen 1970). Heavier particles do not become suspended, but they can be transported as a bed load (bounce and roll) by the water flow.

Although the upper reaches of river systems experience erosion, the lower parts are commonly marked by a state of net deposition, expressed as a thick, laterally extensive spread of alluvial sediment in which the active river courses are embedded. The mean size of deposited particles decreases downstream, as the transporting capacity and turbulence decline (Moss and Walker 1978). The finest particles or wash load, which usually contain the highest contamination levels, will therefore travel the longest distance. These will only accumulate in large lakes or reservoirs. Consequently, the suspended matter transported by rivers is not all destined for the sea bed.

Sedimentation can result in the accumulation in the river bed of particles and surficially active substances, such as heavy metals and POPs, including heavy fractions of oil hydrocarbons, polyaromatic hydrocarbons such as B(a)P, as well as phenols. Resuspension of contaminants occurs when the bedload is disturbed, for example, during the spring snowmelt flood. When bottom sediment particles become suspended, the sorbed contaminants may be transported over long distances by the river.

Lakes and reservoirs can have a significant effect on river hydrology and on sediment accumulation in downstream deltas and estuaries. Eight reservoirs with a total combined volume of 474 km^3, and which together control about 23% of the total river flow have been constructed in the Yenisey River basin. Together they have caused a reduction by a factor of three in sediment transport to the river mouth. In 1961, the load of suspended matter near the river mouth at the community of Igarka was 13×10^6 tonnes, but this had been reduced to 4116 tonnes per year by the end of the 1970s (Alabyan *et al.* 1991). In the Peace River, a tributary of the Mackenzie River, the gates of the W.A.C. Bennett Dam were closed in 1967, creating the Williston Reservoir. Flow routing revealed that while there would be no significant change in the total annual inflow to the Mackenzie Delta, the dam and reservoir would result in an average flow increase of 20-30% to the Delta during the low flow months, especially February to May. Conversely, summer and fall flows would be diminished by as much as 5-10% (Wiens 1991). Subsequent measurements have shown that the monthly discharge of the Peace River has declined 16% for the ice-off period, but increased 40% during ice-on periods. Further, it is estimated that the average annual sediment load downstream has decreased by 33% (373×10^3 tonnes/y) (English *et al.* 1996, Prowse and Conly 1996).

In most cases, sedimentation in large lakes is more or less a permanent sink. Nevertheless, in many shallow lakes, wind induced resuspension of the sediments can occur with subsequent transport downstream. This is likely of significance in lakes with large surface areas and which are oriented with their long axis parallel to prevailing winds. The presence of surface ice throughout much of the year will, however, reduce the extent of wind turbulence. Many Arctic lakes retain extensive ice cover throughout most of the open water season, and some lakes are only free of ice periodically. To our knowledge, there has been no investigation of sediment resuspension in Arctic lakes within the context of contaminant transport.

The rate of sedimentation in, for example, Scandinavian lakes in wooded areas is usually between 0.7 and 1.7 mm/y (Rognerud and Fjeld 1993). Age determinations in lake sediments in subarctic parts of Norway show that the sedimentation rate is usually less than 1 mm/y (Norton 1986, Rognerud *et al.* 1993). Similar rates have been reported for Canadian lakes by Lockhart (1996).

The most important variables regulating gross sedimentation to glacial lakes in Sweden were found to be: the depth relative to wind fetch which together influence resuspension; the form and size of lakes; the proportion of the lake catchment containing forest and open land; the distribution of mires and lakes in the catchment; the relief of the drainage area; and, the theoretical lake water retention time (Håkanson 1994).

The hydraulic conditions change rapidly at the mouth of rivers. The flow pattern in freshwater delta areas is very complex, but bears similarities to the expansion of submerged jets with complementary zones of reverse flow (Jopling 1960). The form of the delta front depends both on fluvial and shore processes, on bed load and suspended load, and on the original topography of the basin. Deltas are generally divided into a topset area, a foreset area constituting the delta front, and a bottomset area beyond the foreset slopes. Bed load transportation of particles larger than 0.18 mm is a necessity for the formation of foreset slopes, and such materials, often highly sorted, constitute the bulk of the foreset deposits. The size of the foreset area depends on the grain size of the material (the coarser the material the larger the foreset area) and on the depth conditions of the river mouth area. When bed-load transportation ceases, the deposition of the suspended load (particles less than 0.18 mm) will systematically reduce the height of the foreset slopes. The bottomset slopes are generally much more stable than the foreset slopes, where mass movement is comparatively frequent. The delta advance can be very rapid in lakes receiving large loads of material (Håkanson and Jansson 1983).

Sediments are resuspended when the bottom shear exceeds a critical shear stress for the sediment bed. The critical shear stress is a function of the properties of the bottom material, such as water content and grain size (Håkanson and Jansson 1983). For example, recently deposited, unconsolidated material is resuspended more easily than compacted material (Bengtsson *et al.* 1990).

Effects of floods

During snowmelt, the water surface in the river rises, and at the same time, the flood waters can mobilize and disperse deposited bottom and bank material. The settled material which previously lay immobile at the bottom becomes dilated, and some may go into turbulent suspension (Friedman and Sanders 1978).

Under normal flow conditions, most of the suspended material moves downstream with the water, without being deposited. However, as a result of ice jams and increased water levels during spring melting, the water may overflow the river banks. The effect of flooding on the transport of suspended matter is variable. When the plain is flooded, material may be picked up (Scrimgeour *et al.* 1994), but both when flow is reduced and in the case of falling water, suspended matter is deposited (Eisma 1993).

The development of vegetation on the tundra can produce hummocky surfaces, which reduce the rate of overland flow by enhancing surface storage, thereby reducing soil erosion and enhancing sedimentation. Sedimentation in flood plains and deltas is also affected by vegetation. Sedimentation rates in the Mackenzie Delta can be predicted from the type of vegetation on the delta (Pearce 1993).

3.3.4.4. **Humic matter in river systems**

While considerable attention in this chapter has been given to the role of inorganic sediment in transporting contaminants in aquatic systems, particulate organic matter (POM), measured as particulate organic carbon (POC), can also play an important role in this regard. Especially when inorganic sediment concentrations are low, autochthonous POM can provide an appropriate substrate for the adsorption of contaminants. Nevertheless, there is an absence of information available on the role of POM in transporting contaminants in temperate rivers and lakes, let alone in Arctic river systems, due in part to the low concentrations of POM relative to that of total (organic and inorganic) suspended particulate matter.

Large amounts of dissolved organic carbon (DOC) are exported from wetlands and taigas, where organic matter accumulates due to slow decomposition rates (Hope *et al.* 1994). The DOC released from wetlands appears to influence the transport of, for example, total and methyl mercury (Driscoll *et al.* 1994). The extent to which contaminants bind to dissolved humic materials depends on the concentration and type of humic materials present, pH, calcium concentration, and ionic strength of the water (Carter and Suffet 1982).

Humic matter is known to be an important carrier for contaminants in freshwater systems (Håkanson and Jansson 1983). OC contaminants were present in the water of five

major rivers of the Hudson Bay lowland, but were found to be almost absent in bottom sediments (McCrea and Wickware 1986). The water also contained high concentrations of organic carbon, iron, and aluminum. It is conceivable that the hydrophobic contaminants were maintained in the water column by being bound to humic substances. The seepage of organic-rich water originating in the surrounding wetlands is a major source of aquatic humic matter to the rivers. Dissolved organic carbon has been found to be a major constituent of these northern waters, and concentrations in the area of 10-14.5 ng/L have been reported (McCrea and Wickware 1986).

Due to their complexing ability, DOC and POC can act as carriers of heavy metals and organic compounds and influence their partitioning. This can change the solubility, mobility, and bioavailability of adsorbed compounds (McCrea and Fischer 1986, Hope *et al.* 1994). Hydrophobic compounds can remain in the water adsorbed to humic substances. Thus, in the presence of high concentrations of organic carbon (DOC and POC), sorption of organic contaminants to sediments may not readily occur, although this is an area requiring further investigation. Humic substances and humic and fulvic acids can also reduce the rate of volatilization of compounds, such as PCBs (McCrea and Fischer 1986).

In the Lena River, 10-11 mg DOC/L has been recorded during summer floods (Martin *et al.* 1993). This is usually accompanied by increased levels of iron, complexed to the humic fraction (McCrea and Fischer 1986). Available data on separate determinations of DOC and POC concentrations and fluxes show that the northern rivers discharge mostly DOC (Table 3·7). The organic matter content is lowest during the summer and autumn periods. The organic matter content is highest in the swampy river basins of the western Siberian lowland. In the weakly mineralized waters, rich in organic substances, which are typical for these Arctic regions, substances such as dissolved ions, copper, lead, and manganese are mostly found in the form of organic complexes.

3.3.4.5. Ice

Ice plays a unique and important role in the Arctic. River and lake ice restrict the exchange between the atmosphere and the water. River ice incorporates particles when it freezes to the bottom, as well as during anchor and frazil ice formation. River and lake ice also receive contaminants from atmospheric deposition throughout the ice-on season. During the spring melt, ice transport can gouge sediments and create ice jams which can result in accelerated stream flows and associated sediment erosion. For these reasons, the role of ice in transporting contaminants must be considered.

Table 3·7. Dissolved and particulate organic carbon concentrations in selected Arctic rivers (Source: WHO/UNEP in press).

River	DOC[a], mg/L	POC[b], mg/L	POC, % in TSS[c]	TOC[d], mg/L	DOC/TOC, %
North Dvina	20.1	3.2	23.4	23.3	86
Pechora	12.7	0.3	16	13	98
Ob	9.1	0.9	2	10	91
Lena	6.6	1.1	3.8	7.7	86
Mackenzie	5.3	7.3	1.7	12.6	42
Average for world rivers	5.3	4.6	1	9.9	55

a. Dissolved organic carbon.
b. Particulate organic carbon.
c. Total suspended sediment.
d. Total organic carbon.

Stable ice cover is formed at river velocities below 0.6 m/s, while the water surface generally remains free of ice at velocities greater than 1.5 m/s (Elíasson 1994). In late winter, ice cover on lakes can be of the order of 2 m thick in the Canadian Arctic Archipelago. River ice can be substantially thicker than this due to the incorporation of slush layers and overflow, and has been reported at up to 2.5 to 3.0 m thick in some Russian Arctic river reaches (Grigoriev and Sokolov 1994).

Also important is the nature of the ice, with so-called white ice forming if snow or slush is incorporated, and black ice forming when freezing occurs rapidly and under calm conditions (or at least without incorporating snow or slush). Thus, black ice is often more typical of open water in a lake proper, away from the effects of shore ice (Bengtsson 1994). The nature of the ice determines the ability of light to penetrate it – white ice severely limits transmission, although snowcover attenuates light more than either black or white ice (Prowse and Stephenson 1986). Some lakes retain substantial ice cover throughout most years (e.g., Lake Hazen). This can impact on light transfer during the summer and can result in earlier freeze-up in the fall.

Anchor ice forms when the entire water column is supercooled and ice nucleates on particles on the bed of the river (Reimnitz *et al.* 1992). A change in river temperature or turbulence, or accumulated buoyancy resulting from the build-up of ice can eventually dislodge the combined ice and sediment mass, rafting it to the surface. Here it is included in the overlying ice cover. Rocks as heavy as 30 kg have been incorporated in river ice by this mechanism (Martin 1981).

Frazil ice also forms when the water column is supercooled. While actively growing, frazil crystals tend to collect particles which can subsequently be incorporated into the ice cover. Ice formed in this way appears turbid, with patchy discolorations due to entrained material (Reimnitz *et al.* 1992). In addition, wind-blown dust and dirty snow accumulate locally on the surface of frozen rivers. As a result of these processes, river ice often contains large amounts of sediment (Zubov 1943).

The surface ice can also freeze into the bed and/or bank, and the rising river stage in the spring will dislodge both the ice and the attached frozen material (Beltaos *et al.* 1993).

In Arctic regions, in-channel ice plays a more critical role in the control of hydrological processes than landscape runoff (Prowse 1994). The presence of floating ice increases the wetted surface of the channel perimeter and the under-ice surface roughness increases the drag on the water. Assuming that the bed and ice-cover underside have identical roughness, then the uniform flow depth will increase by something of the order of 30% (Beltaos *et al.* 1993). For the same discharge, the presence of an ice cover generally reduces the sediment 'driving' variables of shear stress, velocity, and diffusivity, and thus, the sediment transport capacity ought to be reduced, though there has been only limited investigation of this effect. This is especially true for fine particles (<62 µm) (Beltaos *et al.* 1993).

Seasonal low flows and floods are primarily the result of river ice freeze-up and ice jams, respectively. Most of the annual discharge of water and particles in Arctic rivers takes place during the short spring freshet. The large hydrodynamic forces combined with the flow of broken ice result in erosion of the embankments, sediment re-distribution, and other major changes of river geomorphology. A dynamic break-up with associated ice jamming and release will produce higher suspended sediment flux than a thermal break-up (Milburn and Prowse 1996).

Under open water conditions, it is the atmospheric inputs that dominate the heat budget of rivers. Once ice forms, the

Table 3·8. Average dates for the beginning of river ice drift, and the length of ice drifting inthe river mouth regions of selected Russian Arctic rivers (Data source: V. Vuglinsky, pers. comm., State Hydrological Institute, St. Petersburg, Russia, 1996).

River	Average date of the first day of drifting	Length of spring ice drifting
North Dvina	2 May	8 days
Pechora	24 May	4 days
Ob	27 May	4 days
Yenisey	30 May	10 days
Lena	3 June	9 days
Yana	27 May	6 days
Indigirka	3 June	4 days

convective exchanges are decoupled. Also, ice quickly absorbs incoming long wave radiation resulting in strong cooling of the water at the ice surface, thereby creating the potential for high rates of ice growth (Beltaos *et al.* 1993). Ice cover reduces the flux of short wave radiation through greater surface reflection and attenuation. Snowcover on the ice further reduces this flux, as noted by Prowse and Stephenson (1986).

Break-up of the river ice affects water temperature and other important processes, such as nutrient processing and the availability of carbon to the biota (Scrimgeour *et al.* 1994). Average dates for when river ice first begins to drift in the river mouths of selected Russian Arctic rivers are given in Table 3·8. In general, ice break-up occurs in late May or early June and continues for one to two weeks, as considered above in section 3.3.4.1.

Sources of contaminants to the ice

River ice stores and transports contaminants, and may therefore be considered an indirect source of contaminants. Factual information about the rates of uptake of contaminants to the ice or the extent of their subsequent accumulation and transport is scarce. The magnitude of these processes can only be estimated through combining existing information on contaminant accumulation and physical behavior in the ice with the more traditional and ample knowledge on transport processes of sediments, particles, and solutes.

Contaminants are incorporated into the ice cover from the atmosphere, water masses, and sediments. The surface of the ice accumulates snow which has scavenged contaminants from the atmosphere during deposition, and retains particles and associated contaminants deposited as dry deposition. Contaminants which are sorbed to fine suspended particulate matter in the river can be scavenged during the growth of frazil ice (Prowse 1994). The uptake of contaminants takes place along the entire period of ice cover (8-10 months in most Arctic rivers), and their release occurs during a short melting period in summer, when biological production is at its highest. There does not seem to be any evidence to suggest whether or not water-soluble contaminants are frozen into the ice during freezing, or preferentially released to the underlying water. Nonetheless, Lesack *et al.* (1991) report an increase in solute concentrations in the residual water by a factor of 4.3 from the time of initial freeze-up to the development of maximum ice thickness. In rivers, the effects of freezing on the water composition could be less apparent than in lakes, because of constant mixing and through-flow (Cheng *et al.* 1993).

Where the growing ice pack comes into contact with shores and sand banks, the bank and bottom sediments may freeze into the ice. This process happens both in autumn, during the period of stable ice cover formation, and in winter, if the flow of bottom water decreases or ceases and the ice cover lies on the bottom of the river (Beltaos *et al.* 1993). During a freezing period, supercooled water in turbulent reaches can form extensive covers of anchor ice on the river bed. When anchor ice releases from the bottom, it lifts the underlying bed material. The significance of anchor ice on the erosion of the riverbed has been only poorly assessed to date (Prowse 1994).

Transport processes

The contaminants in the water, suspended matter, and bottom sediments are subjected to processes of ice trapping, transfer, and release. These processes are controlled by the varying patterns of freezing, ice growth, and ice cover decay, as well as by the water regime in the autumn-winter period. During freeze-up or ice jams, flow is reduced downstream of the ice accumulation. Ice-induced flood waters upstream can replenish water in the flood plain (Prowse 1994). The reduced water velocity on the flood plain can result in sedimentation of fine-grained material and associated contaminants.

There are two major patterns of ice cover break-up in rivers, mechanical or dynamic break-up and thermal break-up (Prowse 1994). In some rivers, the peak of the spring flood wave is accompanied by rapid ice movement and formation of a large number of strong jams, resulting in a critical rise in water level. A largely irregular river system with many branches contributes to the formation of numerous ice jams, which significantly extend the flood period. Dynamic break-ups are observed in rivers such as the Yenisey, Kotuy, Anabar, Olenek, and Yana. Moving ice is subjected to mechanical decay and melting, gradually releasing particles and contaminants into the water phase, or depositing them on shores and sand banks. The thermal type of ice break-up is less energetic and does not create strong jams in the rivers due to the general decrease in the flexural strength of the ice through the melting and increased porosity of the ice along crystal intersections (Prowse 1994).

The breakup season within the Mackenzie Delta area lasts 4-7 weeks, beginning in late April or early May and ending in mid to late June. In the Mackenzie River, the flood water from the southern part of the basin arrives at the delta before the melting of the ice cover in the delta lakes takes place. Thus, in early May, there is a rapid increase in discharge and suspended-sediment concentrations which accompany the initial period of flow and ice movement along shallow distributary channels. Delta front areas less than 1 m in height become submerged as large volumes of water become confined at the interface between river mouth and seaward bottom-fast ice. The melting process continues until much of the ice has been cleared along major channels. Maximum discharge occurs in early June as a result of the melting snow within the basin. Ultimately, the high volumes of meltwater overflow bottom-fast ice out to the 2 m isobath, accelerating the melting process. Delta-front flooding persists into late June at which time the landfast ice is virtually melted and the river discharge begins to decline.

Dissolved Oxygen (DO)

The long periods of ice cover in northern rivers may result in severe DO depressions during the winter season. Investigations within the Yukon River basin (Schreier *et al.* 1980), revealed that severe DO depressions occurred throughout the basin with lowest levels in late winter. Open water reaches during the winter season did not necessarily aerate the river, as these were frequently linked to groundwater inflows, which often exhibited low oxygen concentrations as well. Nevertheless, recovery from low DO was rapid with ice break-up.

The Takhini River, a groundwater-dominated system, and the Nordenskiold River, a river rich in organic matter and

with many bogs and marshes, (both in the Yukon) were sampled to further investigate DO under ice (Whitfield and McNaughton 1986). DO decreased very rapidly in November and continued to decline in both rivers until February or March with both rivers showing DO recoveries during April under full ice cover. The fact that DO increased while ice was present, concurred with the conclusion of Albright *et al.* (1980) that the Ogilvie and Swift Rivers had greatest microalgal and bacterial biomasses in spring and summer, which were likely controlled by light and dissolved organic carbon.

Lakes receiving this deoxygenated water may become anoxic themselves. Anaerobic bacteria have been identified as being capable of mobilizing contaminants (e.g., Hg) from lake sediments (Bloom and Effler 1990, Mason and Fitzgerald 1991, Regnell and Tunlid 1991, Gillmow *et al.* 1992, Choi and Bartha 1994, Regnell 1994, Zhag and Plonas 1994).

Char Lake, which is a headwater lake and does not receive oxygen-deficient waters, is in most years a typical polar lake, never rising above 4°C and with a brief summer overturn period of up to six weeks duration (Schindler *et al.* 1974, Welch 1994). The lake is extremely oligotrophic, with soluble reactive phosphorus (SRP) measurements consistently less than the detection level (<0.7 mg/L); nevertheless, winter oxygen depletion at the sediment/water interface was considerable, probably reflecting respiration by the benthic community. DO concentrations in Char Lake appear to recover in early spring and were greatest just under the ice when it was thickest in late May (Schindler *et al.* 1974). This probably reflects increased photosynthesis in the surface waters, in association with increased light penetration (24 hours of sunlight and melting snow) at this time of year (Albright *et al.* 1980, Prowse and Stephenson 1986, Whitfield and McNaughton 1986). Schindler *et al.* (1974) also noted that mixing continues after the lake is frozen over, as evidenced by the general uniformity of specific conductance with depth, which may mitigate the DO depression.

The impact of ice on contaminant transfer has not been studied to any great extent, but it is clear that ice will form a reasonably impermeable barrier between the atmosphere and the water throughout large parts of the year. This obviously limits the exchange of atmospheric contaminants with the water, but also retains any contaminants introduced below the ice within the limited water volume. This may also be exacerbated by low DO resulting in release of these contaminants to the water column or a change to a more biologically reactive form (e.g., methylmercury). Sources of contaminants that may be of concern include contaminated groundwater drainage, industrial and municipal discharges below the ice, and natural seeps of hydrocarbons such as occur in the Mackenzie River. The potential impact of contaminant sources on ice-covered ecosystems has not been adequately addressed.

3.3.5. Mass transport

3.3.5.1. Water and suspended matter

The mass of water transported in Arctic river systems is directly relevant to the transport of contaminants, either those which are water soluble or those which are hydrophobic and adsorbed to suspended particulate matter. Increased water flow is often directly correlated with suspended matter load and adsorbed contaminant fluxes. Anthropogenic compounds may be present in different speciations and partitioned between liquid and solid phases, which significantly influences their transport by river flow. The subject of actual transport of contaminants by rivers and loadings to oceans and marginal seas will be dealt with in the relevant chapters (e.g., chapter 6 for POPs and chapter 7 for metals). Discussion here will be limited to water, sediments, and total organic carbon (TOC) which are summarized in Table 3·9.

Most dissolved contaminants are not conservative; their concentrations in the water flow are changed as a result of discharges from various sources to the river and due to various transformation processes in the river. In order to describe and understand the fate of contaminants in river water, concentrations of contaminants should be measured at different points within the entire river basin. However, this is not always possible for remote sites. The difficulties in accessing many Arctic rivers frequently limits even the collection of suspended sediment data in sufficient detail to permit the sediment transport estimates for these rivers.

The unit area discharges (L/s/km^2) and unit area loads (tonnes/km^2/y) of suspended sediments and total organic carbon (TOC) are compared for major Arctic rivers in Table 3·9. While these are large, heterogeneous river basins, there are at least some general patterns evident. Relatively high unit area discharges with generally low sediment and TOC aerial loads are evident for the rivers of Norway and Finland. By comparison, discharges tend to decrease to the east in Russia. The highest unit area sediment loads in Russia are for the Pechora and Indigirka Rivers, essentially on opposite sides of the country, while the highest TOC aerial loadings are in the western drainage basins. The large drainage basins of Canada tend to have relatively low aerial discharges. Unit area sediment loads are also low except for the Mackenzie and Nottaway Rivers. A full explanation of these riverine characteristics and the impact on the receiving marine waters would require a much more intensive assessment than is possible here.

Large Arctic rivers tend to have a high water discharge and a low sediment load, compared to other large rivers of the world. For example, Russian Arctic rivers represent 67% of the total river drainage from the territory of Russia, but only 32% of the suspended matter flux from the same area (WHO/UNEP in press). Unit area discharges and sediment loads are highly variable, depending upon the nature of the watershed. The Mackenzie River has a higher total suspended matter discharge than do any of the reported Eurasian rivers (Table 3·9), although the unit area load of suspended matter from the Mackenzie River is well within the range of the Eurasian rivers. Most of the other large North American rivers actually have very low sediment loads, especially on a unit area basis, due to the minimal surficial material within the watershed and the presence of lakes and reservoirs within the system. In Norway, the rivers have a much higher rate of water delivery per unit area than any other part of the Arctic, due to the high precipitation and relatively short rivers with minimal basin storage. Sediment loads per unit area in Norway are quite low and comparable to many of the rivers in the Canadian Arctic.

While particulate matter is responsible to a great degree for the transport of hydrophobic contaminants in river systems, it does not necessarily follow that higher concentrations of total suspended solids means that there is a greater load of anthropogenic chemicals transported by the river, as this is determined by the actual inventory of contaminants available to the river system from atmospheric and direct sources. Even without a high sediment load, rivers have the potential to transport contaminants either in the dissolved or particulate phase if they are delivered to the system. Rivers contribute a large proportion of the sedimentary and by extension, the contaminant budgets of the Arctic Ocean and marginal seas. For example, the estimated annual discharges of suspended sediments by the Lena and Mackenzie Rivers are 17.6×10^6 tonnes (Martin *et al.* 1993) and 125×10^6 tonnes (Lewis 1991), respectively.

Table 3·9. Drainage area, discharge, surface runoff, concentrations and estimated loads of suspended solids, and TOC for selected Arctic and subarctic rivers (Sources: Gordeev *et al.* 1995, Meybeck and Ragu 1995, Holtan *et al.* 1994, and ENVIRODAT 1996).

				Suspended sediment transport			Total organic carbon transport		
River	Drainage area, 10^3 km^2	Mean annual discharge, m^3/sec	Surface runoff L/sec/km^2	Concentration, mg/L	Annual load, 10^3 t/y	Unit area load, t/km^2/y	Concentration, mg/L	Annual load, 10^3 t/y	Unit area load, t/km^2/y
Norwegian Sea (from 62°N 5°E to 70°N 20°E)									
Gaula	3.7	96.6	26.4	3.9	13	3.5	3.2	11	3.0
Orkla	3.1	66.3	21.7	1.5	3	1.4	2.8	6.2	2.0
Rana	3.8	172.7	44.9	7.1	45	11.7	n.a.	n.a.	n.a.
Vefsa	4.1	181.3	44.0	4.0	23	5.6	3.4	20	5.2
Whole Basin	94.704	7353.5	77.6	–	224	3.7	–	61	1.02
Barents Sea (Norway, from 70°N 20°E to Russian Border)									
Alta	7.4	86.9	11.8	1.8	5	0.7	3.5	11	1.49
Tana	16.4	188.5	11.5	2.1	23	0.8	3.0	n.a.	n.a.
Pasvik	18.4	171.2	9.3	1.4	7	0.4	3.0	20	1.09
Whole Basin	73.141	1316.0	17.9	–	36	0.7	–	33	0.62
Barents and White Sea (Russia)									
Onega	57	501.6	8.8	18	300	4.9	n.a.	n.a.	5.8
North Dvina	357	3462.9	9.7	35	3800	10.6	n.a.	n.a.	7.2
Mezen	78	868	11	32	900	11.1	n.a.	n.a.	2.4
Pechora	322	4089	12.7	80	13500	32.4	n.a.	n.a.	5.2
Whole Basin	1236	13596	11	50*	22000	17.5*	n.a.	n.a.	4.1
Kara Sea									
Ob	2990	12857	4.3	38	16500	6.4	n.a.	n.a.	1.2
Yenisey	2580	19866	7.7	10	5900	2.3	n.a.	n.a.	1.8
Pyasina	n.a.	2727	n.a.	40	3400	18.8	n.a.	n.a.	n.a.
Whole Basin	6248	42486.4	6.8	22*	33200	5.0*	n.a.	n.a.	1.5
Laptev Sea									
Khatanga	364	2693.6	7.4	20	1700	4.6	n.a.	n.a.	1.5
Anabar	100	550.0	5.5	n.a.	n.a.	n.a.	n.a.	n.a.	0.9
Olenjok	219	1138.8	5.2	31	1100	5.1	n.a.	n.a.	1.2
Lena	2486	16656	6.7	34	17600	7.1	n.a.	n.a.	2.1
Yana	238	1094.8	4.6	103	3500	14.8	n.a.	n.a.	1.0
Whole Basin	3643	23679.5	6.5	34*	25100	6.9*	n.a.	n.a.	1.8
East Siberian Sea									
Indigirka	362	1918.6	5.3	210	12900	35.6	n.a.	n.a.	1.3
Kolyma	660	4158	6.3	120	16100	24.3	n.a.	n.a.	1.6
Whole Basin	1342	7917.8	5.9	134*	33600	25.0*	n.a.	n.a.	1.3
Chukchi Sea (excluding Alaska)									
Whole Basin	94.2	640.6	6.9	34*	700	7.4*	n.a.	n.a.	1.0
Bering Sea									
Anadyr	n.a.	1902.6	n.a.	59	1800	17	n.a.	n.a.	n.a.
Yukon	n.a.	6659	n.a.	286	60000	70.4	n.a.	n.a.	n.a.
Whole Basin	n.a.	n.a.	n.a.	n.a.	n.a.	n.a.	n.a.	n.a.	n.a.
Beaufort Sea (Mackenzie is totally dominant)									
Mackenzie	1787	10543.3	5.9	127	125000[a]	24.1	7.8	2597	1.5
Arctic Archipelago									
Coppermine[b]	19.3	105	5.4	1	3.3	0.2	2.3	7.6	0.39
Back[b]	93.9	497	5.3	4	62.7	0.6	3.3	51.7	0.55
Hayes[b]	18.1	195	10	11.07	68.0	3.8	3	18.4	1
Whole Basin	n.a.	n.a.	n.a.	–	n.a.	n.a.	–	n.a.	n.a.
Hudson Bay and Hudson Strait									
Churchill[b]	287	882	3.1	6.5	180.2	0.6	9.8	272.6	0.9
Nelson[b]	1010	2170	2.1	10.8	736.3	0.7	1	68.4	0.06
Moose[c]	60.1	780	12.9	9.2	400	3.7	21	516.5	8.6
Nottaway[b]	57.5	1040	18.1	26.7	1000	15.2	n.a.	n.a.	n.a.
La Grande[b]	96.6	1700	17.6	n.a.	n.a.	n.a.	n.a.	n.a.	n.a.
Koksoak	n.a.	80.4	n.a.	n.a.	n.a.	n.a.	n.a.	n.a.	n.a.
Whole Basin	3607	16952.9	4.7	–	n.a.	n.a.	–	n.a.	n.a.

* Mean Value
a. Lewis 1991.
b. Data for this station were calculated using information provided from HYDAT (1994) and ENVIRODAT (1996).
c. Data for this station were calculated using information provided by HYDAT (1994) and ENVIRODAT (1996). In addition, the Total Organic Carbon data, and the sum of Particulate and Dissolved Carbon (1977-1978) were provided from Water Quality Investigation in Ontario's Arctic Watershed, Inland Water Directorate, Environment Canada, Ontario Region (unpublished).

Norway

Water courses north of the Arctic Circle cover an area of approximately 93 000 km^2, and their discharge to the Norwegian and Barents Seas is approximately 70×10^9 m^3/y, corresponding to a total runoff of 23.9 L/s/km^2. The total amount of suspended particulate matter transported from northern Norway to the sea is in excess of 150×10^3 tonnes/y, or 1.6 tonnes/km^2/y (Holtan *et al.* 1994). A model has been developed to calculate area runoff of total phosphorus, total nitrogen, phosphates, nitrates, and ammonia, using area-specific runoff coefficients (see Holtan and Åstebøl 1991).

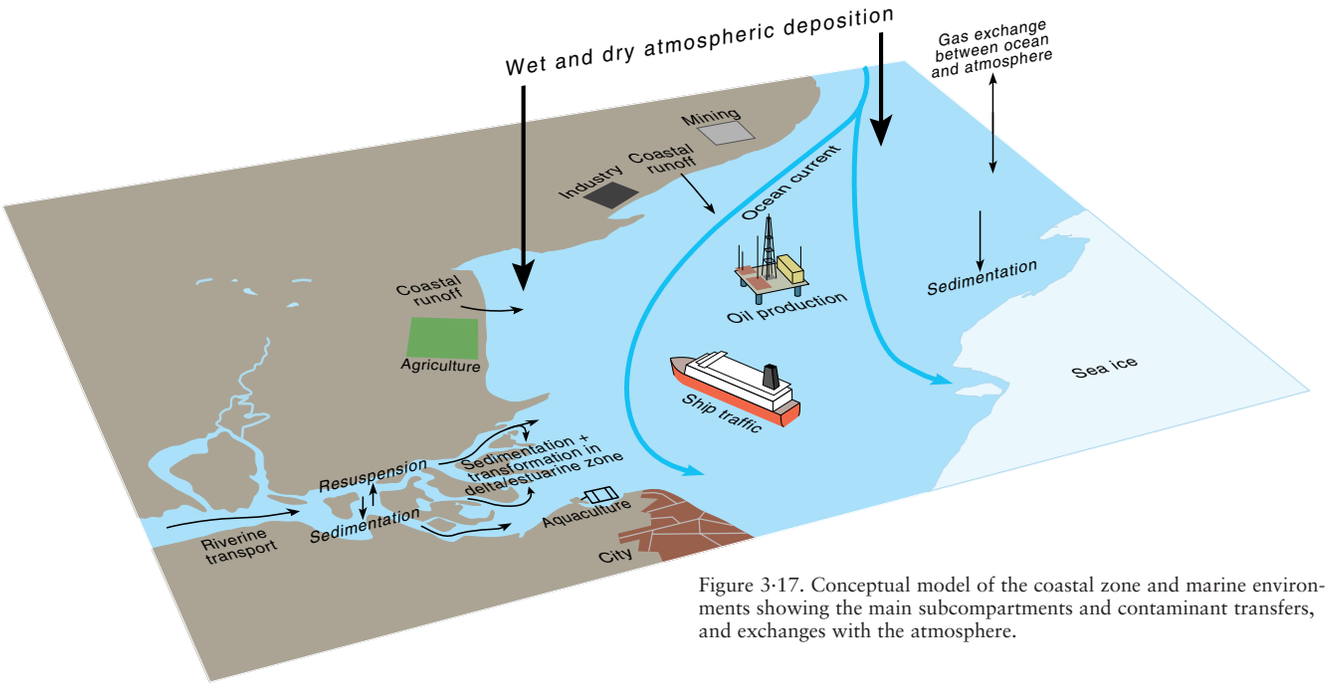

Figure 3·17. Conceptual model of the coastal zone and marine environments showing the main subcompartments and contaminant transfers, and exchanges with the atmosphere.

The rivers in northern Norway are small, relative to the major rivers in northern North America and Russia, and the quantity of particulate matter transported is relatively small. The total amount of suspended particulate matter transported to the Norwegian Sea and the Barents Sea is calculated to be 166×10^6 tonnes per year in a total water runoff of 70×10^9 m^3/y (Holtan *et al.* 1994). The river with the highest annual sediment load is the Rana, transporting 45×10^3 tonnes/y with an average suspended particulate matter concentration of 7.1 mg/L (Holtan *et al.* 1994).

Russia

The mean annual runoff of particulate matter in most Arctic rivers of Russia does not exceed 20 tonnes/km^2/y. The lowest values (5 tonnes/km^2/y) are characteristic of rivers in the forests of the western (European) region, north Caucasus, west Siberia, Kazakhstan, and the mid-Siberian plateau. A moderate runoff of particulate matter (from 5 to 20 tonnes/km^2/y) is characteristic in the eastern part of the European territory, the Ural Mountains, the mountains of south Siberia, the northeast and Far East, and also in the desert regions of Central Asia.

With the exception of Mezen River, rivers of the basins of the Barents Sea and White Sea flow through forests and bogs and the TOC runoff to the rivers is relatively high (mean values of 5.2-7.2 tonnes/km^2/y). The TOC runoff to Siberian rivers is not as high (0.9-2.1 tonnes/km^2/y) despite the occurrence of fairly high TOC concentrations in the water (5-10 mg/L). The TOC runoff from the tundra zones of the basins of the Laptev, East Siberian, and Chukchi Seas is low (0.5-0.8 tonnes/km^2/y), compared to the average global value of 3.7 tonnes/km^2/y (Meybeck 1993).

Canada

The Mackenzie River has been extensively studied with respect to the sediment load to the delta and the Beaufort Sea. The delta is maintained by the Mackenzie and Peel Rivers, which together have a mean annual discharge of almost 10 000 m^3/s and deliver in the order of 125 million tonnes of clayey silt and sand to the delta annually (Lewis 1991). The suspended particles in the Mackenzie River are of mixed biogenic and petrogenic origin. The Mackenzie River receives only minor anthropogenic hydrocarbon inputs (Yunker *et al.* 1991b). Higher plants and peat were sources for the alkanes, alcohols, and stereols. The PAH and pentacyclic triterpanes showed, respectively, alkyl homologue and hopane distributions characteristic of natural seeps of fossil fuels (Yunker *et al.* 1991a). The particulate hydrocarbon flux from the Mackenzie River is by far the most important terrestrial source of hydrocarbons to the Beaufort Sea. The flux of total alkanes is estimated at $440 \pm 94 \times 10^3$ kg/y and for PAH $49 \pm 8 \times 10^3$ kg/y (Yunker *et al.* 1991b). There is a strong seasonality in the hydrocarbon flux, with an estimated winter contribution of less than 0.6% of the total annual flux (Yunker *et al.* 1991a).

Other rivers in Canada have not been studied in the same detail, due to their much lower suspended sediment loads and more difficult access. As noted in Table 3·9, the flows, sediment, and TOC loads in the other rivers are relatively small compared to the Mackenzie River. Unit area loads are also small by comparison, except for the sediment load from the Nottaway River and TOC from the Moose River. The high TOC load of the Moose River may be an artifact resulting from the use of a different analytical method and having had more detailed data available for this river system from the intensive study of McCrea and Wickware (1986).

3.3.5.2. River/lake ice

Although ice on Arctic rivers and lakes is considered to be an important phenomenon with respect to the fate and pathways of contaminants, there seems to be no information available with respect to the mass transport of ice in the freshwater environment. Some preliminary investigations of this transport pathway should be undertaken to determine if quantification of ice transport and associated contaminants is required relative to ocean loadings. This is considered further in the Ocean section (section 3.5.3.1).

3.4. Estuaries, deltas, and fjords

Oceanographic conditions in coastal waters will differ from those in the open ocean, and some of the factors causing these differences are river runoff, tidal currents, and the effect of shore boundaries. The interfaces between the terrestrial/freshwater processes and the oceanic processes are highly complex and unique to both compartments. Deltas and estuaries play an important role in sedimentation in freshwater systems.

Nevertheless, deltas and estuaries have a close connection with the marine environment and have important influences upon oceanic transport and contaminant fate (Figure 3·17).

3.4.1. Estuaries

Estuaries are semi-enclosed, coastal bodies of water, having a free connection to the open ocean, and within which seawater is measurably diluted by freshwater derived from land drainage (Lauff 1967, Pritchard 1967). From a geochemical point of view, any semi-enclosed body of water, where marine waters are mixed with freshwaters, should be considered as estuarine zones. Consequently, river deltas, fjords, bays, and tidal swamps may be considered as estuaries. Because of their high productivity, estuaries often serve as breeding and nursery grounds for many species. The fate of contaminants released from local as well as up-watershed activities is influenced by the characteristics of the estuaries. Arctic estuaries differ from those in temperate regions in their extreme seasonality in water discharge, winter flows being only about 5-10% of the annual average flow (Antonov 1970), and because they are covered with ice from October through June (e.g., Pfirman *et al.* 1995a). The Ob and the Yenisey Rivers have the largest estuaries in the Arctic.

Most estuaries were formed following the last deglaciation, when the rise in sea level inundated coastlines and drowned the mouths of river valleys. However, when sediment discharge is high, the estuary fills, and a delta forms instead. For existing estuaries, either the sediment discharge is low, the inlet is deep, or the tidal action is large enough that the inlet does not fill in.

All estuaries contain a transitional zone where the salt water of the ocean and the freshwater of the river runoff meet. Because freshwater is less dense, it tends to flow out over the saline seawater. Entrainment of some seawater in the freshwater outflow results in a return, replacement flow of seawater up the estuary at depth. In the lower, marine part of the estuary, there is free connection with the open

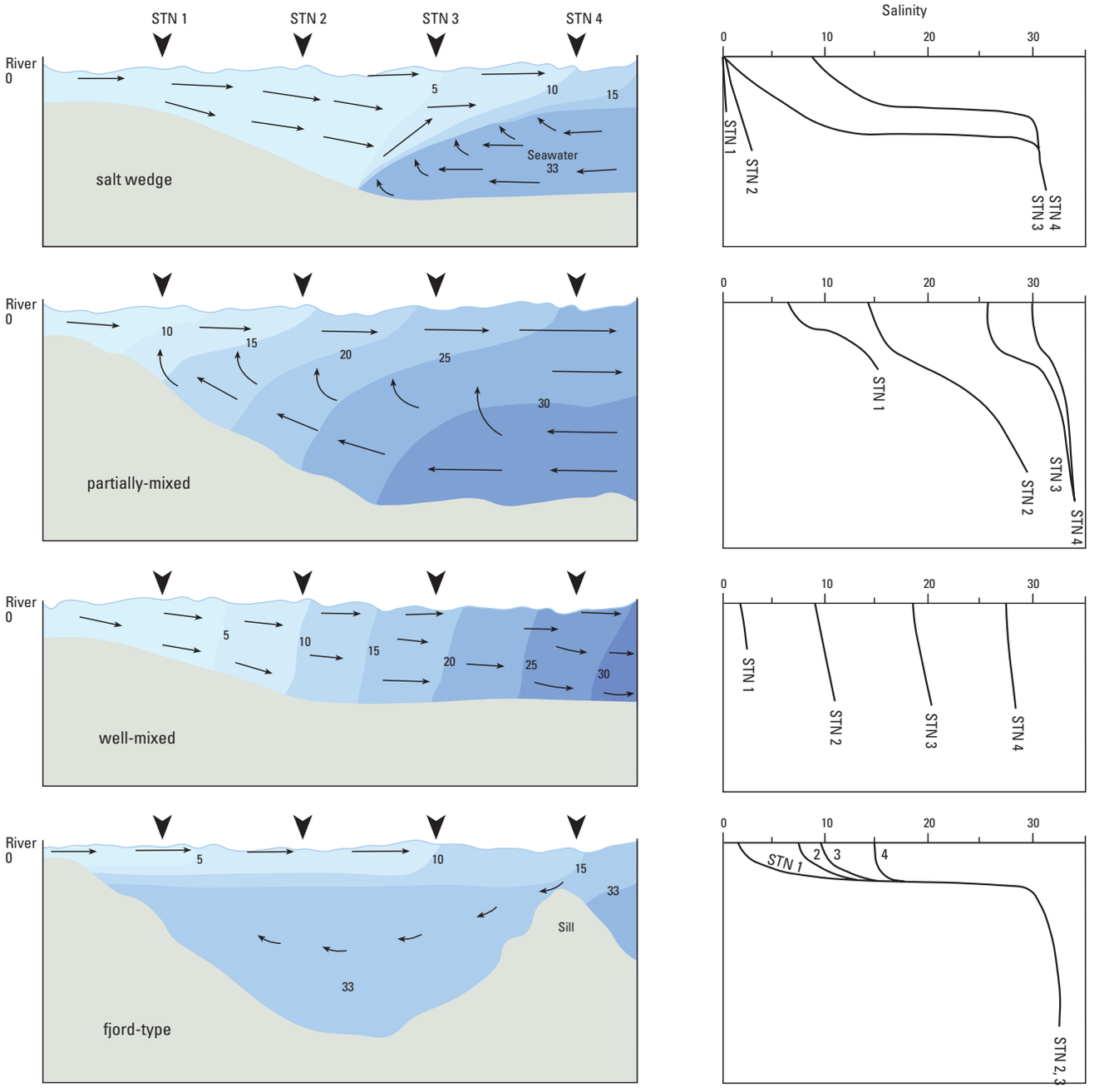

Figure 3·18. Basic circulation and salinity distribution in salt wedge, partially- mixed, well-mixed and fjord-type estuaries as defined by Wollast and Duinker (1982). Numbers and shading show salinity values.

ocean. In the middle part of the estuary, salt water and freshwater mix. Dominated by freshwater river runoff, the upper part of the estuary is also influenced by tides. In some Arctic rivers, tidal influence penetrates as much as hundreds of kilometers upstream (Antonov 1970).

Wollast and Duinker (1982) defined three types of estuaries based on the way that seawater mixes with river runoff. These are salt wedge, partly mixed, and well mixed estuaries. The basic circulation in each of these types of estuaries is illustrated in Figure 3·18. Subsequently, fjord-type estuaries were added by Duxbury and Duxbury (1994). Salt wedge estuaries occur where there is a large amount of river runoff. The less dense freshwater tends to run over the more dense seawater that would otherwise flow upstream at depth, but is held back by the river discharge. A strong front forms between the freshwater and salt water, resulting in the salt wedge. The salt wedge moves upstream when the tide rises, or when the river discharge is low. Conversely, it moves downstream when the tide falls, or the discharge is high.

Partially mixed estuaries have both strong seaward flow of freshwater and strong inward flow of seawater. In well-mixed estuaries, the combined effects of strong tidal mixing and low river discharge result in a slow net seaward flow of water at all depths. The isohalines are nearly vertical.

Fjord-type estuaries (see also Figure 3·20) are deep with a sill at the fjord entrance, and have little tidal mixing. The river water flows out in a thin surface layer over the seawater, with only minor entrainment of the underlying seawater. Because circulation is confined to the surface waters, and the deep waters are isolated by the sill, the deep waters may stagnate and become anoxic.

If the estuary is broad relative to its length, the circulation pattern may have three distinct regimes. Due to the Coriolis force, the out-flowing river discharge within an estuary in the Northern Hemisphere will be forced to its right as it moves out of the estuary. Similarly, the incoming flow is forced to the right looking upstream in the estuary from the perspective of the ocean. As a result, seawater will tend to flow in on one side of the estuary and the river water will flow out on the opposite side. In between, a zone of lateral mixing between the freshwater and seawater is established.

3.4.2. Deltas

The term 'delta' refers to the depositional plain formed by a river at its mouth (Encyclopedia Britannica 1990). Inherent in this definition is the concept that sediments delivered by the river are deposited at or near the coast, and thereby actively build out the land area into the sea. In addition to the subaerial portion of the delta (i.e., above the mean water level and consequently flooded only during the freshet), a subaqueous delta (i.e., below the mean water level of the receiving body of water and consequently subjected to coastal processes rather than terrestrial processes) also builds outward and is usually evident as a bulge in the adjacent bathymetry.

Delta morphology exhibits a lot of variation resulting from: drainage basin characteristics (climate, lithology, basin size), sediment loading and factors affecting it (Milliman and Syvitski 1992), energy along the shoreline (tides, current, and waves), bathymetry of the shelf onto which the river discharges, and human impacts on river systems (GESAMP 1993). The largest deltas are created by major rivers draining large areas and carrying abundant sediment loads. Large subaqueous delta plains are best developed where the continental shelf is shallow and the sediment loads are great.

Within the Arctic, deltas are most obviously formed where rivers discharge directly onto broad continental

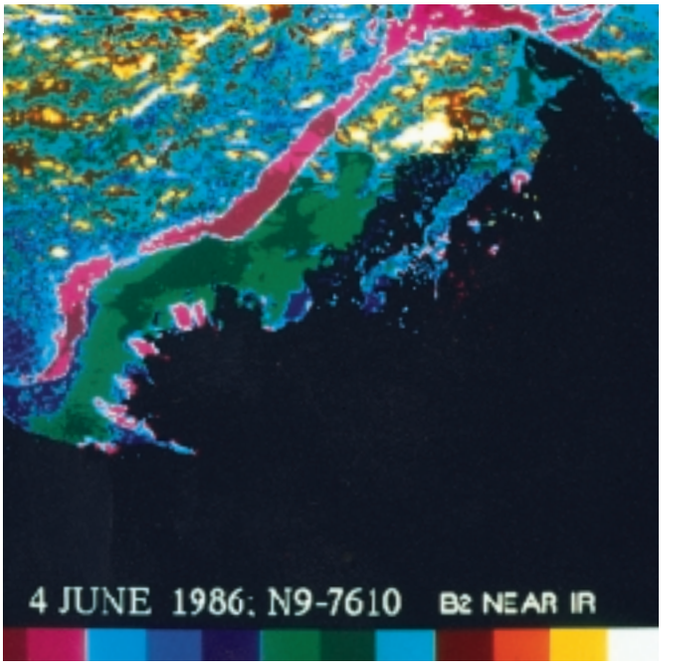

Figure 3·19. Advanced Very High Resolution Radiometer (AVHRR) satellite image (June 4, 1986) showing a color composite of the visible data band for the Mackenzie Delta. River water overflowing the landfast ice can be seen as purple regions extending offshore from the mouths of channels (Source: Dean *et al.* 1994, used with permission of K. Dean and K. Ahlnäs).

shelves. The best examples are the Lena River in Russia and the Mackenzie River in Canada (Figure 3·19), where shallow inshore areas of the shelf provide a wide platform upon which large deltas have been built. Seasonal ice potentially has important effects on the morphology of some deltas in the Arctic. For example, Reimnitz *et al.* (1988) note a flat (<2 m vertical variation in morphology), extensive (16 km) platform in the subaqueous ice-stressed deltas on the Alaskan Arctic shelf. This feature, however, is not seen in the Mackenzie Delta. Because the freshet precedes ice break-up in Arctic deltas, the water level rises rapidly in spring (reportedly more than 10 m for the Lena) and floods the grounded ice in the delta. At this time, water and sediments are transported on top of the ice and in channels under the ice (Figure 3·19 and see Dean *et al.* 1994). Over-flooding may also be associated with 'strudel-scour' which is caused by rapid drainage of ponded waters on the ice surface through melt-holes and fractures in the ice (Reimnitz and Kempema 1987).

Arctic deltas exhibit the characteristics of drowning coastlines. These include features like coastal cliffs showing mass wastage, debris slides, and surface erosion; cliffs showing ground-ice slumps and mud flows; sediment deposits on coastal tundra; inundated tundra; and, breached lakes (e.g., see Harper 1990). This is due to a protracted rise in relative sea level during the Holocene (approximately the past 15 000) which is estimated to total 70 m for the Beaufort shelf (Hequette *et al.* 1995) and possibly as much as 120 m for the Laptev shelf (Nurnberg *et al.* 1995) and other Arctic regions (Pirazzoli 1991, Rasch and Nielsen 1995). Sea-level rise continues globally at a present rate of about 3 mm/y (Douglas 1991). As a consequence of the rising water level, parts of the outer Mackenzie Delta are estimated to be eroding by as much as 20 m/y, although 2 m/y is more typical (Harper 1990). Similarly, the Lena delta is generally retreating (Zenkovitch 1985). Coastal retreat can be expected to be most rapid in regions of low relief, containing poorly consolidated sediments bonded by permafrost (i.e., Arctic deltaic environments). Even though portions of Arctic deltas

are presently being lost, there may still be a net accumulation of sediment in deltas. For example, thaw subsidence could be occurring with subsequent replacement by new sediments. Alabyan *et al.* (1996) found that most of the 21×10^6 tonnes/y of sediments supplied by the Lena River is presently settling within the delta. Similarly, Macdonald *et al.* (1996) estimate that about half of the 127×10^6 tonnes/y of sediments from the Mackenzie River are presently stopping in the Mackenzie Delta.

Deltas are important transition zones between the rivers and the coastal Arctic Ocean and seas. Since deltas capture sediment, they potentially provide a significant sink for particle-reactive contaminants transported by the river and, under conditions of erosion or resuspension, a source. The importance of deltas in the delivery of riverborne contaminants to the Arctic Ocean has been recognized in a number of recent studies (e.g., Martin *et al.* 1993, Peulvé *et al.* 1993, Yunker *et al.* 1993, Coquery *et al.* 1995). Despite their importance, modern deltaic sediment budgets are only poorly known, and establishing such budgets would be a crucial first step to the construction of regional and local budgets for particle-reactive contaminants discharged to Arctic rivers.

3.4.3. Fjords

Figure 3·20 schematically demonstrates the general circulation in connection with a fjord. With a sill at the mouth and a river commonly at the head, the water masses may be split in three depth zones. The freshwater runoff results in the formation of an often shallow, brackish surface layer. The seaward flux of brackish water gradually mixes with the underlying seawater such that its volume may increase 5-10 times before it reaches the fjord mouth. As a consequence, an inflowing compensation current is established to make up for the loss of seawater from the fjord. The intermediate water occupies the zone between the brackish water and the sill. The water exchange in this layer is mainly governed by seasonal and short-term variations in the coastal water.

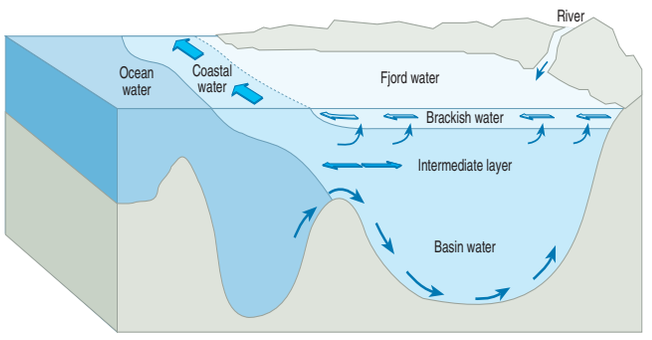

Figure 3·20. Sketch of main circulation pattern in a fjord.

Recirculation is a characteristic feature of fjord circulation driven by the local forces of runoff and wind. Some renewing of water masses takes place due to exchange with the water masses adjacent to the 'open' end of the semienclosed circulation in the frontal area at the mouth of the fjord. However, the main part of the exchange is associated with nonlocal forcing. Several mechanisms governing the exchange have been studied through data analysis, numerical models, and theory. Common to all of these studies are the assumptions of displacement of the vertical density field at the coast caused by the coastal wind; and, that the exchange mainly affects the intermediate and deep-water masses in the fjords. It has been shown that the exchange in the intermediate layer (between the upper layer and sill depth) in narrow stratified fjords takes place as a pressure-driven, mainly two-layer circulation (Svendsen 1977 and 1981, Cannon and Holbrook 1981, Klinck *et al.* 1981, Stigebrandt 1990).

Due to the rotational dynamics, the exchange in broad fjords takes place somewhat differently than in narrow fjords. The transient behavior due to the distortion of the density field at the coast will propagate into the fjord as an internal Kelvin wave, with the shore to the right when looking in the direction of its propagation (Proehl and Rattray 1984). Preliminary simulations indicate that the wave energy, which is dispersed in the fjord, is directed down-fjord on the opposite side (Asplin 1995, Svendsen 1995).

The density of the basin water, below the intermediate water, gradually decreases with time if renewal is not taking place. The speed of this process varies substantially between fjords as a function of topography and the effect of driving forces. In some fjords there is an annual renewal, while in others it may take several years before the density of the basin water is sufficiently reduced to condition a renewal. However, special persistent wind conditions causing strong upwelling on the coast can cause unexpected basin water renewal.

Sometimes the outflow from fjords can be very pronounced, and fjord water can be traced far from the coast. The transport of anthropogenic nutrients and contaminants from the fjords to coastal and open waters strongly depends on their residual time in the fjords.

3.4.4. Particle and nutrient transport

Much of the sediment discharged by rivers is deposited within the confines of the estuary. This is due to two factors: 1) the circulation itself, and 2) flocculation at the freshwater–saltwater front.

Estuarine circulation is characterized by river water and entrained seawater flowing out at the surface, with a replacement flow of seawater at depth (Figure 3·21). This means that particles suspended in river discharge will also flow out at the surface. But, as they settle, they will be transported into the in-flowing seawater at depth, and will be advected back upstream some distance before they finally deposit. In addition, suspended marine sediments will be transported into the estuary by the upstream flow of seawater. Both nutrients and plankton may also remain in the estuary by this circulation pattern (Laws 1993). As a result of this recycling of nutrients, estuaries tend to support high levels of productivity. Fjords represent a special case because of the presence of a sill. For the most part, materials that sink below the level of the sill become trapped in the fjord.

Flocculation is the result of molecular attractive van der Waals forces. In fresh river water, clay minerals carry a net negative charge and repel one another. However, in salt water, free cations neutralize the clay minerals, allowing molecular attractive forces to dominate when clay minerals are brought close enough. As the clay minerals attach to one another, their settling velocity increases, leading to increased deposition.

Similarly, coagulation and biological aggregation result in deposition of particles. At these low salinities, riverborne colloidal iron and humic acids are known to coagulate and settle out of suspension (Sholkovitz 1976, Boyle *et al.* 1977, Sholkovitz *et al.* 1978). Organisms feeding in the estuary excrete particle aggregates as fecal pellets (up to 5 mm long), which have rapid settling velocities.

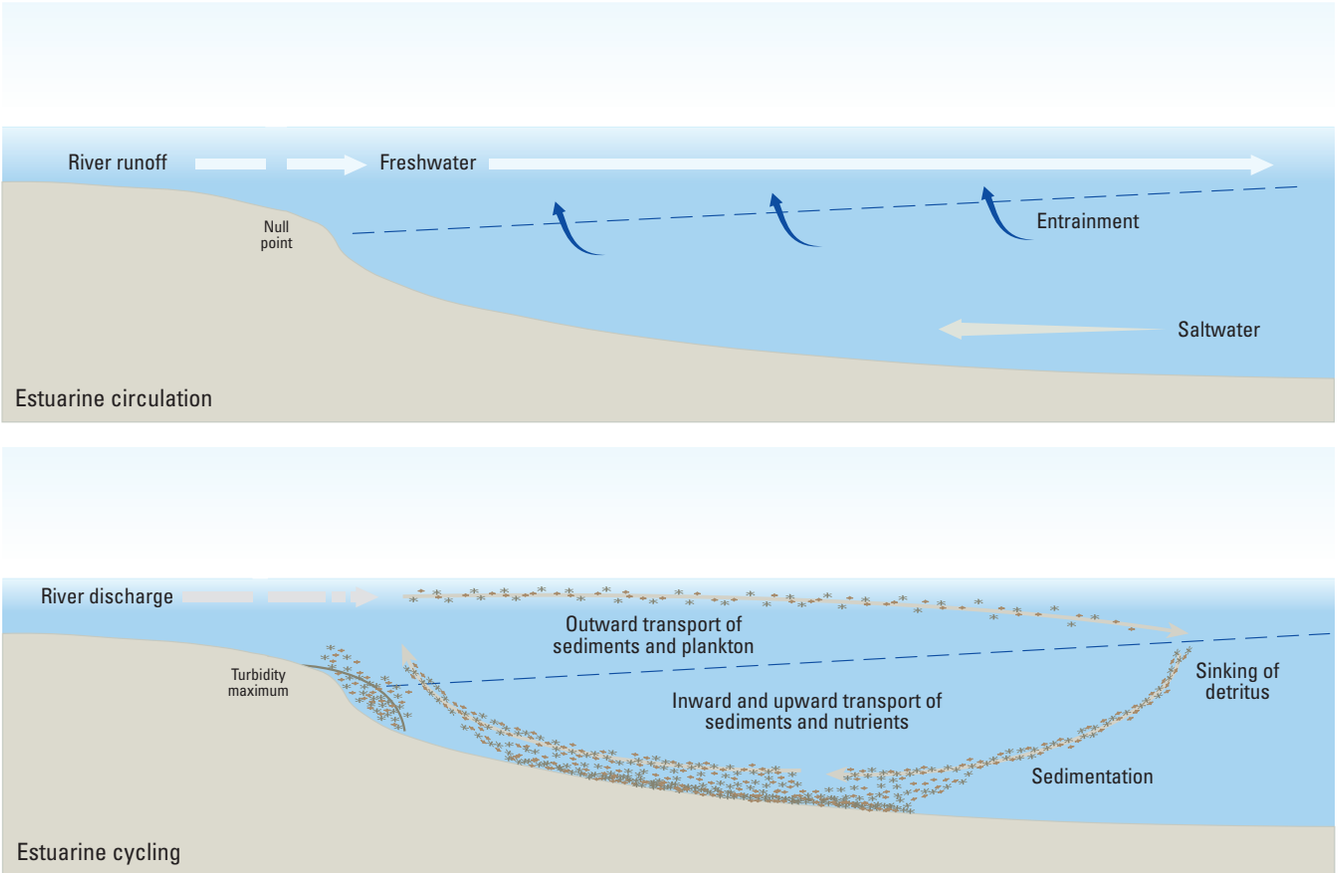

Figure 3·21. Illustration of water, sediment and nutrient cycling in estuaries. Freshwater flows outward, transporting sediments, plankton, and also contaminants. Material that sinks into the inflowing seawater may be trapped in the estuary. Estuaries such as those of the Ob and Yenisey are covered by ice during much of the year (Source: adapted from Laws 1993).

As a result of estuarine circulation, a turbidity maximum with accumulation of fine-grained sediment often forms at the front between river water and seawater (Figure 3·21). Here, particle concentrations are high because clays brought downstream by the river flocculate, and particles transported upstream in the marine flow deposit at the null point in the saltwater flow. Because of the strong seasonality in Arctic river discharge (see section 3.3.4.1), the location of the turbidity maximum will shift, potentially resulting in remobilization of particle accumulations on a seasonal basis. During the spring flood, the rise in waters of the lower regions of the Yenisey River may exceed 20 m, while in the Lena it attains as much as 30 m (Antonov 1970).

3.4.5. Sedimentation

Much of the sediment load transported by Arctic rivers during the high flow, high sediment load season is deposited in river mouth deltas. Overbank sedimentation rates in the Mackenzie Delta can be of the order of several centimeters per year (Pearce 1993). This is likely typical of other deltas and is much greater than the 100-1000 mm/1000 years in estuaries and 1-3 mm/1000 years for ocean sedimentation rates (Lisitsin 1988). Huge amounts of suspended matter are deposited in estuaries and excluded from further transport to the open ocean. Sharp moderation of river flow rate, followed by decrease of a vertical component of turbulent flow and deposition of large particles is the main reason for this effect. Sedimentation of finer particles, which have colloidal properties, is caused by coagulation due to mixing of freshwater with seawater electrolytes.

Suspended matter concentrations in large Arctic rivers are rather low, as a result of the geological and physical-geographical conditions of their basins (see section 3.3.4.3). Sediment can be deposited in deltas upstream in lakes and reservoirs, such as the Slave River delta upstream in the Mackenzie River system and the numerous reservoirs in the upper and middle parts of the largest Siberian rivers. In the Yenisey basin, for instance, eight reservoirs have been constructed, which together control about 23% of the total river flow. Their impact on suspended matter flow is particularly pronounced, with a reduction by a factor of three in sedimentation subsequent to the reservoirs being put in operation (Alabyan *et al.* 1991).

Recent field studies of particulate matter carried out in the Ob and Yenisey estuaries (Lisitsin *et al.* 1994) showed significant sedimentation of riverine suspended matter in the mixing zone of river and sea waters as well as in the shelf zone of the Kara Sea. Estimates show that a maximum of 10-20% of the particulate matter discharged by the rivers Ob and Yenisey passes beyond the borders of estuaries and the Kara Sea shelf. This is a typical situation for rivers which transport sediment material into wide shelves, such as that of the Kara Sea (Milliman 1991).

3.4.6. Ice cover

Arctic estuaries are influenced by ice cover during most of the year. Usually in October, fast ice develops in the estuary, along the coast and in the river itself and the ice remains in place until break-up in June (Ingram 1981, Ingram and Larouche 1987, Macdonald *et al.* 1995, Pfirman *et al.* 1995a). Thus, for most of the year in the Arctic, river runoff enters the ocean under an ice cover. In shallow estuaries (<2 m) ice growth may interfere with inflow in late winter. Under these conditions, the water 'leaks' into the offshore through ero-

sional channels (strudel scour), or in pulses modulated by tidal lifting of the ice (Reimnitz and Kempema 1987). Despite substantially reduced inflow over winter (Antonov 1970, Ingram 1981, Pavlov and Pfirman 1995), estuarine river plumes may be thicker, extend farther offshore and maintain integrity over a larger area because of the ice cover (Ingram 1981).

The lack of wind mixing when ice has formed leads to very sharp vertical stratification with an almost completely fresh layer floating above the salt water. For example, Macdonald *et al.* (1995) were able to account for virtually all of the winter inflow from the Mackenzie River as a large, 5 m thick, 80 km^3 lake under the ice on the inner shelf at the end of winter. The salinity gradient in the estuary becomes extremely strong in the vertical (30 psu over several centimeters) and extremely weak in the horizontal (10 psu over 60 km) (Macdonald and Carmack 1991). The strong vertical stratification can lead to the production of frazil ice at the saltwater interface. This occurs because the freezing temperature of salt water is lower, by as much as 2°C, causing heat to diffuse out of the freshwater layer which is already at its freezing point. Because particle supply is reduced at this time of year, it is expected that contaminant scavenging will be weak and the river water will maintain much of its contaminant load. A significant portion (15% or more) of the winter inflow is incorporated into the growing ice cover in the estuary during winter (Macdonald *et al.* 1995).

During spring break-up, the passage of the powerful flood wave is often accompanied by the deposition of large quantities of ice on the banks and floodplains of rivers. However, the fast ice cover remains in place in the Ob and Yenisey estuaries through the month of June (e.g., Pfirman *et al.* 1995a). Due to the massive discharge of water, the turbidity maximum will move seaward resulting in sediment and contaminant accumulation farther out in the estuary. With the arrival of break-up, the nearshore opens, ice melts, and the accumulated winter inflow is then free to mix as a pulse into the outer shelf during the spring biological bloom.

3.4.7. Contaminant fate

Contaminants strongly sorbed to particles will tend to deposit with the particles within the estuary, and are often found to accumulate at the turbidity maximum. Contaminants with strong particle affinities include PCBs, DDT, lead, and many other metals. Coagulation of colloids also may be implicated in the removal of some dissolved metals (e.g., for Pu, Shen *et al.* 1983, Sholkovitz 1983). For example, although Baskaran and Naidu (1995) observed elevated levels of Pu and ^{137}Cs in surface sediments of the Yenisey estuary, they noted that it was not possible to determine whether the Pu came from coagulation of dissolved Pu, or from simple deposition of particulate material. Such nonconservative contaminants (Dai and Martin 1995) have complicated behavior in estuaries, where the conditions change so radically (i.e., from freshwater to salt water, from high- to low-particle concentration, from well-mixed to stratified, from a shallow regime with constant resuspension in the river to a deeper regime, often dominated by settling). This complexity is compounded in the Arctic by the strong seasonality, resulting in shifts in physical and chemical conditions.

There is a significant difference between summer and winter regimes of estuarine zones which affect contaminant fate. The summer regime is characterized by the most intensive chemical and biological processes and sedimentation rates, as well as maximal discharge of river waters and fluxes of suspended and dissolved matter (55-60% of total annual). The major portion of the suspended matter is trapped and deposited during this season. These sediments may be remobilized during autumn storms, especially in the nearshore (Hill and Nadeau 1989). The winter regime is characterized by increased ice cover of river and sea surfaces, this reducing wind-induced mixing. In addition, a sharp reduction of river discharge and fluxes of suspended and dissolved substances (10-15% of total annual) occurs. The wintertime reduction of biological activity results in less bio-filtration. Although material fluxes are reduced in winter, concentrations of contaminants may be higher than in summer.

Conservative contaminants dissolved in river water mix in the same way as salinity, and are discharged from the estuary. The flushing time of the estuary, that is the length of time required for the estuary to exchange its water, determines how rapidly such wastes are moved out to sea and diluted.

Fast ice often melts in place, releasing its sediment and associated contaminant load (e.g., Reimnitz and Bruder 1972). Fast ice that does drift away from the Kara Sea coast during the summer is likely to melt within the confines of the Kara Sea, perhaps redistributing some incorporated contaminants. Some river-influenced ice may also be exported from the sea, resulting in a wider distribution of incorporated contaminants.

3.5. Ocean

3.5.1. Introduction

The ocean has been for a long time the final resting place for many anthropogenic waste materials. Because of its huge volume, the ocean has been thought a safe place for disposal which would not pose any danger to humans. This view has to be reconsidered. Today, the ocean water column carries too many signatures of our society: radioactive isotopes, such as strontium and cesium, produced during nuclear-bomb detonations and in nuclear fuel reprocessing plants; pesticides, including DDT and its degradation products which have been found in all ocean organisms analyzed; chlorofluoromethanes (freons) which have been measured in the deep waters of the ocean; petroleum products which soil the surface of the ocean; and so on (e.g., Goldberg 1975, Dahlgaard *et al.* 1986, Krysell and Wallace 1988).

Once a contaminant has been introduced into the marine environment it becomes a matter of interest to determine where this contaminant goes and how its concentration varies with time and location. The processes by which contaminants are dispersed in the ocean fall into two basic groups: advection and dilution. Advection transports contaminants from one place to another, while dilution reduces its concentration by mixing (Williams 1979). To be able to understand environmental changes in the Arctic Ocean, it is important to have a good assessment of the present situation, as well as data on which chemicals are being added, subtracted, and transported from one place to another. The following sections describe transport routes and mixing processes that play a role in the redistribution of contaminants.

Contaminants can be delivered, distributed, or removed from the Arctic by different pathways. Atmospheric circulation brings contaminants into and out of the area on a very short time scale (section 3.2). Rivers, streams, and groundwater from the surrounding land (section 3.3) carry their contaminant burdens to the margins of the ocean, where they will be further distributed by ocean currents or by ice. Drifting ice may transport the contaminants into or out of

the Arctic Ocean (section 3.5.3). The North Atlantic Drift (the extension of the Gulf Stream) brings contaminated water from the Atlantic Ocean into the Arctic; the East Greenland Current and currents of the Canadian Arctic Archipelago bring the water back to the Atlantic Ocean once having circulated in the Arctic; a small inflow of water of North Pacific origin enters the Arctic Ocean through the Bering Strait, passes through, and leaves primarily through the Canadian Archipelago (section 3.5.4). Surface-inserted contaminants enter the deeper water column at locations of deep-water formation (section 3.5.4.6). In addition, living organisms within the marine environment may transport contaminants from one place to another.

From scattered observations and deductions based on interpretation of Arctic processes, the following can be postulated (Roots 1982):

1. A considerable proportion of the dissolved and colloidally suspended material, organic or inorganic, which is delivered to the North Atlantic Drift eventually reaches the Arctic Ocean.
2. Material reaching the Arctic Ocean in solution or suspension normally spends several years (and probably much longer if entrained in the Beaufort Gyre) circulating under very stable oceanographic conditions, mainly under an ice cover where photosynthetic reactions and gas exchange are much reduced. The extreme stability of the oceanic stratification probably retards the mixing of contaminants with deeper layers of water, but ensures that those which do reach deeper levels stay there.
3. Airborne contaminants which are deposited on the surface of the Arctic Ocean (typically originating from northern mid-latitude industrialized areas) become trapped on the surface of the sea ice, get flushed into the layer of comparatively fresh water that floods the ocean surface, undergo repeated freezing and melting, and, in general, have less interaction with other oceanic constituents than would similar contaminants in most other oceans.
4. Contaminants and introduced material which remain in or on the surface layers eventually get delivered to the North Atlantic Ocean, less reduced or altered by biological action or chemical interaction than would be the case after the same length of time in oceans at lower latitudes.
5. Material that reaches abyssal depth in the Arctic Ocean appears likely to stay there for very long periods of time due to the semiclosed nature of the basins.

3.5.2. Sources of contamination

Contaminants are delivered to the Arctic marine environment by rivers, ocean currents, atmospheric deposition, domestic and industrial out falls and direct storm runoff, dumped material, and contamination from ships. The marine environment also receives contaminants from secondary sources, such as glaciers and snow and ice melt. In this section, the most important sources for contamination of the ocean are briefly described. A more detailed description of atmospheric and riverine sources is provided in sections 3.2 and 3.3.

3.5.2.1. Rivers

Being nearly landlocked, the Arctic Ocean receives a variety of materials from the surrounding continents, including both anthropogenic and naturally-occurring constituents. Contaminants discharged to rivers will most noticeably influence the coastline and nearby seas.

Ten percent of all riverine discharge to the world oceans occurs in the Arctic. The total discharge is about 3300 km^3/y (Aagaard and Carmack 1989). The Arctic rivers Yenisey, Ob, and Lena are ranked as 5, 6, and 7 in the world, respectively, in order of annual discharge, and the Canadian rivers Mackenzie and Yukon are ranked as 11 and 18, respectively (Goldberg 1976).

Siberian rivers discharging into the Kara, Laptev, and East Siberian Seas have a huge combined drainage area of 9 000 000 km^2 extending far to the south (Shiklomanov and Skakalsky 1994), encompassing many industrial and agricultural regions. The Ob River and its tributaries originate as far south as 45°N (Futsaeter *et al.* 1991). While most smaller rivers are frozen in the winter, some of the major rivers discharge year round as discussed extensively in section 3.3. A unique characteristic of the Arctic Ocean is that the riverine waters can be traced throughout the Arctic Basin due to the extensive ice cover which minimizes mixing.

3.5.2.2. Glaciers

Atmospheric tests of nuclear weapons and nuclear accidents contributed to generally elevated levels of radionuclides in snowfall during the 1950s and 1960s. Because the former Soviet Union used Novaya Zemlya as a nuclear test site, nearby regions, especially glaciers on Novaya Zemlya, Franz Josef Land, Svalbard, and Severnaya Zemlya may be expected to contain elevated levels of radionuclides. Jaworowski (1989) provides some data on levels of radionuclides in glacier ice from Spitsbergen showing that there are elevated levels of ^{137}Cs in ice layers dating from 1955, 1958, and 1965.

Corresponding with these peaks in radioactivity are elevated levels of uranium, vanadium, lead, and cadmium due to sorption onto particles. Heavy metals deposited from Arctic haze similarly are known to accumulate in glacier ice in the circumpolar Arctic (Jaworowski 1989). These contaminants are discharged from glaciers when icebergs calve, and are released to the marine environment upon melting. However, this period of contaminated ice accumulation (i.e., the last 50 years) represents a minor fraction of the total ice in these glaciers (perhaps <1%) so the contribution from this source is likely minor.

3.5.2.3. Atmospheric deposition

Emissions to the atmosphere are returned to the land or the sea as wet and dry fallout as discussed above. Atmospheric transport is recognized as a major route for the transfer of contaminants to the ocean (GESAMP 1985). The time it takes for a contaminant released to the atmosphere on any continent to reach northern waters ranges from days to a few weeks, as compared to years by means of oceanic circulation (Gaul 1989).

Radioactive cesium, strontium isotopes, tritium, and krypton 85 have been deposited from the atmosphere to the ocean as a result of atmospheric weapons testing and nuclear power plant operations in the 1950s and 1960s (Rozanski 1979, Broecker *et al.* 1980, Smethie and Swift 1989). Atmospheric contributions of OC compounds, such as PCBs and DDT, remain significant today. They are released into the atmosphere in the vapor phase and are transported as gases, aerosols, and adsorbed to particles (Duce *et al.* 1983). Eventually, the more persistent contaminants are permanently deposited in the sea floor sediments, but only after cycling through the water, biota, sediments and ice, perhaps many times. Once introduced

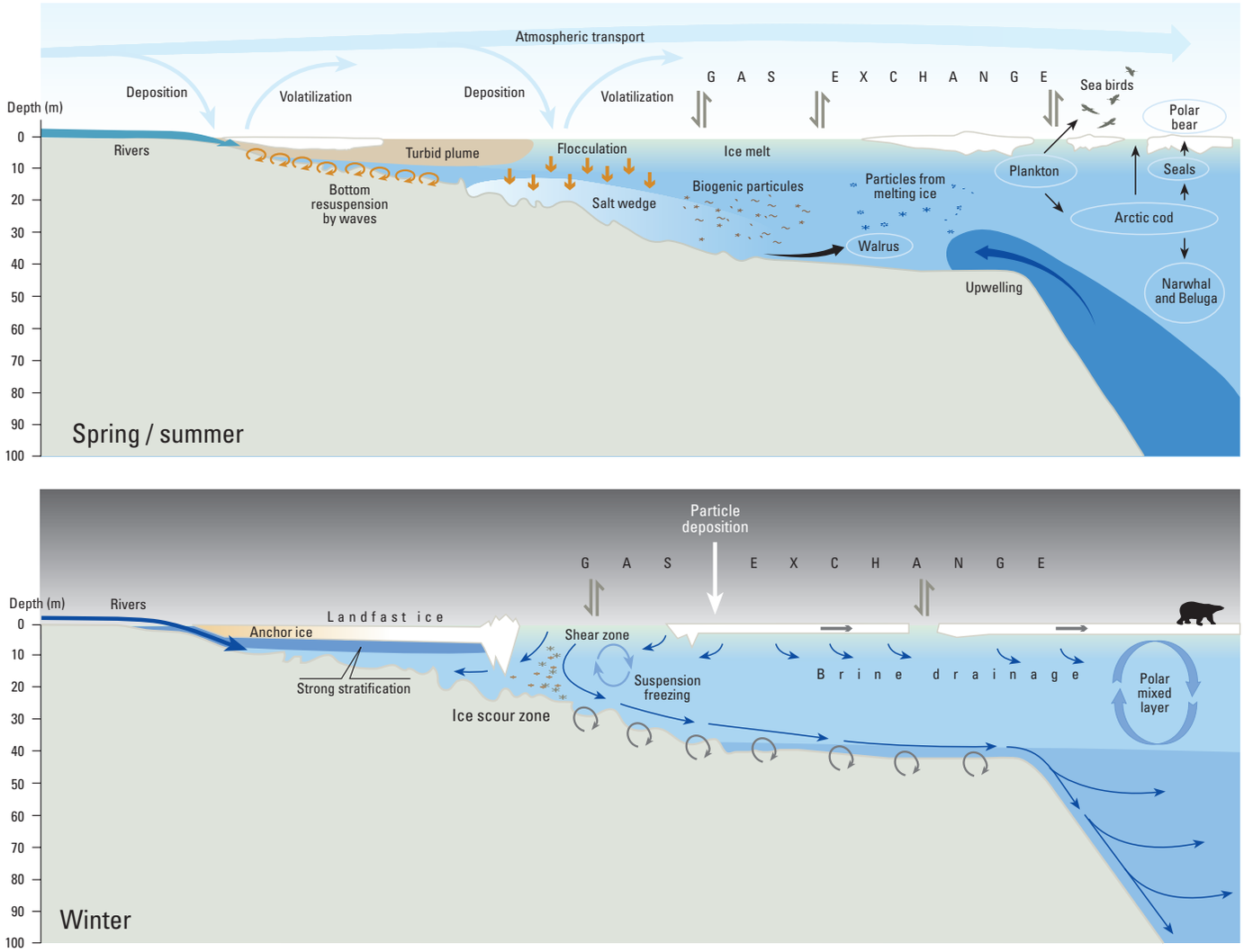

Figure 3·22. Schematic representation of shelf processes involving transport of contaminants and sea ice.

into aquatic environments, synthetic organics partition to all components of the ecosystem. The insecticide DDT, found in the fat of polar bears, is a good example (Ballschmiter and Zell 1980).

In winter and spring, the Arctic atmosphere contains high levels of contaminants from Eurasia, and to a lesser extent from North America, known as Arctic haze. As contaminated particles settle out of the atmosphere, sea ice acts as a lid on the surface of the Arctic Ocean (Figure 3·22). Each year that ice floes drift, contaminants and other materials are deposited on its surface from the atmosphere in the form of snow, rain, fog, and dry deposition (Pfirman *et al.* 1995a, Chernyak *et al.* 1996). Heavy metals accumulating in the snowcover of central Arctic sea ice can reach values that are characteristic of snow deposits on sea ice near Siberian industrial areas (Melnikov 1991). Contaminants deposited on sea ice by atmospheric transport could percolate into the ice surface when meltwater refreezes, and could also be added to the ice underside when meltwater runs off and refreezes. During drift, contaminants concentrated in the oceanic surface microlayer may also be incorporated in the ice (Gaul 1989).

Volatilization

The presence of sea ice in the Arctic Ocean generally inhibits ocean-atmosphere exchange. This is important because many contaminants, such as OCs, are semi-volatile. In winter, when surface water is being convected, the ice acts like a lid, keeping volatile contaminants introduced below it from entering the atmosphere as discussed for river and lake ice in section 3.3.4.6. In summer, stratification of the surface ocean from sea-ice melt or river runoff limits atmospheric exchange to the top 5-10 m. Contaminants discharged in river water and frozen into the sea ice may not be released until the ice breaks up and melts. For example, oil released under the ice is degraded slowly until the ice breaks up (see chapter 10). Polynyas and leads – places where there are breaks in the ice cover – may represent regions for exchange of volatile compounds including OCs (Barrie *et al.* 1992).

Because volatilization increases with temperature, some chemicals deposited from the atmosphere on the ice surface in winter are released back to the atmosphere in the summer when the surface warms and the snow melts (Barrie *et al.* 1992). If deposition occurs on drifting sea ice, release may occur far from the original incorporation location.

3.5.2.4. **Dumping, direct discharge, and accidents**

Contaminants are dumped at sea in designated dumping grounds. The 1972 London Dumping Convention regulates all dumping at sea. Sea dumping of radioactive solid wastes has been practiced since 1946. The Kara and Barents Seas have been the dumping grounds for radioactive waste for the former Soviet Union. Both shipping and oil production contribute to the input of petroleum hydrocarbons to the sea.

The introduction of radioisotopes to the seas of northwestern Europe from industrial installations began in 1952 with discharges from Windscale Works (now Sellafield Works) into the Irish Sea and from Cap La Hague into the English Channel/North Sea. Municipal and industrial wastes, often untreated, are discharged directly to the marine environment. Records of the chemical nature of these discharges are frequently not available.

Contaminants may also be introduced to the marine environment through accidents. Industrial ship traffic and oil exploitation, especially in icecovered areas, should be considered as potential sources.

3.5.2.5. Geology: resuspension and mass flows

Many contaminants of concern are particle reactive, meaning that they are commonly attached to mineral or organic material. The sedimentation of these particles transports contaminants to the sea floor. If accumulations of contaminated sediments are disturbed, contaminants may be resuspended, transported, and deposited elsewhere.

Some contaminants have a low solubility in water and tend to be adsorbed on particulate matter. Fine-grained sediments, with their larger surface area, tend to have greater concentrations of such contaminants than do coarse-grained deposits.

Sedimentation rates in the open ocean may be a thousand times less than coastal deposits. Particles transported to the central parts of basins are generally associated with atmospheric transport, deep ocean currents, ice transport (sea ice and/or icebergs), and biological productivity. In addition to these sources, coastal waters receive matter directly from terrestrial runoff and therefore usually have higher sedimentation rates (Goldberg 1976).

Potentially contaminated particles may be transported off Arctic shelves via mass flows (e.g., submarine landslides, such as slumps, slides, and turbidity currents), as well as in bottom nepheloid layers caused by resuspension by near-bottom currents.

3.5.3. Ice

3.5.3.1. Ice and icebergs

River ice

The potential for contaminant delivery by river and lake ice transported downstream by rivers has been discussed in section 3.3.4. Spring break-up of river ice can be a violent event in addition to being the largest annual hydrologic event. The release of water stored behind ice dams can result in massive discharges of water and ice causing gouging and erosion of river bed and overbank sediments, especially in deltas.

River ice discharged to the marine environment most likely melts and deposits incorporated material in the nearshore zone (Reimnitz and Bruder 1972). This happens because the main period of discharge is during June, when the Arctic summer starts and ice in the marginal seas is just beginning to melt. Where river break-up occurs before there is much melting of the shorefast ice, river water may flow out over the ice, depositing its sediment load on the surface (Reimnitz and Bruder 1972). Because the presence of this surficial sediment effectively lowers the albedo of the ice, it melts rapidly in early summer. In part because of the discharge of river water and ice, river estuaries are usually centers of initial ice melting (Zubov 1943). The river water is warmer than the <0°C shelf water, and rapidly melts sea ice in a region near the river mouth (Antonov 1970, Dean *et al.* 1994). Also, particle-laden river ice has a lower albedo, and therefore melts more quickly than cleaner ice.

Another factor contributing to retention of river ice in the nearshore zone is extensive fast ice cover. This ice is anchored both to the coast and to shallow offshore banks, forming a barrier to offshore transport of the ice that is released behind it. Particle-laden river ice, as well as ice influenced by accumulation of coastal sediments, is largely retained near shore in this way.

Some river and shore fast ice does make its way past these barriers, survives transport across the shelf and is incorporated in the large-scale drift of the Arctic ice pack. At present, there is not enough information on this transport pathway to actually quantify the amount of river ice that is incorporated in the Arctic ice pack.

Sea ice

The area covered by sea ice in the Arctic varies seasonally (Figure 3·23), from 16×10^6 km^2 in March to 9×10^6 km^2 in September (Gloersen *et al.* 1992). The maximum limit of the marginal ice zone extends as far south as 50°N in the Sea of

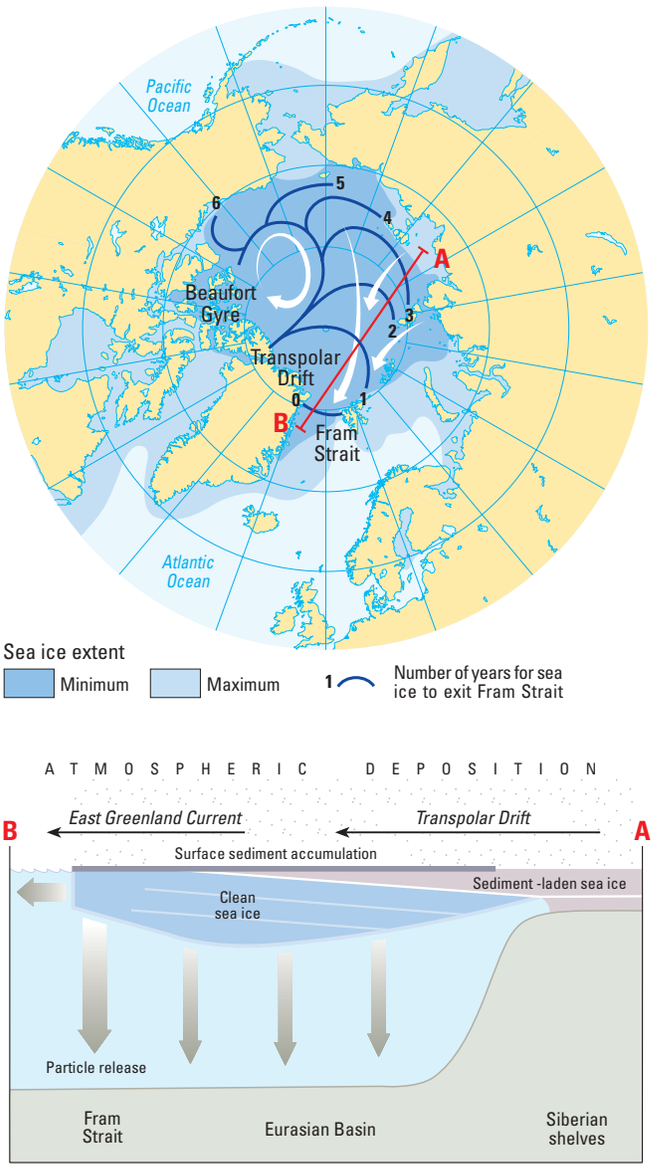

Figure 3·23. Average annual maximum and minimum sea ice extent. The numbered lines show the expected time in years for the ice at that location to exit the Arctic Ocean through the Fram Strait, based on drifting buoy data during 1979-1990. The lower panel shows a schematic representation of ice growth, surface melting, and sediment accumulation during drift of a hypothetical ice floe (Source: Rigor 1992).

Okhotsk and the Labrador Sea, but also as far north as 75°N in the Norwegian and Barents Seas.

There are decadal and inter-decadal fluctuations in the areal sea-ice extent in the Arctic. Shpaiker and Yankina (1971), Mysak and Manak (1989), Zakharov (1994), and Gloersen (1995) attribute these changes to atmospheric pressure anomalies, variations in continental discharge, and El Niño/Southern Oscillation events which influence the influx of Atlantic and Pacific waters. Zakharov (1994) notes that there appears to be a four-year lag between variations in total continental discharge and ice extent in the northern Eurasian Basin.

Formation and melting

Late summer storms are critical to the freezing process, which depends on the temperature contrast between air and ocean water, as well as on the magnitude and distribution of heat in the surface layer. Storms extract heat from the ocean and mix the remaining heat more uniformly and to a greater depth in the water column. New ice formation is first evident in shallow bays, where heat is quickly extracted as the rate of heat loss to the atmosphere increases (Barrie *et al.* 1992).

During sea-ice formation, individual ice crystals develop first, forming spicules called frazil ice. The crystals coagulate to form a solid sheet, or, where agitated by waves or currents, a soupy surface layer called grease ice. With continued freezing, the grease ice forms nilas – thin elastic sheets of ice, or, where there are waves, pancake ice. Pancake ice consists of circular pieces about 0.3-3 meters in diameter with raised rims on the edge produced when the 'pancakes' strike against one another (Parkinson *et al.* 1987).

Continued cold temperatures lead to consolidation of the ice cover. Further thickening of the cover occurs by downward growth of ice crystals, forming columnar ice underneath the surface layer of frazil ice. When the ice section is about 0.3 m thick, it is called first-year ice. Because sea salt is largely excluded during the freezing process, the salinity of young sea ice far from river outlets is about 5 in comparison with surface ocean waters which typically have salinities greater than 34. As sea ice ages, it continues to lose salt because brine that was trapped in the rapidly growing frazil ice drains from it (Parkinson *et al.* 1987).

By the end of the winter, first-year sea ice, generally less than 2 m thick, covers much of the shelf seas (Figure 3·23). In summer, this ice melts, thins, and often moves offshore. If the ice survives the next summer's melt season, it is called second-year ice. Multi-year ice refers to ice that has survived two or more melt seasons. Multi-year ice covers much of the central Arctic and east Greenland areas, and is often thicker than 3 m.

During several years of melting and freezing, the original ice floe is modified substantially (Pfirman *et al.* 1990). Each summer, all of the snow and between 32 and 70 g/cm^2 of ice melts off the surface (average is 40 g/cm^2, Hanson 1965, Romanov 1992). Water produced by the melting snow percolates into the floe surface, accumulates in melt ponds, runs off the floe, and may refreeze on the ice underside, redistributing some contaminants originally located on the ice surface. Extensive surface melting results in formation of meltwater ponds which may cover 25% of the ice surface by mid-July.

Some dissolved and particle-associated contaminants are also lost to the water column with the meltwater. Each winter, more ice is added to the underside of the floe. As a result, while the floe thickens with time, the original first-year ice section, perhaps 1.5 m thick, eventually will melt entirely. Particles, entrained within the ice during formation on the shelves, eventually melt out and often accumulate on the ice surface (Figure 3·23). Zubov (1943) stated that every particle frozen into the ice from below will appear on the surface in two to three years. Because of their darker color, particles near the ice surface absorb more solar energy and melt the ice around them, forming accumulations in pits, called cryoconite holes.

Winds and ocean currents keep most of the ice in constant motion. As a result, the ice is broken up into floes, with open water spaces between the floes. In the central Arctic drift ice, such leads – roughly linear regions of open water between floes – reduce the ice cover to 80-90% in summer from 99% in winter (Gow and Tucker 1990).

Fast ice

Fast ice grows seaward from a coast and remains in place throughout the winter (Figure 3·24). Typically, it is stabilized by grounded pressure ridges at its outer edge, and therefore extends to the draft limit of such ridges, usually about 20-30 m water depth (Wadhams 1986a). Fast ice is environmentally important for several reasons: 1) it hinders and increases the risk to vessel traffic along the coast and through straits resulting in, for example, spills; 2) contaminants in sea floor sediments may be protected from redistribution under the shelter of the ice cover (Pfirman *et al.* 1995); 3) freshwater discharged under the fast ice by some rivers in winter is impounded by the fast ice to a near shore plume (Macdonald *et al.* 1995); 4) it provides a platform for migration of species; and, 5) grounded fast ice disturbs the sea floor.

Polynyas

Polynyas are open water regions ranging in area up to thousands of square kilometers. Flaw leads (also called coastal polynyas) occur at the fast ice border where offshore winds separate the drift ice from the pack ice (Figure 3·24). Polynyas and flaw leads are environmentally important for several reasons: 1) the open water provides opportunities for air/sea exchange of semi-volatile contaminants, such as organochlorines (Barrie *et al.* 1992); 2) they are a source of moisture to the surrounding areas (Müller *et al.* 1976); 3) they typically form the locus of spring ice break-up in late-April to mid-May as an expansion of the flaw leads and polynyas (Barrie *et al.* 1992); 4) they are often locations of intense biological activity where contaminants may be taken up into the food chain; 5) sea ice often forms there in great quantities, perhaps incorporating contaminants (Pfirman *et al.* 1995a); and, 6) dense brines developing from sea-ice formation may result in redistribution of contaminants to the bottom waters in basins (Pfirman *et al.* 1995a).

Important polynyas include (Stirling and Cleator 1981, Parkinson *et al.* 1987): the North Water polynya of Smith Sound (northern Baffin Bay); a polynya off the Bering and Chukchi Sea coasts of Alaska and adjacent islands; the flaw lead off east Greenland; a polynya north of the New Siberian Islands; the flaw leads of the Kara, Laptev, and East Siberian Seas; a polynya around Franz Josef Land; and, a polynya in the Beaufort Sea (Figure 3·24).

Glaciers

The largest glacier ice mass in the Arctic is on Greenland, where ice covers an area of 1800 000 km^2, which is nearly 85% of the land area (Encyclopedia Britannica 1990). Along the coasts of Greenland, Svalbard, Franz Josef Land, Severnaya Zemlya, and the north island of Novaya Zemlya, outlet glaciers terminate in the sea (Solheim and Pfirman 1985, Encyclopedia Britannica 1990, Romanov 1992). These glaci-

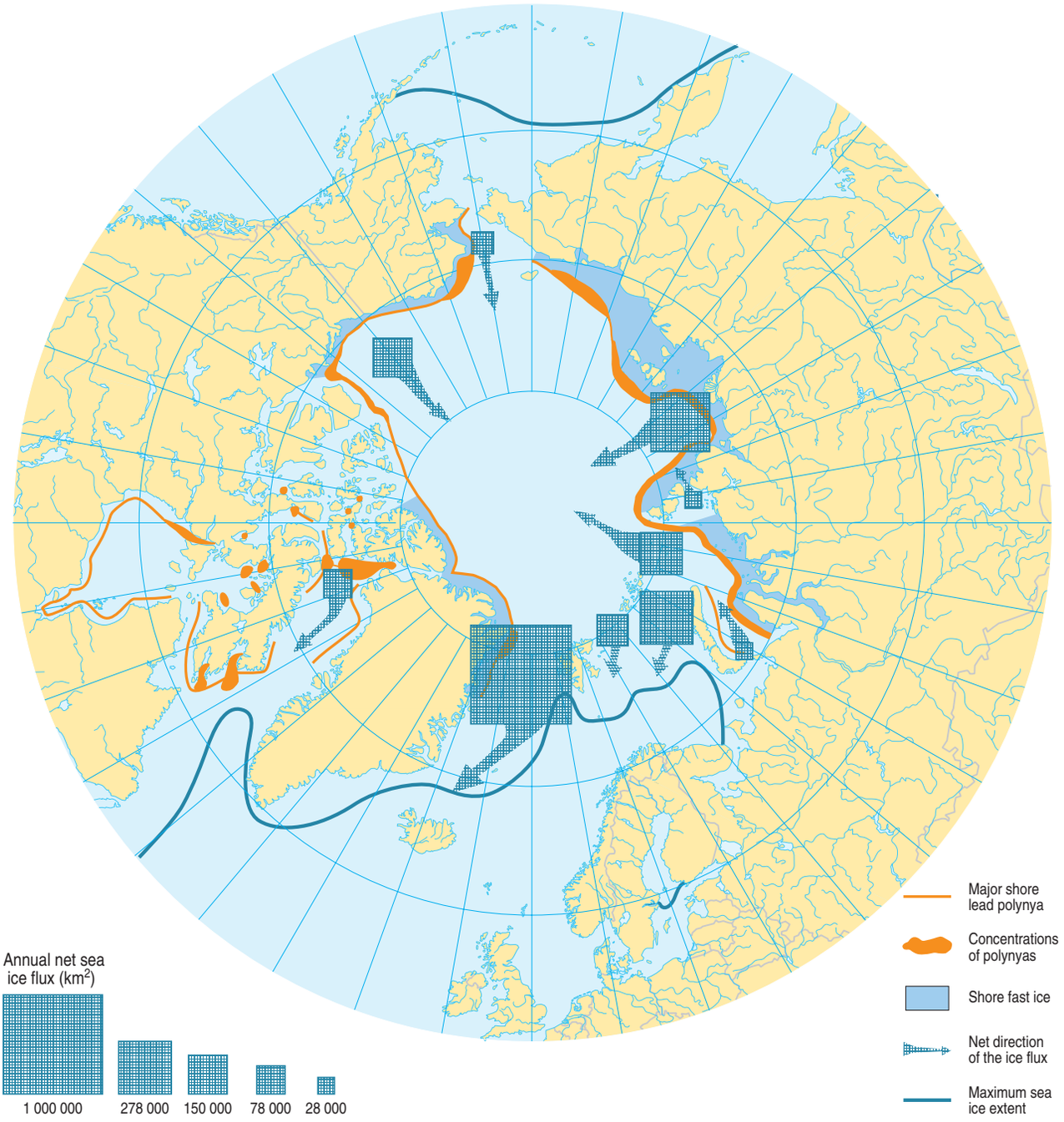

Figure 3·24. Approximate net sea ice exchange (see legend for key to arrow sizes), extent of shore fast ice and winter sea ice, and coastal polynyas and main polynya concentrations. (Source of ice flux data: Zakharov 1976, Vinje 1987, Aagaard and Carmack 1989, Kvambekk and Vinje 1993, and Kotchetov *et al.* 1994; shore-fast ice extent on Siberian shelf after Buzov 1991).

ers periodically break off, or calve, forming icebergs, many of which drift into the North Atlantic Ocean (Figure 3·25). Some 12 000 bergs are calved annually from tidewater glaciers on west Greenland. The most productive of these glaciers is at Illulissat and it contributes an estimated 20×10^6 tonnes of freshwater per day. This is equivalent to a medium size river with a mean annual discharge of 230 m^3/s.

In the Canadian Arctic, tabular and glacier ice is formed in several locations, the most important being the Ward Hunt Ice Shelf off Ellesmere Island and fjords on the north coast of Axel Heiberg Island (Jeffries 1987a, Jeffries *et al.* 1989). The Ward Hunt Ice Shelf has been the source of a number of large tabular ice islands of deep draft (40-50 m) like T3 and, more recently, Hobson's Choice. Between 1983 and 1986, it is estimated that about 25 such ice islands were sighted along the coast of the Queen Elizabeth Islands (Jeffries 1987b). Upon breaking off from the main body of the shelf, the ice islands tend to circulate with the Beaufort Gyre, often completing several circuits before leaving the Arctic Ocean in the Transpolar Drift (Jeffries and Shaw 1993). Some of this tabular ice can enter the Canadian Archipelago where it would eventually disintegrate and melt, but in only one known example has an ice island drifted eastward after calving (Jeffries and Shaw 1993). Icebergs ground close to shore in fjords or are melted on the shelves. They work their way out of fjords from July to September, when coastal regions are often free of sea ice. The role of icebergs and ice islands in disturbing or moving sediments is minor compared to sea-ice pressure ridges. Nevertheless, icebergs and ice islands do pose environmental concerns, for example: 1) they are a hazard to vessel traffic; 2) they can disturb the sea floor when they ground, potentially stirring up contaminants as well as disrupting dumpsites and perhaps rupturing containers (see section 3.5.3.2); 3) they can

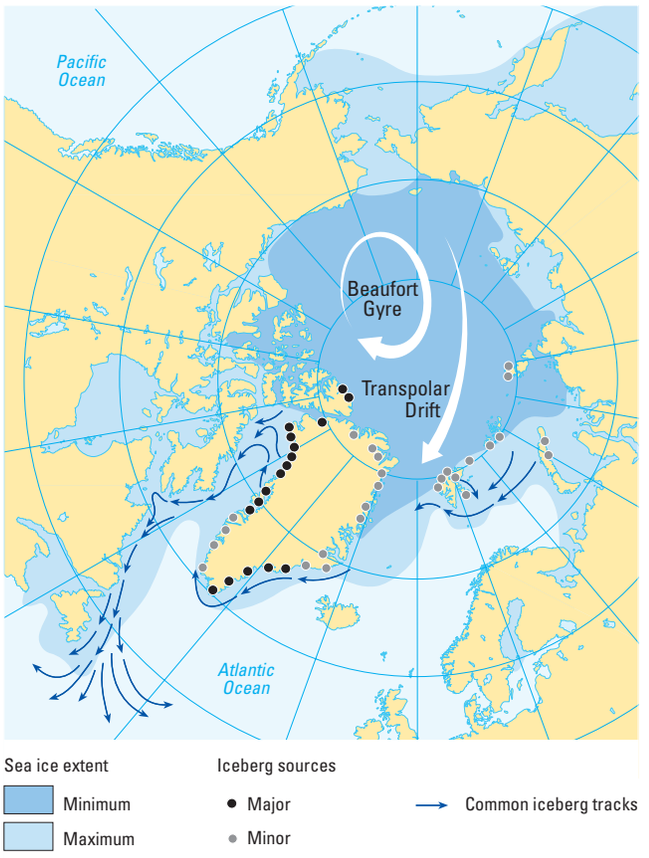

Figure 3·25. Main sources of icebergs and common iceberg drift trajectories. The main ice circulation pattern follows the Transpolar Drift in the eastern Arctic and the Beaufort Gyre in the western Arctic (white arrows) (Source: Sugden 1982).

pose a threat to bottom structures and other equipment used for oil/gas exploration and exploitation (Sackinger *et al.* 1985); and, 4) they contain contaminants deposited from the atmosphere which will be released to the sea surface when they melt although we consider this to be minor due to the fact that the bulk of the ice pre-existed the period of major release of contaminants of concern to AMAP.

Ice drift

Much of the central Arctic drift ice forms in winter in the marginal seas, especially in the wide Siberian Shelf seas, such as the Laptev and the Kara. Ice usually forms over the outer shelf region, because along the coast there is a band of fast ice anchored to the sea floor and/or the shore. A coastal polynya or a flaw lead often exists between the fast ice zone and the drift ice (Figure 3·24).

The two main ice circulation systems are the clockwise Beaufort Gyre in the Amerasian Arctic and the Transpolar Drift in the Eurasian Arctic (Figure 3·25). The Transpolar Drift transports ice primarily from the Kara, Laptev, and East Siberian Seas, toward the Fram Strait, where it exits the central Arctic Basin (Colony and Thorndike 1985). The Beaufort Gyre recirculates ice formed in the Beaufort, Chukchi, and East Siberian Seas, as well as some ice from the Transpolar Drift.

Changes in ice circulation patterns may be related to fluctuations in continental discharge and ice extent, as well as to variations in atmospheric conditions. Over approximately decadal periods, there is an out-of-phase relationship of atmospheric pressure between the Beaufort/Chukchi Sea region and the Greenland Sea (Walsh and Johnson 1979, Mysak and Manak 1989). Kotchetov *et al.* (1994) have documented two different ocean circulation patterns, roughly similar to ice drift patterns (Colony *et al.* in press): a) a large Beaufort Gyre (Figure 3·23), forcing the Transpolar Drift southward with a modest Laptev Gyre, resulting in increased water and ice export to the Greenland Sea and export of ice from the Siberian seas, or b) large gyres in the Chukchi Sea and north of the Laptev Sea, with a reduced Beaufort Gyre, resulting in recirculation of ice and expanded distribution of multi-year floes.

Icebergs released in the Siberian seas may be advected off the shelf to be transported in the Transpolar Drift across the Arctic to the East Greenland Current in the Fram Strait. Here, they join icebergs calved from east Greenland.

Sea ice as well as icebergs released along the west coast of Greenland are advected with the West Greenland Current northward in Baffin Bay. Some ice crosses over to the western side of the bay, and returns southward along the coast of Baffin Island. Continuing to the south, ice is advected in the Labrador Current to the south of Newfoundland (Figure 3·25). Although many icebergs ground or melt during transit, as many as 1400 icebergs have been documented to reach 48°N in one year (Groen 1969). The average number is 386, and such bergs typically have lost about 90% of their mass since calving along the Greenland coast.

Residence time

Transport from the Laptev Sea to the Fram Strait typically takes about three years in the Transpolar Drift (Figure 3·23). Kara Sea ice incorporated in the Transpolar Drift may exit through the Fram Strait in two years (Rigor 1992), while transport to the Barents Sea takes less than a year. Ice in the western Arctic, contributed from the Beaufort, Chukchi, and East Siberian Seas (Figure 3·23), is often incorporated in the Beaufort Gyre where it may circulate for more than five years (Thorndike 1986).

Some ice from the Transpolar Drift may also be entrained in the Beaufort Gyre and recirculate for long periods of time, however, the amount of exchange between the two circulation systems is not well known.

Fluxes

The main exit for ice in the central Arctic is through the Fram Strait (Figures 3·23 and 3·24). Each year, about 2600 km^3 of sea ice (representing about 1 million km^2) is exported through this region in the East Greenland Current (Kvambekk and Vinje 1993).

Within the Arctic region, the combined actions of winds and currents cause large seasonal variations in the transport of ice, both onto and off of the shelves. While Cavalieri and Martin (1994) have made synoptic assessments of sea-ice production in polynyas, estimates of shelf-basin ice fluxes are much cruder, based on different years and use of varying methodology. The Laptev Sea discharges the most ice each year to the Arctic Ocean, from 256 000 km^2/y (Rigor and Colony in press) to 350 000 km^2/y (Zakharov 1976). This is followed by the Kara Sea at 180 000 km^2/y. Export from the Barents Sea to the Arctic Ocean is estimated to range from 17 500 to 100 000 km^2/y (Zakharov 1976, Vinje 1985). The flux of ice (measured in km^3/y) depends on the thickness of the ice.

There are seasonal variations in ice exchange. Both the Barents and Kara Seas export ice to the Arctic Basin in winter and import ice in summer (Zakharov 1976). According to Vinje (1987), approximately 629 km^3/y of ice is exported from the Kara to the Barents Sea through the strait between Franz Josef Land and Novaya Zemlya in winter. During June, July, August, and September, 72 km^3 of ice are imported from the Barents Sea (Vinje 1987), for a net flux of

557 km^3 (278 500 km^2, assuming an ice thickness of 2 m). Other sources indicate that the net annual flux from the Kara to the Barents through this strait could be as low as 198 km^3 (Pavlov *et al.* 1994).

Ice exchange also occurs to the south in the Karskiye Vorota Strait, through which there is a 98 000 km^2 flow from the Barents Sea to the Kara Sea each year from December to April, and 21 000 km^2 flow back to the Barents Sea during the same months (Kuznetsov 1983). Zubakin (1987) estimated the annual net flux from the Barents Sea to the Kara Sea in this region to be about 16.8 km^3/y assuming an ice thickness of 0.6 m (equivalent to 28 000 km^2 of ice). Net flux from the Kara Sea to the Laptev Sea through the Vilkitsky Strait is about 50 km^3/y (ca. 28 000 km^2 based on an ice thickness of 1.8 m).

Although much of the sea ice in the Barents Sea forms locally, it also receives ice from the Kara Sea and the Arctic Ocean. More than 40% of the ice may be multi-year (Loeng and Vinje 1979). According to Vinje (1985), who assumed an average ice thickness of 2 m, the Barents Sea imports 37 km^3 from the Arctic Ocean, and exports 72 km^3. Most of the import from the Arctic Ocean is between the months of April and June. Ice coring in the western Barents Sea in May 1989, confirmed that much of the sea ice sampled was imported from elsewhere. Pfirman *et al.* (1995a) suggest that some of the ice could have formed on the Siberian shelf in waters influenced by river discharge. Abelmann (1992), based on analysis of sea-ice diatom assemblages, also concluded that ice sampled east and north of Svalbard in 1987 probably originated in parts of the Kara or Barents Seas that had some river influence.

Import of ice into the Arctic through the Bering Strait is estimated at about 30 km^3/y (Aagaard and Carmack 1989). Up to 155 km^3/y may advect southward through the Canadian Archipelago (Aagaard and Carmack 1989). However, because much ice in the Archipelago is formed locally, the amount of Arctic ice exported through these passages is not well known.

Ice production in the Beaufort Sea has been estimated directly from records of ice thickness (Melling and Riedel 1995) and indirectly from salt budgets in the water column (Melling and Moore 1995, Macdonald *et al.* 1995). The two methods yield similar rates of ice production from 3 to 4.5 m per year. From ice thickness and velocity measurements, Melling and Riedel (1996) calculated that the maximum net export of ice from the flaw lead on the Beaufort Shelf during winter was about 19 km^3, which is only about 60% of the estimate made by Cavalieri and Martin (1994). Prorating this number for the whole Beaufort Shelf, including the area west of Banks Island, gives a regional annual export of ice during winter of about 60 km^3. However, this estimate does not include ice advected to the interior ocean when the shelves clear at the end of winter. If, for example, two thirds of the ice beyond the landfast zone is advected off the shelf in spring, as much as 450 km^3 of additional ice could be exported from the Beaufort marginal seas to the interior ocean.

3.5.3.2. **Contaminant incorporation in ice**

River and sea ice can become contaminated from above by deposition of atmospheric contaminants, as well as from below, for example, when contaminated sediments are entrained.

River ice

River ice may be an important localized source of contaminants to the nearshore zone where the ice is retained frozen or impounded into landfast ice so that it does not move offshore. River discharge can influence the ice pack on the shelf in several ways. Firstly, sediments deposited from the river on the shelf are resuspended during fall and winter storms, and are incorporated in the developing ice cover, as described below. Secondly, the large river water discharge is primarily in June and July, at which time there is still extensive ice cover in parts of the marginal seas, and the river water (including sediment and contaminants) may flow under or over the fast ice, perhaps contaminating it. Thirdly, although river discharge declines in winter, it does not cease in all rivers, so some water may be contributed to ice forming along the flaw polynya during the rest of the year as well.

Sea ice

Contaminants deposited from the atmosphere are added to the surface of sea ice during drift. Ice forming near major atmospheric sources (such as in the Kara Sea north of Norilsk) or under main atmospheric transport pathways will have elevated contaminant loads.

Ice crystals growing in the sea exclude salt, resulting in ice with a lower bulk salinity than the water from which it forms. In this way, soluble salts (Weeks and Ackley 1986) and some contaminants that are dissolved in the water column are likely to be excluded from the ice (Weeks 1994). However, Arctic ice forming over shallow Siberian seas often includes sediments and organic material. Because many contaminants of concern in the Arctic tend to sorb onto particulate material (Stumm and Morgan 1981), particle-laden ice may also be contaminant-laden (Pfirman *et al.* 1995a). On the other hand, sea ice without incorporated sediments or organic material, probably has less of a dissolved contaminant load than the water from which it grew due to the exclusion of salts and other impurities (Weeks 1994).

Sea ice formed over the Siberian shelves incorporates particles predominantly during suspension freezing and frazil ice formation, but also as a result of anchor ice rafting (Reimnitz *et al.* 1992). Most particle-laden ice appears to form in water depths less than 50 m (Reimnitz *et al.* 1993). This is because the energy needed to resuspend sea floor sediments through the water column increases as the depth increases. Also, anchor ice growth requires that the entire water column is supercooled. Another mode of sediment entrainment is when sea-ice ridges moving over shallow areas act as sediment traps, with resuspended sea floor sediments plating on the underside of the ice.

Processes associated with frazil ice formation tend to cause elevated levels of suspended particulate matter in the water column (Kempema *et al.* 1989). Combined with wave activity and scavenging by ice crystals, the initial ice cover may become enriched in particulate matter relative to normal concentrations observed in the underlying ocean water (Ackley 1982, Garrison *et al.* 1983, Reimnitz *et al.* 1990, Shen and Ackermann 1990, Ackermann *et al.* 1994). Particles entrained during frazil ice formation are silt-sized or smaller. The affinity of hydrophobic contaminants for particles tends to increase with decreasing grain size because of the greater surface area of small particles. As a result, contaminant loads of particle-laden sea ice may be elevated over that of the seabed, which typically contains a mixture of coarse as well as fine grain-sized material (Pfirman *et al.* 1995b).

Suspension freezing could also contribute to the elevated levels of organic material observed in Arctic sea ice. Concentrations of suspended organic carbon in sea ice may be two orders of magnitude higher than in seawater (175-560 μg/L compared with 25-45 μg/L in June to August and approximately 5 μg/L during the remainder of the year) (Melnikov and Pavlov 1978). According to these authors, the elevated

levels appear to result from in-freezing of organic material during ice formation on marginal Arctic seas which have higher biological productivity than the central Arctic Basin. When ice melts in summer, some suspended organic material is contributed to the surface seawater (Melnikov and Pavlov 1978). Dissolved organic carbon may also be enriched within the ice cover due to adsorption. Because of association of many contaminants with fine-grained sediment (clay) and/or organic material, incorporation of such material on the shelves provides a process for contaminant enrichment in sea ice formed there.

The formation of cryoconites during the melt season is important because it concentrates the particles as well as retains much, but not all, of the particle load on the ice surface, even when the ice meltwater runs off the floe, or the floe is tipped or submerged during a rafting event. Therefore, drifting ice that originally contained dispersed contaminant-laden particles tends to form concentrated accumulations at the surface as time progresses. Repeated melting at the surface and freezing at the bottom will cause a transport to the surface of embedded contaminants at the same time that atmospheric deposition continues to add contaminants.

Ice scouring

Another process that affects materials on the sea floor, is gouging by sea-ice pressure ridges and icebergs (Weeks 1994). Sea-ice pressure ridges on the Siberian shelves often have drafts of 25 m (Zubov 1943), and have been documented in the Eurasian Arctic extending down more than 40 m (Wadhams 1986b). While recent iceberg gouging in the Barents Sea by bergs calved from glaciers on Nordaustlandet (Svalbard) and Franz Josef Land have affected the sea floor to water depths of 120-130 m (Elverhøi *et al.* 1989), most icebergs observed today are generally less than 100 m thick (Vinje 1985).

The icebergs documented by Pavlov (1993) to the east of the northern island of Novaya Zemlya, may come from here, although according to Zubov (1943), most of the Novaya Zemlya icebergs are trapped in shallow fjords. Severnaya Zemlya is also a source of icebergs to the Siberian seas. Icebergs in the Laptev Sea reportedly ground in water depths up to 183 m (Kovacs 1972).

While ice gouges may penetrate more than 5 m into the sea floor, in the Barents Sea typical plough mark relief is 2-5 m deep and 10-50 m wide (Elverhøi *et al.* 1989). Plough marks are also common on the Greenland shelf and in the Denmark Strait (S. Malmberg, pers. comm., MRI, Reykjavik, Iceland, 1996). Presumably, the most important effects of ice gouging are: 1) the damage that it could do to waste containers resting on the sea floor (Weeks 1994), and 2) the release of contaminants to the water column when sediments are physically reworked by the ice. Materials dumped in the shallow fjords of Novaya Zemlya (Yablokov *et al.* 1993a, 1993b) could be affected by these processes. Sediment transport via adhering and adfreezing to the ice mass is probably not as important for contaminant transport.

3.5.3.3. **Transport and release of contaminants by ice**

Melnikov (1991) considers processes related to sea-ice formation, drift, and ice and snow melting to be among the main factors governing surface ocean metal concentrations in the Arctic. Similarly, Pavlov and Volkov (1993) and Pavlov (1993) note that sea ice formed in the Kara Sea could incorporate contaminants from the sea as well as those deposited from the atmosphere and release these contaminants when the ice melts. This means that contaminants accumulated throughout the fall and winter are released during spring snowmelt and summer sea-ice decay. The melt period coincides with the spring bloom of biological activity, increasing the potential for biological uptake of contaminants (Melnikov 1991). Organisms feeding on the spring blooms may be subjected to elevated levels of contaminants released from the ice (Figure 3·22). Sea-ice transport of contaminants also has the potential to influence other regions, if the ice exits the shelf and drifts within the central Arctic pack ice. In order to assess potential contaminant transport, detailed data are required on both import and export of ice that is formed in regions where it may entrain contaminants.

Because of formation of cryoconites on the ice floe surface, much of its particle load will be released when the entire floe disintegrates during melting. Sediment traps on moorings deployed across the Fram Strait show that the traps located in the marginal ice zone accumulated much more ice-rafted debris than the traps located underneath the ice stream to the west, where there was a persistent ice cover (Hebbeln and Wefer 1991). Therefore, release of contaminant-laden particles is expected to be greatest along the marginal ice zone.

A mitigating factor that may be important for multi-year ice is that during transport, freeze/thaw cycling tends to aggregate particles into pellets on the ice surface (Barnes and Reimnitz 1974, Barnes *et al.* 1990, Goldschmidt *et al.* 1992). These pellets were also observed in sediment traps located under the ice (Berner and Wefer 1990). Pelletization results in increased sedimentation rates of the particles and their contaminant load, moving them out of the surface layer much more rapidly than if they were released as single particles. Very few data are available on particle release from sea ice to determine the relative importance of particle aggregation.

Marginal ice zone and seas

An important point is that the surface accumulation of particles/contaminants is released to the sea surface when the ice melts. This concept is emphasized by Pavlov and Volkov (1993) and Pavlov (1993), who conclude that contaminated drifting ice will 'partially clean' the area of contaminant incorporation, but will also lead to contamination of surface seawater in the region where ice melt occurs. Most melting, and therefore particle/contaminant release, occurs in the marginal ice zone, where there is a great amount of biological activity in the surface waters. Here, fauna associated with the ice form an important link in the food web between primary producers and fish, sea birds, and mammals (Futsaeter *et al.* 1991). In particular, ice fauna are fundamental to the Arctic marine food chain. If these fauna are contaminated by pollutants in the ice, the contaminants may be passed on and accumulate in the higher trophic levels of the food web.

The large-scale circulation of ice in the Arctic generally results in export of ice from the shelf seas, transport over the central basin, and discharge through the Fram Strait, and to a lesser degree, the Barents Sea and Canadian Archipelago. The main exit for Arctic sea ice is through the Fram Strait. Between 50-85% of the ice discharge consists of multi-year and second-year ice (Vinje and Finnekåsa 1986), which potentially contains accumulated contaminants. The marginal ice zone extends southward from the Fram Strait, along the eastern slope off Greenland. In winter, ice also continues around the southern tip of Greenland and extends up into Baffin Bay.

Ice also melts within the Arctic Basin. Modeling of ice motion (Colony and Thorndike 1985) indicates that much of the ice which melts in shelf regions comes from the cen-

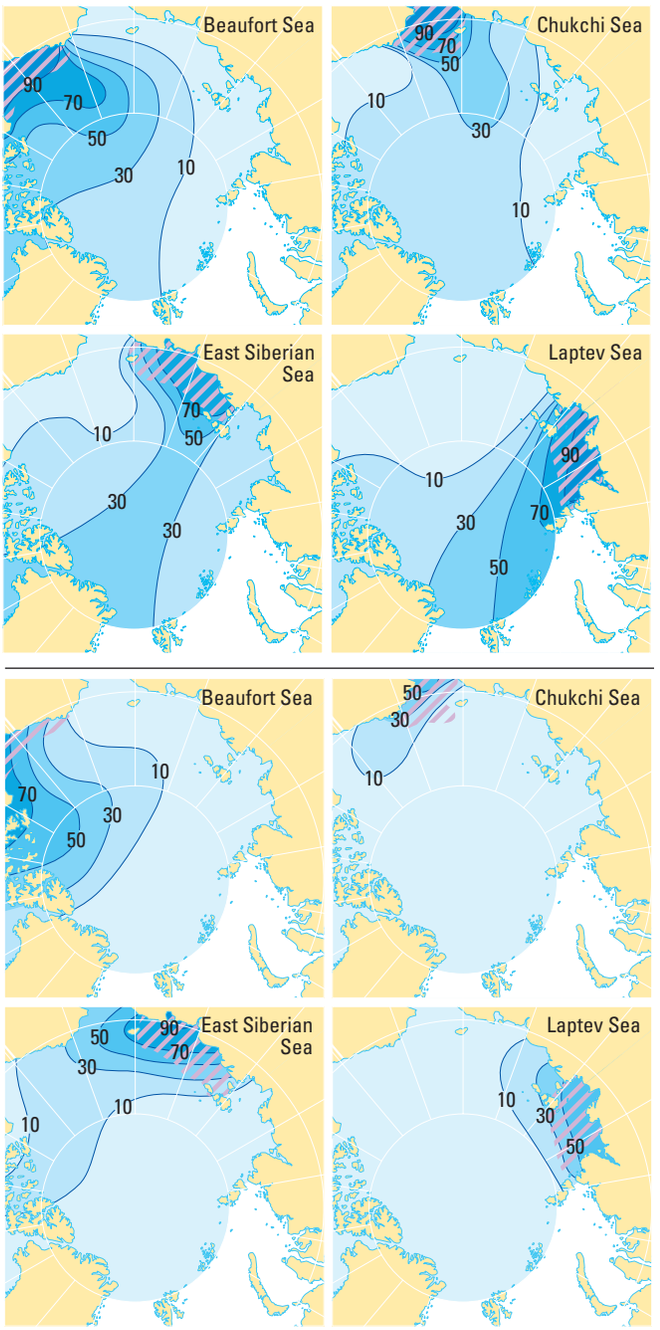

Figure 3·26. Above: contours of the asymptotic probability of ice formed in the hatched region moving into different parts of the Arctic Basin. Below: contours of the asymptotic probability of ice moving from different areas into the hatched region and melting. Note that the Kara Sea is not included in this analysis (Source: Colony and Thorndike 1985).

tral Arctic. For example, sea ice melting in the Beaufort Sea is likely to contain some ice from the north (Figure 3·26), which may have accumulated deposits of atmospheric contaminants over several years during drift in the Beaufort Gyre. The northern Barents Sea is a particularly vulnerable area with a large amount of ice import and melting in relatively close proximity to contaminant sources in the eastern Barents and Kara Seas (Pfirman *et al.* 1995b).

3.5.4. Transport pathways and hydrographic conditions in the Arctic seas

In the ocean, currents are the main transport mechanism of contaminants. Once entrained in a current, contaminants will be carried by it, rather than dispersing uniformly in all directions.

Oceanic circulation is driven by tidal forces, gravitational forces resulting from horizontal density gradients, wind stress directly on the water surface or through an intervening ice sheet, the Coriolis force related to the Earth's rotation, and turbulent shearing. A particular force may dominate in a particular geographical area. For example, wind stress is most important for surface currents in the Canadian Basin (Barrie *et al.* 1992).

Mesoscale eddies are potentially an important transport and redistribution mechanism for water properties in the Canadian Basin (D'Asaro 1988, Aagaard 1989). These features, which are characteristically 20 km in diameter and have maximum speeds of about 25 cm/s, are long-lived and may be one of the most important ways for water properties (including contaminants) introduced at the basin boundaries to penetrate and mix into the interior ocean.

Knowledge of the amount of water transported in a current is important for estimation and modeling of the total transport of contaminants from one area to another. In Figure 3·27, the mean volume fluxes (given in Sverdrup (Svd) = 10^6 m^3/s) in and out of the Arctic Ocean are shown. These fluxes provide the Arctic Ocean with a variety of anthropogenic tracers, although the amount of contaminant carried by the currents is still rather uncertain. Oceanic currents, hydrographic conditions, and physical processes in the ocean are closely linked and are treated jointly in this chapter in order to provide a complete description of the Arctic Ocean and surrounding seas.

3.5.4.1. The Arctic Ocean

A simplified view of the vertical structure in the Arctic Ocean is shown in Figure 3·28. A detailed classification of water masses can be found in Anderson and Jones (1986), Macdonald *et al.* (1989), and Carmack (1990). The Arctic Ocean is usually described as three layers, characterized by different water masses and circulation patterns: the Arctic Surface Water, Atlantic Water, and Deep Water.

The Arctic Surface Water

Surface water (0-200 m) is subdivided into the Polar Mixed Layer (upper 30-50 m) and the halocline (50-200 m). The temperature of the Polar Mixed Layer is kept close to the freezing point because of the ice cover, whereas the salinity exhibits seasonal and geographical fluctuations caused by freezing and melting of sea ice and input of freshwater from the shelf seas by river runoff. The Halocline Layer consists of water advected from the shelves (see section 3.5.4.6), and one can distinguish between Pacific Halocline Water (with salinity 33.1, also called 33.1 water after its characteristic salinity) originating in the Bering and Chukchi Seas, and Atlantic Halocline Water (salinity 34.2) produced on the Eurasian shelves (Jones and Anderson 1986, Aagaard and Carmack 1989). Even though the mechanisms responsible for the transfer of shelf water to the Arctic Ocean are not yet understood in detail, the signature of this transfer can be seen throughout the Arctic Ocean in the distribution of nutrients and other tracers carried by the water masses (Aagaard *et al.* 1981, Jones and Anderson 1986, Wallace *et al.* 1987).

The halocline is markedly stratified in salinity and density, and is maintained by lateral transport of water from the shelves (Aagaard *et al.* 1981, Melling and Lewis 1982, Moore and Smith 1986, Schlosser *et al.* 1994a), where it may have acquired its contaminant burden. The stratification prevents winter convection and deepening of the Polar Mixed Layer to more than about 50 m, and it effectively insulates the Atlantic Layer below from surface processes (Aagaard and

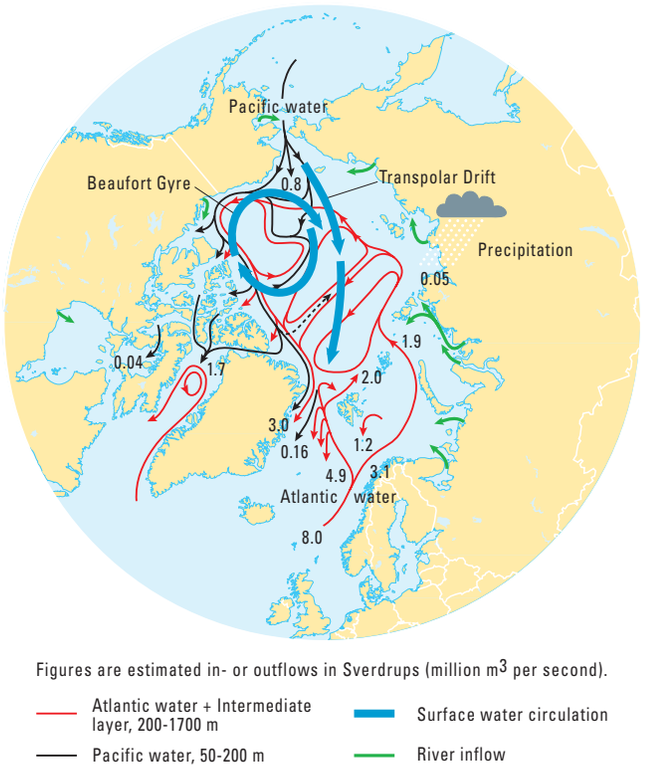

Figure 3·27. The predominant currents in the Arctic Ocean and their major routes around the basin edges of the Arctic (Source: Macdonald and Bewers 1996).

Carmack 1994), since it inhibits the vertical transport of properties, including heat, from the deep water to the surface (Carmack 1990, Jones and Anderson 1986), and provides an effective barrier between the surface water and deeper water, thus reducing contaminant transport.

Two main features characterize the surface water and sea-ice circulation in the Arctic Ocean: the Beaufort Gyre and the Transpolar Drift (Figure 3·29). The Beaufort Gyre is a large clockwise gyre extending over the entire Canadian Basin. The circulation is rather slow between the pole and the Canadian Archipelago, but accelerates in the southern and western regions. Coachman and Barnes (1961) report velocities of 1-5 cm/s around most of the gyre and rather greater velocities (10 cm/s) immediately north of Alaska. From the Beaufort Sea, water is exported to Baffin Bay through the Canadian Archipelago, but some water also enters the Transpolar Drift and exits the central Arctic Basin through the Fram Strait. The Transpolar Drift runs lengthwise across the Eurasian Basin from off the Siberian coast out through the western Fram Strait. Surface waters in the Eurasian Basin tend to move from east to west, toward the North Pole, following the Transpolar Drift. Mean speeds in the central ocean are slow at about 2 cm/s, but increase as the water exits the basin and becomes part of the East Greenland Current (Carmack 1986).

The processes described above are likely to cause variations in the storage of water in the Beaufort Gyre and shifts in the amount of surface water exiting the Arctic either through the Canadian Archipelago or through the Fram Strait. The large freshwater flux from rivers into the Arctic Ocean and subsequent transport of this freshwater into the deep-water formation regions of the Nordic and Labrador Seas might at least in part control the formation rate of North Atlantic Deep Water (Aagaard and Carmack 1989). For example, when more surface water is diverted through the Archipelago, surface waters in the Greenland Sea may be less stable, enhancing deep-water formation. On the other hand, Labrador Sea Water may form more readily when there is a minimal flux of low-salinity surface water through the Archipelago or advection of ice from the Nordic Seas around the southern coast of Greenland (Mysak and Manak 1989).

Tracer studies show that water discharged from Siberian rivers comprises about 10% of the surface water in the main axis of the Transpolar Drift (Östlund 1993, Schlosser *et al.* 1995a). This means that if contaminants are conservative (that is, not modified by biological or chemical processes during transport) and introduced by rivers, they will only be diluted by about a factor of 10 by the time the river water exits the Arctic through the Fram Strait. Outflow pathways for surface water from the Arctic Ocean (Figure 3·27) are mainly through the Fram Strait (1.0 Svd) and the Canadian Archipelago (1.7 Svd), but some surface water (0.4 Svd) also exits through the Barents Sea (Rudels 1986a, Foldvik *et al.* 1988, Loeng *et al.* 1997). Inflows of water to the Arctic Ocean Surface Layer are through the shelf seas (Rudels 1987a, 1987b, Blindheim 1989, Quadfasel *et al.* 1992) and through the Bering Strait (Coachman and Aagaard 1988, Coachman 1993). The shallowness of the Bering Strait (≈50 m) permits only surface water of Pacific origin to enter the Arctic Ocean.

Mean annual flow through the Bering Strait is into the Arctic Ocean and the mean transport is about 0.8 Svd

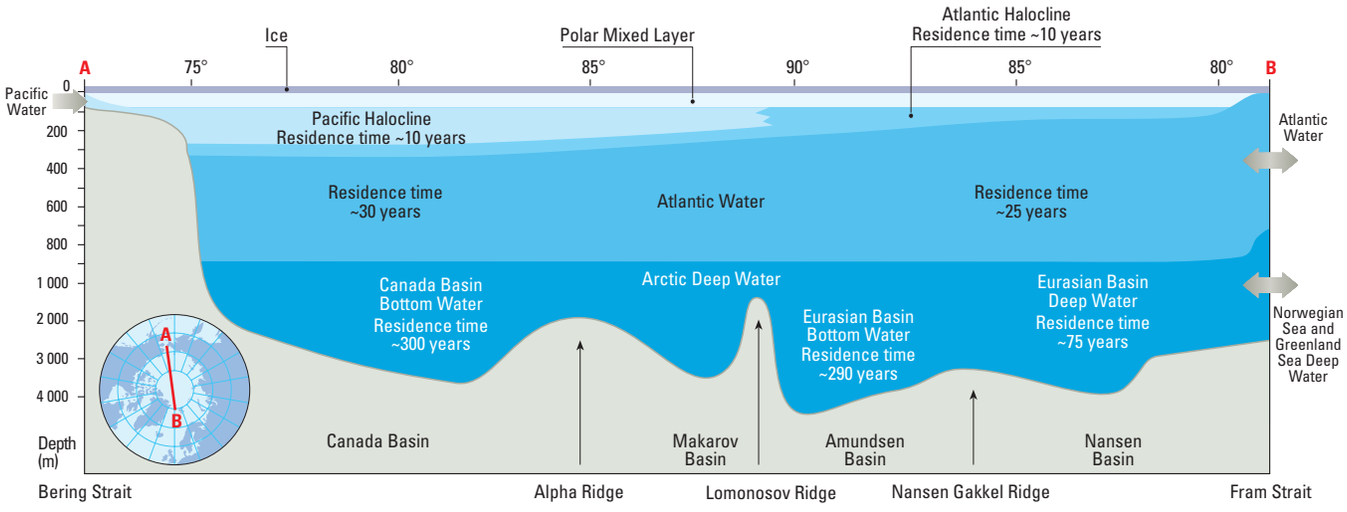

Figure 3·28. A schematic representation of the three-layer structure of the Arctic Ocean, with the Arctic Surface Layer above the Atlantic Water and Arctic Deep Water (Aagaard and Carmack 1989). The residence time for the different water masses are also shown (Bönisch and Schlosser 1995).

Figure 3·29. Surface currents in the Arctic region. Square boxes indicate that the denser inflowing (Atlantic and Pacific) waters are submerging under the Polar Surface Water. The continuation of these flows can be seen in Figure 3·27.

(Coachman and Aagaard 1988). Interannual variability in the transport is about ±0.2 Svd, the seasonal variations in mean monthly transport values are 1-1.5 Svd in summer and 0.3-0.5 Svd in winter. Short-term variations in transport have been observed to range between about 3.0 Svd north and 5.0 Svd south (Coachman 1993).

The Bering Sea Water enters the Chukchi Sea as a surface current (Figure 3·29), but due to its higher density it intrudes under the Polar Mixed Layer and separates the Mixed Layer water from the Atlantic Halocline water. At Point Hope, the Bering Sea Water is split into two branches (Coachman *et al.* 1975) with one turning northwestward to Harold Canyon (65%) and following the flow of the surface water above, the Beaufort Gyre, and thereby spreading out over much of the Canadian Basin. In contrast, the other branch of the water (35%) enters the Barrow Canyon and follows the coast of Alaska as the Alaskan Coastal Current (Overland and Roach 1987). This branch exits the Arctic Ocean through the Canadian Archipelago. Most of the Bering Sea Water that enters the Beaufort Gyre will also eventually leave the Arctic via the passages of the Canadian Archipelago (Codispoti and Lowman 1973). The water mass called Bering Sea Water in the Arctic Ocean is a mixture of Siberian Shelf water (80%) and water from the Bering Sea (20%) (Coachman and Barnes 1961).

The Atlantic Layer

In general, below the surface layer, circulation in the Arctic Ocean is counterclockwise or opposite to that of the sea ice and surface waters (Figure 3·27). The flows into the Arctic Ocean from the Atlantic Ocean are large and difficult to estimate. This is partly because there are at least two main branches into the Arctic Ocean (West Spitsbergen Current and through the Barents Sea) and partly because the flows through the Fram Strait undergo considerable recirculation obscuring the calculation of net import of water. When entering the Arctic Ocean through the Fram Strait, the Atlantic water of the West Spitsbergen Current submerges below the Halocline Layer due to its higher density, and follows the continental slope eastward. Along this path, some water re-

circulates toward the north and follows the direction of the Transpolar Drift (Coachman and Barnes 1963) while the rest passes over the Lomonosov Ridge and enters the Canadian Basin.

Water of Atlantic origin is therefore found at intermediate depths between 200 and 900 m and is defined as saline water with temperatures above 0°C. When Atlantic Water enters the Arctic Ocean north of Spitsbergen and submerges under the Surface Layer, it has a temperature well above 3°C and a salinity of about 35.0%. On its path around the basins, both temperature and salinity decrease as a result of diffusion and mixing with water masses above, below, and alongside the current (Timofeyev 1961, Coachman and Barnes 1963, Newton and Coachman 1974). The coldest core temperature (0.38°C) of the Atlantic Water has been measured north of Ellesmere Island just before it exits the Arctic through the Fram Strait.

Atlantic Water from the Barents Sea can enter the Arctic Ocean at the depth of the Atlantic Halocline and, when density is higher, mix with Atlantic Water or Deep Water (Midttun and Loeng 1987, Anderson *et al.* 1994). Northeast of the St. Anna Trough, the two branches of Atlantic Water (that came through the Fram Strait and the Barents and Kara Seas) meet and merge before continuing eastward along the slope toward the Laptev Sea. Here some of the Atlantic Water turns north and flows as a broad band back toward the Fram Strait, while a smaller fraction crosses the Lomonosov Ridge. The water entering into the Canadian Basin follows the continental slope counterclockwise around the basin, branching off at various topographic features until it reaches the Atlantic Water and flows back over the Lomonosov Ridge and meets the other branch again north of Greenland. Atlantic Water then exits the Arctic Ocean through the Fram Strait, flowing below the cold Polar Water at the surface as an undercurrent of the East Greenland Current (Coachman and Barnes 1963, Aagaard 1989). Bathymetry plays a major role in shaping the circulation patterns of Atlantic Water and deeper waters. A sharp front in water masses centered over the Lomonosov Ridge separates waters in the Eurasian Basin from the Canadian Basin (Anderson *et al.* 1994).

The Arctic Deep Water Layer

Arctic deep water is divided into Canadian Basin Deep Water and Eurasian Basin Deep Water, because of significant differences in the temperature and salinity found in the two basins. Canadian Basin Deep Water is relatively warm and saline (–0.5°C, 34.955) while Eurasian Basin Deep Water is colder and fresher (–0.95°C, 34.945). Eurasian Basin Deep Water is subdivided into deep water and bottom water (Aagaard *et al.* 1981, Smethie *et al.* 1988). Only water above the Lomonosov Ridge (sill depth about 1500 m) can be exchanged between the Canadian Basin and the Eurasian Basin, while between the Eurasian Basin and the Greenland Sea, water down to a sill depth of 2600 m can be exchanged through the Fram Strait. Both inflow and outflow of deep waters can only occur through the Fram Strait because of the shallow sill depths of the Bering Strait, the Canadian Archipelago, and the Barents Sea. In the Fram Strait, deep-water inflow consists of Norwegian Sea Deep Water and Greenland Sea Deep Water (Swift *et al.* 1983, Aagaard *et al.* 1985) while Eurasian Basin Deep and Bottom Water flows out (Smethie *et al.* 1988, Swift and Koltermann 1988).

The temperature difference between deep waters in the Canadian Basin and the Eurasian Basin, as seen in Figure 3·30, is caused by the existence of the Lomonosov Ridge which prevents exchange of bottom water between the two

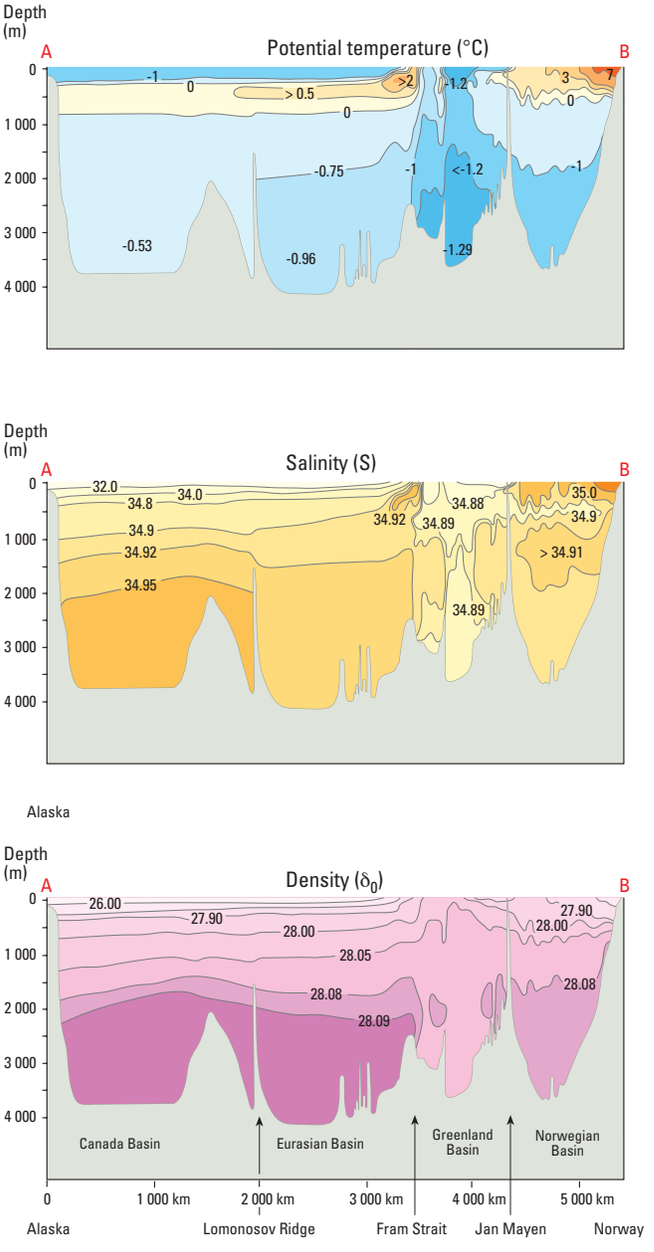

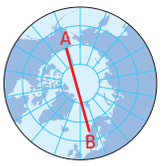

Figure 3·30. Distribution of potential temperature, salinity, and density across the Arctic Ocean and the Greenland and Norwegian Seas (Source: Aagaard *et al.* 1985).

basins. Only the shallower, warmer, deep water of the Eurasian Basin can enter the Canadian Basin (Coachman and Aagaard 1974). Higher salinities in the Canadian Basin are thought to be caused by the addition of brine-rich water from the shelves (Rudels 1987a, 1987b), or could represent relict water derived from an earlier, more saline Arctic Ocean (Macdonald and Carmack 1991). The freshness of the Eurasian Basin is probably linked to the exchange of colder and less saline deep water of the Greenland and Norwegian Seas. The nutrient content of the deep water is also higher on the Canadian side of the Lomonosov Ridge, due to the older age of the Canadian Basin Deep Water (Östlund *et al.* 1987).

The mean flow field in the interior of the Arctic Ocean appears to be very weak (Melling *et al.* 1984, Aagaard 1989). Current measurements near the Lomonosov Ridge on the Eurasian side show that speeds in the abyss are extremely low (mean 0.4 cm/s, maximum 3.8 cm/s), while currents over the crest are considerably higher, reaching 12 cm/s

(Aagaard 1981). The flow over the crest is characterized by a series of pulses which probably represent overflow across the ridge of deep water from the Eurasian Basin destined to sink adiabatically, and fill the Canadian Basin abyss.

The principal large-scale advection in the Arctic Ocean is the subsurface boundary currents, trapped over steep topography which borders each of the major basins, including the flanks of the Lomonosov Ridge (Aagaard 1981, Aagaard 1989). Similar to the flow of Atlantic Water, these deep and apparently narrow currents flow around the basins in a cyclonic (counterclockwise) sense and exit through the Fram Strait. Speed increases with depth through the Atlantic layer and into the deep water. The boundary current is not uniquely associated with a particular water mass. Brine-rich waters flow off the shelves and mix with these boundary currents at different depths depending on density. Contaminants enter the deep Arctic Ocean mainly by the dense water flow off the shelves and can be transported over long distances relatively rapidly by these currents. Contaminant concentrations (chlorofluoromethanes, radionuclides, etc.) are higher in the boundary currents than in the center of the Arctic Basin, and it seems that these currents provide a rapid route out of the basins for newly formed deep waters and associated contaminants (Schlosser *et al.* 1995b).

One example of rapid transport with the subsurface boundary current is the anomalously high $^{137}Cs/^{90}Sr$ ratio observed in 1979 near 1500 m over the Eurasian Basin flank of the Lomonosov Ridge (Livingston *et al.* 1984). It represents a signal from the Windscale nuclear fuel reprocessing plant (now Sellafield) on the Irish Sea. This signal was carried with the boundary current either from Spitsbergen or from the continental slope off the Barents Sea (Livingston 1988) to the North Pole around the perimeter of the Eurasian Basin (about 4000 km). With a speed of about 4 cm/s, which is well within the observed range, the Windscale-tagged water would have taken only three years to travel that pathway.

The deep Arctic Ocean is mainly renewed from the adjacent shelves (Aagaard *et al.* 1985) which results in a net conversion of surface to deeper water (see section 3.5.4.6). Measurements of the chlorofluoromethanes F-11 and F-12 show a slight maximum near the bottom of the Eurasian Basin, suggesting that high-salinity shelf water is transported to the ocean bottom. The F-11, F-12, temperature, and salinity measurements also indicate that Eurasian Basin Deep Water flows southward into the Greenland Sea along the sea floor on the west side of the Fram Strait with a volume transport of about 1.0 Svd (Smethie *et al.* 1988, Bönisch and Schlosser 1995), and from there into the Iceland Sea all the way to the Denmark Strait and the Atlantic Ocean (see section 3.5.4.3).

3.5.4.2. **The Arctic shelf seas**

The marginal seas cover the continental shelves surrounding the Arctic Ocean. The shelf waters are relatively well mixed during the winter and stratified in summer during peak river discharge and ice melts. Shelf seas receive their contaminant load mainly via river discharge and atmospheric pathways from the continents to the south. The shelf seas also provide large open areas during summer where interactions with the atmosphere can take place. Further, they are the sites of oil development both in the Canadian and Russian sector, and they support significant biological production in the spring and summer. As a result of biological production, deposition occurs of organic material and its decomposition products, including incorporated contaminants (Wallace *et al.* 1987).

During winter, with the formation of dense bottom water, entrained contaminants will be transferred off the shelves and into the interior of the Arctic Ocean. Shelf-derived contaminants, injected mainly into the halocline (Aagaard 1994), may spread throughout the entire Arctic Ocean (Macdonald and Carmack 1991). Ten years after their injection, tritium and helium had spread with shelf-derived waters throughout the upper Arctic Ocean (Östlund 1982, Schlosser *et al.* 1990).

The Barents Sea

The main circulation pattern in the Barents Sea consists of relatively warm Atlantic Water flowing eastward with the North Cape and Murman Currents in the south and cold Arctic waters flowing southwestward with the Bear Island, Persey, and East Spitsbergen Currents in the north (Loeng 1991). The southern part of the Barents Sea is therefore characterized by relatively warm waters of the Coastal Water ($t > 3°C$, $S < 34.7$) and Atlantic Water ($t > 2°C$, $S > 35.0$). The northern part of the Barents Sea is characterized by Arctic Water ($t < 0°C$, $34.3 < S < 34.7$). During summer, the Arctic Water is covered with a thin layer, 5-20 m, of meltwater ($t > 0°C$, $S < 34.2$). The Arctic and Atlantic Waters meet and mix at the oceanic Polar Front which is an important area for biological production (Loeng 1989, Pavlov 1993). The bottom topography of this shelf sea strongly influences its current distribution.

Bottom Water ($t < -1.7°C$, $S > 35.0$) is formed over shallow banks as a result of cooling and ice formation (see section 3.5.4.6), and flows down slopes to local depressions (Midttun 1985). This cold and saline Bottom Water will eventually leave the Barents Sea and enter the Arctic Ocean through the strait between Svalbard and Franz Josef Land or through Saint Anna Trough, or enter the Norwegian Sea through Bear Island Trough.

Atlantic and Coastal Waters enter the Barents Sea from the west (Blindheim 1989), mainly between northern Norway and Bear Island, while Arctic Water enters between Svalbard and Franz Josef Land, as well as via the Kara Sea (Pfirman *et al.* 1994, Loeng *et al.* 1995). The main exit for water leaving the Barents Sea is between Novaya Zemlya and Franz Josef Land. Mean monthly volume transports through this strait, calculated from current measurements, show an increased outflow in winter with maximum in December (3.3 Svd) and a weaker flow in summer (1.0 Svd). To the south of Novaya Zemlya, there is also an exchange of water with the Kara Sea. Between Svalbard and Franz Josef Land there is only a small net outflow of water to the Arctic Ocean. Along the western margin of the Barents Sea, the main outflow occurs south of Bear Island. Water exchange through the section Bear Island-Sørkapp (Svalbard) is negligible - the Atlantic Water that enters the Storfjordrenna recirculates back into the Greenland Sea (Loeng *et al.* 1995).

The Murman Coastal Current is the northeastern extension of the Norwegian Coastal Current and follows the coast of Russia. Part of it enters the White Sea where the general circulation is counterclockwise. The water exchange between the Barents Sea and the White Sea is very small. With an inflow of 0.167 Svd from the Barents Sea and an outflow of 0.174 Svd from the White Sea, the net transport is 0.007 Svd to the Barents Sea. This value is balanced by river runoff into the White Sea (Uralov 1960, Altshuler *et al.* 1970, Potanin and Korotov 1988). The freshwater inflow from rivers to the Barents Sea is very small, 5000-6000 m^3/s, of which the Pechora River runoff accounts for 90% of the total.

The Barents Sea comprises a mixture of locally formed sea ice, and ice advected in from the Arctic Basin. While the southern part of the sea is kept free of ice by the warm North

Cape Current, locally formed and multi-year ice advected from the Arctic Basin cover much of the Barents Sea north of about 74°N in winter. Beginning in December, ice growth proceeds westward from Novaya Zemlya, so that by March most of the sea east of 45°E may be icecovered. Ice decay begins in May, with the ice edge retreating back to about 79-80°N by September.

The Kara Sea, the Laptev Sea, and the East Siberian Sea

Inflow from the Barents Sea and the Arctic Ocean together with the river runoff governs the water structure of the Kara Sea (Pavlov *et al.* 1993). In the southwestern Kara Sea, water is exchanged in both directions through Karskiye Vorota (Pavlov and Pfirman 1995). The water entering from the Barents Sea submerges because of higher density under the surface water ($t = -1.4°C$, $22.0 < S < 25.0$). The northern Kara Sea is influenced by Atlantic Water entering from the Arctic Ocean through the deep troughs of Saint Anna and Voronin. The southeastern Kara Sea is strongly influenced by continental runoff from the rivers Ob and Yenisey.

Ice formation begins in the northern Kara Sea in September and in the southern regions in October, persisting until May (Pavlov *et al.* 1994). Fast ice developed along the coast may remain in place until July. Flaw leads along the fast ice margin are the main areas of new ice production (Pavlov and Pfirman 1995). Typical ice thicknesses are 1.5-2 m. Ice is exported northward, into the Arctic Basin as well as into the Barents and Laptev Seas.

The surface water of the Laptev Sea and the East Siberian Sea is of low salinity ($22.0 < S < 25.0$) and cold ($t = -1.4°C$) and occupies the central part of these seas. To the north is the Polar Water and to the south is the river water (only present in summer). The local surface water is a mixture of these. In the deep northern part of the two seas, a temperature maximum is found between 100 and 400 m, from intruding Atlantic Water. Inflowing Polar Water and Deep Atlantic Water from the Arctic Ocean influence much of the Laptev Sea (Kotchetov *et al.* 1994). In the East Siberian Sea, the eastern part is covered with Bering Sea Water in the winter (Pavlov *et al.* 1994).

Ice begins to develop in the Laptev Sea in late September, with persistent ice cover ranging from October to May (Pavlov *et al.* 1994). Fast ice, extending over 30% of the sea, covers the regions that are less than 20-25 m deep. New ice forms along the persistent flaw lead at the northern margin of the fast ice. Large amounts of ice formed in the Laptev Sea are exported to the Arctic Basin. As a result, the Laptev is often called the ice factory of the Arctic.

The East Siberian Sea has the most persistent ice cover of all the Siberian seas. It is completely covered with ice from October or November to June or July (Pavlov *et al.* 1994). Fast ice develops out to about the 25 m isobath, and reaches thicknesses of 2 m. Although flaw leads and new ice develop in the western and eastern regions of the sea, large amounts of ice are also imported from the Arctic Basin. In the summer, multi-year ice often covers the northeastern portion of the sea.

The Kara, Laptev, and East Siberian Seas all exhibit similar patterns of circulation (Figure 3·29). There is a counterclockwise circulation with currents directed eastward along the coast and westerly setting currents along the northern limits where the seas adjoin the Arctic Ocean. The circulation is greatly dependent upon local winds. Persistent easterly winds may reverse the usual easterly currents along the Siberian coast and cause westerly sets at the surface in any of the marginal seas. The effect of winds on the subsurface currents depends upon the strength and duration of the winds. Very little is known about the deep and near bottom currents (Timokhov 1994).

Through these Siberian seas, vast amounts of river runoff enter the Arctic Ocean. The seasonal runoff cycle influences the current circulation which becomes stronger and flows more toward the sea when runoff is high, and becomes weaker and flows closer to the coast when runoff is low (Pavlov *et al.* 1993, Pavlov *et al.* 1994, Kotchetov *et al.* 1994). The strong continental runoff is considered to be one of the most significant features of the Kara Sea, the freshwater input totals 0.03 Svd, mainly from the Ob River (0.01 Svd) and the Yenisey River (0.02 Svd). The average annual volume of river runoff to the Laptev Sea is about 0.02 Svd, most of it from the Lena River, while freshwater input to the East Siberian Sea is smaller, less than 0.01 Svd (Pavlov *et al.* 1994).

The Chukchi Sea

Relatively warm water enters the Chukchi Sea through the Bering Strait. One branch flows northward and then west-northwest in a broad stream, and enters the Arctic Ocean just east of Herald Island; while a northeasterly branch narrows into a high-speed jet-like stream closely following the Alaskan coast into the Beaufort Sea (Paquette and Bourke 1981).

Water from the East Siberian Sea enters the Chukchi Sea and mixes with the branch of water from the Bering Sea that flows northward, and this product is what is called Bering Sea Water in the Arctic Ocean (see section 3.5.4.1). The western and central parts of the Chukchi Sea are dominated by this Bering Sea Water ($31.0 < S < 33.5$, $0°C < t < 8°C$ in summer), whereas the eastern part is dominated by Alaskan Coastal Water ($S < 31.0$, $10°C < t < 15°C$ in summer), representing 'unmixed' water from the Bering Sea (Coachman *et al.* 1975). In winter, the water column is near the freezing point ($t = -1.8°C$) over the entire Chukchi Sea, and intermediate and deep water is formed by brine release. The deep water settles to the sea floor and flows down the Barrow Canyon. During summer, freshwater inflow (mostly from the Yukon River) and ice melt provide a low-density surface layer which absorbs solar energy and only gradually mixes with the water below (Ahlnäs and Garrison 1984).

The ice cover of the Chukchi Sea retreats in summer to the shelf break north of the Bering Strait. It has characteristics similar to the Arctic drift ice, but with a greater proportion of first-year ice.

The Beaufort Sea

The Canadian Beaufort Shelf is the largest shelf on the North American side of the Arctic Ocean, but because it is so narrow it represents less than 2% of the total Arctic shelf area. Due to oil exploration in the 1970s and 1980s and the ease of ship access, the Canadian Beaufort shelf has been the focus of many oceanographic and contaminant studies (Thomas *et al.* 1990, Macdonald and Thomas 1991). The dominant bathymetric feature is the Mackenzie Trough which separates the Alaskan and Canadian shelves. Freshwater input comes from the Mackenzie River, the fourth largest river draining into the Arctic, discharging about 0.001 Svd, most of it (70%) between May and September (Carmack *et al.* 1989, Macdonald *et al.* 1995), providing a dominating influence on the regional oceanography, sedimentology, and biogeochemistry. Water masses in the surface layer (< 200 m) are freshwater from the Mackenzie River, icemelt water, and water of the Polar Mixed Layer and Pacific Halocline Layer (Macdonald *et al.* 1989, Macdonald and Carmack 1991, Melling and Moore 1995). In certain winters, the Mackenzie shelf produces sufficient dense water to ventilate the offshore halocline (Melling and Lewis 1982).

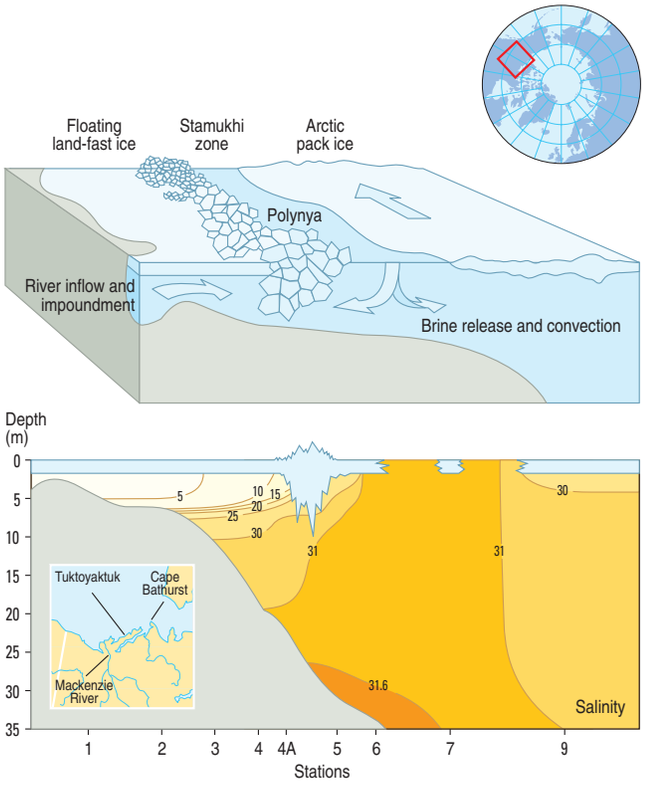

Figure 3·31. A schematic diagram showing the inflow from the Mackenzie River trapped in the nearshore zone beneath the landfast ice. Beyond the stamukhi zone, intermittent opening and refreezing in the flaw lead produces brine which encourages mixing and convection. Numbers in lower panel are salinity values. (Source: Macdonald and Carmack 1991).

Along the coast of the Beaufort Sea there is generally a westward flow driven by the prevailing easterly winds, but the circulation responds rapidly to changing wind conditions, such that under westerly winds the motion is eastward. Significant flow on the inner shelf is primarily a summer phenomenon, when the shelf water is ice free. Strong easterly winds can produce coastal upwelling which displaces the Mackenzie plume offshore and replaces the brackish water with saline water (Giovando and Herlinveaux 1981). Seaward of about the 50 m isobath, the flow is substantially different: strong flow occurs throughout the year, locally aligned with the isobaths. The dominant feature is the Beaufort Undercurrent, a bathymetrically-steered eastward flow extending seaward from the 40-50 m isobaths to at least the base of the continental slope (Paquette and Bourke 1974, Aagaard 1984).

A zone of landfast ice progresses from the shore to the 20 m isobath each winter. Between the landfast ice and the westward-moving pack ice, there is a shear zone where a persistent lead forms. In this region, the ice cover opens and refreezes several times during the winter, producing dense, brine-enriched water. Ice formed in the Beaufort Sea is typically advected along shore to the west and may be incorporated in the westward circulating Beaufort Gyre. At the seaward edge of the landfast ice, a deeply ridged rubble zone forms an effective barrier to Mackenzie River water (which flows throughout the year), keeping the freshwater dammed up near the shore under the ice as shown in Figure 3·31. Minimum ice concentrations occur in September, when the area near the Mackenzie Delta forms a region of open water.

3.5.4.3. **The Nordic Seas**

The Nordic Seas include the Norwegian, Greenland, and Iceland Seas. All of the upper waters of the Nordic Seas are supplied, either through mixture or local modifications, by Atlantic Water ($t > 3°C$, $S > 35.0$) and Polar Water ($t < 0°C$, $S < 34.4$) (Figure 3·32). The Atlantic Water occupies the eastern side, whereas Polar Water is found on the western side of the Nordic Seas. A distinct hydrographic regime lies between these two regions, and the general term Arctic Water or Arctic Intermediate Water ($t > 0°C$, $S < 34.9$) is used to distinguish the upper layer waters of this transition region from those of more direct Polar or Atlantic origin. All three domains (Polar, Arctic, and Atlantic) overlie a vast layer of cold (<0°C), nearly isohaline (34.88-34.94) deep water. Overviews of the Nordic Seas oceanography are given by Swift (1986) and Hopkins (1991).

The Nordic Seas are thus a transition zone for warm and saline water on its way from the Atlantic Ocean to the Arctic Ocean, and for cold and less saline water from the Arctic Ocean to the Atlantic Ocean (Figures 3·32 and 3·33). The Greenland-Scotland Ridge forms a barrier between the deep waters of the Nordic Seas and the North Atlantic which constrains the exchange of deep water.

The Norwegian Sea

The surface layer of the Norwegian Sea is dominated by warm, saline Atlantic Water, except for the coastal area of Norway where Coastal Water with low salinity and variable temperature is transported northward by the Norwegian Coastal Current (Figure 3·33). Norwegian Coastal Water is colder than the Atlantic Water in winter and early spring, and warmer the rest of the year. Where these two water masses meet, a sharp surface front is formed. The lateral extent of Coastal Water varies during the year.

A slight salinity minimum ($34.85 < S < 34.91$) can be traced all over the Norwegian Sea as a result of Arctic Intermediate Water (lower AIW in Figure 3·32) intruding between the Atlantic Water and the deep water. Arctic Intermediate water enters the Norwegian Sea from both the Greenland and Iceland Seas, and prohibits direct mixing of the Atlantic Water and Norwegian Sea Deep Water (Blindheim 1990).

The Norwegian Sea Deep Water has lately been categorized as two water masses: young and old Norwegian Sea Deep Water. The young Norwegian Sea Deep Water forms in the periphery of the Greenland Gyre as a 50-50 mixture between Greenland Sea Deep Water and Eurasian Basin Deep

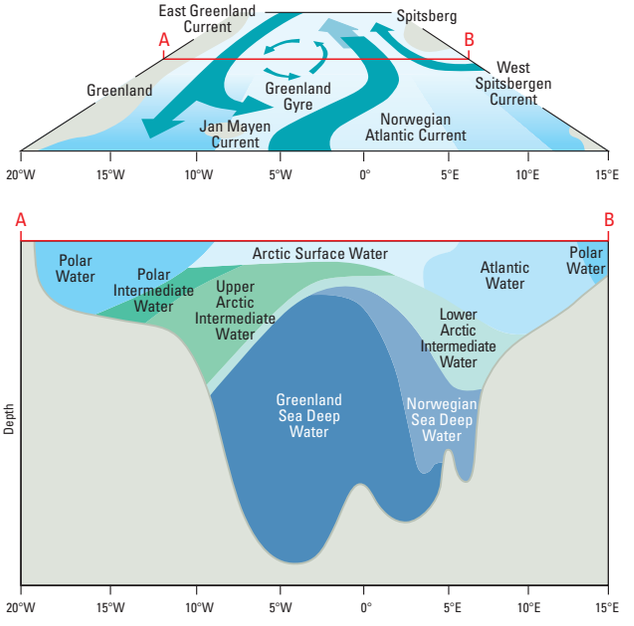

Figure 3·32. Schematic diagrams of the Greenland Sea showing the surface circulation (above) and water mass structure at a section across the central gyre (below) (Source: Carmack 1986).

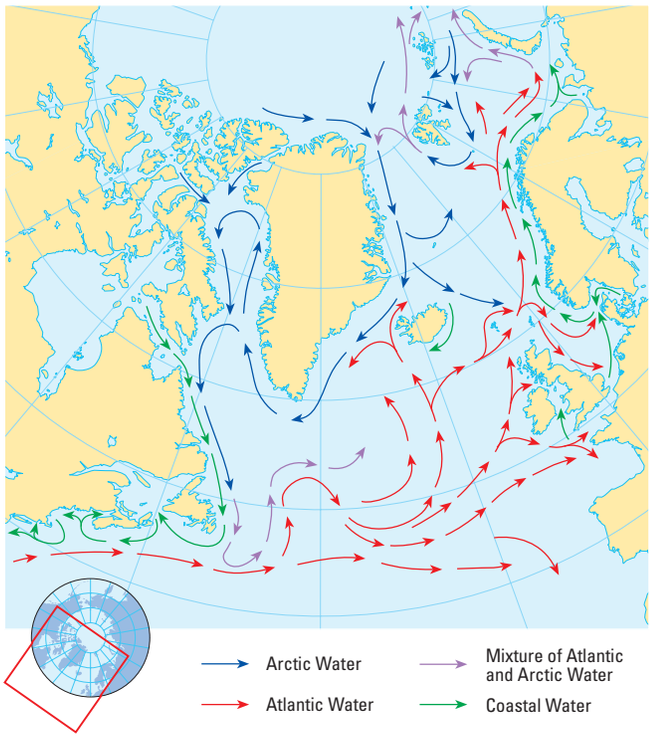

Figure 3·33. Major surface currents in the North Atlantic Ocean.

Water, and enters the Norwegian Sea through gaps in the mid-ocean ridge. The old Norwegian Sea Deep Water is found in the deep basins of the Norwegian Sea and the Iceland Sea, and is an aged version of the mixture (Aagaard *et al.* 1985, Swift and Koltermann 1988).

Atlantic flow through the Nordic Seas

The main inflow of Atlantic water into the Norwegian Sea occurs along the continental slope west of the Shetland Islands and across the Iceland-Faeroe ridge north of the Faeroe Islands (Figure 3·33). Transport via these inflows is uncertain, estimates have varied between 2 and 10 Svd (Tait 1957, Timofeyev 1963, summarized in Hopkins 1991). From direct measurements, Gould *et al.* (1985) derived a flux of 7.8 ± 2.3 Svd, while Blindheim (1993), on a section a little north of Shetland, found volume transports ranging from 2.4 to 7.9 Svd. This section was situated north of the offshoots from the Norwegian Atlantic Current into the North Sea, and therefore covers the flow which continues northward into the Nordic Seas. Transport was highest in winter. Atlantic water also enters the Iceland Sea through the eastern side of the Denmark Strait, as the Irminger Current. This inflow is small (Kristmannsson *et al.* 1989), and after mixing with the local waters north of Iceland its last traces may be found in the shelf area east of Iceland (Stefánsson 1962).

The Norwegian Atlantic Current follows the Norwegian continental slope north to about 70°, where the current bifurcates into the North Cape Current and the West Spitsbergen Current (Figure 3·33). The West Spitsbergen Current sends several branches westward on its way through the Greenland Sea. Since this water is denser than the surface water of the region, the Atlantic Water submerges to intermediate depths. Much of the water of the West Spitsbergen Current, after passing 79°N, recirculates in the Fram Strait instead of entering the Arctic Ocean. This so-called 'Return Atlantic Water' eventually enters the southward flowing water of the East Greenland Current, and could represent as much as 70-80% of this flow (Bourke *et al.* 1988, Jónsson and Foldvik 1992). The contaminant load carried by the West Spitsbergen Current will either enter the Arctic Ocean through the Fram Strait, or be carried across the Fram Strait and enter deeper waters of the East Greenland Current.

The Norwegian Coastal Current

Inshore of the Norwegian Atlantic Current flows the Norwegian Coastal Current, which is a continuation of the Baltic Current. Freshwater from the Baltic Sea mixes in the Skagerrak with local water, North Sea Water, and Atlantic Water to form the Norwegian Coastal Current (Blindheim and Loeng 1981).

The current follows the coast of Norway into the Barents Sea, and transports contaminants from both the Baltic and the North Sea toward the north. For instance, radionuclides discharged with waste water from Sellafield Works into the sea are transported in part over the Central North Sea, through

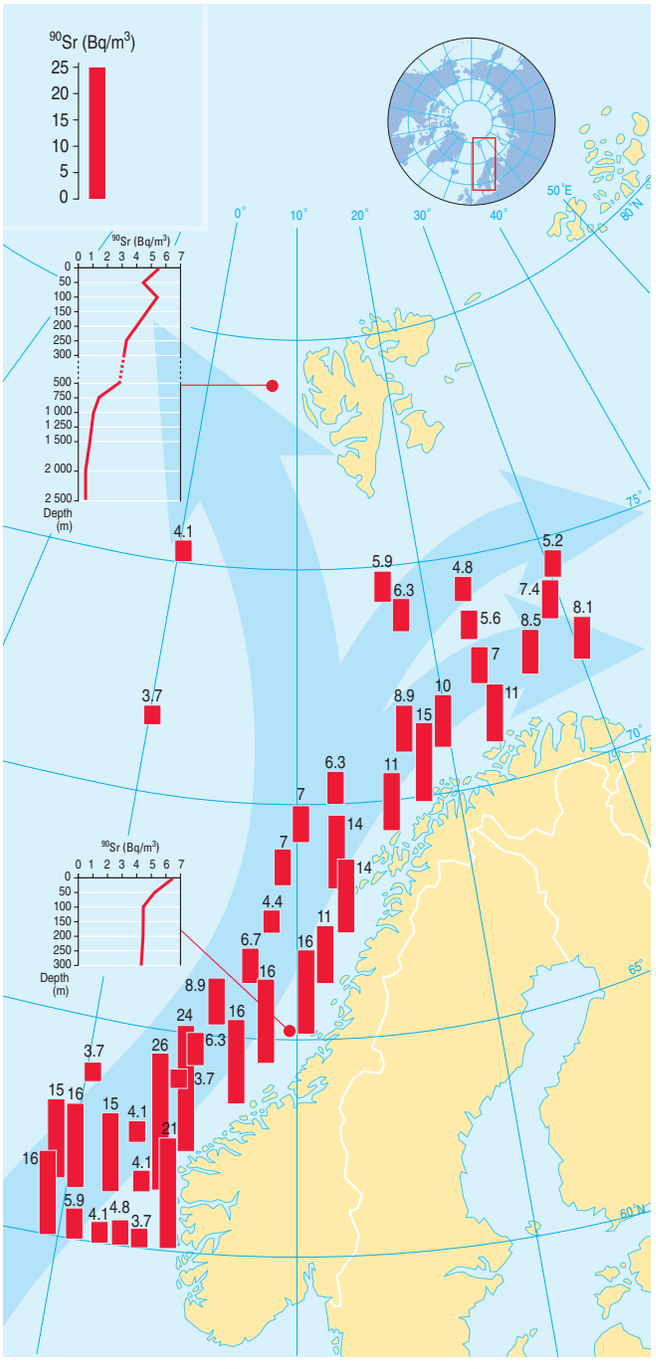

Figure 3·34. Transport of ^{90}Sr, originating from Sellafield, along the coast of Norway. The highest values are found in the Norwegian Coastal Current and decrease northward (Source: Kautsky 1987).

Skagerrak, and alongside the Norwegian Deep Water toward the north (Dahlgaard *et al.* 1986, Kautsky 1987). Close to the Norwegian Coast, one can follow a narrow strip of water with relatively high transport of ^{90}Sr (Figure 3·34), with decreasing values westward and northward. The ratio $^{137}Cs : {}^{90}Sr$ is much higher in this area than the ratio expected from atomic bomb tests, which indicates that the additional content of ^{137}Cs in the water originates mainly from the Sellafield Works. Radiocesium from the Sellafield Works is found mainly in the surface layer of the ocean (0-200 m).

The Greenland Sea

The most prominent feature of the Greenland Sea is the cyclonic Greenland Sea Gyre, centered on the prime meridian at about 74-75°N (Figure 3·32). The Greenland Sea Gyre exhibits only a small variation in seasonal temperature, varying between –0.8°C and –1.5°C, and both horizontal and vertical temperature gradients are much smaller than in the Atlantic Water (Quadfasel and Meincke 1987). The well-defined East Greenland Polar Front separates the Polar Water from warmer and more saline Arctic Water to the east. There are marked changes in both temperature and salinity across the front, which are usually identified with the 0°C isotherm (Paquette *et al.* 1985, Manley *et al.* 1987). In addition, we have the Arctic Front between the Arctic Water and the Atlantic Water.

The upper layer of the Greenland Sea is rather thin in the Greenland Sea Gyre compared to the other areas of the Greenland Sea. Greenland Sea Deep Water fills the basin from about 800 m to the sea floor in the peripheral areas while in the center of the gyre it fills the water column from 50-200 m to the sea floor. Greenland Sea Deep Water is nearly homogeneous, although deep water ($-1°C < t < 0°C$) has been distinguished from bottom water ($t < -1.0°C$). The Greenland Sea Deep Water constitutes at least 85% of the total volume of water in the Greenland Sea, and is produced locally by convection during winter. Vertical mixing occurs in winter when the surface waters cools and sea ice forms, rejecting salt, resulting in increased surface density in the Greenland Sea Gyre (see section 3.5.4.6 and Figure 3·39).

Freshwater influx to the upper Greenland Gyre from the East Greenland Current may inhibit the formation of the dense water during any given winter (Clarke *et al.* 1986, Muench 1990). This happened, for example, during the winter of 1988-89 when convection reached just to an intermediate depth of 1600 m. Hydrographic observations and measurements of the concentrations of chlorofluorocarbons (CFCs) have suggested that the formation of Greenland Sea Deep Water slowed considerably during the 1980s, related to a weakened convection in the Greenland Sea (Schlosser *et al.* 1991, Malmberg and Jónsson 1997). The formation of Greenland Sea Deep Water is estimated at 0.1-0.47 Svd (Schlosser *et al.* 1991, Bönisch and Schlosser 1995), with the value of 0.47 Svd being the deep-water formation rate from 1965 to 1980, and 0.1 Svd since 1980. A decrease in the salinity in the upper water column in the Greenland Sea could be the cause of this reduction, which seems to have started at the time of the appearance of the salinity anomaly in the East Greenland Current between 1981 and 1982 (Dickson *et al.* 1988).

The western portion of the Greenland Sea has perennial ice cover, due to ice formed locally as well as ice advected from the Arctic Basin through the Fram Strait. The Jan Mayen Gyre entrains some ice from the East Greenland Current into the center of the sea. This feature, known as the 'Odden', is located at about 74°N (Parkinson *et al.* 1987). Ice extent reaches its maximum in February-March and its minimum in August-September. The eastern portion of the Greenland Sea is kept free of ice by the warm waters of the West Spitsbergen Current.

Polar flow through the Nordic Seas

The East Greenland Current brings water from the Arctic Ocean southward along the East Greenland coast to the Atlantic Ocean. This current consists of three water masses: Arctic Surface Water (Polar Water), Atlantic Water that has completed a cyclonic gyre in the Arctic Ocean (Intermediate Atlantic Water) or has recirculated in the Fram Strait (Return Atlantic Water), and deep waters, mainly Eurasian Basin Deep Water. Year-long moored measurements from the East Greenland Current near 79°N show a mean southward transport of about 3.0 Svd in the upper 700 m, of which about 1.0 Svd is Polar Water (Foldvik *et al.* 1988). The southward flux of Eurasian Basin Deep Water is about 1 Svd (Bönisch and Schlosser 1995).

The East Greenland Current follows the edge of the Greenland continental shelf as a southward boundary current. Highest velocities are centered over the continental slope. The main body of the current forms a surface layer between 100 and 200 m thick. Seasonal variations are well pronounced, with the current being deflected offshore during summer because of runoff along the east coast of Greenland and the surface broadening during winter.

Deep water entering the Greenland Sea through the Fram Strait can be separated into three different water masses (Aagaard *et al.* 1991, Rudels and Quadfasel 1991). The densest of these water masses is found at a depth of approximately 2000 m in the Greenland Sea. Since the depth of the ridge between Greenland and Jan Mayen is about 1600 m, the flow of the most dense water turns eastward north of the ridge. Along the path, it mixes with Greenland Sea Deep Water and forms Norwegian Sea Deep Water. Part of the newly formed Norwegian Sea Deep Water will recirculate in the Greenland Sea or enter the Arctic Ocean below the West Spitsbergen Current (Smethie *et al.* 1988), while the rest (about 0.9 ± 0.1 Svd, Swift and Koltermann 1988) enters the Norwegian Sea mainly through the Jan Mayen Fracture Zone (Sælen 1983). Some of this water eventually enters the North Atlantic through the Faeroe-Shetland Channel.

The two other deep-water masses pass through the Greenland Sea as narrow cores along the East Greenland continental slope at depths of around 1000 m and 1500 m, and enter the Western Iceland Sea. Signals of the densest Eurasian Basin Deep Water, however, have also been seen in the Western Iceland Sea (Malmberg *et al.* 1990, Aagaard *et al.* 1991, Rudels and Quadfasel 1991). Transport between the Greenland Sea and the Iceland Sea through the passage between Greenland and Jan Mayen is about 2.5 Svd (Buch *et al.* 1996).

The Jan Mayen and the East Icelandic Currents are formed by branches of the East Greenland Current. The Jan Mayen Current completes the southern rim of the counterclockwise gyre north of Jan Mayen, while the East Icelandic Current augments the counterclockwise gyre north of Iceland.

The Iceland Sea

Atlantic Water is found over the north Icelandic continental shelf, where it interacts with shelf water (Stefánsson 1962, Swift and Aagaard 1981). Polar Water is found over the Greenland continental shelf, but is also occasionally carried into the Iceland Sea by the East Icelandic Current (Malmberg 1984). The Polar Front separates the Polar Water from

the Arctic Water. The location of this front depends on water transport in the Irminger Current, as well as in the East Icelandic Current.

Hydrographic conditions in the Iceland Sea are highly variable because of its location near the boundary between warm and cold currents. Changes in the inflow of Atlantic Water and variability in the extent of Polar Water lead to marked fluctuations in salinity and temperature, both in space and time (Stefánsson 1962, Swift and Aagaard 1981, Malmberg 1984, Hopkins 1991, Buch *et al.* 1992 and 1996, Malmberg and Kristmannsson 1992).

Below approximately 600 m, the deep water is mostly Norwegian Sea Deep Water (nearly 60% of the total volume), but some Eurasian Basin Deep Water has also been detected near the Denmark Strait (Buch *et al.* 1992). Arctic Intermediate Water accounts for 30%, and the remaining 10% is distributed amongst the surface water masses (Swift and Aagaard 1981). The Arctic Intermediate Water is partially formed locally in winter and comprises much of the overflow water that enters the North Atlantic (Swift *et al.* 1980).

Overflow waters

Below the Atlantic inflow to the Nordic Seas, intermediate and deep waters flow out into the North Atlantic basin. Because of the ridge system in the southern part of the Nordic Seas, only a small amount of deep water, 10-15% of the circulation in the deep basins (>1500 m), will escape to the North Atlantic. Flow through the deep channels (500-800 m) of the Greenland-Scotland Ridge consists mainly of Arctic Intermediate Water (Swift *et al.* 1980, Blindheim 1990, Bönisch and Schlosser 1995), but also some deep waters.

The Faeroe channels are the deepest connections across the Greenland-Scotland ridge system. They have complex topography. Cold water ($t < 3°C$) leaves the Norwegian Sea along the bottom of the Faeroe-Shetland channel and through the Faeroe Bank Channel in a relatively thin near-bottom flow, with mean velocities of 50 cm/s (Saunders 1990). Strong mixing and entrainment of North Atlantic Water occurs when the Overflow Water leaves the channel and starts sinking into the deep basins of the North Atlantic. This is where production of North East Atlantic Deep Water (mixing between North Atlantic Water and Overflow Water) begins. The upper boundary of the North East Atlantic Deep Water is found at about 2000 m all the way from the Faeroe Bank Channel to the east coast of North America.

The Iceland-Faeroe ridge, with a sill depth less than 500 m, is the shallowest portion of the Greenland-Scotland ridge system. Intermittent overflow (Meincke 1983) across the ridge joins the waters of the Faeroe Bank Channel outflow and undergoes the same modifications. How much North Atlantic Water is entrained into the Overflow Water is not easy to say, but it is thought that most of the mixing takes place just south of the ridges. The combined southward flow of North East Atlantic Deep Water along the eastern flank of the Reykjanes Ridge is estimated at 3.5-5.7 Svd (Dickson and Brown 1994, Price and O'Neil Barringer 1994). The densest component of this water mass remains in the northeastern basin, while the rest enters the northwestern Atlantic through the Charlie Gibbs Fracture Zone.

The topography and current distribution in the Denmark Strait is relatively simple. Cold southward currents are located along the Greenland slope, with Polar waters in the near surface layers and the Arctic intermediate and deep waters in the deeper layers. The currents in the Denmark Strait are strongest in the near-bottom layer over the Greenland slope. Current measurements indicate velocities between 40-95 cm/s (Aagaard and Malmberg 1978, Meincke 1983). The maximum observed velocity was 167 cm/s at 100 m above the sea floor (Ross 1978). Over the Iceland slope, the northward current flows at about 10 cm/s (Kristmannsson *et al.* 1989).

The southward transport of deep water through the Denmark Strait varies between 1 and 7 Svd, and these variations typically occur in bursts of one-day duration at intervals of several days (Meincke 1983). The cause of these fluctuations is not yet fully understood. A representative figure of 2.9 Svd is used as a mean value for the Denmark Strait overflow (Dickson and Brown 1994). The overflow from the Denmark Strait increases rapidly by entrainment to 5.2 Svd at 160 km downstream from the sill. Its speed decreases to about 33 cm/s south of Dohrn Bank, and further decreases to 25-30 cm/s from Angmagssalik to Cape Farewell. At Angmagssalik, the volume transport has increased to 10.7 Svd by merging of the eastern deep waters and entrainment of Labrador Sea Water. By the time the overflow current reaches Cape Farewell, its transport has further increased to 13.3 Svd.

Water masses associated with the different overflows over the Greenland-Scotland ridge are Arctic Intermediate Water and Arctic Deep Waters (Norwegian Sea Deep Water, Greenland Sea Deep Water, and Eurasian Basin Deep Water). The characteristics of these overflow streams are that they are fast (up to 60 cm/s long-term mean), thin (100-150 m), follow topography with intense near-bottom shear, have maximum entrainment close to the source, and nonlinear deceleration and deepening occurs downstream as a result of frictional effects (Dickson and Brown 1994).

Water from the Iceland-Scotland overflow undergoes stronger cross-isopycnal mixing near its origin than does the Denmark Strait overflow. The North East Atlantic Deep Water is therefore less dense, and thus is found above North West Atlantic Deep Water from the northern Irminger Sea to the continental margin of North America. The densest water does not pass southward around the Grand Banks (Swift 1984).

3.5.4.4. **The Labrador Sea, Baffin Bay, Canadian Archipelago, and Canadian inland seas**

Labrador Sea

The East Greenland Current, after passing through the Denmark Strait, is joined by a branch of the Irminger Current. Intense mixing between the two water masses takes place during the subsequent southward flow (Buch 1985). Off southeast Greenland, the current is augmented further by water recirculating from the North Atlantic Current. The West Greenland Current is the continuation of these water masses and follows the west coast of Greenland to the northern part of Baffin Bay. Along its northward course, the current branches several times westward into the Labrador Sea. Just south of the Davis Strait, the West Greenland Current divides and sends a major branch westward, while the inshore portion continues northward through the Davis Strait and into Baffin Bay (Figure 3·33).

The hydrographic conditions in the upper layers on the eastern side of the Labrador Sea depend on a variable mixture of cold, low-salinity Polar Water and warmer, more saline Irminger Water. Beneath this upper water mass is a water mass that forms from a mixture of Irminger Water and Labrador Sea Water (Lazier 1973, Clarke and Gascard

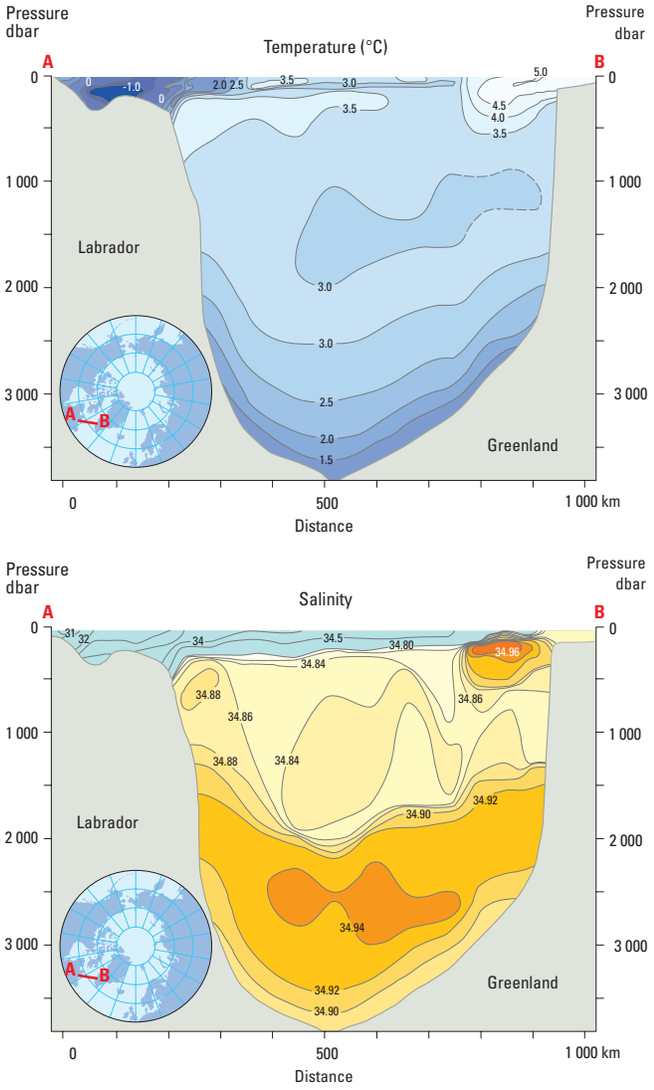

Figure 3·35. Temperature and salinity of the Labrador Sea. The cold freshwater from the Arctic Ocean and Baffin Bay is seen above the continental shelf (Source: Stein and Wegner 1990).

1983, Clarke 1984). Vertical distributions of temperature and salinity for the Labrador Sea are shown in Figure 3·35.

The Labrador Current (Figure 3·33) flows southward over the continental shelves and slopes of Labrador and Newfoundland from the Hudson Strait around the Tail of the Grand Banks of Newfoundland and the coast of Nova Scotia. The Labrador Current is comprised of water from the Hudson Strait, the Baffin Island Current, and the branch of the West Greenland Current that turns westward in the Davis Strait. The Labrador Current transports 3.8 ± 0.9 Svd, of which 85% occurs over the slope between the 400 and 1200 m isobath and 15% occurs over the shelf (Lazier and Wright 1993).

The upper layers of the western part of the Labrador Sea consist of cold, low-salinity water from the Hudson Strait and the Baffin Bay, as evidenced by temperatures as low as –1.5°C and salinities less than 34.0. This water often extends offshore to form the surface layer over most of the sea (Lazier 1973). Offshore of the Labrador Current, one can frequently find Irminger Water at depths of 200 to 1000 m that has been carried all the way around the Labrador Sea.

An important feature at intermediate depth is Labrador Sea Water, a low-salinity water mass, formed as a result of mixing and cooling surface water masses transported into this region. This intermediate water mass is renewed via convection (see section 3.5.4.6) to as deep as 2000 m in winter. Renewal occurs in the central Labrador Sea, where the isopycnals rise to meet the sea surface because of the cyclonic circulation of the sea. Surface water cooled here sinks to intermediate depths along isopycnal surfaces (Lee and Ellett 1967, Lazier 1973, Talley and McCartney 1982, Clarke and Gascard 1983, Gascard and Clarke 1983). At a depth of 1500 m, the water has a temperature of about 3.4°C and a salinity of about 34.9. Labrador Sea Water is advected into the Irminger Sea, into the North Atlantic Ocean, and southward along the western boundary of the North Atlantic Ocean.

The Deep Western Boundary Current is found along the lower continental slope. It flows north along the West Greenland slope and continues around the entire Labrador Sea until it exits north of Flemish Cap. Water masses associated with this current are the North East Atlantic Deep Water and the Denmark Strait Overflow Water (also called the North West Atlantic Deep Water). The North East Atlantic Deep Water, characterized by a salinity maximum between σ_θ values of 27.80 and 27.88, originates in the Iceland-Scotland overflow (Clarke 1984). It circulates above and seaward of the cold Denmark Strait Overflow Water (Swift 1984, Lazier and Wright 1993).

Davis Strait sea ice formed in the fall is advected southward in the Labrador Current where it is joined by floes exported from the Foxe Channel of the Hudson Strait. Carried rapidly to the south, the ice reaches the eastern coast of Newfoundland by January-February. By March-April, it has reached its southern extreme, approximately at the limits of the current. In April, the marginal ice zone retreats rapidly back to the north. In some years, Arctic ice of the East Greenland Current rounds the southern tip of Greenland and makes its way northward in the West Greenland Current.

Baffin Bay

Baffin Bay is a relatively deep basin (>2100 m), but communication with the Arctic Ocean and the Labrador Sea is limited by sills (250 m in the north, 640 m in the south). The overall circulation is cyclonic, and the two dominant features of the circulation are the West Greenland Current and the Baffin Island Current, also called the Baffin Land Current or the Canadian Current (Bailey 1957, Collin and Dunbar 1964, Muench 1971, Buch 1985, Rudels 1986b).

The lower part of the West Greenland Current shows clear influence of Atlantic Water as it enters Baffin Bay, with a temperature maximum at about 500 m, but it experiences a rapid temperature decrease as it moves northward along the Greenland coast. In the northern parts of Baffin Bay, the influence of Polar Water flowing southward from the Nares Strait is strong. When the 'Atlantic' layer exits through the Davis Strait (as part of the Baffin Island Current), it might contain as little as 1/6 water from the south and as much as 5/6 water from the Arctic Ocean (Rudels 1986b).

The Baffin Island Current, flowing south along the east coast of Canada, is much stronger and more voluminous than the West Greenland Current. The reason for this is that the Baffin Island Current is augmented by inflowing currents from Smith Sound, Jones Sound, and Lancaster Sound. South of the sounds, the Baffin Island Current continues southward along the east coast of Baffin Island, through the Davis Strait, and into the Labrador Sea, where it becomes part of the Labrador Current. The Baffin Island Current generally has higher speeds toward the south, as it accumulates water from the various inflows.

Three water masses can be distinguished in Baffin Bay:

1. the surface water (upper 200 m), characterized by cold temperatures of about –1.6°C and a salinity of about 33.7; in summer a layer of fresher (30-32) and warmer (2-5°C) water covers the surface. Winter convection is thought to be limited to this layer, because of a strong thermocline below;
2. the Atlantic Water, which is warm ($t > 0$°C) and saline (34.5) with a temperature maximum at about 500 m (0.5-1.5°C); and,
3. the Baffin Bay Deep Water (below 1400 m), which is a very uniform water mass with a temperature of – 0.44°C and salinity of 34.4.

In the central portion of Baffin Bay, a depression (>2200 m deep) is filled with Baffin Bay Bottom Water. The deep and bottom waters of Baffin Bay originate in the Arctic Ocean (from depths of about 250 m) and enter Baffin Bay mainly through the Nares Strait. Because of higher density, these Arctic Ocean waters sink to the bottom (Bailey 1956, Tchernia 1980, Rudels 1986b, Bourke and Paquette 1991).

The sea ice of this region is comprised mostly of locally generated, first-year ice, with a small amount of multi-year Arctic ice transported southward through the Nares Strait.

Nares Strait

The Nares Strait lies between the Canadian Archipelago and Greenland. It connects the Smith Sound of Baffin Bay with the Lincoln Sea of the Arctic Ocean. The water in the Nares Strait is advected almost unchanged from the Lincoln Sea. There are seasonal changes in the water structure due to freezing and heating, but these are confined to the near-surface layer of 50 m. The most obvious feature of the water structure is a layer of cold water with a temperature minimum ($t = -1.4$°C, $32 < S < 33.5$) at a depth of about 75 m. Below the sill depth (250 m), the water is warmer (about 0°C) and more saline ($34.0 < S < 34.8$) (Sadler 1976).

Canadian Archipelago

The Canadian Archipelago lies on the extensive polar continental shelf of North America and constitutes a network of shallow channels that forms a transition zone between the waters of the Arctic Ocean and Baffin Bay. The water which flows through the many straits and sounds of the Canadian Archipelago originates mainly in the surface layer of the Arctic Ocean, the net transport being from the Arctic Ocean. The volume transport through the different channels is not confidently known, but is thought to be about 1.7 Svd (Fissel *et al.* 1988). These flows are likely to be important to the freshwater and contaminant budgets of the Arctic Ocean since they consist mostly of Polar Surface Water. About half the Polar Surface Water which ultimately discharges into the Atlantic Ocean passes through these channels (Stigebrandt 1981).

In the western part of the Archipelago, the water is identical in physical properties to that of the Canadian Basin, the upper layer being characterized by Polar Surface Water and the lower layer with Atlantic Water. Moving eastward, the halocline is warmed up as a result of heat diffusion from the underlying Atlantic water, and the Atlantic Water found in the different basins of the western Archipelago is therefore colder than Atlantic Water with the same salinity in the Canadian Basin (Melling *et al.* 1984).

The water leaves the Archipelago by three main exits. The two largest, Jones Sound (150 m × 12 km) and Lancaster Sound (130 m × 55 km) empty into Baffin Bay, while the smaller, Fury and Hecla Strait, empties into Foxe Basin and ultimately passes through the Hudson Strait and into the Labrador Sea. Water flowing through Jones and Lancaster Sounds has a much higher Bering Sea Water component than water entering Baffin Bay through Smith Sound (Codispoti and Owens 1975, Jones and Coote 1980).

An important feature of this region is the high velocity currents, especially in some passages, that run through the Arctic Islands. Maximum speeds can be more than 2.0 m/s and the energy available in these currents is sufficient to bring warmer, more saline water from below the sill depth up to the surface. The result is a reduced rate of sea-ice formation. Enhanced heat flow and mechanical removal of ice by these strong currents are in many places responsible for large open-water areas, polynyas, that are so common in this area and which often remain ice-free even in midwinter (Topham *et al.* 1983, Melling *et al.* 1984).

The new ice cover in the Archipelago has generally developed by the middle of October. Ice within the channels of the Archipelago is shorefast, typically reaching thicknesses of 1.7 to 2.3 m. It breaks up by the middle of July. The break-up of sea ice proceeds into the Archipelago from Amundsen Gulf. Break-up is not always complete, allowing multi-year ice to develop, in some areas reaching great thicknesses. Once break-up has occurred, there is a general easterly drift of the locally formed ice, together with some ice advected from the Arctic through the M'Clure and other straits.

Foxe Basin

Foxe Basin is a shallow inland sea with an average depth of less than 100 m. Water from the Arctic Ocean enters Foxe Basin through the Fury and Hecla Strait (Figure 3·36). Outside the strait, the Arctic Water is stratified, but intense mixing takes place as it passes the sill of the Fury and Hecla Strait and the water enters Foxe Basin as a homogeneous water mass. Very high current speeds, up to 3 m/s, have been observed in the strait (Collin and Dunbar 1964, Sadler 1982). The inflow is rather small, 0.04 Svd in the winter (Sadler 1982)

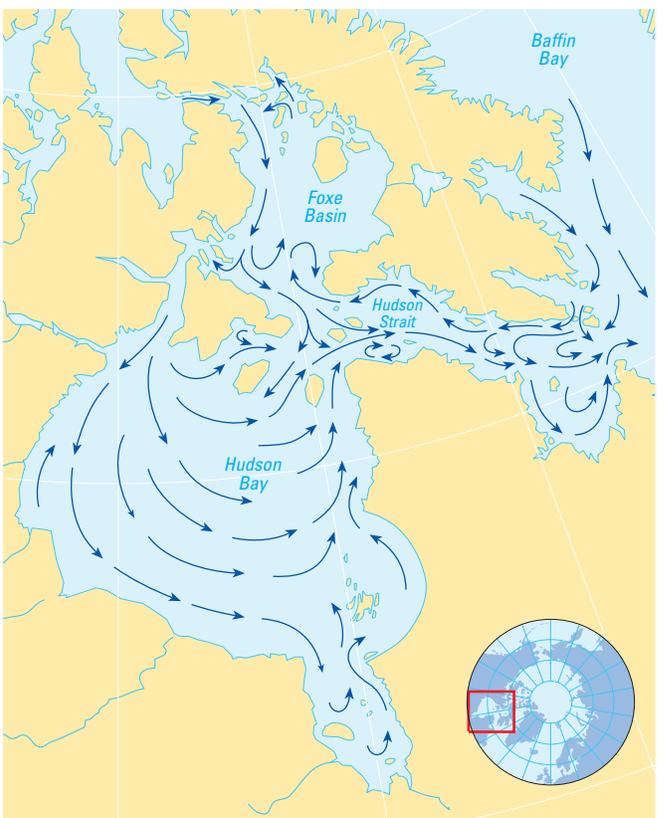

Figure 3·36. Surface currents in Hudson Bay, Hudson Strait and Foxe Basin.

and 0.1 Svd in the summer (Barber 1965), but even so, it fills the northern half of the Foxe Basin in one year, and has a substantial influence on the circulation in the basin (Prinsenberg 1986a).

Arctic Water is lighter than the water in Foxe Basin and flows southward, on top of it, along the coast of Melville Peninsula. Northeast of Southampton Island, a branch moves westward into the Frozen Strait, through Roes Welcome Sound and into the Hudson Bay. A second branch turns northeasterly and joins water entering Foxe Basin from the Hudson Strait. Both branches enter a counterclockwise gyre in the area south of Prince Charles Island. A third branch continues through Foxe Channel and into the Hudson Strait.

In the eastern and central part of the Foxe Basin, the large tides (up to 8 m) result in a well mixed and essentially homogeneous water mass from top to bottom; whereas on the western side, the water is stratified (Campbell 1964, Prinsenberg 1986a). Seasonal changes in surface temperature are very small, from –1.7°C to about 3.0°C. Surface salinity can occasionally fall far below 20.0, reflecting dilution by meltwater and river runoff. By late summer and early autumn, surface salinities are back to a level of 29.0-32.0. During winter, the density of the surface water increases due to cooling and brine release. The cold, saline bottom water (t = –1.97°C, S = 34.07) in deeper parts of Foxe Basin and Foxe Channel is a result of dense water formation over shallow shelves in the eastern basin during winter (Campbell 1964).

A sill (185 m) separating Hudson Bay and Foxe Channel prevents the inflow of this cold, saline bottom water into Hudson Bay, except for intermittent occasions when this water mass reaches a depth of 185 m or less (Campbell 1964). Even so, the deep, homogeneous bottom layer in Hudson Bay is assumed to be a result of intermittent overflow, rather than the formation of dense water inside Hudson Bay (Prinsenberg 1986a).

Hudson Bay, James Bay, and Hudson Strait

Hudson Bay, which is a broad, shallow, semi-enclosed sea, lies almost entirely south of the Arctic Circle. It does not interact directly with the Arctic Ocean; rather, it is externally forced by the Atlantic Ocean via the Hudson Strait, and the waters within the bay are modified by substantial runoff (Prinsenberg 1991).

Hudson Bay has an average depth of 125 m. Water column properties vary throughout the year because of melting, freezing, and river runoff. Surface cooling and wind mixing cause the seasonal pycnocline to deepen from 10 m in the summer to 40 m in the late fall. During winter, salt is rejected from the developing sea-ice cover and the pycnocline deepens even more, to about 90 m.

Circulation in Hudson Bay (Figure 3·36) is cyclonic with southward flow on the west side and northward flow on the east side (Hachey 1935, Barber 1967). No return loop has been observed in the northern part of the bay, rather the surface water exits into the Hudson Strait (Prinsenberg 1983). Watershed contribution to Hudson Bay from its shores is large (0.02 Svd). As this water flows over the surface of the bay, it is deflected to the right by the Coriolis force and adds to the cyclonic circulation (Prinsenberg 1986b). The surface layer of Hudson Bay is strongly influenced by the river runoff - salinities lie between 24.0 and 30.0 in summer. Surface temperatures in summer are between 5 and 9°C.

Surface water entering from Foxe Basin and the Hudson Strait sinks below the surface layer in the Hudson Bay because of its higher density. Deep water exchange with the adjacent seas is limited by the sill depths, the deepest (185 m) being the one between Hudson Bay and the Hudson Strait (Prinsenberg 1986a).

Hudson Bay is almost completely covered with ice during the winter, and is completely free of ice in the summer. With the exception of some influx through Foxe Basin, the ice is local. It begins to form in November, and has almost completely covered the bay by December. The bay remains covered until at least May, when break-up begins. By June, the ice retreats from the northeastern and northwestern coastlines, but it remains in the southwestern portion through July, not disappearing totally until August.

James Bay is extremely shallow, with only a few locations having depths over 50 m. In summer, the water in James Bay is warmer and fresher than Hudson Bay water, and is therefore easily identified as it flows northward along the west coast of Quebec. The large runoff rates (0.01 Svd) of the James Bay region account for 61% of the freshwater brought into Hudson Bay (Prinsenberg 1986b). In James Bay, a cyclonic gyre exists, partly caused by wind stress and partly by freshwater runoff. Water from James Bay enters the Hudson Bay with velocities above 15 cm/s (Prinsenberg 1986c).

The main hydrographic feature of the Hudson Strait is a marked across-channel gradient in the surface temperature and salinity, with higher temperature and lower salinity in the south (Drinkwater 1986). The southeastward flow in the Hudson Strait originates in the outflows from Foxe Basin and Hudson Bay (Figure 3·36). As these waters proceed toward the east, they tend to be confined to a thinner surface layer and finally lose most of their identity as they reach the waters of the open ocean (Collin and Dunbar 1964). At the northern side of the strait, water from the Baffin Island Current flows northwestward (Iselin 1927, LeBlond 1980), sending out branches to the southern side that join the southeastern outflowing current. Water from Hudson Bay is modified through mixing with colder surface water from Foxe Basin and some colder, higher-salinity deep water in the strait. When this water approaches the eastern entrance to the Hudson Strait, it undergoes intense vertical mixing and further modification.

3.5.4.5. **The Bering Sea**

The Bering Sea is the northernmost extension of the Pacific Ocean, separated from the Pacific by the Aleutian Islands, which form a partial barrier to water exchange between the North Pacific Ocean and the Bering Sea. The water entering the Bering Sea from the south is Alaskan Stream Water. The Alaskan Stream is the northern boundary current of the Pacific subarctic gyre and extends from the head of the Gulf of Alaska to the western Aleutian Islands (Figure 3·37). The Alaskan Stream flows along the Aleutian Islands in a narrow, high-speed and very stable westward current, generally seaward of the 1000 m isobath (Stabeno and Reed 1991). Exchanges to the north (and south) are small, relative to the total volume transport (15-20 Svd) of the Alaskan Stream (Reed 1984). The maximum sill depths of the major openings are 430 m (Amukta Pass), 1155 m (Amchitka Pass), 2000 m (Near Strait), and 4420 m (Kamchatka Strait) (Favorite 1967). The easternmost pass through which significant northward transport (>1 Svd) of Alaskan Stream Water occurs is Amchitka Pass (Reed 1990, Stabeno and Reed 1994), while water transport through the passes east of 180° are intermittent and limited. The major inflow occurs through the Near Strait (10 Svd), but is variable. In 1991, there was essentially no inflow of Alaskan Stream Water (Stabeno and Reed 1992), but in 1992, there was a well developed northward flow (Reed

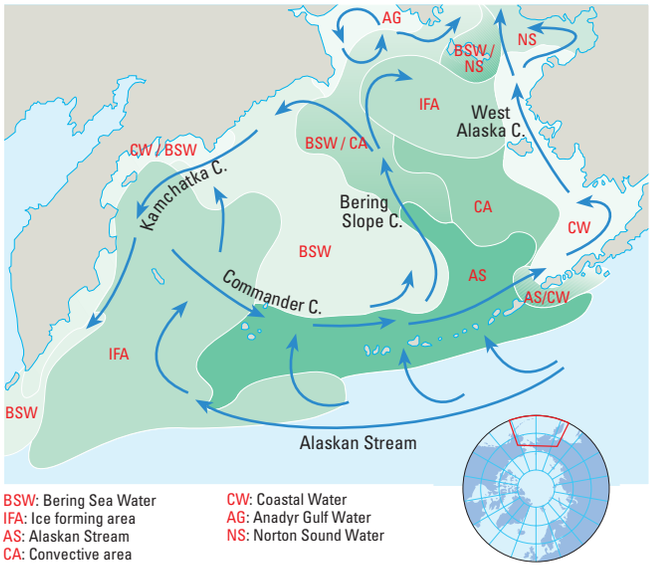

Figure 3·37. Schematic diagram of circulation and the extent of different water masses in the Bering Sea (Source: Takenouti and Ohtani 1974).

and Stabeno 1993). All deep-water inflow to the Bering Sea has to take place through the Kamchatka Strait.

The Bering Sea has a vast continental shelf that occupies about 44% of the total area – 43% of the shelf is abyssal with water depths generally >3000 m, and 13% is continental slope (Hood and Kelley 1974). Bering Sea Water is comprised of Pacific Ocean water that enters through the Aleutian passes and is modified by local processes. Figure 3·37 is a schematic diagram of circulation and the extent of water masses and their characteristics.

Circulation within the Bering Sea basin is generally cyclonic. Most of the flow through the Near Strait turns eastward and follows the Commander Current along the north side of the Aleutian Islands. Inflows through the other passes join this flow eastward. The Bering Slope Current (5 Svd) follows the continental slope along the Aleutian basin up to Cape Navarin where it bifurcates; a smaller part (about 10%) of the flow follows the 60-70 m isobath around the Gulf of Anadyr, and the rest turns south and joins the Kamchatka Current (Paluskiewicz and Niebauer 1984, Royer and Emery 1984, Kinder *et al.* 1986). The Kamchatka Current forms the western boundary current of the Bering Sea Gyre. Outflow from the Bering Sea to the Pacific Ocean is confined to the Kamchatka Strait. The latest measurement of the outflow from the Bering Sea through the Kamchatka Strait ranges from 6 Svd in 1991 (Stabeno and Reed 1992) to 12 Svd in 1990 (Verkhunov and Tkachenko 1992).

The vertical density structure of the southwestern Bering Sea can be represented by a surface layer, about 200 m thick, a deeper transition layer near 500 m, and a bottom layer. The deep Bering Sea is a vast plain lying at a depth of 3800 m with occasional hollows up to 4150 m deep (Tsunogai *et al.* 1979). The Bering Sea Deep Water has the highest silica concentration in the world ocean (Mantyla and Reid 1983).

The Bering Sea Shelf is very broad (500 km), unusually flat, and featureless. The shelf is divided into three regimes (Kinder and Schumacher 1981): 1) the inner shelf (<50 m); 2) the central or middle shelf (50-100 m); and, 3) the outer shelf (>100 m). The shelf break occurs near the 200 m isobath.

On the southeastern shelf there are two water masses: Alaskan Coastal Water and Central Shelf Water (Coachman 1986). The Alaskan Coastal Water (CW in Figure 3·37) is a mixture of seawater and freshwater runoff from land, formed in the coastal zone from the shore to the 50 m isobath. It tends to be vertically homogeneous because of mixing by tidal currents and wind (as shown in Figure 3·38), except near river mouths where the freshwater input is sufficient to create a two layered structure. Estimates of the mean annual runoff are about 8.0-10.0 $\times 10^3$ m^3/s, with a minimum in

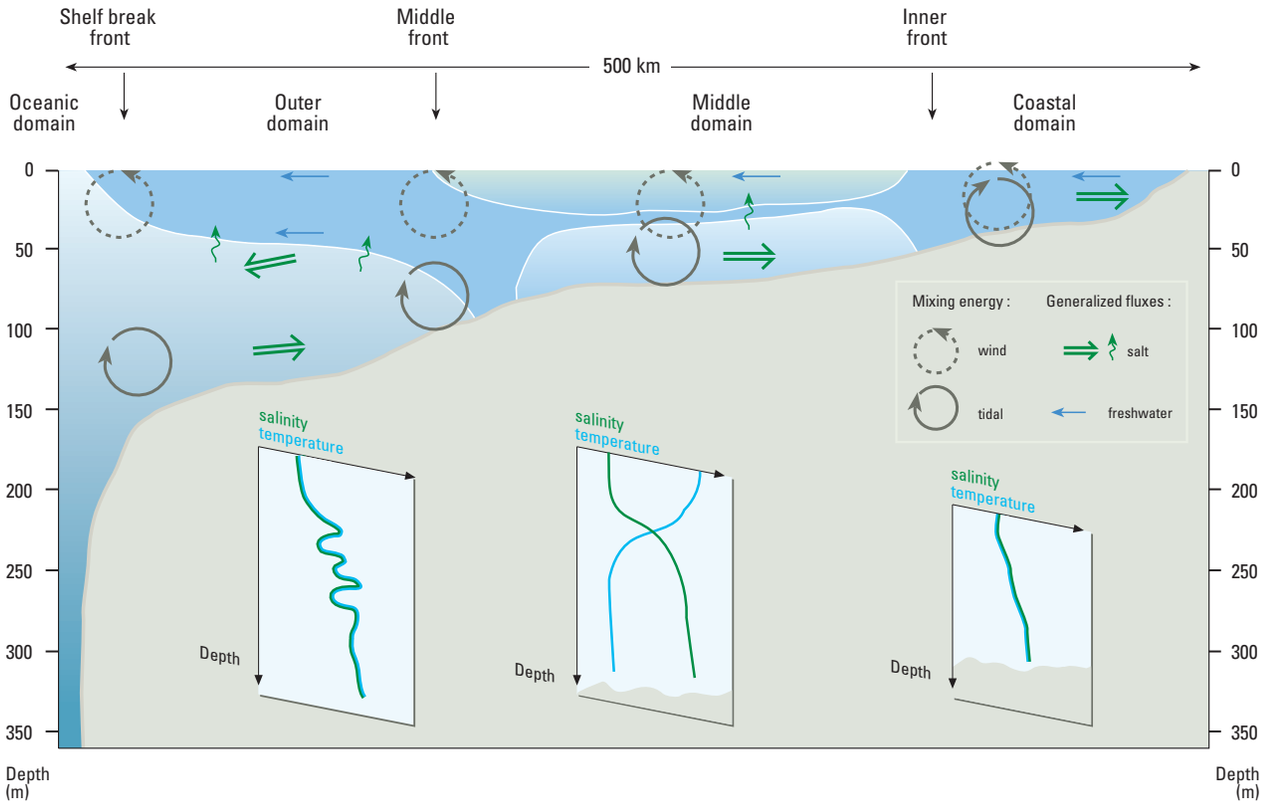

Figure 3·38. The different domains of the Bering Sea continental shelf are separated by fronts. The coastal domain (depth <50 m) tends to be vertically homogeneous, the middle domain (50-100 m) shows a clear two-layered structure, while the outer domain (100-170 m) is dominated by lateral interaction between the shelf water and the Bering Sea Water (Source: Coachman and Walsh 1981).

spring and maximum in early summer (Roden 1967, Coachman *et al.* 1975, Overland 1981).

The Central Shelf Water is formed between the 50 m and 100 m isobaths from a mixture of seawater and freshwater (from ice melting and precipitation). It has a tendency toward a two-layered structure (Coachman and Walsh 1981, Kinder and Schumacher 1981, Muench 1983) with a surface layer 10-40 m thick overlying a relatively homogeneous deep layer (Figure 3·38). In winter, the shallower part of this area (<70 m) becomes a cold, homogeneous water column because of cooling and wind mixing. In spring, when ice starts to melt and the winter storms cease, the two-layered structure is re-established. Horizontal gradients in both salinity and temperature are small. The Central Shelf Water is found in the convective areas (CA) and ice-formation areas (IFA) (Figure 3·37). A strong inner front separates the Central Shelf Water from the Alaskan Coastal Water (Coachman and Walsh 1981) and an outer front also inhibits lateral fluxes from the west.

The outer continental shelf (>100 m isobath) is a zone of lateral water mass interaction (Figure 3·37) between Central Shelf Water and Bering Sea Water (BSW). A northwest current (1-10 cm/s) exists over the outer shelf, while the flow over the middle shelf is insignificant (Schumacher and Kinder 1983).

Mean salinity in July ranges from 31‰ near the Alaskan coast to 33 at the 200 m isobath (Kinder *et al.* 1986). Because of the low salinities in the surface layer on the continental shelf, the depth of vertical convection due to ice formation is only about 50 m. Particularly in the Gulf of Anadyr (Figure 3·37), where oceanic water enters at a lower level, convection is restricted to the upper 30 m, and no cold high-salinity water is found at the bottom (Takenouti and Ohtani 1974).

Over the continental shelf, the West Alaska Current follows the coastline from north of the Alaska Peninsula to the Bering Strait, entering the Arctic Ocean on the eastern side of the strait. The current is influenced by water transports from the local rivers: the Kvichak, Nushagak, and Kuskokwim Rivers, and most of all by the Yukon River farther north. Any contaminant load brought by these rivers to the sea enters the West Alaskan Current, and is thereby transported to the north and into the Arctic Ocean. The current appears to be weak (only a few cm/s), at least in the southern part (Kinder *et al.* 1986), transporting about 0.1 Svd to the Bering Strait.

The northern Bering Shelf (also called the Chirikov Basin) lies north of St. Lawrence Island and south of the Bering Strait. Two water masses, Norton Sound water (NS) and Gulf of Anadyr water (AG), that are warm and have low salinity, are formed in the upper 10 m during summer, overlying a bottom layer of colder and more saline water (Figure 3·37).

Circulation in the Chirikov Basin is dominated by a northward net water transport into the Arctic Ocean. This flow is driven by a sea surface slope down to the north which results from the sea level difference between the North Pacific and Arctic Ocean (Stigebrandt 1984, Aagaard *et al.* 1985, Overland and Roach 1987). The regional circulation is therefore normally northward in the Anadyr, Bering, and Shpanberg Straits. Mean currents within these straits are about 25 cm/s in the Bering Strait, 15 cm/s within the Anadyr Strait, and 5 cm/s in the Shpanberg Strait (Aagaard *et al.* 1985). Strong northerly winds coincide in general to weaken the northward currents.

The flow through the Bering Strait to the Arctic Ocean is subject to an annual cycle, with maximum transport (1.0-1.5 Svd) during the summer months and minimum transport (0.3-0.5 Sv) during the winter months (Coachman 1993). The winds are the main cause of these seasonal variations. When strong winds (>8 m/s) from the northeast or east prevail, which is mostly a fall phenomenon, the flow through the Bering Strait reverses (Coachman and Aagaard 1988). Most of the water that finally crosses the Bering Strait originates from the branch of the Bering Slope Current that enters the Gulf of Anadyr (Anadyr Current) before going through the Anadyr Strait or the Shpanberg Strait (Coachman *et al.* 1975).

Small amounts of ice may also be imported into the Arctic Ocean through the Bering Strait, but this can be safely ignored in first-order budgets, since it is much smaller that the errors in the other terms. The calculations of property transport into the Arctic Ocean from the Pacific Ocean are relatively straightforward, provided contaminant data are available, and can probably be better constrained than any of the other ocean exchanges.

The flow of Bering Sea Water through the Bering Strait is less than 5% of the total inflow into the Bering Sea and is not considered an important factor in the water budget. However, this flow does permit the exit of a considerable amount of the freshwater runoff along the coast of the eastern Bering Sea, as well as some of the dilute water found off the coast after the sea ice over the continental shelf melts in late spring. Contaminants delivered by rivers to the shelf will therefore eventually end up in the Arctic Ocean.

The sea ice in the Bering Sea is comprised mostly of locally generated ice, although there is some imported ice southward through the Bering Strait from the Chukchi Sea. The first-year ice is thinner than on many of the northern shelf seas, typically reaching a thickness of 20-40 cm. Formation occurs primarily in the northern Bering Sea, especially in coastal polynyas in Norton Sound and to the south of St. Lawrence Island. The ice then circulates to the southwest in the Bering Gyre, where it moves toward the marginal ice zone and is destroyed by melting. The marginal ice zone is located at the shelf break of the southeastern Bering Sea in winter, and retreats rapidly back to the north in mid-May.

3.5.4.6. **Vertical mixing**

In the Arctic, near-surface seasonal variations can be accounted for by a combination of winter cooling, freezing, and convective mixing, and summer meltwater addition. Different mechanisms for vertical mixing or a combination of these may result in formation of denser water masses. The density of the water produced determines to what depth the water sinks. Especially important is the process of deep convection which helps ventilate the deep basins. Convection is a result of unstable distribution of density in the water column with heavy water above lighter water (Rudels 1993). This situation can arise from cooling and by evaporation or freezing, which increase surface salt concentration.

There are two main types of deep convection (Killworth 1983), shown schematically in Figure 3·39. The first is convection near an ocean boundary (shelf convection), and involves the formation of a dense water mass on the shelf, which then descends down a continental slope and into the deep basin of the ocean (brine formation, left hand side of the figure). The second is open ocean deep convection (mid-gyre convection), occurring far from land, and especially in regions with a shallow thermocline or halocline (i.e., in the center of cyclonic eddies). When the upper layer density is increased, local open ocean convection chimneys may be formed (Killworth 1979).

Cooling and the release of salt into the water from the generation of sea ice are the driving factors in the process of vertical convection and formation of dense water in the Arc-

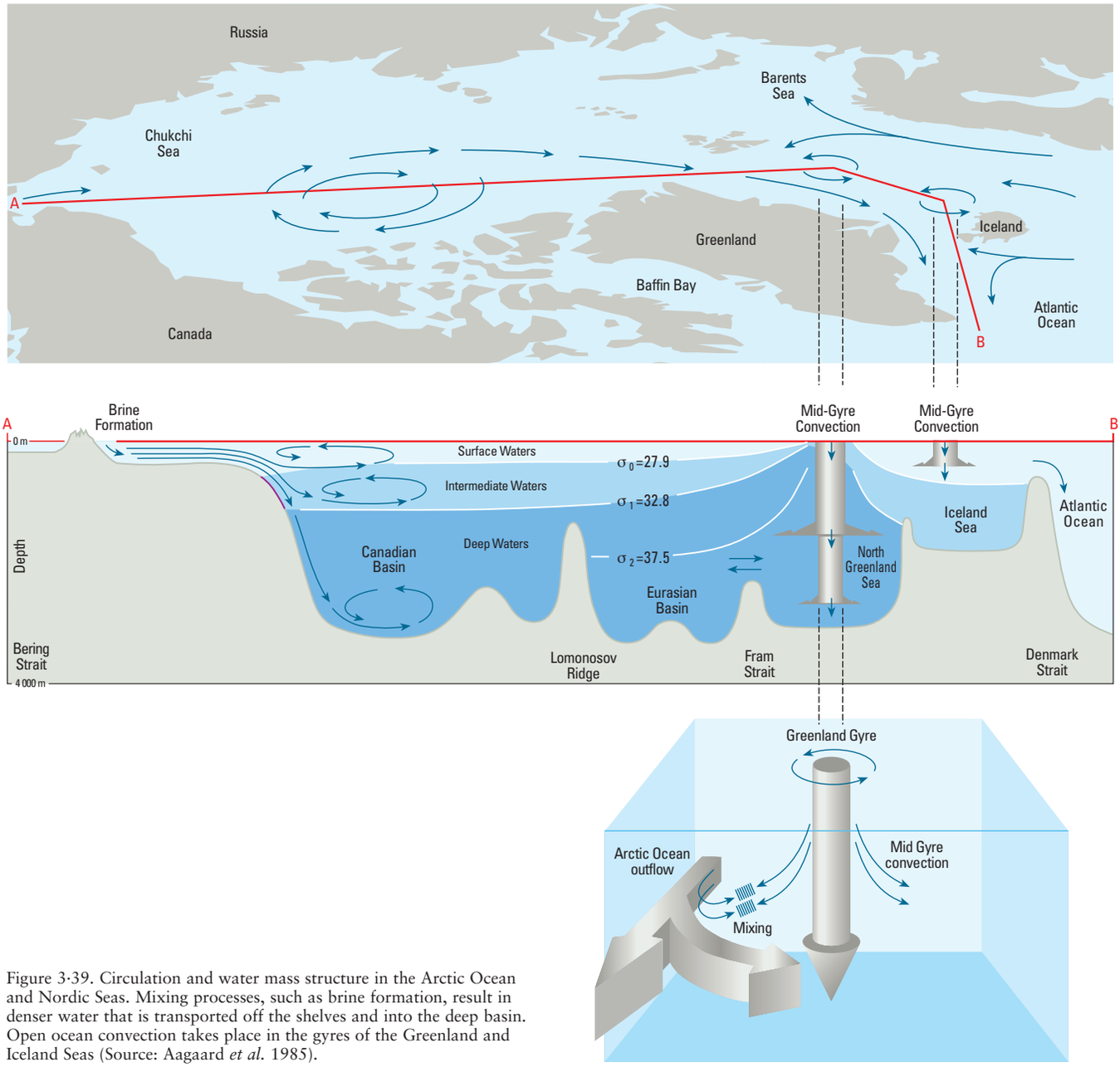

Figure 3·39. Circulation and water mass structure in the Arctic Ocean and Nordic Seas. Mixing processes, such as brine formation, result in denser water that is transported off the shelves and into the deep basin. Open ocean convection takes place in the gyres of the Greenland and Iceland Seas (Source: Aagaard *et al.* 1985).

tic (Killworth 1983, Carmack 1986, Carmack 1990, Rudels 1993). The first type of convection takes place on the continental shelves surrounding the Arctic Ocean, whereas the second type of convection is found in the Greenland, Iceland, and Labrador Seas. Because ice forms on open water at a greater rate than under existing ice, persistent divergence of the ice cover maximizes the formation of dense water (Melling *et al.* 1984).

Shelf convection in the Arctic

The waters on the shelves surrounding the Arctic Ocean are normally stratified during summer due to ice melt, freshwater inflow from rivers, and precipitation. During winter this stratification is broken down as a result of freezing and brine release, and vertical mixing takes place (Aagaard 1994). If the water column becomes homogeneous down to the sea floor, further brine release will result in a movement of the densest water (called bottom water) toward the edge and down the continental slope. Eventually these dense water plumes detach from the slope and move into the interior of the Arctic Ocean at the appropriate density levels (Aagaard *et al.* 1985, Rudels 1993). Water at freezing temperature with a wide range of densities is produced in this manner, depending on initial salinity, bathymetry, ice cover, and wind condition.

On shelves with complicated topography, such as the Barents and Kara Seas, it is likely that bottom-water accumulates in hollows and enclosed depressions (Midttun 1985). When the accumulation is sufficient to overtop and overflow shelf depressions, and where shelf troughs extend across the shelf to the edge, the bottom water runs off and sinks to its density level. The flow from the shelves is thought to be both localized and intermittent.

The higher the surface salinity, the less brine has to be introduced to achieve the density required to produce bottom water. In order to maximize bottom-water production, it is therefore important that the upper layers are preconditioned by removal of freshwater components prior to freezing, and that inflow of river water during winter is blocked (Macdonald *et al.* 1989, Macdonald and Carmack 1991, Omstedt *et al.* 1994, Melling and Moore 1995).

Bathymetry is of great importance for this process, since vertical convection reaches the bottom earlier in shallow areas. Here the water column quickly homogenizes, and bottom-water formation starts.

The strong winds that are typical for the autumn, together with reduced river inflows, can result in well-mixed, relatively saline nearshore water (Carmack *et al.* 1989) before ice starts to form. Also, upwelling of denser water in periods with offshore winds may bring more saline water to the surface. When ice starts to form, wind is important in moving the existing ice away, so that new ice can form in the same area. The reason for this is that most of the salt is rejected back to the underlying water during the freezing process (Gow and Tucker 1990) and faster ice growth in open water areas means that more brine will then be released there than under thicker ice cover.

Due to its high density, bottom-water flows along the sea floor under the influence of the buoyancy, friction, and Coriolis forces. Unfortunately, no concurrent observations of the temperature, salinity, and speed of such currents exist. Calculations with a stream-tube model indicate that drainage currents require a long time to cross a featureless shelf (more than 40-60 days), chiefly because of the predominance of the Coriolis force, which discourages down slope flow. However, more rapid drainage is possible through submarine canyons (Melling and Lewis 1982).

Bottom water formed on the shallow banks around Novaya Zemlya (Midttun 1985) fills the western and eastern Novaya Zemlya troughs. From here, it flows through the St. Anna Trough into the Arctic Basin. The topography of the troughs inhibits strong advection and mixing and allows the salt to accumulate. The St. Anna Trough outflow is therefore dense and can penetrate into the deep water of the Eurasian Basin and contribute to its ventilation. In contrast, the bottom water of the Laptev Sea is less dense and will only intrude into the layer of Atlantic Water (Quadfasel *et al.* 1993). Bottom water has also been observed in the Bear Island Channel, on the Svalbard Bank, and in Storfjordrenna (Sarynina 1969, Anderson *et al.* 1988, Quadfasel *et al.* 1988, Blindheim 1989). In the Chukchi Sea (Aagaard *et al.* 1981), Beaufort Sea (Melling and Lewis 1982, Melling and Moore 1995), and Barrow Canyon, similar water has been observed descending into the Canadian Basin and mixing with existing subsurface water of the same density (Garrison and Becker 1976).

Much of the bottom water produced on the shelves is not dense enough to sink into the deep basins, but enters the depths of the halocline in the Arctic Ocean. The signature of this shelf water can be seen over most of the Arctic Ocean in the temperature-salinity structure of the halocline (Figure 3·40). Both physical and chemical properties indicate that the origin of the upper halocline is in the Chukchi Sea (Aagaard *et al.* 1981, Jones and Anderson 1986), where-

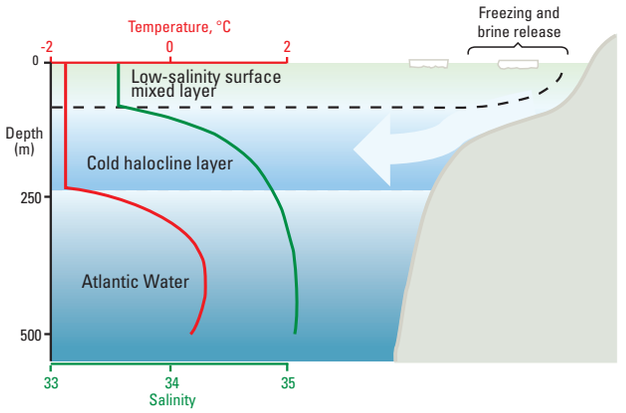

Figure 3·40. Schematic representation of the temperature and salinity structure of the upper Arctic Ocean and how the halocline layer is maintained by brine-rich water produced on the shelves (Source: Aagaard *et al.* 1981).

as the lower halocline originates in the Barents and Kara Seas, but winter convection in the interior of the Arctic Ocean can also be of importance in forming the Arctic Ocean halocline (Rudels *et al.* 1996).

The bottom waters that run off the banks and flow into neighboring depressions and eventually into the deeper basins may transport with them suspended sediments and associated contaminants.

Open ocean convection in the Arctic

Open ocean convection requires cyclonic circulation in a gyre, a preconditioning phase to create low static stability within the gyre, and intense and rapid surface forcing (e.g., by wind) (Killworth 1983). These conditions for open ocean convection occur in the Greenland, Iceland, and Labrador Seas.

The Greenland Sea has been recognized as a source for deep and bottom-water formation since the time of Nansen (1906). Water produced in the Greenland Sea Gyre, that is Greenland Sea Deep Water, is one of the world's densest water types. In the Greenland Sea, cold, fresh, less dense surface water must sink through the warmer, more saline, denser water underneath. Since the surface salinity is too low to allow for deep-reaching convection even if the water is cooled to the freezing point, the freshwater has to be removed to create a water dense enough to convect into the deeper layers. Formation of sea ice aids initiation of deep convection, since freshwater is extracted in the ice while most of the salt remains in the water (Rudels 1993).

Earlier theories about the origin of bottom-water generally involved mixing the surface (Polar Water) and intermediate water (Atlantic Water) via diffusion, turbulence, eddies, ice edge upwelling, or other processes (Carmack and Aagaard 1973, McDougall 1983, Clarke 1986, Rudels 1990). The mixed water, which was then saltier, further cooled at the surface and sank. A more recent theory, also based on mixing of water masses, adds the 'salinization' mechanism of brine rejection by early winter ice formation: ice forms at the surface in early winter, rejecting salt and thus increasing the density of the surface water. Arctic winds then blow the ice away, exposing the 'preconditioned' surface water to cooling and mixing by the strong, cold winter winds. Deep convection then occurs in a series of short, episodic bursts (Pawlowicz *et al.* 1994).

Quadfasel and Rudels (1990) monitored the buildup of a salty layer in the top 5 m of the water column in the Greenland Sea Gyre with a drifting bag equipped with temperature and conductivity sensors. The layer became unstable and ejected a plume draining this top layer. Such plumes entrain ambient water and the upper Arctic layer will eventually be enriched with salt, so that consequent plumes penetrate through the halocline and into the relatively warm intermediate layer (Rudels *et al.* 1989, Rudels 1990).

This warm intermediate water must rise to the surface so that continuity can be preserved. Here it melts the ice and temporarily stops the convection, but after cooling of the surface layer and new ice formation, the haline convection cycle can start again. CTD (conductivity, temperature, depth) profiles obtained in the central Greenland Sea Gyre during several winter cruises apparently confirmed this concept of convection cycles by showing that apparent convection depths increase stepwise rather than continuously (Muench 1990). The severity of the winter cooling influences the amount of deep water that is produced in a given year, and to which depth the convection will take place (Aagaard 1968, Carmack and Aagaard 1973, Schott *et al.* 1993).

Water produced by convection in the Iceland Sea is an intermediate water mass nearly as cold as the deep water, but

slightly less saline, and therefore lying above the deep water (Swift and Aagaard 1981). The key to the formation of this dense intermediate water in winter is seasonal heat loss. The salinity of the Arctic domain waters ultimately limits the density of the water cooled at the sea surface in winter. Maintenance of relatively high salinities in the northern and central Iceland Sea is important for the convective process. The East Greenland Current, carrying relatively low-salinity water, if spread over the Iceland Sea, could bring about sufficient stratification to block winter formation of the densest water masses. A salinity of 34.7 from the surface downward to about 100 m proved to be the critical value in this area. At salinities of 34.7 and lower, the surface water does not reach a density high enough to start a deep convection, even at a freezing temperature of –1.8°C. Salinities of 34.8 or more, however, make this possible (Malmberg 1984).

The part of the Iceland Sea with the highest surface layer densities in winter is well away from the areas that in summer and fall show the strongest influence of the relatively low-salinity surface water carried by the East Greenland Current and East Icelandic Current. The layer formed in winter spreads laterally along isopycnal surfaces throughout the Iceland Sea. The water produced constitutes a major proportion of the overflow of dense water into the North Atlantic.

The development of cyclonic circulation and concentrated cooling and mixing within a cyclonic gyre, together with the presence of a source of warm, salty water (i.e., the Irminger Sea Water) lead to deep convection in the Labrador Sea (Clarke and Gascard 1983). This scenario will probably only occur in the Western Labrador Sea during winters in which there has been a significant cold westerly wind during the early winter (January-February). Since the Labrador Shelf is normally ice-covered during winter, the Arctic air reaches out to the deep western Labrador Sea before it meets open water. Here the heat and vapor flux (evaporation) into the air rises dramatically, resulting in intense cooling and a rise in salinity of the water in this area. This is the preconditioning phase of Labrador Sea Water renewal.

When a cyclonic gyre forms in the Western Labrador Sea (scale ≈200 km), various water types (i.e., remnants of Irminger Water and Atlantic Water) present within this gyre are mixed into the mixed layer and eventually cooled by the cold and dry northwest winds blowing offshore from Labrador. It is believed that the gyre retains the developing deep mixed layer in this general area long enough for the transformation to Labrador Sea Water to take place (Clarke and Gascard 1983). The intensity of the convection varies from year to year. Data suggest that significant renewal of Labrador Sea Water occurs on only 6 out of 10 years studied (Lazier 1980), and it occurs to varying depths (Lazier 1973, Gascard and Clarke 1983). Convection in this region will not reach to the bottom, however, because the North Atlantic Deep Water is a denser water mass than the Labrador Sea Water. Instead, the water produced will spread out over large parts of the North Atlantic on top of the North Atlantic Deep Water.

Upwelling

The potential importance of upwelling in the Arctic in connection with deep-water formation is that it can bring deeper, usually more saline water (Atlantic water) to shelf sites where the water can be cooled by surface exchange and returned to the deep basins with increased density (Aagaard *et al.* 1981). How efficient this process is in producing dense water is still uncertain, but the net fluxes associated with upwelling seem to be small, except maybe in some of the canyons (Aagaard and Roach 1990).

Double diffusion

In areas where warm and salty (e.g., Atlantic) water underlies cold and fresher (e.g., Polar) water, a high density subsurface layer can be produced by double diffusive processes at the interface. Heat is lost from the saline layer into the upper layer, and from there it is expelled to the atmosphere (Carmack and Aagaard 1973, McDougall 1983). The diffusion of salinity into the upper layer is much, much slower than the heat diffusion, so the lower layer will remain salty while it cools, and the density of the layer will increase.

Both open ocean convection and shelf convection introduce waters with different temperature-salinity characteristics into the water column. Open ocean convection leads to large horizontal gradients which may be so strong that a slight disturbance results in vertical gradients capable of establishing double diffusive convection, which can drive horizontal mixing of the waters. Shelf convection results in large vertical gradients and inversions of temperature and salinity induce double diffusive processes, which act to remove these anomalies (Rudels 1993).

Vertical particle fluxes

Vertical mixing is limited in the Arctic Ocean by the stratification of the water column produced by freshwater inputs of runoff and ice melt. Therefore, settling particles may form a significant component of the vertical transport of material which short circuits the sluggish diffusive transport. Vertical particle fluxes in the Arctic Ocean vary widely among the marginal seas, where strong seasonal inputs of terrestrial and marine particles occur; along slopes where sediments are advected and redeposited by boundary currents; and, in the interior ocean, in which surface water is isolated from both terrestrial and atmospheric inputs, and where productivities are much lower (Subba Rao and Platt 1984, O'Brien *et al.* 1991, Macdonald *et al.* 1993, Wheeler *et al.* 1996).

On shelves, in the marginal ice zone, and under the Transpolar Drift, particle fluxes may be relatively large due to supply from coastal sediments or from high biological productivity. Pfirman *et al.* (1990) proposed that sediment contributed from sea ice forming along the Siberian margin would result in elevated particle flux and sedimentation rates under the Transpolar Drift. Stein *et al.* (1994) further proposed that oceanic and turbidity currents are even more important than sea ice as sources of sediment to the Eurasian Basin, with active resuspension and redeposition along the sea bed. One of the more important regions for vertical particle flux occurs in marginal ice zones, where algal mats falling off the melting ice during break-up can result in separation of algal blooms from grazers, allowing phytodetritus to settle relatively undegraded to depth (Carey 1987, Hsiao 1987, Bruland *et al.* 1989, Hebbeln and Wefer 1991, Riebesell *et al.* 1991). These regions, which deliver carbon-rich material to the benthos, are potentially important for the rapid transport of sediments and contaminants from the ocean surface to the sea floor. Another kind of process produces pellets that are released where ice melts. During its transit, particle-laden ice is reworked by freeze-thaw cycles which tend to move enclosed sediment to the surface of the ice. Surface ablation of the dirty ice can then form 'cryoconites', or pellets, which are effective scavengers of particle-reactive contaminants, and settle quickly through the water column once the ice has melted (Pfirman *et al.* 1990).

In contrast to shelves and margins, permanently ice-covered regions have very low particle fluxes (Fischer *et al.* 1988, Hargrave *et al.* 1994) because they are far from inorganic sediment sources and, although moderate primary production may occur, much of the production is recycled in the surface

water (Wheeler *et al.* 1996). In support of this, Ku and Broecker (1967), Finkel *et al.* (1977), Moore and Smith (1986), and Bacon *et al.* (1989) concluded from various natural radionuclide inventories (^{230}Th, ^{10}Be, ^{210}Pb) that scavenging intensity, and hence particle production and sinking, in the interior Arctic Ocean is low. Variations in particle fluxes occur between basins in the interior ocean as suggested by Scholten *et al.* (1995). Distributions of ^{230}Th and ^{231}Pa suggest low flux in the deep waters of the Makarov Basin and higher flux in the Eurasian Basin.

Particle-reactive contaminants, such as some of the artificial radionuclides, will be incorporated into the vertical particle flux, and since sinking particles are often carbon-rich and contain biogenic components, bioaccumulating contaminants, such as OCs and mercury, are likely to be involved too. For example, Cochran *et al.* (1995) found that rapid ventilation and scavenging at the Nansen Basin margin resulted in the removal of particle-reactive radionuclides at rates comparable to those of the North Atlantic. Inorganic components of the particle flux will tend to be coupled to the biogenic flux because 'indiscriminate packaging' by zooplankton of small particles produces larger aggregates which then dominate the flux (Honjo 1990).

Due to logistical difficulties, there are few direct measurements of particle fluxes in the interior Arctic Ocean. Hargrave *et al.* (1989, 1994) used sediment traps at the Canadian Ice Island to measure fluxes characteristic of regions under permanent ice cover. Peaks in particle sedimentation were observed during late summer (August-September) and mid-winter (December-January). Average particle fluxes were low (1.1 g/m^2/y), compared to other year-round measurements made in marginal seas (3-120 g/m^2/y), as summarized in Hargrave *et al.* (1994). Not enough sedimenting material was collected to analyze for contaminant content, but the seasonal pattern of deposition suggests that scavenging of particle-associated compounds from the water column would be greatest during the late summer months.

In locations where there is seasonal ice cover, biological fluxes are usually found to undergo strong variability, with maximum fluxes 10 to 1000 times the minimums (Atkinson and Wacasey 1987, Honjo *et al.* 1988, Wefer *et al.* 1988, Wefer 1989, Honjo 1990). In winter, biogenic fluxes are extremely low, but near shelves these may be augmented by particles carried off the shelves in dense-water flows (Honjo *et al.* 1988, Wefer 1989).

3.5.4.7. **Oceanic time scales**

Understanding water mass characteristics and renewal rates are important for the determination of the sensitivity of the Arctic waters to environmental changes. The northern water masses interact extensively with the surface ocean in their formation regions, and hence have been tagged with anthropogenic substances that have entered the surface layer of the ocean during the past several decades. Measurements of these tracers can be very useful in calculations of the time required for a water mass to travel from its source region to another region. Salinity and temperature anomalies that are advected with the currents can also be used to estimate transport times.

Atlantic Water flowing north from the Rockall Channel will probably take two to three years to reach Bear Island (Blindheim and Loeng 1981) and half a year from Bear Island to the west coast of Novaya Zemlya. Using cesium and strontium released from Sellafield on the Irish Sea as a tracer, one can see that the isotopes follow the main currents, allowing calculation of transport times (Dahlgaard *et al.* 1986, Kautsky 1987). Livingston *et al.* (1984), using the same tracers, deduced that water could transit from Spitsbergen to the North Pole in about three years.

Current velocities in the Greenland and Iceland Seas have been used to calculate the time it will take the Deep Water to flow from the Fram Strait to the Denmark Strait (Buch *et al.* 1996). The result was about 700 days. Based on satellite-tracked drifter observations taken in 1982-83, Royer and Emery (1984) found a transit time around the Bering Sea on the order of one year.

Ages and residence times

Estimates of ages and residence times of water masses in the Arctic Ocean and adjacent seas have been based mostly on distribution of transient tracers, including ^{14}C, tritium, and chlorofluoromethanes. The residence time is a measure of the average time a water parcel spends in a certain reservoir, while the age is defined as the mean time elapsed since the water parcel left the surface. The different ^{14}C radioactivities in the surface and the deep water can be used to calculate the age of the deep water, since the only change in the amount of ^{14}C in seawater is due to decay.

The residence time for waters in the Arctic Ocean (Figure 3·28) varies with location and depth. On the Eurasian shelf, the residence time is one to three years (Codispoti and Lowman 1973, Hanzlick and Aagaard 1980, Östlund and Hut 1984, Pavlov and Pfirman 1995). Mean residence time of river runoff on the shelves of the Siberian seas, however, has been estimated from salinity and tracer data (tritium, ^{3}He, and the ^{18}O/^{16}O ratio) to be 3.5 ±2 years (Schlosser *et al.* 1994b). On the Canadian shelf, the residence time for freshwater is less than a year (Thomas *et al.* 1986). Over the deep basins, the residence time for the surface and halocline waters is about ten years (Aagaard and Coachman 1975, Östlund 1982, Livingston *et al.* 1984), although surface water in the Transpolar Drift may take less than five years to cross from the Siberian shelf to the Fram Strait (Schlosser *et al.* 1995a).

Atlantic Water has a shorter residence time in the Eurasian Basin than in the Canadian Basin, about 25 and 30 years, respectively (Aagaard and Greisman 1975, Wallace and Moore 1985). Eurasian Basin Deep Water has the shortest residence time of the deep waters of the Arctic Ocean, about 75 years, because of its connection with the Greenland-Norwegian Seas (Bönisch and Schlosser 1995). ^{14}C and ^{39}Ar data show an estimated mean residence time of 250-300 years for Eurasian Basin Bottom Water and 300 years for Canadian Basin Bottom Water (Schlosser *et al.* 1994b, Bönisch and Schlosser 1995). The Amundsen and Nansen Basins are treated as one reservoir, i.e., the Eurasian Basin, since the mean renewal times of the deep and bottom water of the two basins are fairly similar.

In the Nordic Seas, the mean age of the waters between 50 to 500 m depth (i.e., Upper Arctic Intermediate Water; Fig. 3·32) is five to ten years, while the mean age for the upper 500 m in the Norwegian Atlantic Current is only one to two years (Schlosser *et al.* 1995b). The less saline component of Arctic Intermediate Water represents a rapid turnover of a small system, and the residence time is three to four years (Swift *et al.* 1980).

Measurable concentrations of the chlorofluoromethanes F-11 and F-12 have penetrated to the deep basins of the Nordic Seas. They show progressively lower concentrations with increasing depth, reflecting the greater isolation of deeper waters from air-sea exchange. Calculations based on these chlorofluoromethanes give a time scale for deep-water con-

vection in the Greenland Sea of 40 years and a time scale for lateral mixing between the deep Greenland Sea and the deep Norwegian Sea of 20 to 30 years (Bullister and Weiss 1983). The residence times for the Greenland Sea Deep Water and the Norwegian Sea Deep Water have been estimated from tracer balances to be 28 and 31 years, respectively (Bönisch and Schlosser 1995).

Tritium and ^{85}Krypton have been used to estimate the age of the Denmark Strait Overflow Water and the North East Atlantic Deep Water just south of the Denmark Strait. Denmark Strait Overflow Water was the densest water observed south of the Denmark Strait, and there are two types, a low-salinity type and a slightly higher salinity, more dense type. Tritium and ^{85}Krypton data reveal that the low-salinity type resided behind the Greenland-Iceland ridge for about one year, before flowing into the Irminger Sea, compared to about 15 years for the higher salinity type. North East Atlantic Deep Water forms in the northeastern Atlantic from a mixture of water flowing out of the Norwegian Sea and North Atlantic Water. About 70% of the tritium and ^{85}Krypton burden of North East Atlantic Deep Water comes from North Atlantic Water and 30% from Norwegian Sea water. The average age of the North East Atlantic Deep Water just south of the Denmark Strait, relative to its formation in the northeast Atlantic, is approximately 7.5 years (range: 1-11.5 years) (Smethie and Swift 1989).

The ventilation time of the Labrador Sea Water depends on the production rate. With a production rate of 8 Svd (McCartney and Talley 1984), the ventilation time is nine years; but if the production rate is lower, the ventilation time is higher. Using the 2 Svd value calculated by Worthington (1976), a ventilation time of 36 years is derived (Talley and McCartney 1982).

In Baffin Bay, the upper layer (200 m) has a residence time of about two years (Top *et al.* 1980, Rudels 1986b), while the warmer layer below has a residence time of 8 to 20 years. From oxygen consumption, Top *et al.* (1980) calculated the residence time of the bottom water in Baffin Bay to be 500-1000 years.

The normal residence time for water in the Chirikov Basin (between St. Lawrence Island and the Bering Strait) is about two weeks, and varies little during the summer; but with the appearance of reversed flows in the fall, the residence times are two to four times longer (Coachman 1993).

3.6. Modeling

3.6.1. Introduction

A complete review of modeling as it relates to the physical and chemical fate of contaminants in the various compartments of the Arctic environment is beyond the scope of this report. Consequently, only a summary of some of the more relevant models that have been adapted for northern conditions, or specifically applied to contaminant transport in the Arctic are reviewed here. Within the terrestrial/freshwater compartment, only models related to the fluvial transport and fate of contaminants in freshwater systems will be considered. However, some of the atmospheric models do consider the soil surface in the context of sources and exchanges. It appears that data gaps and data inconsistencies among different compartments remain a problem for these kinds of linkages.

To date, there has been no attempt to fully integrate all of the compartments in a single model, due to the complexity that would be required. However, the recent advances in atmospheric models directed at understanding contaminant transport from temperate source regions to the Arctic and the exchanges between the atmosphere and the land and ocean in the northern hemisphere have made significant progress toward this end. These models could perhaps be enhanced through greater coupling with compartment and subcompartment specific models, though whether or not the increased parameterization would effectively enhance the predictive ability of the model is not known.

3.6.2. Atmospheric modeling

As mentioned in section 3.2, for most contaminants, the atmosphere provides the fastest transport medium. Therefore, in order to understand how contaminants are brought to the Arctic, it is important to quantitatively calculate the atmospheric transport in an explicit manner. Furthermore, having established a measurement-validated modeling tool, the model can be used to estimate the relative importance of different emission sources, to evaluate possible effects of new emissions, and to increase our understanding of the relative importance of various processes involved in the transport. There are two types of models used for contaminant pathways studies: 1) three-dimensional atmospheric models suitable for studying the movement of one-hop compounds and, to a lesser extent, multi-hop compounds; and, 2) two-dimensional multi-compartmental models suitable for multi-hop compounds. Both types are usually run on a domain that is global, although single-hop compounds can often be studied effectively with a hemispheric scale model.

3.6.2.1. Three-dimensional atmospheric models

Models for meteorological fields

There are two different classes of models used to simulate the air motions and dispersion of contaminants in the atmosphere. Physical models are physical analogues to the atmosphere, consisting of tanks filled with liquids set in rotation in order to reproduce the effects of the planetary rotation. External forcings of motions can be controlled, and the resulting motions and their transport capacities can be observed and measured. Physical models are no longer in wide use.

The second class of models are numerical models – mathematical tools which calculate the physical quantities utilizing electronic computers. The elementary laws of nature (mass conservation, Newton's second law, the laws of thermodynamics) and the properties of the air (the equation of state) and its composition are all formulated as mathematical differential equations. It is presumed that it is not necessary to calculate the motion of each molecule in air, but that the physical laws can be formulated for separate air parcels. These are assumed small enough to be treated as homogeneous and large enough to disregard molecular discontinuities. In particular, molecular diffusion of total mass between air parcels is neglected. Thus, the law of mass conservation can be applied for each individual air parcel, and a unique air velocity can be defined as the velocity of each parcel. The size of each air parcel is assumed to be small enough to be mathematically treated as an infinitesimal quantity. The mathematical equations contain derivatives of physical quantities (wind velocity, temperature, pressure, etc.) in all space directions and in time. The time derivatives are of first order and, in principle, the time-evolution of all the quantities in any point in the atmosphere can be found, provided proper initial values are given, as well as boundary conditions describing the interactions with the Earth's surface and the universe.

In practice, however, the equations for these models are generally impossible to solve in analytic fashion. They are

nonlinear and coupled, so that the distribution of one quantity determines the distribution of other quantities. Furthermore, motions, which vary in time with a typical frequency and have a typical spatial size, cannot be treated without taking into account the influence from motions with other frequencies and sizes. For example, the development of cyclones the size of 1000 km depends, among other things, on the structure and strength of turbulent eddies ranging in size from 10-100 m. Initial values and boundary conditions cannot be given accurately, but are subject to uncertainties, due to measurement errors and insufficient coverage of measurement networks. Research initiated by Lorenz (1963) has shown that the equations governing atmospheric motions are crucially dependent on the initial conditions. Thus, the time-development of two initial conditions which are arbitrarily close, but not exactly equal, will lead to completely different states of the atmosphere within a limited time span (the predictability limit). This difficulty is why all weather prediction is based on regular meteorological observations which are disseminated in real-time to forecast centers around the world. This is not the case, for example, for predictions of tidal water.

The mathematically complex nature of the equations for atmospheric state quantities provokes a need for approximations. It is also clear from the chaotic properties of the atmosphere that observations must be incorporated in some way in order to be able to reproduce time-resolved features similar to those observed. First of all, it must be accepted that it is impossible, at least so far, to calculate motions and features on scales of variations from fractions of millimeters and seconds to thousands of kilometers and months simultaneously. The equations are therefore subject to Reynolds-averaging, i.e., separating turbulent and small-scale flows from larger-scale flows. Nonlinear terms give rise to terms in the averaged equations which describe the influence of the turbulent flow on the larger-scale flow. Thus, the problem of turbulence closure is encountered, an area of research which has produced a large amount of scientific literature. The Reynolds-averaged equations are still analytically unsolvable, and so must be further approximated by so-called discretization methods. For example, all derivatives in space and time can be replaced by finite differences over discrete intervals in the time and space coordinates, but discretizations can also be made by, for example, using finite Fourier transforms (spectral discretization), or so-called finite element methods. In any case, the method of discretization directly or indirectly defines a grid of node-points, in which the state quantities are defined and known, but not the space and time in between. As for the Reynolds averaging, the procedure of discretization gives rise to new terms in the equations which describe the influence of the scales that are unresolved by the grid. These are called subgrid processes, which must be parameterized as a function of the resolved scale quantities in order to close the system.

These parameterizations are made in all routine meteorological models, and they frequently involve crude assumptions for parameter values, which are difficult to defend independently from observations and measurements. Such parameters must often be tuned in order to obtain reasonable model results (as compared with actual measurements). Clouds and precipitation processes are heavily involved in subgrid parameterizations; thus, these are the most uncertain components of atmospheric models.

In order to produce quantitative results which can be compared with actual measurements taken at specific points and time-levels, calculations with the numerical models have to use initial data which are based on measurements. Such initial conditions, called analyses, are made through a process called data assimilation. Modern data assimilation is a method which permits information from observations to propagate in space downwind of the observation points. Thus, the influence of good observations can be seen as well in data sparse regions, such as the Arctic. Fields of meteorological quantities from a numerical model which is run using data assimilation can be taken out in all grid nodes with equally spaced intervals. The resultant data set is considered to be time resolved, in that it is the best available estimate of the quantities in each grid node at the given time levels, reflecting the scales of motion resolved by the grid. A model which is not using data assimilation, but only calculates the meteorological quantities with no corrections will produce fields which may resemble analyzed fields, but they cannot be viewed as valid for specific dates and times. Such fields can be taken as possible realizations of the given climate, determined by the insolation and ground surface boundary conditions, but in many cases even this is not possible as the 'model-climate' may deviate considerably from the real climate due to factors such as weak subgrid parameterizations.

Atmospheric models can be solved for parts of the Earth (limited area models, LAM), or for the whole globe (general circulation models, GCM). LAMs cannot be run without lateral boundary conditions, presumably from a GCM run with a coarser resolution (larger distance between the grid nodes) than the LAM. LAMs are run in national weather centers for the purpose of weather prediction over a few days, while GCMs are run at fewer centers (e.g., European Center for Medium Range Weather Forecasts, ECMWF, or National Meteorological Center, NMC in USA) for the whole period of predictability, approximately five to ten days depending on flow type. GCMs are also run at certain locations without data assimilation in order to study general circulation and climate-related topics in a research model. Full climate simulations and climate predictions can only be made using models that incorporate ocean circulations, sea ice, and land ice. Such model runs require enormous data resources and machinery to handle all the model output. They are run at only a few locations around the world (see IPCC (1996) for an overview).

Dispersion models

Atmospheric dispersion models are numerical models which produce approximate numerical solutions to mass budget equations for a given set of contaminants. The contaminants are in our case always considered to be gravitationally neutral (i.e., they follow the motion of the air precisely). The only exception is contaminants that are captured by precipitation, in which case they follow the precipitation until they hit the ground and deposit there, or they are reintroduced as air contaminants by evaporation of the precipitation element.

Dispersion models need information about emission sources, in addition to meteorological fields, which cause transport and precipitation scavenging. Many physical and chemical processes are also linked to meteorological conditions, in particular inside clouds. The modeling of contaminants seriously influenced by the presence of clouds (e.g., a major part of the production of sulfate from sulfur dioxide takes place inside clouds) is highly impacted by the uncertainty related to clouds in meteorological models. In relation to dry deposition to the ground, data on the properties of vegetation, snowcover, ice cover, or open water may be required, as well as the state of boundary layer turbulence, which determines the aerodynamic resistance toward dry deposition. For some contaminants, the state of the boundary layer may also be of crucial importance for natural

emissions from the sea, or for the re-emission of multi-hop contaminants.

For single-hop contaminants, a pure atmospheric dispersion model will be sufficient. As long as the emissions, deposition processes, and the meteorological fields influencing them are determined, the system is closed. To further evaluate the fate of a single-hop contaminant being deposited, modeling of freshwater and/or oceanic transport is required. But these models do not have to interact any further with the atmospheric model. Dispersion models aimed at understanding Arctic distribution of single-hop contaminants should at least include coverage of emission sources in the major areas of the northern hemisphere.

For multi-hop contaminants, distribution in all compartments of the environment must be carefully studied so that rates of revolatilization can be predicted. However, since many of the multi-hop contaminants (e.g., semivolatile organic compounds (SOC) or mercury) have a large fraction of their total mass in the other compartments (e.g., ocean, terrestrial), and have been accumulating in these compartments over decades, the day-to-day transport in the other compartments is not crucial. A more reasonable approach is to map the concentrations in the land, freshwater, and oceanic compartments. Modeling the whole accumulation process over decades requires multi-compartmental models with full interaction (see section 3.6.2.2). Dispersion models aimed at understanding Arctic distribution of multi-hop contaminants should have global coverage.

Off-line dispersion models

Dispersion models which are not part of models for meteorological fields, are called off-line models. This is a natural choice for modelers who do not run their own meteorological model, or who want to produce time-resolved calculations of contaminants for comparison with measurements. In principle, such modeling could be made on-line inside the full meteorological model run with assimilation of meteorological observations. In practice, however, there are still large problems in the initial phase after inserting measurements. These so called 'spin-up' problems reveal a serious under-prediction of clouds and precipitation due to a mismatch between the vertical motions produced in the model and the analyzed field of relative humidity. Therefore, until better methods come in to use (e.g., the 4D-VAR assimilation method being developed at several numerical weather prediction centers), the 'spin-up' problem is avoided by using short-range forecasts (~ 6-12 hours) as input to the dispersion model. These data are not available for each time-step in the dispersion model, thus, off-line modeling necessitates some kind of time interpolation between the inputs.

Off-line modeling with the scope of understanding Arctic contaminants has so far been mainly concerned with Arctic haze and sulfur compounds. Iversen (1989b) developed and applied a hemispheric-scale model for sulfur dioxide and particulate sulfate. Based on meteorological data from NMC, the model was run for March 1983, and a period in June-July 1983. Emissions were taken from Semb (1985). The model output was compared with observations taken at ground level and with aircraft in the Norwegian Arctic. Seasonal contrasts as well as episodic behavior were reasonably well reproduced. Later, the model was run for October 1982 and January 1983, with a more comprehensive model validation (Tarrason and Iversen 1992). Recently, the model has been run for a full year (1988), with meteorological data from ECMWF (Tarrason and Iversen 1996). Results can be found in chapter 8 of this report. Christensen (1995) developed a model with almost hemispheric coverage and used ECMWF data as input to produce dispersion calculations for three full years. These results showed good comparability with actual measurements.

Full three-dimensional global modeling of multi-hop contaminants has so far not appeared in the literature. Strand and Hov (1993) used a two-dimensional, zonally-averaged model to calculate the global distribution of the α- and γ-HCH isomers. The model also included the oceans and land/soils as separate model compartments. Meteorological data were taken from Plumb and Mahlman (1987) which are zonally-averaged, based on a GCM without data assimilation.

There are several model results published which cover Arctic areas, but none are specific to Arctic contaminant behavior. Langner and Rodhe (1991) calculated global distributions of sulfur compounds based on monthly-averaged meteorological data, with relatively coarse resolution. Benkowitz *et al.* (1994) calculated sulfur distributions based on ECMWF meteorological data for October and November 1986, focusing on the North Atlantic Ocean.

On-line dispersion models

The main benefit of running a dispersion model as an integrated part of a meteorological model, in spite of the loss of actual time-resolution, is the possibility of including feedback effects between the contaminant and the meteorological variables determining the transport, chemistry, and deposition of the contaminant. For example, sulfur may change the atmospheric contents of cloud condensation nuclei, and thus the lifetime of clouds and their optical properties. Increased cloudiness may increase the efficiency of sulfur dioxide oxidation to sulfate. Sulfate also directly causes an increase in clear air scattering of solar radiation and thus an increase of planetary albedo. Soot, or black carbon, may likewise cause a decrease of the clear air albedo over regions with very high natural surface albedo (e.g., in the Arctic). In total, these processes may perturb the natural radiation balance in a way which can cause changes in large-scale wind systems.

Another benefit of using on-line models is the availability of full meteorological data with the same accuracy as the dispersion model. Thus, no interpolation is needed. The main drawback is that day-to-day comparisons with measurement data is impossible. Agreements must be relied on in a more statistical sense.

Dastoor and Pudykiewicz (1996) recently made calculations of Arctic sulfur transport in the Canadian global spectral model. So far the model does not include feedbacks to the meteorological fields, although the results appear promising. With little focus on the Arctic, Taylor and Penner (1994) used the Lawrence Livermore National Laboratory version of the Community Climate Model 1 of the US National Center for Atmospheric Research to calculate the sulfur distribution with sulfate radiative forcing and feedback on the meteorological fields. Similar calculations have also be made by Pham *et al.* (1995) and Feichter *et al.* (1996).

Joussaume (1990) modeled dust of crustal origins in a GCM, although without any feedback mechanisms to atmospheric processes. A minor, but still significant amount was calculated to be transported to the Greenland icecap through elevated routes (height 5-10 km above ground) from the Sahara, Middle East, and desert areas in Asia. Similar calculations made for conditions during the last glacial maximum (18 000 years before present) lead to larger burdens of crustal dust, but still underestimated compared with ice-core observations (Joussaume 1993). Genthon and Armengaud (1995) have also calculated desert dust distributions, as well as sea salt and radioactive isotopes, with special emphasis on deposition in Greenland and Antarctica.

3.6.2.2. **Multi-compartmental models**

Global scale multi-compartmental models have the potential to:

1. contribute significantly to our understanding of the extent of transport of contaminants from sources in tropical and temperate zones to the Arctic and Antarctic;
2. assist in the formulation and testing of hypotheses surrounding the 'cold condensation' effect tending to concentrate substances in regions of cold climate (Wania and Mackay 1993);
3. quantify fluxes of contaminants to the Arctic;
4. estimate the fraction of the total global use of each contaminant which reaches the Arctic; and,
5. predict the time response to contamination and decontamination (e.g., 5 years or 50 years).

Since the models necessarily treat several media including air, soils, and ocean water, as well as a variety of biota, they synthesize or integrate the components of the global and Arctic systems (Figure 3·1). The application to developing rational international contaminant control strategies is obvious. For example, an early attempt to model the global DDT cycle with a four latitude-zone box model by Ostromogil'skii *et al.* (1985) led to the conclusion that DDT contamination will persist for many decades and impact the Arctic much more than the Antarctic. After checking their model with observations in various environmental media, they estimated that after a global ban of DDT, the rate of decline in atmosphere, soil, and ocean will be a factor of 10-20, 30, and 1-2% per decade, respectively.

Although more comprehensive models are still in their infancy, considerable progress in model development has been made in recent years. Existing global models for persistent organics cover a wide range of complexity. These models are all based on a multi-compartmental global system, shown in Figure 3·1, with varying degrees of complexity. For instance, the atmospheric compartment has been treated by Wania and Mackay (1995) and by Strand and Hov (1993).

Modeling studies are conducted in one of two ways as determined by the type of question to be answered and the type of model. These two are as follows:

1. Long-term, low-spatial resolution model – starting with a 'clean' global environment and simulating the entire time period a chemical has been used on a global scale/or as long as it has been persistent in the environment. This is the approach taken in the 2-D and 1-D models described below. At this time, this is impractical for a 3-D model, as a result of the immense demand in computing time and input parameters; and,
2. Short-term, high-spatial resolution model – defining the global contaminant loading in system compartments (Figure 3·1) at one point in time, and simulating a shorter time period (e.g., one year). This is the approach taken by the 3-D models.

The Bergen and Toronto Models

There have been two attempts at simulating the dispersion of OCs on a zonally-averaged, global scale. Strand and Hov (1996) modeled the distribution of HCHs using a 2-D, atmospheric model (Bergen Model), while Wania and Mackay developed a multimedia compartment model for OCs based on the fugacity approach (Toronto Model) (Wania and Mackay 1993, Wania 1994, Mackay and Wania 1995, Wania and Mackay 1995).

The Bergen Model is a global multi-compartmental model for HCHs with atmosphere-soil and atmosphere-ocean exchange represented with a two-dimensional zonally-averaged atmospheric model. An existing, detailed atmospheric model was simplified (Strand and Hov 1993) by reducing the vertical and meridional resolution to six equally spaced latitude zones and four vertical layers. This was then combined with a modified oceanic transport model (Siegenthaler and Joos 1992) and a soil-atmosphere exchange model for trace organics developed by Jury *et al.* (1983, 1984a, 1984b). In summary, the model includes the atmosphere, ocean water, cultivated and uncultivated soil, and the processes of atmospheric advection and convection, diffusive gas exchange between atmosphere and soil or water, wet deposition, and chemical degradation. Seasonality is taken into account by defining specific temperatures, precipitation rates, and atmospheric transport parameters for four seasons.

One weakness of this model is that no consideration is given to particle-associated chemicals in atmosphere and surface water, and, therefore, to particle-mediated transport processes, such as dry particle deposition from the atmosphere or contaminant scavenging by settling suspended matter in the surface ocean. This may be an acceptable simplification in the case of HCHs, which, due to relatively high volatilities and water solubilities, occur mostly in the gaseous or in the truly dissolved phase, but would require adjustments for less volatile or less soluble chemicals. It is also not totally appropriate for Arctic precipitation which for much of the year is dominated by snowfall, an effective scavenger, even of highly volatile contaminants at low temperatures (Gregor 1996, Hoff *et al.* 1995). Also, no land-to-ocean exchange is taken into account, which may be very important for river-transported chemicals. Furthermore, ocean-atmosphere exchange is assumed to occur at ocean water temperatures, which are considered to be constant throughout the year and which often differ considerably from the temperature of the overlying atmospheric boundary layer. Since a sensitivity analysis revealed the Henry's Law constant as one of the most influential input parameters, this is potentially a very serious source of error.

The Combined Model (Figure 3·41) is essentially an expansion of a regional multimedia model developed by Mackay *et al.* (1992), designed to describe the fate of chemicals in smaller regions of approximately 10^5 km^2. It consists of ten linked, latitudinally-determined climatic zones, with each zone consisting of air, fresh and marine water, cultivated and uncultivated soil, and freshwater sediments. The

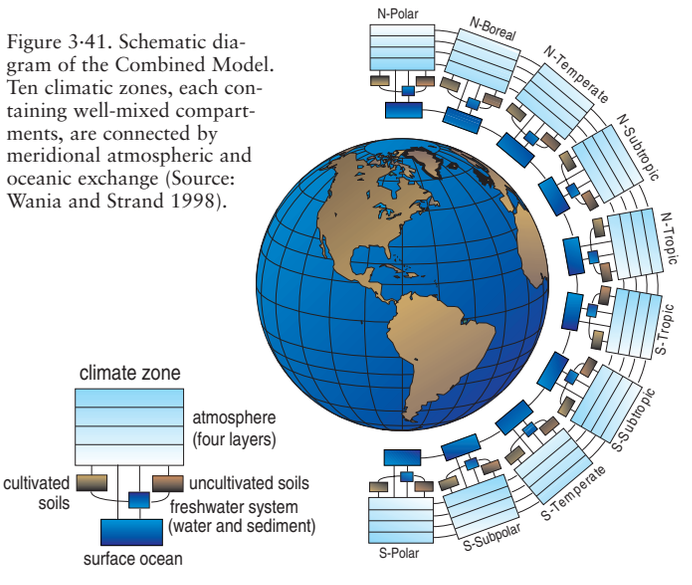

Figure 3·41. Schematic diagram of the Combined Model. Ten climatic zones, each containing well-mixed compartments, are connected by meridional atmospheric and oceanic exchange (Source: Wania and Strand 1998).

zonally-averaged climatic bands are similar to the zones defined in the Bergen Model. Transport and exchange processes between these compartments as well as degradation and export to the deep sea are parameterized. The model includes the phase partitioning of chemicals between air and aerosols, as well as between air and suspended matter. However, there is no vertical subdivision of the atmospheric compartments, which makes the description of atmospheric transport processes very simplistic. Seasonally varying parameters, such as temperature and atmospheric exchange rates, are defined as sinusoidal functions.

The Bergen Model is superior in its treatment of advective and diffusive transport processes in the global atmosphere, while the Toronto Model succeeds better in describing the reversible climate-dependent exchange processes between the atmosphere and the Earth's surface. Recently, Wania and Strand (in prep.) have combined the best parts of both approaches by incorporating into the Toronto Model a 2-D description of the atmosphere which adopts the vertical layering and the deduction of transport parameters from the Bergen Model. This 'combined' model is the first fugacity-based model which includes stacked atmospheric

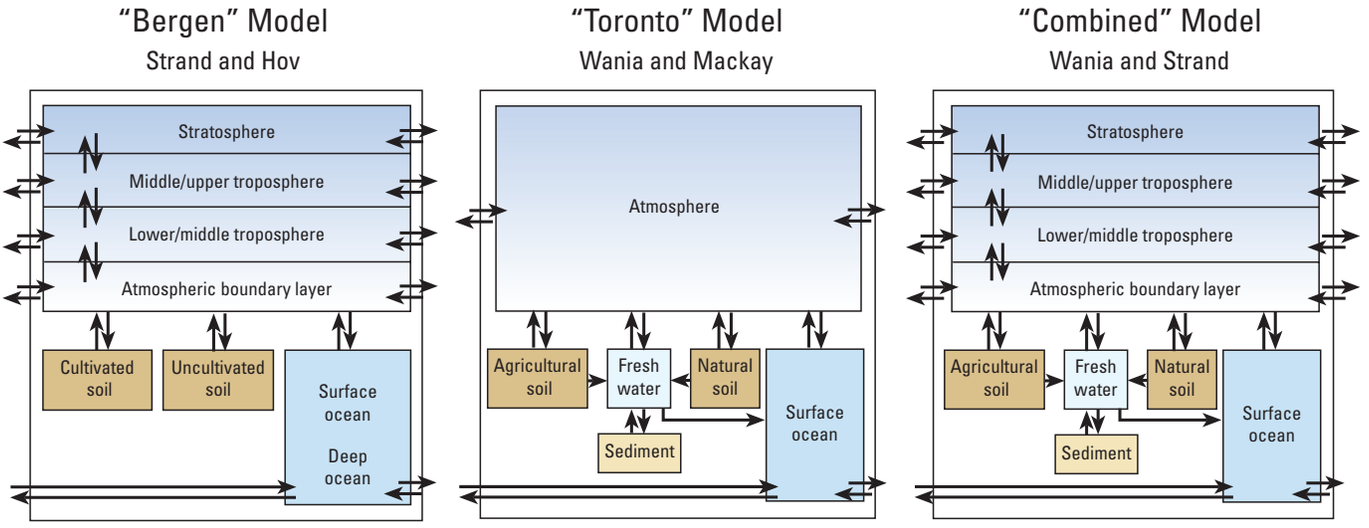

Figure 3·42. A comparison of the structures of the Bergen, Toronto, and Combined zonally-averaged global models (Source: Barrie *et al.* 1997).

Table 3·10. A comparison of characteristics of global zonally-averaged multi-compartmental toxics models.

	Bergen Model	Toronto Model	Combined Model
Zonal subdivision	6 zones, equally spaced	9 zones, based on climatic criteria	10 zones, based on climatic criteria
Compartments in each zonal 'building block'	4 atmospheric layers (stratosphere, middle/upper and lower/middle troposphere, atmospheric boundary layer), surface ocean, deep ocean (subdivided into several layers), cultivated and uncultivated soil	1 atmospheric layer (entire troposphere), surface ocean, cultivated and uncultivated soil, freshwater, freshwater sediment	4 atmospheric layers (stratosphere, middle/upper and lower/middle troposphere, atmospheric boundary layer), surface ocean, cultivated and uncultivated soil, fresh water, freshwater sediment
Treatment of atmospheric transport	Meridional and vertical exchange described with horizontal and vertical advection velocities and eddy diffusion coefficients	Meridional exchange described with latitude-dependent horizontal eddy diffusivities, lumping advective and and diffusive processes	Meridional and vertical exchange described with horizontal and vertical advection velocities and eddy diffusion coeficients
Treatment of oceanic transport	Modified High-Latitude-Exchange/ Interior Diffusion-Advection Model (HILDA) by Siegenthaler and Joos (1992)	Meridional exchange described with estimated horizontal eddy diffusivities, lumping advective and diffusive processes	Meridional exchange described with estimated horizontal eddy diffusivities, lumping advective and diffusive processes
Treatment of atmosphere–ocean exchange	Diffusive gas exchange at ocean water temperature, dissolution in rain	Diffusive gas exchange (at different air and ocean water temperatures), dissolution in rain, dry and wet particle deposition	Diffusive gas exchange (at different air and ocean water temperatures), dissolution in rain, dry and wet particle deposition
Treatment of atmosphere–soil exchange	Description of soil–atmosphere exchange based on Jury *et al.* (1983, 1984a, 1984b)	Description of soil–atmosphere exchange based on Mackay and Stiver (1991)	Description of soil–atmosphere exchange based on Mackay and Stiver (1991)
Treatment of seasonality	4 seasonal values for air temperature, precipitation, evaporation, and atmospheric transport parameters	Sinusoidal functions for air and ocean water temperature, sea ice coverage, and atmospheric exchange parameters	12 monthly values for air and ocean water temperature, sea ice coverage, and atmospheric exchange parameters
Technicalities	Zonally-averaged continuity equation, step-wise solution using finite difference approximation	54 linear mass balance equations in fugacity notation solved step-wise using finite difference approximation	90 linear mass balance equations in fugacity notation solved step-wise using finite difference approximation
Test chemicals	α-HCH and γ-HCH	α-HCH and γ-HCH, DDT	α-HCH and γ-HCH
Reference	Strand and Hov (1996)	Wania (1994), Wania and Mackay (1995)	Wania and Strand (1998)

compartments of variable density, and special consideration is given to the treatment of vertical atmospheric transport and wet deposition processes. Temperatures in ocean water and the four atmospheric layers, as well as the vertical and horizontal atmospheric transport parameters are input as monthly averages. Figure 3·42 and Table 3·10 compare various characteristics of the three zonally-averaged models.

3.6.3. Freshwater systems

3.6.3.1. Introduction

In order to understand how contaminants are transported within and from the terrestrial/ freshwater compartment, it is important to quantitatively link the processes that control transport. Such a modeling tool, once validated with measurements, can be used to increase our understanding of the relative importance of individual processes as well as to ultimately estimate contaminant deliveries. Although the different processes in river systems influence each other, most models address only one or a few of these aspects, and tend to focus on a specific question or location.

The river system as a whole, with all its processes, from watershed runoff and riverine processes to the discharge via estuaries into the ocean, is not yet adequately represented by a single model or even coupled models. As well, unlike atmospheric and oceanic models, which are larger in scale and not confined by national boundaries, freshwater models tend to be country-specific and are presented as such below.

3.6.3.2. Norway

A new computer model system has recently been developed in Norway. This River System Simulator (RSS) combines 14 different models to describe river processes, with particular emphasis on the environmental effects of river regulations. The system integrates only well-tested models, and makes use of one common database and a common user interface (Killingtveit and Harby 1994).

The RSS consists of three main parts: the main user interface, the simulation models, and the database. The parts are briefly described separately below. The relational database is based on a common logical data model or database scheme, which reflects as closely as possible the real physical system, rather than the data structure used by the individual models. The computations are performed by a number of individual models, exchanging data through the database via a standard database query language (Structured Query Language, SQL).

The 14 models included in the River System Simulator can be grouped into four main categories. These are:

1. input from the watershed into the river system;
2. hydropower system simulation models;
3. physical, chemical, and biological processes in rivers and lakes; and,
4. consequences for humans and ecosystems.

Only the latter two will be considered further, since they are most relevant to contaminant issues.

Physical, chemical, and biological processes in rivers and lakes

This group contains the largest number of models in the RSS, including models for river hydraulics, ice and water temperature, sediment transport, and water quality. Most models in this group were developed previously by the US Army Corps of Engineers – Hydraulic Engineering Center (HEC) or the Environmental Protection Agency (EPA). These models, listed below, are well established and thoroughly tested, and were included in the RSS with as few modifications as possible.

HEC-2 is used to compute water-surface profiles for steady, gradually varying flow in both prismatic and nonprismatic channels. Both subcritical and supercritical flow profiles can be estimated, as well as the effects of various obstructions, such as bridges, culverts, weirs, and structures in the overbank region.

DAMBRK is used for simulation of rapidly changing, unsteady flow, for example from a dam breach or a flood wave.

HEC-6 is used for computation of sediment transport, erosion, and deposition in rivers. Its hydraulic capabilities are similar to those of HEC-2. In addition, the model can simulate bed changes due to erosion and deposition of sediments.

RICE simulates hydraulics and ice processes in rivers. The most important ice simulation processes are frazil ice production, icecover generation, and decay and transport of ice.

FINNECO is a water quality model for lakes. The model is based on the EPAECO model and has subsequently been modified in Finland and Norway to enable it to be used in ice-covered lakes. The model can compute water quality and algal growth in a lake as a function of climatic conditions and the water quality of the lake inflow. The model can also compute the vertical temperature distribution in the lake.

QUAL2E is a water quality model for rivers. The model is based on the EPA model with the same name, but has been extended to include benthic algae in the RSS version.

AKVASS is a groundwater model that describes the interaction between river and groundwater in the river plain. The model can compute effects, for example, in the form of lowered groundwater level when streamflow is reduced due to hydropower regulation, or dynamic fluctuations in groundwater level due to rapidly varying flow downstream from peaking hydropower plants.

Consequences for humans and ecosystems

Most of the models in this group have been designed and implemented as part of the RSS project. The reason for this was that there were few such models in existence, and they were poorly documented and tested, or for other reasons were regarded as unsuitable for inclusion in the RSS.

BIOLAKE estimates the potential fish harvest from a lake based on simple relations to zooplankton and benthos. Fish harvests are estimated for pelagic and benthic fish species. If both types of species exist in the same lake, the total harvest is reduced by competition. BIOLAKE also estimates the impacts of lake regulation on fish harvests.

BIORIV is a model used to describe biological conditions in rivers, and the effect of changing physical conditions. In the first version, the effect of water temperature is primarily considered. Time from spawning to hatching, juvenile fish

growth, and time to smoltification are all strongly water temperature-related simulations done by the model.

HABITAT simulates physical habitat (living conditions) in rivers, and how this is affected by changes in streamflow. The model is useful in studies of how the habitat of different fish species is affected by river regulation.

RECREATE is a model used to compute how a proposed change in stream flow will affect the recreational value of the river.

Examples of the use of River System Simulator

Testing has been an important issue in the complete development of the RSS. Three Norwegian rivers were chosen as reference rivers, each posing different problems and possessing different biological, hydrological, and geographical conditions. They are the Gjengedal River, Halden River, and Stjørdal River. Only the Gjengedal and Stjørdal River systems are discussed here.

Gjengedal River system

The Gjengedal River is situated in western Norway, in the county of Sogn og Fjordane. The catchment area is 32 km long and includes 171 km^2 at the outlet to the Hyen Fjord. The catchment area rises from sea level to 1077 m.a.s.l. The largest lake is Storevatnet, with an area of 31 km^2. Hydrologically, the river is typical of rivers in the middle part of western Norway, with a distinct spring flood, several rain storms in the fall, and very low runoff during the winter period. The mean annual runoff is 11.6 m^3/s.

The RSS was used to study possible impacts of a planned hydropower development. The lake Storevatnet was proposed as a storage reservoir for the hydropower plant. Alternative locations of the power station outlet were investigated. The most significant impacts on the environment were predicted in the river reaches between the power station outlet and the original lake outlet at the dam site.

The RSS was also used to analyze the economic potential of different locations of the hydropower plant with alternative restrictions of minimum flow and reservoir filling level. The model ENMAG was set up to simulate these alternatives. The regulation of the lake Storevatnet will affect the growth and stock of brown trout, the only fish in the lake. The model BIOLAKE was used to simulate the expected changes in fish harvest. The planned regulation height is 28 m, which probably will lead to approximately an 80% decrease in harvest. This model is based on empirical data, and may be too conservative for the Storevatnet site, since brown trout is the only species of fish.

Stjørdal River system

A 70 year old hydropower system is about to be refurbished in the upper part of the Stjørdal River system in the middle part of Norway. The major impacts will be in the upper part of the river system, with pronounced changes in the flow regime. Different types of changes and impacts will also take place all the way downstream to the outlet in the fjord. Altogether, eight models were tested for both the upper and lower part of this river system. The RSS was used to study topics, such as:

- the effects of floods and changes in the flood and flow regime;
- ice conditions and water temperature changes;
- economic revenue of hydropower production;
- possible groundwater level changes in the river valley;
- improvements of the juvenile fish habitat;
- possible water temperature-related impacts on fish growth; and,
- possibilities for canoeing/rafting.

Although the RSS has proven very useful in its applications, there has been no consideration, apparently, of using this model to predict the effect of these changes on contaminant transport within the system, though this project seems quite feasible. More effort should be put into applying the RSS to help understand contaminant transport and fate in Arctic river systems.

3.6.3.3. **Canada**

Much of the modeling work in Canada has focused on the Mackenzie River, especially hydrology and ice. See for example the following sources for:

- 1-D hydrodynamic modeling for the Mackenzie Delta (J. Kerr, pers. comm., Studies Engineer, Environment Canada, Yellowknife, NWT, 1996);
- a multi-channel suspended sediment transport model for the Mackenzie Delta (S. Fassnacht, pers. comm., Department of Civil Engineering, University of Waterloo, Waterloo, Ontario, Canada, 1996) also based on the 1-D hydrodynamic model;
- river ice (Beltaos *et al.* 1993, Martinson *et al.* 1993, Chambers *et al.* 1994); and,
- hydrology of small systems (Cassell and Pangburn 1991, Munro 1991).

Other modeling efforts have looked at evapotranspiration from Arctic wetlands, snowfall, and fresh snow and snowpack processes, but there is as yet no attempt at integrating these on a larger scale.

Data from an intensive study of the processes controlling contaminant fate at Amituk Lake, NWT (Diamond *et al.* 1996) has been used to attempt to fully integrate physical process data with contaminant fate data. These modelers built a general, whole lake, mass balance model based on the QWASI model (Quantitative Water Air Sediment Interaction), developed originally by Mackay and coworkers (Mackay 1991). The model uses equivalence as the equilibrium criterion, which is suitable for most chemicals, rather than fugacity, which is suitable for VOCs only. A multi-species time-dependent model was developed to represent the large proportion of meltwater and chemical loadings that flow through the lake without mixing with the water column, because of the rapid and dominant spring freshet. The model also accounts for ice cover for up to 46 weeks of the year, during which no air-water exchange of chemicals occurs, and contaminant concentrations in the water column may increase as they are excluded from the ice layer. The application of this model to understanding the fate of contaminants will be considered further in chapter 6.

Models have been developed for a portion of the Yukon River system (Diamond *et al.* 1996, Barrie *et al.* 1997), however, since these are still in the early stage of development, they will not be considered here.

3.6.3.4. **United States**

Model development in the United States parallels that in Canada. Emphasis has been on developing models that are concerned with one or several physical transport processes specific to Arctic conditions, but little effort has been directed

at fully integrating these processes to provide, for example, estimates of contaminant delivery, even seasonally, from large river systems. Some examples of these models include Kane *et al.* (1993) for energy-related modeling of snowmelt and Cassell and Pangburn (1991) who modified the Streamflow Synthesis and Reservoir Regulation (SSARR) model to account for cold region effects.

3.6.3.5. **Russia**

A deterministic, mathematical model has been developed for runoff, called the HYDROGRAPH SHI-96. It covers all types of runoff and may be applied to any physiographic region and basins of any size. The design interval of the model is daily or shorter and the model input includes precipitation amount and duration, air temperature, and air humidity deficit. The model generates a continuous hydrograph for the design interval. Other information required by the model includes:

- formation and melting of snowcover;
- evapotranspiration;
- infiltration and surface runoff;
- dynamics of soil moisture and drainage water;
- formation of underground runoff;
- runoff transformation as part of overland flow and within the channel; and,
- runoff at the outlet.

This model is part of the 'Runoff – Erosion – Contamination' System model (V. Vuglinsky, pers. comm., State Hydrological Institute, St. Petersburg, Russia, 1996).

In conclusion, it is clear that additional effort should be directed at more comprehensive, circumpolar modeling activities to quantify delivery of contaminants from the land surface to the fluvial system. Subsequently, existing river models, such as the RSS, the SSARR, or the HYDROGRAPH SHI-96, need to be tested and calibrated for estimating contaminant transport and river-mouth loadings to the marine environment. Testing of these models with existing data will help determine information needs for their refinement. International coordination and cooperation in this effort is required to enhance information compatibility.

3.6.4. Marine system modeling

3.6.4.1. **Objectives of modeling**

One of the latest attempts in marine system modeling has been to define the major Arctic Ocean transport pathways for contaminants through application of a coupled dynamic–thermodynamic ice-ocean model to the geographical area encompassing the Arctic Basin and adjacent seas. Numerical models must utilize both historical and newly acquired field data to provide information on physical transport. Concurrent analyses of field data will contribute to understanding the model output within the context of pertinent physical transport processes.

Models can provide a quantitative, climatological picture of water mass and contaminant transports everywhere in the Arctic. The pathways for both bottom-released and river-origin contaminants can be described by the model. Since prediction of the ice drift is included, the pathways for contaminants in the ice from riverine sediments can be simulated. All of these modeling components can provide a basis for the design of a long-term monitoring plan for the interpretation of measurements and for the design of future modeling scenarios.

3.6.4.2. **Types of models**

Numerical modeling is a tool that has proven useful and will continue to prove itself useful in understanding and simulating the Arctic Ocean and, indeed, the whole climate system. There has been evolutionary progress toward completely coupled, ice-ocean numerical models. At first, decoupled models were being used. Semtner (1976a) performed an ocean modeling study of the Arctic Basin wherein ice properties were prescribed, and the general circulation was calculated by the model. On the other hand, there have been many more modeling studies where ice was explicitly modeled and where oceanic parameters were prescribed.

Maykut and Untersteiner (1971) developed a one-dimensional, thermodynamic ice model which was simplified and shown by Semtner (1976b) to perform well, even if ice is represented by a low-resolution vertical grid. Parkinson and Washington (1979) used Semtner's model and a simplified ice dynamics model to simulate the yearly ice cycle in the Arctic and Antarctic. Hibler (1979) developed a horizontal, two-dimensional, transport model of the Arctic Basin which exhibited realistic properties. Ice growth rates were prescribed *a priori* as a function of ice thickness and time of the year. A one-dimensional, bulk mixed-layer model has been developed by Lemke (1987) and coupled to Semtner's ice model. Mellor and Kantha (1989) coupled a one-dimensional, turbulence closure model to an ice model. The ice model also explicitly recognized the importance of ice to the ocean heat transfer role of open leads.

The papers by Hibler and Bryan (1987) and Semtner (1987) brought forth simulation studies of the Arctic Basin using a full three-dimensional, coupled ice-ocean model. It is apparent from these papers that oceanic heat distribution does play an important role in determining the location of the marginal ice zone and the other icecover properties, such as mean ice thickness and concentration. These models did not incorporate mixed layer physics even though, as remarked by Hibler and Bryan, the mixed layer ought to be considered the essential coupling medium between ice and ocean. A three-dimensional, coupled ice-ocean model which incorporated coupling with the mixed-layer physics was developed by Mellor and Kantha (1989).

Until the last decade or two, modeling studies have been somewhat idealized and lacking in adequate resolution. Due to the availability of increasingly affordable and powerful computer resources, numerical modeling is now entering an age where ever more realistic simulations of oceans are to be expected.

Ice models

Häkkinen and Mellor (1992) developed a coupled dynamic model that will predict ice motion, which is primarily driven by winds. The model is built on governing ice equations. The dynamic prognostic variables are ice concentration, mass, and velocity. The ice mass equations provide an accurate balance between advection of ice mass and sources and sinks of ice. There are some empirical coefficients in the ice concentration equations which deal with how to convert ice growth in open water to an increase in fractional ice cover, and ice melt to a decrease in fractional ice cover. The ice momentum balance consists of Coriolis force, advection of momentum, wind stress, interfacial ice-ocean stress, and forcing from internal stresses. Away from the coastal areas, the main balance is between wind stress and ice-ocean stress. Near the coasts, the ice internal stresses become important (Hibler 1979, Häkkinen and Mellor 1992).

Thermodynamics

The pioneering study of ice thermodynamics was done by Maykut and Untersteiner (1971), in which vertical structure of sea ice was highly resolved, but ice concentration and horizontal variability were neglected. The ice models that will be discussed below are essentially slab models in which vertical structure is simplified to minimally model the conduction process (Semtner 1976b). The following conduction description used in Häkkinen and Mellor (1992) resembles the model of Semtner (1976b), with modifications to account for leads. A schematic of the thermodynamics is shown in Figure 3·43.

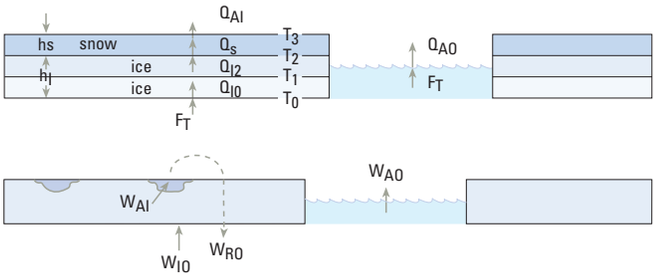

Figure 3·43. A schematic of the three-level thermodynamic snow ice system model (Source: Häkkinen and Mellor 1992).

In the model, the conductive heat flux at the sea-ice surface is balanced by the atmospheric heat flux, including radiative, sensible, and latent components, if surface temperature is below freezing. If there is a net heat gain at the surface and the surface is at or above freezing, the heat gain is used to melt the snow and ice. At the ice/water interface, any imbalance between the conductive heat flux from the ice slab and the sensible heat flux from the water column results in either freezing or melting. The surface temperature over snow or ice, T_3, is determined iteratively (a single iteration for monthly winds, but several iterations for daily varying winds) from the surface energy balance, where the atmospheric flux, Q_{AI}, has to equal the conductive heat flux through snow, Q_s. However, the heat capacity of the snow is neglected, so that conductive flux through ice, Q_{I2}, equals Q_s. Q_{AI} consists of the solar radiation and longwave back radiation formulas, which are adapted from Parkinson and Washington (1979), and turbulent sensible and latent heat fluxes modeled using bulk formulas. The surface albedo is assumed to be a function of surface temperature (Robock 1980). The ice cover is considered as a single slab, rather than dividing it into several thickness classes, each of which would have their separate heat balance. Up to 10 cm of water is allowed to accumulate at the surface; excess water can drain to the ocean. In the fall, this surface water freezes before bottom accretion begins.

A common conclusion from the ice modeling studies is that the snow-ice system has its largest sensitivity to the surface albedo. In effect, all other variability in surface forcing components, such as cloudiness and sensible and latent heat flux, are secondary compared to the albedo effect. However, once one defines the albedo model, in which the Arctic sea ice will not vanish during summer in the present climate, the other forcing components, i.e., oceanic heat flux, ice divergence, snowfall, cloudiness, and air temperatures (and winds), also show strong sensitivity in determining the Arctic ice mass. Considering all the uncertainties in all of the forcing components listed above, the ice models appear to be relatively stable in giving an average Arctic sea-ice thickness of about 2.5-3.3 m when climatological radiative and turbulent heat fluxes, snowfall, and oceanic heat fluxes representative of the central Arctic are used.

It should be noted that, whereas the models include some vertical variability for the thermodynamics, the equations for momentum are invariably slab models. They do not allow for vertical variability in velocity, a reasonable simplification.

Requirements and constraints

This is a review of sea ice-ocean models which will be/are used as components of global coupled atmosphere-ocean-land-ice models. Using numerical ocean models, the research goal is to understand the numerous interactions between lateral and vertical exchanges of heat and salt that dominate the high latitude ice-ocean system. Exactly the same processes of advection and mixing which govern temperature and salinity also govern the advection and diffusion of contaminants.

This discussion is limited to a review of models and modeling studies of the Arctic and its peripheral seas. Furthermore, discussion is restricted to three-dimensional, primitive equation, numerical ocean models, which acknowledge temperature and salinity variations and which have been used or are currently being developed for Arctic studies in a coupled ice-ocean model. These types of ocean models are the focus because the inclusion of thermodynamics and salinity effects are important for both short-term and long-term simulations. Secondly, any contaminants can be modeled as scalar variables, just like temperature and salinity, but they will have different surface boundary conditions and sources and sinks. Finally, some examples on how models can be used to describe different scenarios for transport and spreading of contaminants are given.

Quality and availability of data

Initialization of realistic three-dimensional ocean models requires good quality hydrographic data. This will considerably shorten the spin-up time of the model and improve its accuracy in anticipated one- to five-year simulations. The first available historical data set was compiled by Levitus (1982), and was based on a sparse set of hydrocasts. An improved version was compiled by Levitus and Boyer (1994) and Levitus *et al.* (1994). Prognostic model simulations require forcing fields consisting of atmospheric data (winds, air temperatures, humidity, short and long wave radiation fields, cloudiness, precipitation) and lateral transports of water at the open boundaries. The analyzed atmospheric data set most useful for this work is available from ECMWF. The transports through the Norwegian Sea and the Denmark and Bering Straits are derived from available transport estimates. There are several sets of river runoff values available. However, the accuracy of total river input is questionable because of the large year-to-year variability, and because many smaller rivers are usually not included.

Availability of models

A coupled ice-ocean model using multi-layer sigma coordinates accommodating both shallow shelf regions, such as the Kara and Barents Seas, and the deep basins is now available. This model traces the flow of contaminants in surface/subsurface layers and their (possible) sinking to the deep ocean.

3.6.4.3. **Ocean Models**

Detailed discussion here is restricted to three-dimensional, primitive equation numerical ocean models which include description of temperature and salinity variations and which have been used in large-scale Arctic studies in a coupled ice-ocean model. These models have the potential to describe con-

taminant transport. Exceptions will be identified. For mesoscale ice-ocean models and ice-ocean process studies, the reader is referred to a review by Häkkinen and Mellor (1990).

Specific ocean models

The first numerical ocean model and the present day standard is the Bryan-Cox Model (Bryan 1969, Cox 1984), which was later numerically improved by Semtner (1976a) so that it is sometimes called the Bryan-Cox-Semtner Model. It is conceptually the simplest of the models, an immediate advantage, in that it uses a conventional z-level vertical coordinate and spherical coordinates. It is used by many large-scale ocean modelers (Bryan and Holland 1989, Semtner and Chervin 1992).

The Princeton Ocean model (POM) (Blumberg and Mellor 1980, Mellor 1993) was initially developed for application to estuaries and coastal oceans, although it is currently being applied to ocean basins. In estuarine applications, the sigma coordinate system, together with a free surface and the turbulence closure submodel (Mellor 1973, Mellor and Yamada 1974, Mellor and Yamada 1982), provided a bottom boundary which converted tidal energy into turbulence and mixing. Comparisons with current meter measurements, tide gauge data, and salinity intrusion into estuaries were favorable. The model's horizontal grid is orthogonal curvilinear, which supports rectilinear or spherical coordinates as special cases.

A variation on the theme of sigma-coordinate models is offered by the Spectral, Primitive Equation Model (SPEM) developed by Haidvogel (Hedstrom 1990, Haidvogel *et al.* 1991). It is similar in some respects to the POM model, except that it has a rigid lid and is distinguished by the fact that variables on the sigma coordinate are expanded vertically in series of Chebyshev polynomials (i.e., it is a spectral model in the vertical, instead of a level model). It has been used in a number of process studies, but not yet for coupled ice-ocean studies, although such a coupled version is under development.

The forerunner of the isopycnal layer models is the Bleck and Boudra Model (Bleck and Boudra 1986, Bleck *et al.* 1992). This particular model has not yet been coupled to sea ice, but the isopycnic formulation was adopted by Oberhuber (1993a) in his version of the isopycnal model with a sea-ice cover using Hibler's viscous-plastic rheology and Semtner's thermodynamics. An advantage of isopycnal coordinates is that increased resolution is automatically obtained in regions with strong density gradients. The code is complicated due to the need to cope with vanishing isopycnal layer thicknesses near the ocean surface and bottom.

Coupled ice-ocean, Arctic modeling studies

In the Arctic Ocean and the peripheral seas, the Greenland, Iceland, Norwegian, and Barents Seas, the overall stratification structure is determined by both river runoff and Atlantic and Pacific inflow, and by dynamic and thermodynamic interactions with the ice cover. As a result of heat exchange with the atmosphere, deep waters are formed in this region, a process which is augmented by brine rejection due to ice formation. Alternatively, since density is strongly salinity-dependent, freshwater fluxes at the ocean surface are especially important because of their stabilizing effect. In the Arctic Ocean, the freshwater layer prevents heat exchange between upper and deeper parts of the water column, and in the Greenland Sea, an excess freshwater cap in the form of ice can prohibit the renewal of deep waters. These processes prescribe the needs of a limited-area coupled Arctic model: a good description of mixing (which poses further demands on the surface forcing) and good estimates for river runoff, lateral inflows and outflows, and their spatial distribution. Either of these elements can be circumvented by using a diagnostic description for parts of the ocean model, such as relaxation to climatology, however, this limits a model's usefulness.

Partially diagnostic models

Hibler and Bryan (1987) were the first to present results from a coupled ice-ocean model for the Arctic. The ocean model was partially diagnostic for the deeper ocean, in that a Newtonian damping factor forced the temperatures and salinities toward climatological values, while the upper ocean could adjust prognostically to the surface forcing determined by ice freezing and melt. The main result from the simulations was to show the importance of the northward heat transport by the Norwegian Atlantic Current, which is responsible for determining the ice extent in the Greenland and Barents Seas. This same heat source is responsible for year round ice melt in the Greenland Sea. The coupling also intensified the oceanic Beaufort Gyre and the East Greenland Current, which the authors described as a readjustment to the forcing because the initial salinity and temperature fields were smoothed estimates of the observations.

The climatology of the Arctic ice thickness field supports high ice thicknesses north of Greenland due to the mechanical pileup of ice transported by the Transpolar Drift to the vicinity. However, the model, using surface forcing from 1979, produced a highly anomalous ice thickness field with a large ice buildup along the East Siberian coast and a weak build up north of Greenland.

This Hibler-Bryan Model has been implemented for operational use at the US Navy's Fleet Numerical Oceanography Center (Riedlinger and Preller 1991). Forecasted seasonal ice trends are in good overall agreement with observations for growth and decay. However, the ice cover in the Barents and Greenland Seas appears to be somewhat excessive, which the authors attribute to poor model resolution to describe narrow currents like the West Spitsbergen Current.

Another coupled ice-ocean model by Piacsek *et al.* (1991) is also partially diagnostic. The Hibler ice model is coupled to a high resolution mixed layer, where turbulence is calculated according to the level 2.5, Mellor and Yamada turbulence closure model (Mellor and Yamada 1982). However, the deeper ocean is diagnostic with a geostrophic velocity field determined from Levitus' (1982) climatology. Corresponding to a perpetual year, 1986 forcing, the model produces a very realistic seasonal variability, with the exception of the wintertime ice extent in the Barents Sea. They consider the inclusion of the mixed layer dynamics to give a superior ice thickness field compared to coupled models without mixed layer dynamics. The mean oceanic heat flux in the model varies in the ice-covered area from 5 to 15 W/m^2, attaining even larger values northeast of Spitsbergen in the area of the submerged Atlantic waters. These values are on the high side compared to the traditional view of about 2 W/m^2, and to even lower values, less than 0.5 W/m^2, as suggested by other one-dimensional modeling studies (Mellor and Kantha 1989). Comparison of observed buoy tracks and simulated drift tracks are in reasonably good agreement considering the coarse resolution of the model.

Prognostic models

The first comprehensive prognostic ocean model for the Arctic Ocean was described by Semtner (1976a) using the Bryan-Cox-Semtner (BCS) ocean model. The model was later ex-

panded by Semtner (1987) to include a dynamic-thermodynamic ice cover comprised of a three-level snow-ice system (Semtner 1976b) and an ice rheology simplified from the model by Hibler (1979). This ice-ocean system was driven by monthly surface forcing and specified inflow-outflow fluxes at the boundaries as in the Semtner (1976a) model.

Overall, the results from the ice model component showed agreement with the observed ice extent, but ice thicknesses were much lower compared to the generally accepted average values of 2.5-3 m. The model predicted a modest ice growth in the Beaufort Sea Gyre and much larger growth occurring on the Eurasia coast. The model also showed that ice melt occurred in the Greenland Sea even in mid-winter. The simulated oceanic circulation produced the main circulation features in the upper ocean, such as the Beaufort Gyre, Transpolar Drift, East Greenland Current, Norwegian Atlantic Current, and Barents Shelf circulation. Surface salinities were reasonably well reproduced in the model, except that their gradients were not strong enough in the central Arctic.

This model has been applied to the study of inter-annual ice variability by Fleming and Semtner (1991) for the period of 1971-1980. Their main conclusion is that using inter-annually varying forcing produces much improved sea-ice cover variability for the annual cycle, compared to the model forced by mean monthly climatology. The inter-annual forcing produced large variability in ice thickness fields, with much less degree of variability in sea-ice extent. The oceanic heat flux variability has the strongest influence in determining the monthly average ice edge positions. However, overly thin ice thickness is still a problem in the model which is, according to the authors, probably a result of an excessive melt-freeze cycle. Also, the authors consider that not having an explicit treatment of mixed layer dynamics produces inadequacies in the vertical mixing processes.

In particular, the model is used to test the conjecture of Aagaard and Carmack (1989) that the Great Salinity Anomaly was a consequence of an anomalously large ice export in 1968. The model simulations explored the high latitude, ice-ocean circulation changes due to wind field changes while other forcing components, such as air temperatures, cloudiness, snowfall, and river runoff, were climatological. The simulated ice extent in the Greenland Sea increased during the 1960s, reaching a maximum in 1968, as observed. The maxima in ice extent coincided with large pulses of ice export through the Fram Strait. The ice export from the Arctic Ocean to the Greenland Sea in 1968 was the largest in the simulation, being about twice as large as the simulated average for 1955-1975 and corresponding to 1600 km^3 of excess freshwater. The simulated upper water column in the Greenland Sea has a salinity minimum in the fall of 1968, followed by very low winter salinities. In addition to the above average ice export to the Greenland Sea, there was also a supply of freshwater from the Arctic Ocean. The total simulated freshwater input of 2500 km^3 to the Greenland Sea compared well with the estimated total freshwater excess of the Great Salinity Anomaly of about 2200 km^3, as it passed through the Labrador Sea (Dickson *et al.* 1988).

A paper by Oberhuber (1993b) used the OBH Model for most of the Atlantic Ocean from 30°S to 90°N. Thus, a sector of the Arctic Ocean was included in the model domain. The ice model was as described in section 3.6.4.2; however, the sensible heat storage in the ice was neglected. The model resolution is 2° by 2°. This model has been adopted into a limited area Arctic–Nordic seas model by Holland *et al.* (1993). Their paper presents a set of sensitivity studies of nearly all possible forcing components. They find that cloud cover is one of the least known, but most sensitive components, while snow fall (up to 2 m/y) did not appear to be crucial.

Evaluation and verification of model results

There now exist fairly sophisticated, numerical models for ice cover and oceans. They appear to give fairly realistic results even though they are mostly coarse resolution models. The basic criterion of evaluating an equilibrium ocean model is the question of how well it can reproduce the seasonal hydrography. The comparison is inadvertently limited to scalar variables instead of velocity fields of which we know very little except for coarse features, such as the cyclonic flow of the Atlantic origin waters around the Arctic Basin. Remote sensing gives an ideal way to validate ice model results, at least for ice concentration fields. Also the Arctic Buoy Program can provide information on ice drift for validation purposes. The least known quantity observationally is the ice thickness. To date, the best means of measuring ice thickness is through submarine sonar observations, but this type of data is classified, and thus is largely unavailable for monitoring and validation.

3.6.4.4. Modeling of oceanic contaminant transport in Arctic seas

The starting point for modeling the transport of contaminants in Arctic seas, is a coupled ice-ocean model as described above. In addition, a transport model is needed, either as an extension integrated into the ocean model or as a separate model driven by the results from the ocean model.

Depending on the contaminant in question, the transport model can be more or less complicated. If the contaminant is dissolved in seawater, it is treated as a passive tracer. This can be done in two ways. In the Eulerian approach, an advection-diffusion equation is solved for the development of the tracer concentration in a similar way to the equations for salinity and heat in the ocean model itself. An alternative is the Lagrangian, or particle-tracking approach. Here, trajectories of passive particles representing the contaminant are calculated from the current field of the ocean model. Both methods are well developed, and have well-known good and bad properties.

If the contaminant is bound to particles, the situation is a lot more complex. The particle may go into the sediments, be resuspended, captured in ice, etc. The physical, chemical and geological processes are not known well enough. Realistic models are not available at present. Further process studies and modeling are needed to gain knowledge before these processes can be incorporated or parameterized into regional or large-scale pollution transport models.

Examples of dispersion modeling

There has been relatively little activity on modeling of dispersion of oceanic contaminants in Arctic areas. Recently, the activity has increased somewhat, but most of the results are so fresh that they have not yet reached the reviewed literature. This increased activity is mostly concerned with the potential threats of nuclear contamination from former Soviet sources, in particular in the Kara Sea.

The largest modeling effort has been in the USA under the Arctic Nuclear Waste Assessment Program (ANWAP). The model used is the coupled ice-ocean model of the US Naval Research Laboratory. This model consists of a Bryan-Cox ocean model coupled with a Hibler ice model. The modeling work is reported in Preller and Edson (1995).

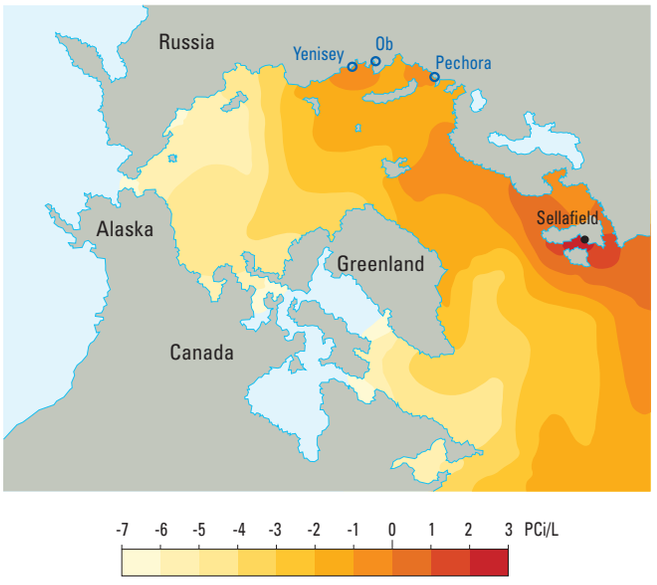

Figure 3·44. Distribution of radioactivity (PCi/L) in the surface layer of the ocean after ten years of simulation of Preller's model. Source locations are the Ob, Yenisey. and Pechora Rivers, as well as Sellafield. (Source: Preller and Edson 1995).

The model area contains the Arctic Ocean, the Nordic Seas, and the subpolar gyre in the North Atlantic and parts of the North Pacific as shown in Figure 3·44. The main contaminant sources are the rivers Ob and Yenisey in the Kara Sea, Pechora in the Barents Sea, and the Sellafield plant in the Irish Sea. The contaminants are transported as passive tracers in an Eulerian way. A Lagrangian approach is used to look at contaminant transport by the ice. For the Nordic and Barents Seas, the modeled contribution from Sellafield agrees with observed radiation levels. For the Kara Sea, the local river sources must be added to obtain high enough radiation levels. Figure 3·44 shows the levels of radiation in the surface with both Sellafield and the river sources after 10 years.

More regional work for the Kara and Barents Seas has been done by Harms (1997). He uses the Hamburg Shelf Ocean Model (HamSOM) documented by Backhaus (1985), together with an ice model based on Hibler's model. The Eulerian transport model is used to study the dispersion from waste dump sites east of Novaya Zemlya. In addition

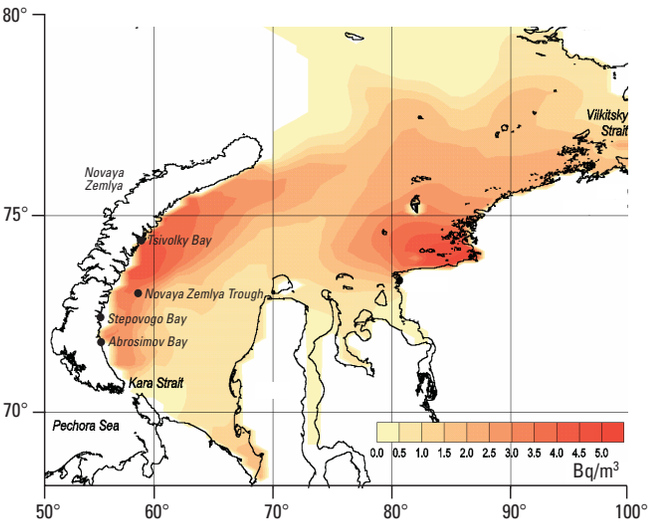

Figure 3·45. Yearly and depth-averaged concentrations (Bq/m^3) of ^{137}Cs after 6 years from Harms' model. The sources are instantaneous releases of 1 PBq from the dump sites in Abrosimov Bay, Stepovogo Bay, Tsivolky Bay, and Novaya Zemlya Trough (Source: Harms 1997).

to passive transport with the currents, a simple formulation is used to remove a fraction of the concentration from water into the sediments. He concludes both for ^{137}Cs and ^{239}Pu that a serious contamination of adjacent seas is unlikely. Figure 3·45 shows the modeled concentration of ^{137}Cs six years after release east of Novaya Zemlya.

Canada's Institute of Ocean Science (IOS) uses a prognostic ocean model coupled with a sea-ice model to investi-gate how a tracer is transported within the Arctic Ocean. A novel feature of the IOS model is the representation of the subgridscale eddies as a driving force in the mean circulation rather than as traditional eddy viscosity. This eddy force ('neptune') was described by Holloway (1992) and implemented in models by Alvarez *et al.* (1994). Other features of the IOS model include the use of flux corrected transport (FCT) after Gerdes *et al.* (1991). The model includes inflow at the Bering Strait, passages through the Barrow and Nares Straits in the Canadian Archipelago, and an open boundary in the Greenland Sea. Forcing by seasonal wind and buoyancy is applied for 120 years, at which time a tracer source is 'turned on' in the Norwegian Atlantic Current, then followed for 15 years. This represents a simplified European radionuclide source. Subsequent evolution can be compared with the tracer observations.

Profound differences between the models are seen in column-integrated tracer burdens (Figure 3·46) and in vertical sections (Figure 3·47). Even though diffusion was made as small as possible (while not allowing large negative concentrations), usual modeling (Figure 3·46) produces a diffuse picture in an unrealistic circulation. In particular, Fram Strait inflow is too weak along the Eurasian slope and transport north of Greenland is westward, counter to observed circulation (Rudels *et al.* 1989, Schlosser *et al.* 1995b). In contrast, when the model includes neptune effect and FCT (Figure 3·46), there is persistent eastward flow all along the Eurasian slope, returning flow along the Lomonosov Ridge, cyclonic circulation in the Makarov Basin and an anticyclonic flow around the Chukchi Plateau/Northwind Ridge. North from Greenland, mid-depth flow is eastward. (Here, a caution is warranted in that these remarks are based upon studies from the particular IOS model using geopotential coordinates. Another model, using isopycnal layers (Holland *et al.* 1995) would be expected to behave differently. Careful model intercomparisons remain to be done).

The tracer distribution shown in Figure 3·46 is more consistent with flows inferred from current meter data (Aagaard 1989) and water properties (Rudels *et al.* 1994, McLaughlin *et al.* 1995, Schlosser *et al.* 1995b). Ice motion (not shown) resembles the synthesis by Rigor (1992). Perhaps most importantly, Figure 3·46 is consistent with what is known about the entry of European reprocessing radionuclides into the Arctic Ocean (Livingston 1988) and their distributions as revealed by recent submarine and icebreaker sections (Ellis *et al.* 1995, Smith *et al.* 1995).

Figure 3·47 shows a vertical section through the North Pole along Y = 0 in Figure 3·46. Striking differences between usual modeling and the model with FCT/neptune (Figure 3·47) are seen in stronger tracer inflow from the Fram Strait and a return flow along the Lomonosov Ridge. A tracer core (Figure 3·47) has circulated around the Laptev slope and is returning along the Lomonosov Ridge.

Velocities, normal to Y = 0, are shown in Figure 3·47. Both models produce westward flow over the Eurasian Basin. However, the FCT/neptune model exhibits two important differences. A strong eastward flow along the Eurasian slope displaces westward flow to the interior, and flow along the Amundsen flank of the Lomonosov Ridge is evident throughout the water column.

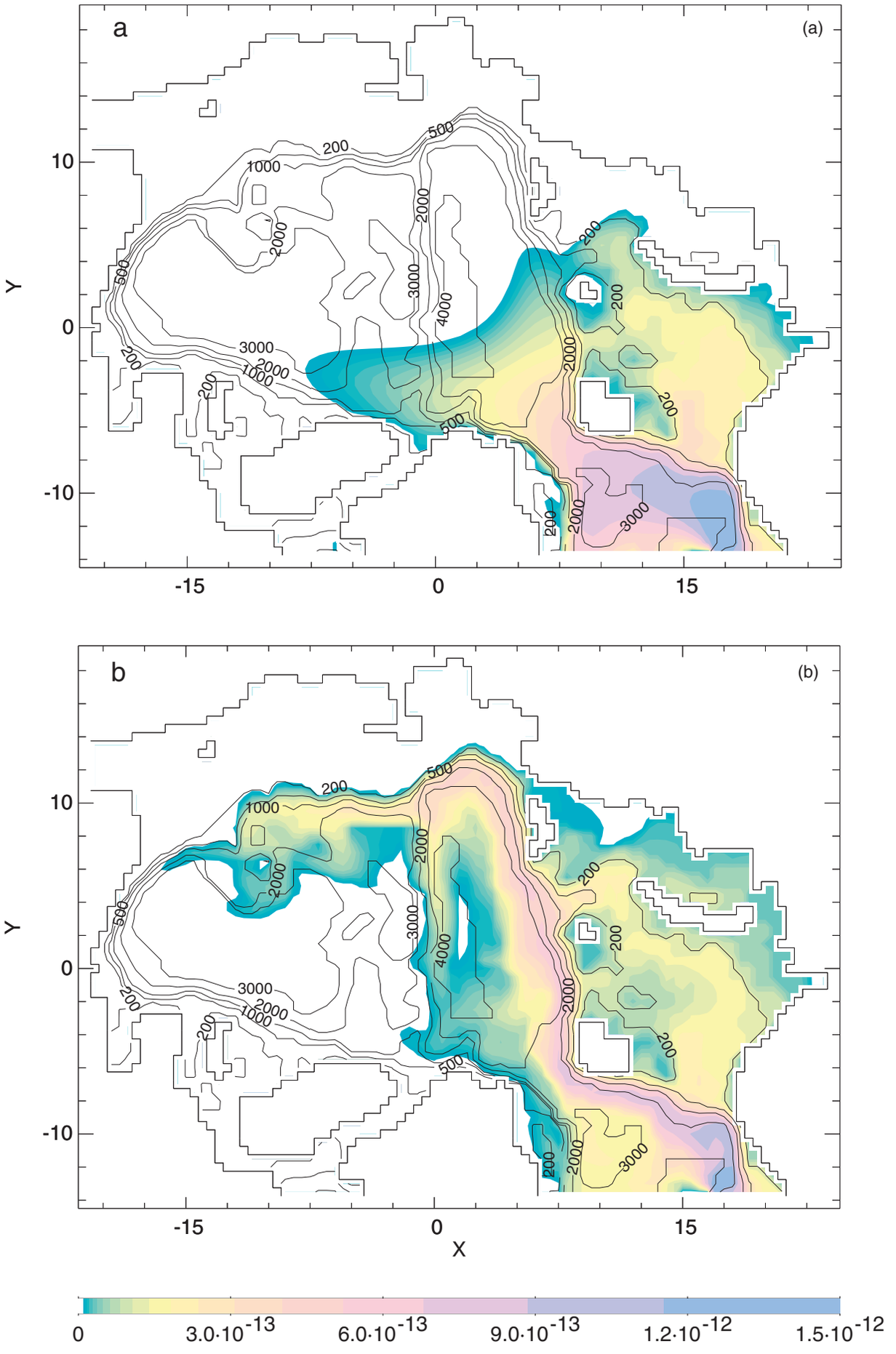

Figure 3·46. Vertically integrated tracer burden shown after 15 years. Units are burden per unit surface area, normalized by cumulative release. Bottom topography is in meters; a) no neptune, centered difference, and b) neptune, flux-corrected transport (Source: Alvarez *et al.* 1994).

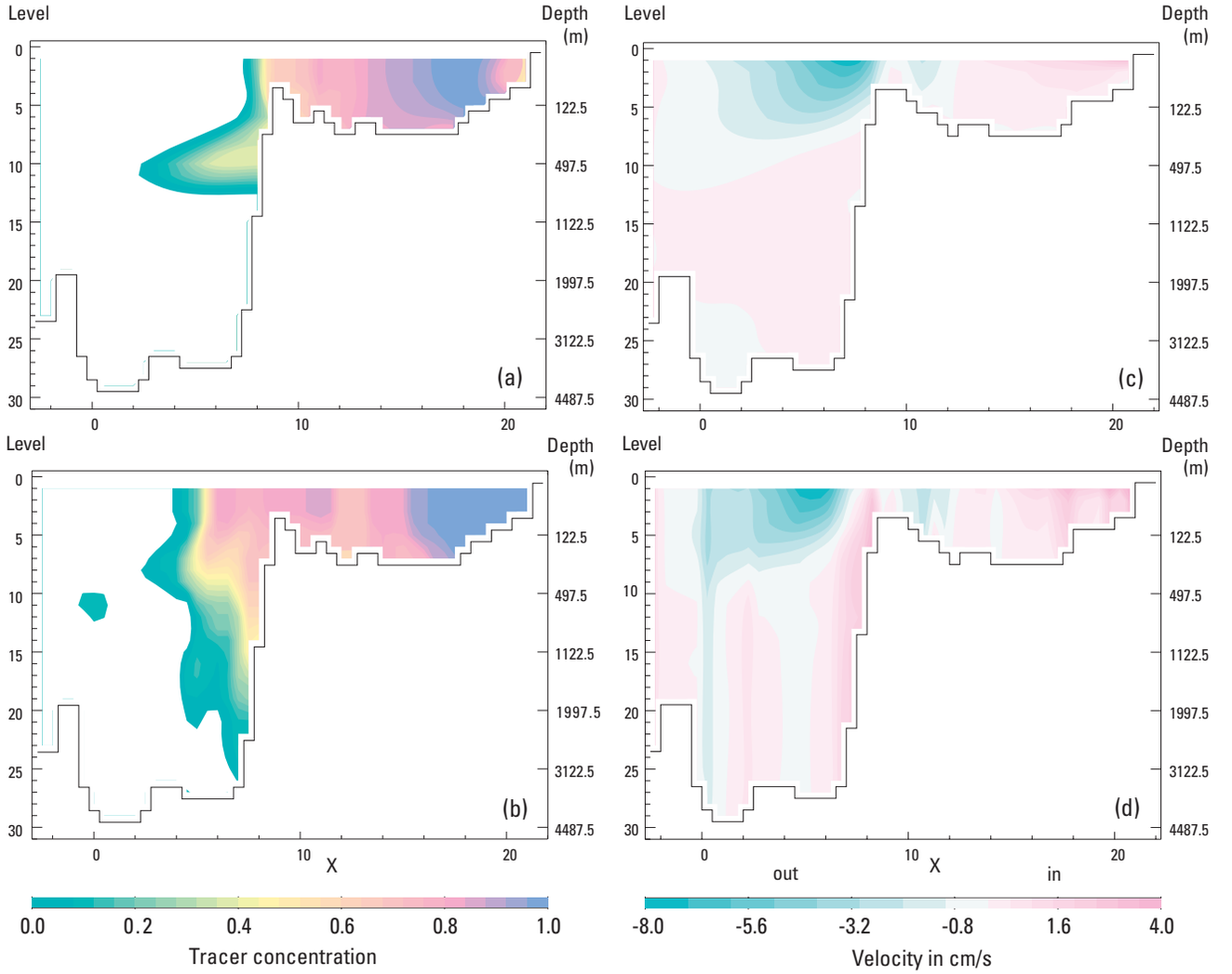

Figure 3·47. Tracer concentration on a vertical section (along Y = 0 on Figure 3·46) after 15 years; a) no neptune, centered difference; b) neptune, flux-corrected transport; c,d) velocity normal to the section with positive 'into' the page, negative 'out' of the page; c) no neptune, centered difference; and, d) neptune, flux-corrected transport (Source: Alvarez *et al.* 1994)

3.7. Summary and information gaps

3.7.1. Atmospheric pathways

Atmospheric pathways are important in the overall context of the delivery of contaminants to the Arctic. The atmosphere is the most important pathway relative to ocean and terrestrial/freshwater pathways for one-hop compounds (acids, metals except mercury, involatile organics). Given the current configurations of anthropogenic sources at mid-latitudes, the most favored pathway into the Arctic is from the Eurasian continent from November to May. The relative importance of atmospheric transport compared to marine and terrestrial/freshwater is very contaminant-specific for the multi-hop compounds, such as OC pesticides, Hg, and PCBs. While all of the compartments (Fig. 3·1) play a role in transporting these contaminants, the speed of transfer through the atmosphere suggests that this compartment is particularly important in the global cycling of these types of compounds. The airshed for the Arctic is northern hemisphere for one-hop contaminants, but global for multi-hop contaminants.

Models exist that quantitatively simulate atmospheric pathways. These have been derived from general circulation models, which have required extensive international cooperation, resulting in models that cover a large geographic area, including the Arctic. Thus, it has been a natural extension to apply these models to understanding contaminant transport from source regions to the Arctic.

The most accurate models for studying atmospheric transport pathways are those using globally or hemispherically gridded meteorological fields based on climatic observations. The density of meteorological observations in the Arctic is lower than elsewhere, due to the remoteness and high cost of operating these stations, and consequently, the accuracy of the predictions is reduced. These models have proven invaluable in that they can mathematically describe physical/chemical processes that help explain observed atmospheric levels of contaminants and inter-pathway exchanges.

Physical/chemical processes in the polar atmosphere are unique, and not as well understood or documented as those for temperate regions. Some of the processes that need to be understood better to improve the modeling capability and the general understanding of contaminant transport include:

- cloud, fog, and precipitation scavenging of contaminants in the Arctic during the summer when there is extensive low-level cloud and light precipitation under conditions of continuous daylight;
- chemical transformation of contaminants in air under Arctic conditions of temperature and sunlight;
- scavenging of contaminants by Arctic precipitation under low temperature conditions, especially the role of large surface area snow crystals that descend slowly through the air column;

- air-surface exchange of contaminants to better understand the recycling possibilities of multi-hop compounds under Arctic conditions; and,
- gas-particle phase partitioning within the atmosphere, and the role of temperature and other conditions in controlling this process.

Arctic atmospheric pathway studies suffer from a paucity of observations, both spatially and temporally. This is especially a problem with respect to multi-phase studies, such as the simultaneous measurement at the surface (land, freshwater, and marine, including ice surfaces for both lakes and oceans) and through the air column. This deficiency can only be addressed through greater use of fully integrated observational platforms (i.e., surface-based stations combined with aircraft and ships). In some cases, these observations would need to be augmented by surface-level routine observations from additional locations using observatories and buoys. In addition, the intensive observations would have to be supplemented by remote sensing techniques (e.g., satellite imagery, lidars, etc.) as this is the only means of providing broad spatial coverage cost-effectively.

3.7.2. Terrestrial/freshwater pathways

The deposition of contaminants from the atmosphere through snow, rain, and dry fallout is a major regional-scale source of contamination in the Arctic. However, the processes controlling scavenging, fate, and release are poorly understood. Since the atmosphere serves as a relatively homogeneous source, spatial variability of contaminant deposition seems to be largely controlled by the precipitation fluxes to the land and ocean surfaces. Precipitation measurements are spatially limited in the Arctic, especially over the ocean, and remotely sensed data are currently imprecise. Consequently, mass fluxes of contaminants to the land and ocean surfaces are difficult to estimate at present. Improved sampling devices for contaminants in precipitation, developed for Arctic climatic conditions, together with better accounting of precipitation accumulation in remote areas, would enhance the accuracy of deposition information.

Just as the processes that control scavenging from the atmosphere are poorly understood and quantified, so too are the physical and chemical processes that control the exchange between snowpacks and the atmosphere. For example, only recently has it been recognized that there is a large difference between the air/snowpack exchange of shallow and deep snowpacks. The fate of contaminants in cold and metamorphosing snowpacks is largely controlled by snowmelt and refreezing, solar radiation, changing snow particle size and surface area, and exchange with the atmosphere and surface soil. These processes have only begun to be investigated. Field studies provide evidence that up to 80% of the total solute load in the snowpack is released with the first 20-30% of meltwater. Laboratory studies indicate that, whereas dissolved pollutants (organic compounds with high water solubility) are rapidly dispersed into the water at the onset of melting, those that are adsorbed (to particles) are more recalcitrant, and only leave the snow with the final meltwater. An understanding of the rates of these processes and the factors controlling them is necessary in order to model the delivery of contaminants to the aquatic system from land and ice runoff. This is a clear gap in our understanding of contaminant delivery to the oceans from the terrestrial/freshwater compartment.

The contaminants delivered to the Arctic and deposited to the terrestrial/freshwater environment are readily transported to and within the freshwater system. At present, discharge and sediment concentration in freshwater systems are reasonably well documented. Estimates of contaminant loads from rivers to the oceans, on the other hand, are quite crude, being dependent upon a very limited set of observations and lacking a large-scale modeling capability. The paucity of site-specific and larger-scale studies in the Arctic limits the understanding of processes and determination of mass transport. Site-specific investigations of contaminant transport and fate in Arctic freshwater systems are required to understand the basic processes and to evaluate and calibrate site-specific and larger-scale models. For example, studies are needed on freeze and thaw effects on snowpack release; permafrost effect on infiltration and on ground and drainage waters; humic acids and their influence on adsorption of hydrophobic compounds; and, inorganic particles and sorption processes. Larger-scale studies and monitoring are required to more precisely measure the total mass of contaminants delivered to oceans and the temporal distribution of this delivery, as well as to characterize the particulate and dissolved phase contributions. This information is necessary in order to improve the estimation of the transport of hydrophobic and soluble contaminants from the land surface to headwater systems using large-scale mass transport models (e.g., the River System Simulator), which have not been used extensively for the Arctic.

Our knowledge of transport and levels of contamination of surface waters in the Arctic is restricted, but even less is known about processes and levels in drainage waters and their discharge to Arctic rivers. The transport and fate of contaminants in drainage waters are probably partly controlled by similar variables as those controlling surface waters (e.g., organic matter, pH, ions), but these processes, as well as the extent or potential for contamination of Arctic groundwater, have hardly been investigated. Such knowledge would be most useful for areas where local contamination sources are a concern.

There has been no investigation of sediment resuspension in Arctic lakes in the context of contaminants transport. As well, there are few investigations of shallow lakes (2-3 m deep), which are the most common in the Arctic. Their heat budget (warmer and not stratified during the summer, but often totally frozen in the winter) is likely to influence the fate of contaminants, but this has not been investigated.

Ice cover is an important phenomenon in the Arctic. It plays a role in freshwater systems, especially with respect to oxygen exchange and consumption, which in turn could influence the fate of contaminants in the environment. Although not studied to any great extent, it is clear that ice will form a reasonably impermeable barrier between the atmosphere and the water for the majority of the year. This obviously limits the exchange of atmospheric pollutants with the water, but also retains any pollutants introduced below the ice within the limited water volume. Sources of contaminants that could be a concern include contaminated groundwater drainage, industrial and municipal discharges below the ice, and natural seeps of hydrocarbons such as occur in the Mackenzie River. Also, the role of ice in remobilizing contaminants in rivers and in delivering contaminants to the ocean has received minimal attention. The role of ice in controlling exchanges and the magnitude of contaminant loadings by ice should be evaluated to determine if more extensive work is required.

Hydrophobic contaminants sorb to particles and their transport is strongly related to the quantity and nature of suspended loads in rivers. Areas with reduced water velocity, such as lakes, floodplains, and freshwater deltas, are possi-

ble deposition zones for contaminants. The quantities and physical aspects of sediment transport are relatively well known. This is important for determining the relative contribution of the different phases of contaminants (dissolved or associated with particles and ice) transported in the river. However, the concentrations of contaminants in the different phases and their spatial and temporal variability remain largely unknown.

Much emphasis has been placed on the pathways for long-range transport of contaminants, nevertheless, the contribution of local Arctic sources of contaminants to the total contaminant transport budget requires further investigation. In Canada, this seems to be only a local concern, whereas in Russia, Arctic sources may be a major component of the total budget. Many large river basins draining to the Arctic extend well into temperate latitudes in both Canada and Russia. Investigations in Canada have shown that there is little industrial and agricultural impact on Canadian river systems flowing to the north; however, in Russia, there is much greater potential for both industrial and agricultural discharges to directly affect the quality of water. Some information is available for industrial and municipal sources, but little seems to be known about the agricultural impacts on these river systems.

3.7.3. Ocean pathways

Our schematic knowledge of the general circulation in the Arctic Ocean has improved over the past decade due especially to tracer studies carried out during basin transects. However, there are still large gaps in our knowledge of the current structure in the Makarov and Canada Basins, of the exchange between the ocean margins and the interior, of the coupling between basins, and of the relative importance of the Canadian Arctic Archipelago and the Fram Strait for surface water exiting the Arctic. Tracer fields often give a direct measure of the rate of propagation of a property and, in the most widely cited example, radionuclide tracers from the European reprocessing plants have shown dramatically that transport times are much faster than earlier believed. But tracer fields often do not provide good estimates of volume flows. Poorly constrained volumetric flows, together with a very poor knowledge of the contaminant concentrations (particulate and dissolved), mean that, at present, only approximate guesses of quantitative transport rates are possible within the Arctic Ocean. Although volumetric flows are better constrained at the entrances and exits from the Arctic Ocean, there is still considerable uncertainty and variance, and the contaminant concentrations are, as yet, poorly determined or not determined at all. Therefore, we need better documentation of volume transports of ice and water, and their contaminant burdens into, out of, and within the Arctic.

Due to ice cover, circulation in the central Arctic Ocean has not been as well documented as in the adjacent seas. For example, the amount of water exchanged between the Beaufort Gyre and the Transpolar Drift is not well quantified. This is important since the Beaufort Gyre can retain a contaminant and recirculate it for many years, while contaminants in the Transpolar Drift exit the Arctic Ocean in just a few years. Similarly, water leaving the Beaufort Gyre through the Canadian Archipelago could be important for contaminant flux out of the Arctic.

The Arctic Ocean is more dynamically coupled to its surrounding seas than believed earlier. Little is known about the variability in the different seas and how they affect the main system. For example, river runoff is transported with relatively little dilution over remarkably large distances in the Arctic – more so than in any other ocean basin. Our understanding of the role of this redistributed river water in long-range contaminant transport is limited, as is the influence of variable riverine discharge on ocean circulation.

The Arctic is not in a steady-state, but how it oscillates is still uncertain. Because most data are from the summer and have been obtained relatively recently, there is less known about winter conditions and interannual variability. The Beaufort Gyre seems to shift between a small gyre and a larger one, but the causes of these changes and their effects are unknown. The Atlantic layer seems to have warmed by about 0.5-1°C during recent years. The invasion of warm water, following boundary currents around the Eurasian and Canadian Basins, is accompanied by a shift in the front separating the Atlantic and Pacific water masses in the upper part of the Arctic Ocean. The fate of this displaced Pacific water, including its pathway out of the Arctic Ocean, is not known.

Transport pathways and mechanisms are not the same for all contaminants. Some contaminants tend to become bound to particles while others remain in the dissolved phase. Since particles tend to sediment and therefore take different pathways than dissolved constituents, it is crucial to understand both the phase geochemistry of the contaminant and the ocean processes of particle production and vertical flux. Presently, there are few data with which to estimate the relative importance of particles in the transport of contaminants and the movement of contaminants from surface water and coastal zones to deeper parts of the ocean.

Sea ice acts as a lid on the surface of the ocean, hindering ocean-atmosphere exchange of contaminants. Clearly, ice controls the seasonal cycle of semivolatile constituents in the ocean surface, but measurements are limited.

Recent studies indicate that sea ice also plays a role in transport and redistribution of contaminants, although little concrete information is available on the quantitative significance of this pathway, as detailed below. The process of retaining particles/contaminants during transport and releasing them at the sea surface far away makes sea ice a unique transport mechanism.

Many dissolved pollutants are excluded with salt during the freezing process, thus, sea ice without incorporated sediments or organic material may be less contaminated than the water from which it was formed. However, much of the ice formed in shallow regions of the Siberian seas entrains resuspended sediments and organic material, and may therefore incorporate associated contaminants. Some of this ice is exported from the shelf and transported over thousands of kilometers. The relative importance of atmospheric deposition versus marine and river sources of contaminants to sea ice is not clear. As well, information is lacking on the significance of contaminated ice being exported from a large region where it is formed, into a smaller region where it dissipates and/or is exported.

Due to continued atmospheric deposition of aerosols and condensates during transport, and perhaps entrainment from the surface ocean microlayer, contaminant loads may increase in older sea ice. The fate of contaminants deposited to sea ice in snow as the snow melts is unknown. Some portion may be lost in meltwater runoff, some may volatize, and some may adsorb to sediments in the ice, but the distribution among these is unknown.

Most particles and associated contaminants are probably released at the sea surface along the marginal ice zone. Because of biological activity in this region, it is possible that contaminants released here enter the food chain. Sea-ice transport could provide a link between pollutant source

areas and distant wildlife. The biological communities that seem to be most at risk from long-range pollutant transport by sea ice are those along the marginal ice zones, where large amounts of ice melt. Such areas are found in the Barents and Greenland Seas, the Iceland Sea, the west coast of Greenland and Baffin Bay, and to a lesser degree the other marginal seas. The degree to which sea-ice transport of contaminants contributes to body burdens in these regions is not known.

Presently, models of ocean and ice circulation are often of too low resolution to resolve boundary currents and eddies, both of which are likely to be the main modes of contaminant transport. Furthermore, contaminants enter the models only as passive tracers, and future modeling efforts need to incorporate more realistic contaminant properties including uptake by biota, particle scavenging, and kinetic losses.

3.7.4. Conclusions

Following from the summary and information gaps discussed above, it can be concluded that a number of steps are required to better understand the pathways of contaminants into and within the Arctic. These are presented below as general conclusions which are relevant to all compartments:

1. Tracers are important in determining and confirming pathways. To date, these have been used in the ocean pathway studies (e.g., radionuclides released from Sellafield), but greater use needs to be made of natural and anthropogenic tracers in all compartments. Emphasis should be placed on tracers that mimic the major contaminants, or are representative of groups of contaminants, thereby enhancing pathway studies, as well as perhaps reducing their cost. Selected PAHs, PCB congeners, stable isotopes, and a range of other contaminants could prove to be very useful in this regard and need to be examined more fully.
2. Arctic processes are largely understood qualitatively, however, the ability to quantify them is inadequate. In particular, it is essential that transport processes and their relative importance or magnitude within and between compartments (air, terrestrial, water, ice, sediments, biota) be determined. There is a need for prioritization to ensure that the most important processes are investigated within the context of contaminant delivery to the Arctic environment.
3. In general, there is a qualitative understanding of the transformation and fate of different contaminants or groups of contaminants under varying Arctic conditions. However, detailed information and the ability to quantify these processes is lacking. While a considerable amount of information is available on this subject for many of the contaminants under temperate conditions, there is still little or no understanding as to how, for example, temperature and light affect the rate of these processes. In order to be able to fully assess the magnitude and direction of pathways, a better understanding of transformation and fate of pollutants in the Arctic is required.
4. Ice is a dominant multi-compartment medium of the Arctic. However, the role of ice in modulating contaminant fate and controlling pathways is poorly understood. This is an important gap.
5. There is ample evidence of the limited effectiveness of sporadic and poorly integrated process, pathway, and flux studies. Through the use of multi-media models, a great deal could be achieved efficiently by fully integrating processes, observed levels, and trends. In other words, integrating the observed environmental measurements with the pathways and sources information, so as to provide assessment and feedback on the design and implementation of future monitoring and process research activities, as well as management and/or mitigation measures. Models are also essential in assessing the sensitivity of individual or linked processes, which in turn can be instructive in assigning priorities to often complex research questions. In particular, models have not been used to their fullest in the area of terrestrial/freshwater pathways. There is also a need for integrated models to help assess complex questions, including evaluation of the relative importance of processes, estimation of transport fluxes, and assessment of remedial measures.

3.7.5. Recommendations

The overriding conclusion from this work is the general inability to quantify fluxes and rates on a circumpolar scale. Consequently, these recommendations are intended to enhance our understanding of the inter- and intra-compartmental delivery of contaminants by providing guidance for future system-based monitoring and research activities. This can be approached in two ways, either through the evaluation of pathways to determine 1) 'contaminant focusing zones' or 2) 'zones of influence' of known source regions. These concepts are illustrated in Figure 3·48a and b (next page), respectively.

1. Accordingly, it is recommended that contaminant pathways be evaluated in a comprehensive and systematic way to determine contaminant focusing zones as a result of long-range transboundary transport through one or more environmental compartments. Specific focusing zones include:

- atmospheric and ocean conduits and deposition areas;
- marginal ice zones and polynyas; and,
- zones of increased precipitation (e.g., coastal and mountainous areas).

This approach will help to account for existing areas of relatively elevated contaminant levels and to identify other potential zones of impact based on the physical/chemical data.

Some examples to illustrate what is meant by contaminant focusing zones include:

- Atmospheric pathway convergence and terrestrial/freshwater focusing: The mountain range on the west coast of North America focuses the deposition of atmospheric contaminants through precipitation. These are then carried through runoff into sensitive drainage systems resulting in accumulation in lakes;
- Estuaries: In productive environments, estuaries act as a trap for sediments and contaminants, especially where nearby sources contribute contaminants to river or ocean ice and water; and,
- Marine convergence: This may be an important factor for a number of areas, as suggested by both pathway and contaminant residue information. For example, in the Svalbard area, air masses, precipitation scavenging, ocean currents, and sea ice may all interact to focus contaminants. In the Canadian Arctic Archipelago, the flux of water and contaminants out of the Arctic Ocean takes place almost entirely in the upper 100 m and is consequently coupled with air exchange and freshwater inputs which together could uniquely impact upon the local marine ecology.

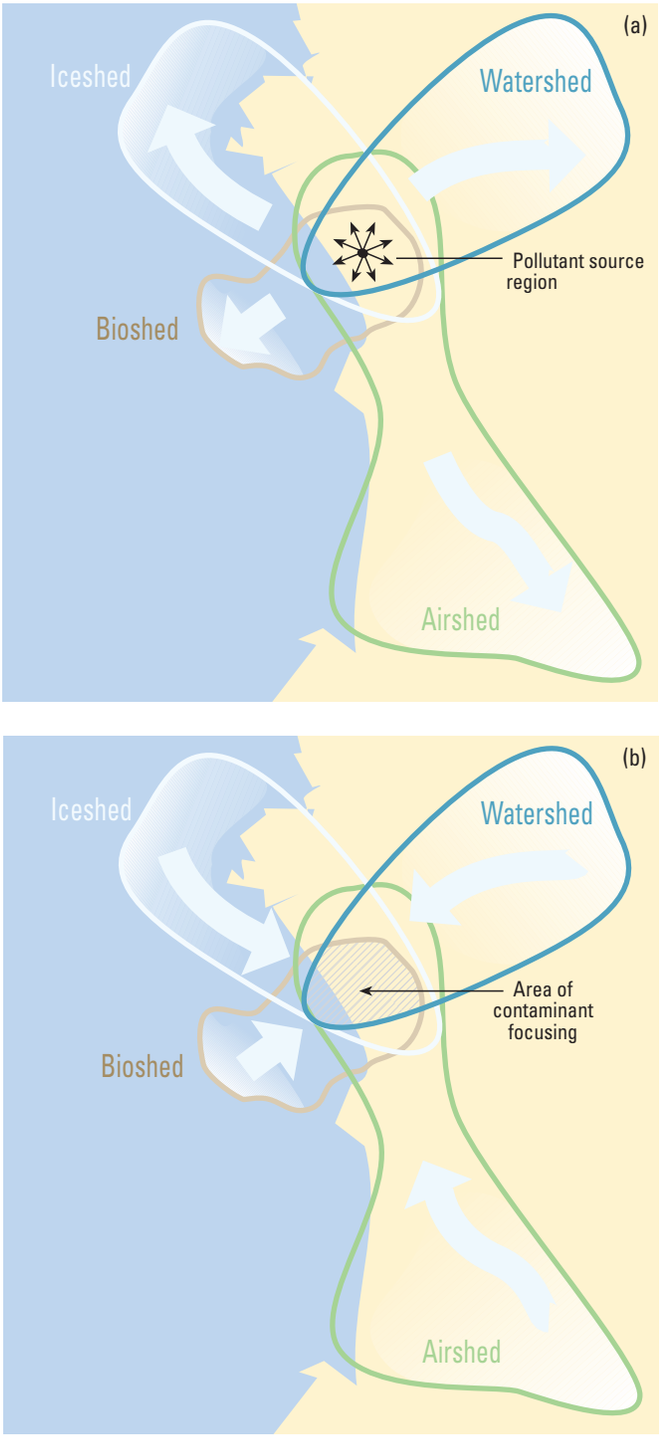

Figure 3·48. Illustration of the concept of a) the 'zone of influence' through major contaminant pathways from a major source region, and b) the 'contaminant focusing zone' resulting from the convergence of pathways carrying contaminants from a variety of sources to a single zone.

2. Subsequently, it is also recommended that the zones of influence of known regional or local sources be investigated based upon an understanding of processes, pathways, and flux rates. This will lead to the identification of local, or at most regional zones of influence for specific sources of contaminants.

The first priority in this exercise would be to understand the zone of influence of sources locally, regionally, and over long distances, pointing to areas for which impact studies may be required. Second and subsequent priorities would have to consider information needs with respect to pathways. Some examples which illustrate the applicability of determining zones of influence of contaminant sources include:

- the Murman area, for which the long-range zone of influence is not well known, despite having large industrial and municipal atmospheric emissions and wastewater discharges with extensive local and regional effects;
- the fate and impact of contaminants from regional sources upon the Kara Sea; and,
- the extent of impact from point sources within the Arctic (e.g., DEW Line sites) relative to long-range sources.

In order to fulfill the intent of these recommendations, investigations of both contaminant focusing zones and the zones of influence of source regions will have to consider the usefulness of tracers, quantify the main processes, assess transformation and fate in the specific situation, consider the unique conditions of the Arctic, such as ice, and fully integrate the use of multi-media models. Development of comprehensive investigations to address these recommendations will require further definition and development within the context of the information provided on contaminant levels and the effects of specific contaminants as outlined in subsequent chapters.

Acknowledgments

Editors
Dennis J. Gregor, Harald Loeng, Len Barrie.

Authors
Len Barrie, Eva Falck, Dennis J. Gregor, Trond Iversen, Harald Loeng, Rob Macdonald, Stephanie Pfirman, Trond Skotvold, Elleke Wartena.

Contributors
B. Ådlandsvik, A.C. Brown, M. Diamond, P. Fellin, V. Gordeev, S. Häkkinen, W. Hart, G. Holloway, V. Kimstach, L. Lockhart, H. Martin, K. Puckett, W. Schroeder, G. Stephens, W. Strachan, H. Svendsen, V. Vuglinski, B. Welch, A. Zhulidov.

Reviewers
Oceans: K. Aagaard, B. Hansen, S. A. Malmberg, T. Vinje, G. Björk, S. Carlberg, E. Reimnitz, T. Rossby, T. Tucker
Atmosphere: W. Schroeder
Terrestrial/Freshwater: T. Prowse, M. Jansson
Entire chapter: D. Landers, M. Bewers.

References

Aagaard, K., 1968. Temperature variations in the Greenland Sea deep water. *Deep-Sea Res.* **15**: 281-296.
Aagaard, K., 1981. On the deep circulation of the Arctic Ocean. *Deep-Sea Res.* **82**: 251-268.
Aagaard, K., 1984. The Beaufort undercurrent. *In:* P.W. Barnes, D.M. Schell and E. Reimnitz (eds.). The Alaskan Beaufort Sea, ecosystems and environments, pp. 47-71. Academic Press, Orlando.
Aagaard, K., 1989. A synthesis of the Arctic Ocean circulation. *Rapp. P.-v. Réun. Cons. int. Explor. Mer* **188**: 11-22.
Aagaard, K., 1994. Contamination of the Arctic: Ocean processes. *Arct. Res. U.S.* **8**: 21-33.
Aagaard, K. and E.C. Carmack, 1989. The role of sea ice and other fresh water in the arctic circulation. *J. Geophys. Res.* **94(C10)**: 14485-14489.
Aagaard, K. and E.C. Carmack, 1994. The Arctic Ocean and climate: a perspective. The polar oceans and their role in shaping the global environment. *Am. Geophys. Un.* **85**: 5-20.
Aagaard, K. and L.K. Coachman, 1975. Toward an ice-free Arctic Ocean. *EOS* **56**: 484-486.
Aagaard, K. and P. Greisman, 1975. Towards new mass and heat budgets for the Arctic Ocean. *J. Geophys. Res.* **80**: 3821-3827.
Aagaard, K. and S.-A. Malmberg, 1978. Low frequency characteristics of the Denmark Strait overflow. ICES C.M. 1978 C: 47. International Council for the Exploration of the Sea, Copenhagen.
Aagaard, K. and A.T. Roach, 1990. Arctic Ocean-shelf exchange: Measurements in Barrow Canyon. *J. Geophys. Res.* **95(C10)**: 18163-18175.
Aagaard, K., L.K. Coachman and E.C. Carmack, 1981. On the halocline of the Arctic Ocean. *Deep-Sea Res.* **28**: 529-545.

Aagaard, K., J.H. Swift and E.C. Carmack, 1985. Thermohaline circulation in the Arctic Mediterranean seas. *J. Geophys. Res.* **90**: 4833-4846.
Aagaard, K., E. Fahrbach, J. Meincke and J.H. Swift, 1991. Saline outflow from the Arctic Ocean: Its contribution to the deep waters of the Greenland, Norwegian, and Iceland seas. *J. Geophys. Res.* **96**: 20433-20441.
Abelmann, A., 1992. Diatom assemblages in Arctic sea ice – indicator for ice drift pathways. *Deep-Sea Res.* Special Issue **39**: S525-S538.
Ackermann, N.L., H.T. Shen and B. Sanders, 1994. Experimental studies of sediment enrichment of Arctic ice covers due to wave action and frazil enrichment. *J. Geophys. Res.* **99**(**C4**): 7761-7770.
Ackley, S.F., 1982. Ice scavenging and nucleation: Two mechanisms for incorporation of algae into newly-forming ice. *EOS Trans. Am. Geophys. Un.* **63**: 54-55.
Ahlnäs, K. and G.R. Garrison, 1984. Satellite and oceanographic observations of a warm coastal current in the Chukchi Sea. *Arctic* **37**: 244-254.
Alabyan, A.M., D.B. Babich and A.L. Bogomolov, 1991. Recent processes of delta formation and history of the Yenisey Delta development. VINIT1, Moscow. (In Russian). 151p.
Alabyan, A.M., R.S. Chalov, V.N. Korotaev, A.Y. Sidorchuk and A.A. Zaitsev, 1996. Natural and technogenic components of water and sediment supply to the Laptev sea. *Ber. Polarforsch.* (in press).
Albright, L.J., K.V. Masuda, G.L. Ennis and H. Schreier, 1980. Microbial dynamics of two sub-Arctic Canadian rivers. *Water Resour. Res.* **14**(**9**): 1353-1362.
Allan, R.J., 1979. Heavy metals in bottom sediments of Great Slave Lake (Canada): A reconnaissance. *Environ. Geol.* **3**: 49-58.
Allen, J.R.L., 1970. Physical processes of sedimentation: An introduction. *In:* J. Sutton and J.V. Watson (eds.). Earth Science series No.1, 248p. Unwin University Books. George Allen and Unwin Ltd., London, U.K.
Altshuler, V.M., Y.V. Sustavov and Y.M. Kazakova, 1970. On the energy and water exchange between the White and Barents Seas. *Trudy Polyarn. Naucho-Issled. Inst. Morsk. Ryb. Khoz. Oceanogr.* **27**: 114-118. (In Russian).
Alvarez, A., J. Tintore, G. Holloway, M. Eby and J.M. Beckers, 1994. Effect of topographic stress on the circulation in the western Mediterranean. *J. Geophys. Res.* **99**: 16053-16064.
Anderson, L.G. and E.P. Jones, 1986. Water masses and their chemical constituents in the western Nansen Basin of the Arctic Ocean. *Oceanol. Acta* **9**: 277-283.
Anderson, L.G., E.P. Jones, R. Lindegren, B. Rudels and P.-I. Sehlstedt, 1988. On the chemistry of the cold, high salinity bottom waters of the Arctic Ocean shelves. *Cont. Shelf Res.* **8**: 1345-1355.
Anderson, L.G., G. Björk, O. Holby, E.P. Jones, G. Kattner, K.P. Koltermann, B. Liljeblad, R. Lindegren, B. Rudels and J. Swift, 1994. Water masses and circulation in the Eurasian Basin: results from the Oden 91 expedition. *J. Geophys. Res.* **99**: 3273-3283.
Antonov, V.S., 1970. Siberian rivers and Arctic seas. *Probl. Arktiki Antarktiki* **36/37**: 142-152.
Arnesen, R.T. and E.R. Iversen, 1995. Transport of heavy metals from Norwegian mines. NIVA Report O-94021. NIVA (Norwegian Institute for Water Research), Oslo, Norway. (In Norwegian).
Asplin, L., 1995. Examination of local circulation in a wide, stratified fjord and exchange of water with the adjacent ocean due to constant local up-fjord wind. *In:* H.R. Skjoldal, C. Hopkins, K.E. Erikstad and H.P. Leinaas (eds.). Ecology of fjords and coastal waters. Elsevier Science B.V., Amsterdam.
Atkinson, E.G. and J.W. Wacasey, 1987. Sedimentation in arctic Canada: Parcticulate organic carbon flux to a shallow marine benthic community in Frobisher Bay. *Polar Biol.* **8**: 3-7.
Backhaus, J.O. 1985. A three-dimensional model for the simulation of shelf dynamics. *Dt. Hydrogr. Z.* **38**: 165-187.
Bacon, M.P., C.-A. Huh and R.M. Moore, 1989. Vertical profiles of some natural radionuclides over the Alpha Ridge, Arctic Ocean. *Earth Planet. Sci. Lett.* **95**: 15-22.
Bailey, W.B., 1956. On the origin of Baffin Bay deep water. *J. Fish. Res. Bd Can.* **13**: 303-308.
Bailey, W.B., 1957. Oceanographic features of the Canadian archipelago. *J. Fish. Res. Bd Can.* **14**: 731-769.
Ballschmiter, K. and M. Zell, 1980. Baseline studies of the global pollution – l. Occurence of organohalogens in pristine European and Antarctic aquatic environments. *Int. J. Environ. analyt. Chem.* **8**: 15-35.
Barber, F.G., 1965. Current observations in Fury and Hecla Strait. *J. Fish. Res. Bd Can.* **22**: 225-229.
Barber, F.G., 1967. A contribution to the oceanography of Hudson Bay. Mar. Sci. Br., Dept. of Mines and Technical Surveys, Ottawa, Ms. Rep. Ser., No. 4, 69p.
Barnes, P.W. and E. Reimnitz, 1974. Sedimentary processes on Arctic shelves off the northern coast of Alaska. *In:* J.C. Reed and J.E. Sater (eds.). The coast and shelf of the Beaufort Sea, pp. 439-476. The Arctic Institute of North America, Washington D.C.
Barnes, P.W., E.M. Kempema and E. Reimnitz, 1990. Source, characteristics and significance of sediment pellets formed on the sea ice of the Arctic Basin. *In:* S.F. Ackley and W.F. Weeks (eds.). Sea ice properties and processes: Proceedings of the W.F. Weeks Sea Ice Symposium, pp. 106-108. Cold Regions Research and Engineering Laboratory, Hanover, New Hampshire, CRREL Monograph 90-1.
Barrie, L.A., 1985. Atmospheric particles: their physical and chemical characteristics and deposition processes relevant to the chemical composition of glaciers. *Ann. Glaciol.* **7**: 100-108.
Barrie, L.A., 1986. Arctic air pollution flow of current knowledge. *Atmos. Environ.* **20**: 643-663.
Barrie, L.A., 1991. Snow formation and process in the atmosphere that influence its chemical composition. *In:* T.D. Davis, M. Tranter and H.G. Jones (eds.). Seasonal Snowpacks. NATO ASI Series, Volume 28, pp. 1-20. Springer-Verlag, Berlin and Heidelberg, Germany.
Barrie, L.A., 1992. Scavenging ratios: black magic or a useful scientific tool. *Precip. Scavenging Atmos.-Surface Exchange* **1**: 403-415.
Barrie, L.A., 1995. Arctic aerosols: composition, sources and transport in ice core studies of global biogeochemical cycles. *In:* R.J. Delmas (ed.). Global Environmental Change. NATO ASI Series, Volume 30, pp. 1-22. Springer-Verlag, Heidelberg, Germany.
Barrie, L.A., 1996b. Occurrence and trends of pollution in the Arctic troposphere. *In:* E. Wolff and R.C. Bales (eds.). Chemical exchange between the atmosphere and polar snow. Global Environmental Change. NATO ASI Series I, Volume 43, pp. 93-130. Springer-Verlag, Heidelberg, Germany.
Barrie, L.A., 1996a. Personal communication. Atmospheric Environment Service, Environment canada, Downsview, Ontario, Canada.
Barrie, L.A. and R.S. Schemenauer, 1986. Pollutant wet deposition mechanisms in precipitation and fog water. *Water Air Soil Pollut.* **30**: 91-104.
Barrie, L.A. and R.S. Schemenauer, 1989. Wet deposition of heavy metals. *In:* J.M. Pacyna and B. Ottar (eds.). Control and fate of atmospheric trace metals. NATO ASI Series C 268, pp. 203-231. Kluwer Academic Publishers, Dordrecht, The Netherlands.
Barrie, L.A., M.P. Olson and K.K. Oikawa, 1989b. The flux of anthropogenic sulphur into the Arctic from mid-latitudes in 1979/80. *Atmos. Environ.* **23**: 2505-2512.
Barrie, L.A., D. Gregor, B. Hargrave, R. Lake, D. Muir, R. Shearer, B. Tracey and T. Bidleman, 1992. Arctic contaminants: sources, occurrence and pathways. *Sci. Total Environ.* **122**: 1-74.
Barrie, L.A., R. Macdonald, T. Bidleman, M. Diamond, D. Gregor, R. Semkin, W. Strachan, M. Alaee, S. Backus, M. Bewers, C. Gobeil, C. Halsall, J. Hoff, A. Li, L. Lockhart, D. Mackay, D. Muir, J. Pudykiewicz, K. Reimer, J. Smith, G. Stern, W. Schroeder, R. Wagemarm, F. Wania and M. Yunker, 1997. Chapter 2. Sources, occurrence and pathways. pp 25-182. *In:* J. Jensen, K. Adare and R. Shearer (eds.). Canadian Arctic Contaminants Assessment Report. Indian and Northern Affairs Canada, Ottawa. 460p.
Baskaran, M. and A.S. Naidu, 1995. ^{210}Pb-derived chronology and the fluxes of ^{210}Pb and ^{137}Cs isotopes into continental shelf sediments, East Chukchi Sea, Alaskan Arctic. *Geochim. Cosmochim. Acta* **59**: 4435-4444.
Beltaos, S., D.J. Calkins, L.W. Gatto, T.D. Prowse, S. Reedyk, G.J. Scrimgeour and S.P. Wilkins, 1993. Physical effects of river ice. *In:* T.D. Prowse and N.C. Gridley (eds.). Environmental aspects of river ice, pp. 3-74. Ministry of Supply and Services, National Hydrology Research Institute, Saskatoon, Saskatchewan.
Bengtsson, L., 1994. Northern hydrology in Sweden. *In:* T.D. Prowse, C.S.L. Ommaney and L.E. Watson (eds.). Northern hydrology: International perspectives, pp. 109-127. Environment Canada, Saskatoon, Saskatchewan, NHRI Science Report No. 3.
Bengtsson, L., T. Hellström and L. Rakoczi, 1990. Redistribution of sediments in three Swedish lakes. *Hydrobiologia* **192**: 167-181.
Benkowitz, C.M., C.M. Berkowitz, R.C. Easter, S. Nemesure, R. Wagener and S.E. Schwartz, 1994. Sulfate over the North Atlantic and adjacent continental regions: Evaluation for October and November 1986 using a three-dimensional model driven by observation-derived meteorology. *J. Geophys. Res.* **99**: 20725-20756.
Benson, C.S., 1982. Reassessment of winter preciptiation on Alaska's Arctic Slope and measurments on the flux of windblown snow. University of Alaska, Geophysical Institute, Fairbanks, Alaska, Report No. 288, 26p.
Berner, H. and G. Wefer, 1990. Physiographic and biological factors controlling surface sediment distribution in the Fram Strait. *In:* U. Bleil and J. Thiede (eds.). Geological history of the polar oceans: Arctic versus Antarctic, pp. 317-335. Kluwer Academic Publishers, Dordrecht, The Netherlands.
Bidleman, T.F., 1988. Atmospheric processes. *Environ. Sci. Technol.* **22**(**4**): 361-367.
Bidleman, T.F. and L. McConnell, 1995. A review of field experiments to determine air-water gas exchange of persistent organic pollutants. *Sci. Total Environ.* **159**: 101-117.
Bleck, R. and D.B. Boudra, 1986. Wind-driven spin-up in eddy resolving ocean models formulated in isopycnic and isobaric coordinates. *J. Geophys. Res.* **91**: 7611-7621.
Bleck, R., C. Rooth, D. Hu and L.T. Smith, 1992. Salinity-driven thermocline transients in a wind-and thermohaline-forced isopycnic coordinate model of the North Atlantic. *J. Phys. Oceanogr.* **22**: 1486-1505.
Blindheim, J., 1989. Cascading of Barents Sea bottom water into the Norwegian Sea. *Rapp. P.-v Réun. Cons. int. Explor. Mer* **188**: 49-58.
Blindheim, J., 1990. Arctic intermediate water in the Norwegian Sea. *Deep-Sea Res.* **37**: 1475-1489.
Blindheim, J., 1993. Seasonal variations in the Atlantic inflow to the Nordic Seas. ICES C.M. 1993 C: 39. International Council for the Exploration of the Sea, Copenhagen.
Blindheim, J. and H. Loeng, 1981. On the variability of Atlantic influence in the Norwegian and Barents Seas. *Fiskeridir. Skr. Ser. Havunders.* **17**: 161-189.
Bloom, N. and S.W. Effler, 1990. Seasonal variations in the mercury speci-

ation of Onodoga Lake (New York). *Water Air Soil Pollut.* **53**: 251-265.
Blumberg, A.F. and G.L. Mellor, 1980. A coastal ocean numerical model. *In:* J. Sunderman and K.-P. Holz (eds.). Mathematical modelling of estuarine physics. Proc. Int. Symp., Hamburg, 1978, pp. 203-214. Springer-Verlag, Berlin.
Bönisch, G. and P. Schlosser, 1995. Deep water formation and exchange rates in the Greenland/Norwegian Seas and the Eurasian Basin of the Arctic Ocean derived from tracer balances. *Prog. Oceanogr.* **35**: 29-52.
Borys, R.D., E.E. Hamilton and P.J. DeMott, 1988. The chemical fractionation of atmospheric aerosol as a result of snow crystal fromation and growth. *J. Atmos. Chem.* **7**: 213-239.
Borys, R.D., D. Del Vecchio, J.-L. Jaffrezo, C.I. Davidson and D.L. Mitchell, 1993. Assessment of ice parcticle growth processes at Dye-3, Greenland. *Atmos. Environ.* **27A**: 2815-2822.
Bourke, R.H. and R.G. Paquette, 1991. Formation of Baffin Bay bottom and deep waters. *In:* P.C. Chu and J.C. Gascard (eds.). Deep convection and deep water formation in the ocean. Elsevier, Amsterdam.
Bourke, R.H., A.M. Weigel and R.G. Paquette, 1988. The westward turning branch of the West Spitsbergen Current. *J. Geophys. Res.* **93**: 14065-14077.
Boyle, E.A., J.M. Edmond and E.R. Sholkovitz, 1977. The mechanism of iron removal in estuaries. *Geochim. Cosmochim. Acta* **41**: 1313-1324.
Brimblecombe, P., M. Tranter, P.W. Abrahams, I. Blackwood, T.D. Davies and C.E. Vincent, 1985. Relocation and preferential elution of acidic solute through the snowpack of a small, remote, high-altitude Scottish catchment. *Ann. Glaciol.* **7**: 141-147.
Brimblecombe, P., S.L. Clegg, T.D. Davies, D. Shooter and M. Tranter, 1987. Observations of the preferential loss of major ions from melting snow and laboratory ice. *Water Resour. Res.* **21**: 1279-1286.
Broecker, W.S., T.-H. Peng and T. Takahashi, 1980. A strategy for the use of bomb-produced radiocarbon as a tracer for the transport of fossil fuel CO_2 into the deep sea source regions. *Earth Planet. Sci. Lett.* **49**: 463-468.
Bruland, K. W., P.K. Bienfang, J.K.B. Bishop, G. Eglinton, V.A.W. Ittekkot, R. Lampitt, M. Sarnthein, J. Thiede, J.J. Walsh and G. Wefer, 1989. Group report: Flux to the seafloor. *In:* W.H. Berger, V.S. Smetacek and G. Wefer (eds.). Productivity of the ocean: Present and past. Report of the Dahlem workshop on productivity of the ocean: Present and past, Berlin, April 24-29, 1988. pp. 193-215. Wiley, Chichester. 471p.
Brunskill, G.J., 1986. Environmental features of the Mackenzie System. *In:* B.R. Davies and K.F. Walker (eds.). The ecology of river systems, pp. 435-471. Dr. W. Junk, Dordrecht, The Netherlands.
Bryan, K., 1969. A numerical model for the study of circulation of the world oceans. *J. comput. Phys.* **4**: 347-376.
Bryan, F. and W.R. Holland, 1989. A high resolution simulation of the wind and thermohaline-driven circulation of the North Atlantic. Taha Hulikoua, Proc. of the Hawaiian Winter Workshop, pp. 99-116. University of Hawaii.
Buch, E., 1985. Seasonal and year to year variations of West Greenland waters in recent years. *Rapp. P.-v. Réun. Cons. int. Explor. Mer.* **185**: 141-151.
Buch, E., S.-A. Malmberg and S.S. Kristmannsson, 1996. Arctic Ocean deep water masses in the western Iceland Sea. *J. Geophys. Res.* **101**: 11965-11973.
Bullister, J.L. and R.F. Weiss, 1983. Anthropogenic chlorofluoromethanes in the Greenland and Norwegian Seas. *Science* **221**: 265-268.
Bursey, G.G., T.W.D. Edwards and S.K. Frape, 1991. Water balance and geochemistry studies in a tundra watershed, district of Keewatin, Northwest Territories. *In:* T.D. Prowse and C.S.L. Ommanney (eds.). Northern hydrology: Selected perspectives. Proceedings of the Northern Hydrology Symposium, 10-12 July 1990, Saskatoon, Saskatchewan, pp. 17-31. Environment Canada, Saskatoon, Saskatchewan, NHRI Symposium No. 6.
Buzov, A.Y., 1991. Natural factors and their influence on transit sailing on the Northern sea Route - Part I. The Northern Sea Route Project - Pilot Studies Report. The Fridtjof Nansen Institute, Oslo.
Cadle, S.H., J.M. Dasch and N.E. Grossnickle, 1984a. Northern Michigan snowpack - a study of acid stability and release. *Atmos. Environ.* **18**: 807-816.
Cadle, S.H., J.M. Dasch and N.E. Grossnickle, 1984b. Retention and release of chemical species by a northern Michigan snowpack. *Water Air Soil Pollut.* **22**: 303-319.
CAFF (Conservation of Arctic Flora and Fauna), 1994. The state of protected areas in the circumpolar Arctic 1994. Directorate for Nature Management, Trondheim, CAFF Habitat Conservation Report No. 1., 163p.
Calles, B., 1977. The river Elvegårdselv and its delta; a study of fluvial transport and topographical changes. University of Uppsala, Dept. of Physical geography, UNGI report 45.
Campbell, N.J., 1964. The origin of cold high-salinity water in Foxe Basin. *J. Fish. Res. Bd Can.* **21**: 45-55.
Cannon, G.A. and J.R. Holbrook, 1981. Wind induced seasonal interaction between coastal and fjord circulation. *In:* R. Sætre and M. Mork (eds.). Norwegian coastal current, pp. 131-151. University of Bergen.
Carey, A.G., 1987. Parcticle flux beneath fast ice in the shallow southwestern Beaufort Sea, Arctic Ocean. *Mar. Ecol. Prog. Ser.* **40**: 247-257.
Carey, A.G., 1995. Importance of site-specific factors in influencing contaminant distributions in ecosystems. *In:* (Anon. ed.) Abstract book. 2nd. SETAC World Congress (16th Annual Meeting), 5-9 November 1995, Vancouver, B.C., Canada.
Carlson, T.N., 1981. Speculations on the movement of polluted air to the Arctic. *Atmos. Environ.* **15**: 1473-1477.
Carmack, E.C., 1986. Circulation and mixing in ice-covered waters. *In:* N. Untersteiner (ed.). The geophysics of sea ice, pp. 641-712. Plenum, New York.
Carmack, E.C., 1990. Large scale physical oceanography of polar oceans. *In:* W.O. Smith (ed.). Polar oceanography, pp. 171-222. Academic Press, San Diego, California.
Carmack, E.C. and K. Aagaard, 1973. On the deep water of the Greenland Sea. *Deep-Sea Res.* **20**: 687-715.
Carmack, E.C., R.W. Macdonald and J.E. Papadakis, 1989. Water mass structure and boundaries in the Mackenzie shelf estuary. *J. Geophys. Res.* **94(C12)**: 18043-18055.
Carter C.W. and I.H. Suffet, 1982. Binding of DDT to dissolved humic materials. *Environ. Sci. Technol.* **16(11)**: 735-740.
Cassell, E.A. and T. Pangburn, 1991. Interactive modelling of cold regions watersheds. *In:* T.D. Prowse and C.S.L. Ommanney (eds.). Northern hydrology: Selected perspectives. Proceedings of the Northern Hydrology Symposium, July 10-12, 1990, pp. 363-377. Environment Canada, National Hydrology Research Institute, Saskatoon, Saskatchewan, Canada.
Cavalieri, D.J. and S. Martin, 1994. The contribution of Alaskan, Siberian and Canadian coastal polynyas to the cold halocline layer of the Arctic Ocean. *J. Geophys. Res.* **99**: 18343-18362.
CCN, 1986. PCBs in perspective. *Can. Chem. News* **38**: 15-17.
CCREM (Canadian Council of Resource and Environment Ministers), 1987. Canadian water quality guidelines, prepared for the Task Force on Water Quality Guidelines of the Canadian Council of Resource and Environment Ministers by Water Quality Objectives Division. Water Quality Branch, Inland Waters Directorate, Environment Canada, Ottawa, Ontario.
CGEIC (Canadian Global Emission Inventory Centre), 1996. Atmospheric Environment Service, Environment canada, Downsview, Ontario. Unpublished.
Chambers, P., G.J. Scrimgeour, A. Pietroniro, J.M. Culp and I. Loughran, 1994. Oxygen modelling under river ice covers. *In:* T.D. Prowse (ed.). Proceedings of the workshop on environmental aspects of river ice, August 18-20, 1993, pp. 235-260. National Hydrology Research Institute, Saskatoon, Saskatchewan, Canada.
Cheng, H., S. Leppinen and G. Whitley, 1993. Effects of river ice on chemical processes. *In:* T.D. Prowse and N.C. Gridley (eds.). Environmental aspects of river ice. National Hydrology Research Institute, Saskatoon, Canada, NHRI Science Report No. 5.
Chernyak, S.M., C.P. Rice and L.L. McConnell, 1996. Evidence of currently used pesticides in air, ice, fog, seawater and surface microlayer in the Bering and Chukchi Seas. *Mar. Pollut. Bull.* **32**: 410-419.
Christensen, J.H., 1995. Transport of air pollution in the troposphere to the Arctic. PhD thesis, National Environmental Research Institute, Roskilde, Denmark, 377p.
Church, M., 1974. Hydrology and permafrost with reference to northern North America. *In:* Proceedings Workshop Seminar on Permafrost Hydrology, pp. 7-20. Canadian National Committee for IHD, Ottawa.
CIP, 1995. Natural environment in Russia. A brief survey. *ECOS J.*: 1-119.
Claridge, F.B. and A.M. Miira, 1981. Erosion control along transportation routes in northern climates. *Arctic* **34(2)**: 147-157.
Clarke, R.A., 1984. Transport through the Cape Farewell-Flemish Cap section. *Rapp. P.-v. Réun. Cons. int. Explor. Mer* **185**: 120-130.
Clarke, R.A., 1986. The formation of Greenland Sea deep water. ICES C.M. 1986 C: 2. International Council for the Exploration of the Sea, Copenhagen.
Clarke, R.A. and J.-C. Gascard, 1983. The formation of Labrador Sea water, Part I: Large-scale processes. *J. Phys. Oceanogr.* **13**: 1764-1778.
Clarke, R.A., J.L. Reid Jr. and J.H. Swift, 1986. The Greenland Sea in winter. ICES C.M. 1986 C: 32. International Council for the Exploration of the Sea, Copenhagen.
Coachman, L.K., 1986. Circulation, water masses, and fluxes on the southeastern Bering Sea shelf. *Cont. Shelf Res.* **5**: 23-108.
Coachman, L.K., 1993. On the flow field in the Chirikov Basin. *Cont. Shelf Res.* **13**: 481-508.
Coachman, L.K. and K. Aagaard, 1974. Physical oceanography of Arctic and subarctic seas. *In:* Y. Herman (ed.). Marine geology and oceanography of the Arctic Seas, pp. 1-72. Springer-Verlag, New York.
Coachman, L.K. and K. Aagaard, 1988. Transports through Bering Strait: Annual and inter-annual variability. *J. Geophys. Res.* **93(C12)**: 15535-15539.
Coachman, L.K. and C.A. Barnes, 1961. The contribution of Bering Sea water to the Arctic Ocean. *Arctic* **14**: 147-161.
Coachman, L.K. and C.A. Barnes, 1963. The movement of Atlantic water in the Arctic Ocean. *Arctic* **16**: 9-16.
Coachman, L.K. and J.J. Walsh, 1981. A diffusion model of cross-shelf exchange of nutrients in the southeastern Bering Sea. *Deep-Sea Res.* **28A(8)**: 819-846.
Coachman, L.K., K. Aagaard and R.B. Tripp, 1975. Bering Strait: the regional physical oceanography. University of Washington Press, Seattle.
Cochran, J.K., D.J. Hirschberg, H.D. Linvingston, K.O. Buesseler and R.M. Key, 1995. Natural and anthropogenic radionuclide distributions in the Nansen Basin, Arctic Ocean: Scavenging rates and circulation timescales. *Deep-Sea Res. II* **42(6)**: 1495-1517.
Codispoti, L. and D. Lowman, 1973. A reactive silicate budget for the

Arctic Ocean. *Limnol. Oceanogr.* **18**: 448-456.
Codispoti, L.A. and T.G. Owens, 1975. Nutrient transports through Lancaster Sound in relation to the Arctic Ocean's reactive silicate budget and the outflow of Bering Strait waters. *Limnol. Oceanogr.* **20**: 115-119.
COGLA, 1989. Database listing of onshore wells, N.W.T. and Yukon. Canada oil and gas lands administration, Ottawa (Computer database).
Collett Jr., J.L., B. Oberholzer and J. Staehlin, 1993. Cloud chemistry at Mt. Rigi, Switzerland: dependence on drop size and relationship to precipitation chemistry. *Atmos. Environ.* **27A**: 33-42.
Collin, A.E. and M.J. Dunbar, 1964. Physical oceanography in Arctic Canada. *In:* H. Barnes (ed.). pp. 45-75. Ocean. Mar. Biol. Ann. Rev. 2, George Allen and Unwin, London.
Colony, R. and A.S. Thorndike, 1985. Sea ice motion as a drinkard's walk. *J. Geophys. Res.* **90**: 965-974.
Cooper, L.W., C.R. Olsen, D.K. Solomon, I.L. Larsen and R.B. Cook, 1991. Stable isotopes of oxygen and natural and fallout radionuclides used for tracing runoff during snowmelt in Arctic watershed. *Water Resour. Res.* **27(9)**: 2171-2179.
Cooper, L.W., C. Solis, D.L. Kane and L.D. Hinzman, 1993. Application of oxygen-18 tracer techniques to arctic hydrological processes. *Arct. alp. Res.* **25(3)**: 247-255.
Coquery, M., D. Cossa and J.M. Martin, 1995. The distribution of dissolved and particulate mercury in three Siberian estuaries and adjacent arctic coastal waters. *Water Air Soil Pollut.* **80(1/4)**: 653-664.
Cotham, W.E. and T.F. Bidleman, 1991. Estimating the atmospheric deposition of organochlorine contaminants to the arctic. *Chemosphere* **22(1-2)**: 165-188.
Cowardin, L.M., V. Carter, F.C. Golet and E.T. LaRoe, 1979. Classification of wetlands and deepwater habitats of the United States. US Department of the Interior, Fish and Wildlife Service, Washington D.C., 103p.
Cox, M.D., 1984. A primitive equation, 3-dimensional model of the ocean. Princeton University, GFDL, GFDL Ocean Group Tech. Rep. No.1, 141p.
D'Asaro, E.A., 1988. Observations of small eddies in the Beaufort Sea. *J. Geophys. Res.* **93**: 6669-6684.
Dahlgaard, H., A. Aarkrog, L. Hallstadius, E. Holm and J. Rioseco, 1986. Radiocaesium transport from the Irish Sea via the North Sea and the Norwegian Coastal Current to East Greenland. *Rapp. P.-v. Réun. Cons. int. Explor. Mer* **186**: 70-79.
Dai, M.-H. and J.-M. Martin, 1995. First data on trace metal level and behaviour in two major Arctic river-estuarine systems (Ob and Yenisey) and in the adjacent Kara Sea, Russia. *Earth Planet. Sci. Lett.* **131**: 127-141.
Dastoor, A.P. and J. Pudykiewicz, 1996. A numerical global meteorological sulphur transport model and its application to Arctic air pollution. *Atmos. Environ.* **30**: 1501-1522.
Davidson, C.I., 1989. Mechanisms of wet and dry deposition of atmospheric contaminants to snow surfaces. *In:* H. Oeschger and C.C. Langway (eds.). The environmental record in glaciers and ice sheets. Report of the Dahlem workshop on the environmental record in glaciers and ice sheets, Berlin, March 13-18, 1988. pp.29-51. Wiley, Chichester. 400p.
Davies, T.D., C.E. Vincent and P. Brimblecombe, 1982. Preferential elution of strong acids from a Norwegian ice cap. *Nature* **300**: 161-163.
Dean, K.G., W.J. Stringer, K. Ahlnäs, C. Searcy and T. Weingartner, 1994. The influence of river discharge on the thawing of sea ice, Mackenzie River Delta: albedo and temperature analyses. *Polar Res.* **12**: 93-94.
Diamond, M.L., H. Freitas and M. Kawai, 1996. Modelling inorganic and organic contaminants in arctic freshwater lakes. *In:* J.L. Murray, R.G. Shearer and S.L. Han (eds.) Synopsis of research conducted under the 1994/95 Northern Contaminants Program, pp. 119-130. Department of Indian and Northern Affairs, Ottawa, Canada, Environmental Studies No. 73.
Dickson, R.R. and J. Brown, 1994. The production of North Atlantic deep water: Sources, rates, and pathways. *J. Geophys. Res.* **99**: 12319-12341.
Dickson, R.R., J. Meinke, S.A. Malmberg and A.J. Lee, 1988. The "great salinity anomaly" in the northern North Atlantic. *Prog. Oceanogr.* **20**: 103-151.
Doskey, P.V. and A.W. Andren, 1981. Modeling the flux of atmospheric polychlorinated biphenyls across the air/water interface. *Environ. Sci. Technol.* **15**: 705-711.
Douglas, B.C., 1991. Global sea level rise. *J. Geophys. Res.* **96**: 6891-6992.
Drinkwater, K.F., 1986. Physical oceanography of Hudson strait and Ungava Bay. *In:* I.P. Martini (ed.). Canadian inland seas, pp. 237-264. Elsevier Oceanography Series 44, Elsevier, New York.
Driscoll, C.T., C.L. Schofield, R. Munson and J. Holsapple, 1994. The mercury cycle and fish in Adirondack lakes. *Environ. Sci. Technol.* **28(3)**: 136-143.
Duce, R.A., V.A. Mohnen, P.R. Zimmerman, D. Grosjean, W. Cautreels, R. Chatfield, R. Jaenicke, J.A. Ogren, E.D. Pellizzare and G.T. Wallace, 1983. Organic material in the global troposhere. *Rev. Geophys. Space Res.* **21**: 921-952.
Duxbury, A.C. and A.B. Duxbury, 1994. An introduction to the world's oceans. Wm.C. Brown Publisher, Dubuque, Iowa, 472p.
Dynesius, M. and C. Nilsson, 1994. Fragmentation and flow regulation of river systems in the northern third of the world. *Science* **266**: 753-762.
ECMP, 1995. Information prepared by the Environmental Committee of Murmansk province for the AMAP expert group. *In:* Proposals for environmentally sound investment projects in the Russian part of the Barents region, Volume 1: Non-radioactive contamination. The Nordic Environment Finance Corporation (NEFCO), Barents Region Environmental Programme, Phase I report. AMAP, Oslo. 147p.
Eisma, D., 1993. Suspended matter in the aquatic environment. Springer-Verlag, Berlin-Heidelberg, 315p.
Eitzer, B.D. and R.A. Hites, 1989. Atmospheric transport and deposition of polychlorinated dibenzo-r-dioxins and dibenzofurans. *Environ. Sci. Technol.* **23**: 1396-1401.
Elíasson, J., 1994. Northern hydrology in Iceland. *In:* T.D. Prowse, C.S.L. Ommaney and L.E. Watson (eds.). Northern hydrology: International perspectives, pp. 41-80. Environment Canada, Saskatoon, Saskatchewan, NHRI Science Report No. 3.
Ellis, K.M., J.N. Smith, R.P. Nelson, L. Kilius, R. Macdonald, E. Carmack and S.B. Moran, 1995. Distribution of artificial radionuclides in the Arctic Oceans from the 1994 Arctic Ocean Section. *In:* P. Strand and A. Cooke (eds.). Environmental Radioactivity in the Arctic. Proceedings of the second International Conference on Environmental Radioactivity in the Arctic, Oslo, August 21-25, 1995, pp. 204-207. Norwegian Radiation Protection Authority, Østerås, Norway. 416p.
Elverhøi, A., S.L. Pfirman, A. Solheim and B.B. Larssen, 1989. Glaciomarine sedimentation on epicontinental seas – exemplified by the northern Barents Sea. *Mar. Geol.* **85**: 225-250.
Encyclopedia Britannica, 1990. The New Encyclopedia Britannica, 15th ed., vol. 14, pp. 288-292. Encyclopedia Britannica Inc., Chicago.
English, M.C., M.A. Stone, B. Hill, P.M. Wolfe and R. Ormson, 1996. Assessment of impacts on the Slave River Delta of Peace River impoundment at Hudson Hope. Northern River Basins Study, Edmonton, Alberta, Project Report No. 74, p. 91.
ENVIRODAT, 1996. Water Quality data Base. Environment Canada, Ottawa, Canada.
Evans, S.M., 1996. Biomagnification of persistent organic contaminants in Great Slave Lake. *In:* J.L. Murray, R.G. Shearer and S.L. Han (eds.). Synopsis of research conducted under the 1994/95 Northern Contaminants Program, pp. 215-220. Indian Affairs and Northern Development, Ottawa, Canada, Environmental Studies No. 73.
Favorite, F., 1967. The Alaskan Stream. *Int. N. Pac. Fish. Com. Bull.* **21**: 20.
Feichter, J., E. Kjellstrom, H. Rodhe, F. Dententer, J. Lelieveld and G.-J. Roelfs, 1996. Simulation of the tropospheric sulfur cycle in a global climate model. *Atmos. Environ.* **30**: 1693-1707.
Fellin, P., L.A. Barrie, D. Dougherty, D. Toom, D. Muir, N. Grift, L. Lockhart and B. Billeck, 1996. Air monitoring in the Arctic; results for selected persistent organic pollutants for 1992. *Environ. Toxicol. Chem.* **15**: 253-261.
Finkel, R., S. Krishnaswamit and D.L. Clark, 1977. Be-10 in Arctic Ocean sediments. *Earth Planet. Sci. Lett.* **35**: 199-204.
Fischer, G., D. Fütterer, R. Gersonde, S. Honjo, D. Ostermann and G. Wefer, 1988. Seasonal variability of parcticle flux in the Weddell Sea and its relation to ice cover. *Nature* **335**: 426-428.
Fissel, D.B., J.R. Birch, H. Melling and R.A. Lake, 1988. Non-tidal flows in the Northwest Passage. Canadian Institute of Ocean Science, Sidney, British Columbia, Canada, Tech. Rep. Hydrogr. Ocean Sci. 98, 157p.
Fleming, G.H. and A.J. Semtner, 1991. A numerical study of interannual ocean forcing on Arctic ice. *J. Geophys. Res.* **96**: 4589-4603.
Foldvik, A., K. Aagaard and T. Torresen, 1988. On the velocity field of the east Greenland Current. *Deep-Sea Res.* **35**: 1335-1354.
Franz, T.P., D.J. Gregor and S.J. Eisenreich, (in press). Snow deposition of atmospheric semivolatile organic chemicals. *In:* J.E. Baker (ed.). Atmospheric deposition of contaminants to the Great Lakes and coastal waters. Society for Environmental Toxicology and Chemistry (SETAC).
Freitas, H., M. Diamond, R. Semkin and D. Gregor, 1997. Contaminant fate in High Arctic lakes: Development and application of a mass balanced model. *Sci. Total Environ.* (submitted)
French, H.M., 1978. Sump studies I. Indian and Northern Affairs Canada, Ottawa, Environmental Studies No. 6, 52p.
Friedman, G.M. and J.E. Sanders, 1978. Principles of sedimentology. John Wiley and Sons Inc., New York, 792p.
Futsaeter, G., G. Eidnes, G. Halmo, S. Johansen, H.P. Mannvik, L.K. Sydnes and U. Witte, 1991. Report on oil pollution. The State of the Arctic Environment Reports, University of Lapland, Arctic Centre, Rovaniemi, pp. 270-334.
Garland, T.R., R.G. Riley, E. Snyder-Conn and D.F. Woodward, 1988. Drilling fluids and the Arctic tundra of Alaska: Assessing contamination of wetlands habitat and the toxicity to aquatic invertebrates and fish. *Arch. Environ. Contam. Toxaphene* **17(5)**: 638-697.
Garrison, G.R. and P. Becker, 1976. The Barrow submarine canyon: a drain for the Chukchi Sea. *J. Geophys. Res.* **81**: 4445-4453.
Garrison, D.L., S.A. Ackley, K.R. Buck, 1983. A physical mechanism for establishing algal populations in frazil ice. *Nature* **306**: 363-365.
Gascard, J.C. and R.A. Clarke, 1983. The formation of Labrador sea water. Part II: Mesoscale and smaller scale processes. *J. Phys. Oceanogr.* **13**: 1779-1797.
Gaul, H., 1989. Organochlorine compounds in water and sea ice of the European Arctic Sea. *In:* R. Shearer and A. Bartonova (eds.). Global significance of the transport and accumulation of polychlorinated hydrocarbons in the Arctic, The 8th international conference of Comité Arctique International, Oslo, 18-22 September 1989.
Genthon, C. and A. Armengaud, 1995. GCM simulations of atmospheric

tracers in the polar latitudes: South Pole (Antarctica) and Summit (Greenland) cases. *Sci. Total Environ.* **160/161**: 101-116.
Gerdes, R., C. Koberle and J. Willebrand, 1991. The influence of numerical advection schemes on the results of ocean general circulation models. *Climate Dynamics* **5**: 211-226.
GESAMP, 1985. Interchange of pollutants between the atmosphere and the ocean. IMO/FAO/UNESCO/WMO/WHO/IAEA/UN/UNEP. GESAMP Reports and Studies No. 23, 55p.
GESAMP, 1993. Anthopogenic influences on sediment discharge to the coastal zone and environmental consequences. IMO/FAO/UNESCO. GESAMP Reports and Studies No. 52, 66p.
Giorgi, F., 1986. A particle dry-deposition parameterization scheme for use in tracer transport models. *J. Geophys. Res.* **91**(**D9**): 9794-9806.
Giovando, L.F. and R.H. Herlinveaux, 1982/1 (1982 or 1981?). A discussion of factors influencing the dispersion of pollutants in the Beaufort Sea. *Pacif. mar. Sci. Rep.* **81**(**4**): 198.
Gloersen, P., 1995. Modulation of hemispheric sea-ice cover by ENSO events. *Nature* **373**: 503-506.
Gloersen, P., W.J. Campbell, D.J. Cavalieri, J.C. Comisco, C.L. Parkinsona and H.J. Zwally, 1992. Arctic and Antarctic-1987, Satellite passive-microwave observations and analysis. NASA SP-511, 290p.
Goldberg, E.D., 1975. Synthetic organohalides in the sea. *Proc. R. Soc. Lond.* Ser.B **189**: 277-289.
Goldberg, E.D., 1976. The health of the oceans. Unesco, Paris, 172p.
Goldschmidt, P.M., S.L. Pfirman, I. Wollenburg and R. Henrich, 1992. Origin of sediment pellets on the Arctic sea floor: sea ice or icebergs? *Deep-Sea Res.* Special Issue **39**: S539-S565.
Gordeev, V.V. and I.S. Sidorov, 1993. Concentrations of major elements and their outflow into the Laptev Sea by the Lena River. *Mar. Chem.* **43**(**1-4**): 33-46.
Gordeev, V.V., J.-M. Martin, I.S. Sidorova and M.V. Sidorova, 1995. A reassessment of the Eurasian river input of water, sediment, major elements and nutrients to the Arctic Ocean. *Am. J. Sci.* (accepted)
Gosselink, J.G. and R.E. Turner, 1978. The role of hydrology in freshwater wetland ecosystems. *In:* R.E. Hook, D.F. Whigham and R.L. Simpson (eds.). Freshwater wetlands. Ecological processes and management potential. New York, 378p.
Gould, W.J., J. Loynes and J. Backhaus, 1985. Seasonality in slope current transports N.W. of Shetland. ICES C.M. 1985 C: 7. International Council for the Exploration of the Sea, Copenhagen.
Gow, A.J. and W.B. Tucker III, 1990. Sea ice in the polar regions. *In:* W.O. Smith Jr. (ed.). Polar oceanography. Part A, Physical science. Academic Press Inc., San Diego, California.
Graedel, T.E. and J.P. Franey, 1975. Field measurements of submicron aerosol washout by snow. *Geophys. Res. Lett.* **2**: 325-328.
Graf Pannatier, E. and D.J. Gregor, 1996. Mackenzie delta overbank and lake sedimentation and contaminant accumulation study. IWD-NWT NOGAP Progress Report #3, May 1996, 41p. (Unpublished report).
Gray, C.B., 1994. Lake Laberge. *In:* R.J. Allan, M. Dickman, C.B. Gray and V. Cromie (eds.). The book of Canadian lakes, pp. 474-484. The Canadian Association on Water Quality, Gloucester, Ontario, Canada. Monograph Series #33.
Gray, C.B., M. Dickman, B. Krushelnicki and V. Cromie, 1992. A survey of Canadian lakes. National Water Research Institute, Environment Canada, Burlington, Ontario, Canada. NWRI Contribution #91-18 (unpublished).
Gray, D.M., D.I. Norum and J.M. Wigham, 1973. Infiltration and physics of flow of water through porous media. *In:* D.M. Gray (ed.). Handbook on the principles of hydrology, pp. 5.1-5.41. Water Information Center Inc., New York.
Gregor, D.J., 1990. Deposition and accumulation of selected agricultural pesticides in Canadian Arctic snow., *In:* D.A. Kurtz (ed.). Long range transport of pesticides, pp. 373-386. Lewis Publishers, Chelsea, Michigan.
Gregor, D.J., 1991. Organic micropollutants in arctic snow and firn. *In:* M.-K. Woo and D.J. Gregor (eds.). Arctic environment: Past, present and future, p. 164. Proceedings of a symposium held at McMaster University, Nov. 14-15, 1991. McMaster University, Department of Geography, Hamilton, Ontario.
Gregor, D.J., 1996. Snow, ice and temperature as determinants of organic chemical fate in northern ecosystems. *In:* J.L. Murray and R.G. Shearer (eds.) Synopsis of research conducted under the 1994/95 Northern Contaminants Program, pp. 57-59. Ottawa, Canada, Environmental Studies No. 73.
Gregor, D. and J. Eamer, 1993. Base flow water quality and contaminant levels in the upper Yukon River system. *In:* J.L Murray and R.G. Shearer (eds.). Synopsis of research conducted under the 1992/93 Northern Contaminants Program, pp. 69-77. Department of Indian and Northern Affairs, Ottawa, Canada, Environmental Studies No. 70.
Gregor, D.J. and W. Gummer, 1989. Evidence of atmospheric transport and deposition of organochlorine pesticides and PCB in Canadian Arctic snow. *Environ Sci. Technol.* **23**(**5**): 561-565.
Grigoriev, V.Y. and B.L. Sokolov, 1994. Northern hydrology in the Former Soviet Union (FSU). *In:* T.D. Prowse, C.S.L Ommaney and L.E. Watson (eds.). Northern hydrology: International perspective, pp. 147-179. Environment Canada, Saskatoon, Saskatchewan, Science report No.3.
Groen, P., 1969. The waters of the sea. Van Norstrand, New York.
Gross, G.W., C.-H. Wu, L. Bryant and C. McKee, 1975. Concentration dependent solute redistribution at the ice/water phase boundary. II. Experimental investigation. *J. Chem. Phys.* **62**: 3085-3092.
Gubala, C.P., D.H. Landers, M. Monetti, M. Heit, T. Wade, B. Lasorsa and S. Allen-Gil, 1995. The rates of accumulation and chronologies of atmospherically derived pollutants in Arctic Alaska, USA. *Sci. Total Environ.* **160/161**: 347-361.
Haas, J., 1991. Estimates of evaporation in the Yukon and Northwest Territories. *In:* T.D. Prowse and C.S.L. Ommanney (eds.). Northern hydrology: Selected perspectives, pp. 189-203. Proceedings of the Northern Hydrology Symposium, 10-12 July, 1990, Saskatoon, Saskatchewan. Environment Canada, Saskatoon, Saskatchewan, NHRI Symposium No.6.
Hachey, H.B., 1935. The circulation of Hudson Bay water as indicated by drift bottles. *Science* **82**: 275-276.
Haidvogel, D.B., J.L. Wilkin and R.E. Young, 1991. A semi-spectral primitive equation ocean circulation model using vertical sigma and orthogonal curvilinear horizontal coordinates. *J. comput. Phys.* **94**: 151-185.
Håkanson, L., 1994. A model to predict gross sedimentation in small glacial lakes. *Hydrobiologia* **284**: 19-42.
Håkanson, L. and M. Jansson, 1983. Principles of lake sedimentology. Springer-Verlag, Berlin and Heidelberg, Germany. 316p.
Häkkinen, S. and G.L. Mellor, 1990. One hundred years of Arctic ice cover variations as simulated by a one dimensional coupled ice-ocean model. *J. Geophys. Res.* **95**: 15959-15969.
Häkkinen, S. and G.L. Mellor, 1992. Modeling the seasonal variability of the coupled Arctic ice-ocean system. *J. Geophys. Res.* **97**: 20285-20304.
Hansen, A.D.A. and H. Rosen, 1984. Vertical distribution of particulate carbon, sulfur and bromine in the Arctic haze and comparison with ground-level measurements at Barrow, Alaska. *Geophys. Res. Lett.* **11**: 381-384.
Hanson, A.M., 1965. Studies of the mass budget of Arctic pack-ice floes. *J. Glaciol.* **5**: 701-709.
Hanzlick, D. and K. Aagaard, 1980. Freshwater and Atlantic water in the Kara Sea. *J. Geophys. Res.* **85**: 4937-4942.
Hardisty, P., V. Schilder, T. Dabrowski and J. Wells, 1991. Yukon and Northwest Territories ground-water data base. *In:* T.D. Prowse and C.S.L. Ommanney (eds.). Northern hydrology : Selected perspectives, pp. 465-482. Proceedings of the Northern Hydrology Symposium, 10-12 July, 1990, Saskatoon, Saskatchewan. Environment Canada, Saskatoon, Saskatchewan, NHRI Symposium No. 6.
Hargrave, B.T., W.P. Vass, P.E. Erickson and B.R. Fowler, 1988. Atmospheric transport of organochlorines to the Arctic Ocean. *Tellus* **40B**: 480-493.
Hargrave, B.T., B. von Bodungen, R.J. Conover, A.J. Fraser, G. Phillips and W.P. Vass, 1989. Seasonal changes in sedimentation of particulate matter and lipid content of zooplankton collected by sediment trap in the Arctic Ocean off Axel Heiberg Island. *Polar Biol.* **9**: 467-475.
Hargrave, B.T., B. von Bodungen, P. Stoffyn-Egli and P.J. Mudie, 1994. Seasonal variability in particle sedimentation under permanent ice cover in the Arctic Ocean. *Cont. Shelf Res.* **14**: 279-293.
Harms, I.H., 1997. Modeling the dispersion of ^{137}Cs and ^{239}Pu released from dumped waste in the Kara Sea. *J. Mar. Sys.* **13**(1997): 1-13.
Harper, J.R., 1990. Morphology of the Canadian Beaufort Sea coast. *Mar. Geol.* **91**: 75-91.
Hart, K.M., J. Tremp, E. Molnar and W. Giger, 1993. The occurrence and the fate of organic pollutants in the atmosphere. *Water Air Soil Pollut.* **68**: 91-112.
Hebbeln, D. and G. Wefer, 1991. Effects of ice coverage and ice-rafted material on sedimentation in the Fram Strait. *Nature* **350**(**4**): 409-411.
Hecky, R.E., R.W. Newbury, R.A. Bodaly, K. Patalas and D.M. Rosenberg, 1984. Environmental impact prediction and assessment: the southern Indian Lake experience. *Can. J. Fish. aquat. Sci.* **41**: 720-732.
Hedstrom, K.S., 1990. User manual for a semi-spectral primitive equation regional ocean circulation model. Version 3.0. Institute for Naval Oceanography, Technical Note FY 90-2, 90p.
Hequette, A., M.-H. Ruz and P.R. Hill, 1995. The effects of the Holocene sea level rise on the evolution of the southeastern coast of the Canadian Beaufort Sea. *J. coast. Res.* **11**(**2**): 494-507.
Hibler III, W.D., 1979. A dynamic sea ice model. *J. Phys. Oceanogr.* **9**: 815-846.
Hibler III, W.D. and K. Bryan, 1987. A diagnostic ice-ocean model. *J. Phys. Oceanogr.* **17**: 987-1015.
Hill, P.R. and O.C. Nadeau, 1989. Storm-dominated sedimentation on the inner shelf of the Canadian Beaufort Sea. *J. Sedimentary Petrology* **59**: 455-468.
Hobbie, J.E., 1973. Arctic limnology: a review. *In:* M.E. Button (ed.). Alaskan Arctic tundra. Arctic Institute of North America, Washington D.C., Technical Paper No. 25.
Hoekstra, P. and R.D. Miller, 1967. On the mobility of water molecules in the transition layer between ice and a solid surface. *J. Colloid Interface Sci.* **25**: 155-173.
Hoff, J.T., F. Wania, D. Mackay and R. Gilham, 1995. Sorption of nonpolar organic vapours by ice and snow. *Environ. Sci. Technol.* **27**: 2174-2180.
Holland, D.M., L.A. Mysak, D.K. Manak and J.M. Oberhuber, 1993. Sensitivity study of a dynamic thermodynamic sea ice model. *J. Geophys. Res.* **98**: 2561-2586.
Holland, D.M., L.A. Mysak and J.M. Oberhuber, 1995. An investigation of the general circulation of the Arctic Ocean using an isopycnal ocean

model. *Tellus* **48A**: 138-157.
Holloway, G., 1992. Representing topographic stress for large scale ocean models. *J. Phys. Oceanogr.* **22**: 1033-1046.
Holtan, G., D. Berge, H. Holtan and T. Hopen, 1994. Annual report on direct and riverine inputs to Norwegian coastal waters during the year 1993 – Paris Convention. SFT (Norwegian State Pollution Control Authority), Oslo. SFT Report 580194 (NIVA-report 090001), 138p..
Holtan, H. and S.O. Åstebøl, 1991. Handbook for collection of data on pollutant inputs to fjords and water courses. Revised edition – November 1991. SFT (Norwegian State Pollution Control Authority), Oslo. SFT Report No. 91:10. (In Norwegian).
Honjo, S., 1990. Particle fluxes and modern sedimentation in the Polar Oceans. *In*: W.O. Smith (ed.). Polar oceanography, Part B: Chemistry, biology and geology, pp. 687-739. Academic Press, San Diego, California.
Honjo, S., S.J. Manganini and G. Wefer, 1988. Annual parcticle flux and a winter outburst of sedimentation in the northern Norwegian Sea. *Deep-Sea Res.* **35**(**8**): 1223-1234.
Hood, D.W. and E.J. Kelley, 1974. Summary of early exploration and oceanographic features. *In:* D.W. Hood and E.J. Kelley (eds.). Oceanography of the Bering Sea with emphasis on renewable resources, pp. xv-xxi. University of Alaska, Institute of Marine Science, Fairbanks, Alaska.
Hope, D., M.F. Billett and M.S. Cresser, 1994. A review of the export of carbon in river water: Fluxes and processes. *Environ. Pollut.* **84**: 301-324.
Hopkins, T.S., 1991. The GIN Sea – A synthesis of its physical oceanography and literature review 1972-1985. *Earth-Sci. Rev.* **30**: 175-318.
Hsiao, S.I.C., 1987. Sedimentation in Arctic Canada: species composition and biomass of phytoplankton contributed to the marine sediments of Frobisher Bay. *Polar Biol.* 7: 245-251.
Hunter, J.G., 1960. Hazen Lake. Fish. Res. Board Canada, Arctic Unit Annual Report and Investigators Summaries, April 1, 1959 to March 31, 1960.
HYDAT, 1994. Hydrology Data Base, version 4.94. Environment canada, Ottawa, Canada.
Ibrahim, M., L.A. Barrie and F. Fanaki, 1983. An experimental and theoretical investigation of the dry deposition of particles to snow, pine trees and artificial collectors. *Atmos. Environ.* **17**: 781-788.
Igamberdiev, V.M., V.N. Lystsov and V.M. Makeev, 1995. Identification and assessment of land-based activities in Russian Federation that contribute to the degradation of the Arctic marine environment. Report prepared by Arctic workshop of ACOPS (Advisory Committee on Protection of the Sea), Moscow. (In Russian). 192p.
Ingram, R.G., 1981. Characteristics of the Great Whale River plume. *J. Geophys. Res.* **86**: 2017-2023.
Ingram, R.G. and P. Larouche, 1987. Variability of an under-ice river plume in Hudson Bay. *J. Geophys. Res.* **92**: 9541-9547.
IPCC, 1996. Climate change 1995. The science of climate change. Cambridge University Press, Cambridge, 572p.
Iribarne, J.V. and L.A. Barrie, 1995. The oxidation of S(IV) during riming by cloud droplets. *J. Atmos. Chem.* **21**: 97-114.
Iribarne, J.V. and T. Pyshnove, 1990. The effect of freezing on the composition of supercooled droplets - I. Retention of HCl, HNO_3, NH_3, and H_2O_2. *Atmos. Environ.* **24A**: 383-387.
Iribarne, J.V., L.A. Barrie and A. Iribarne, 1983. Effect of freezing on sulphur dioxide dissolved in supercooled droplets. *Atmos. Environ.* **17**: 1047-1050.
Iselin, C.O., 1927. A study of the northern part of the Labrador Current. *Bull. Nat. Res. Council* **61**: 217-222.
Iversen, T., 1984. On the atmospheric transport of pollution to the Arctic. *Geophys. Res. Lett.* **11**: 457-460.
Iversen, T., 1989a. Some statistical properties of ground level air pollution at Norwegian Arctic stations and their relation to large scale atmospheric flow systems. *Atmos. Environ.* **23**: 2451-2462.
Iversen, T., 1989b. Numerical modelling of the long range atmospheric transport of sulphur dioxide and particulate sulphate to the Arctic. *Atmos. Environ.* **23**: 2571-2595.
Iversen, T., 1996. Atmospheric transport pathways for the Arctic. *In:* E. Wolff and R.C. Bales (eds.). Chemical exchange between the atmosphere and polar snow. Global Environmental Change. NATO ASI Series I, Volume 43, pp. 71-92. Springer-Verlag, Berlin and Heidelberg, Germany.
Jaffrezo, J.L., M.P. Clain and P. Masclet, 1994. Polycyclic aromatic hydrocarbons in the polar ice of Greenland. Geochemical use of these atmospheric tracers. *Atmos. Environ.* **28**: 1139-1145.
Jantunen, L.M. and T.F. Bidleman, 1995. Reversal of the air-water gas exchange direction of hexachlorocyclohexanes in the Bering and Chukchi Seas: 1993 versus 1988. *Environ. Sci. Technol.* **29**: 1081-1089.
Jaworowski, Z., 1989. Pollution of the Norwegian Arctic: A review. Norsk Polarinsitutt Rapportserie **55**. Norwegian Polar Institute, Oslo, Norway. 93p.
Jeffries, M.O., 1987a. The growth, structure and disintegration of Arctic ice shelves. *Polar Record* **23**: 631-649.
Jeffries, M.O., 1987b. Stucture and growth of Arctc ice shelves and ice islands. NRC of Canada Associate Committee on Geotechnical Research, Ottawa, Technical Memorandum 41, pp. 39-48.
Jeffries, M.O. and M.A. Shaw, 1993. The drift of ice islands from the Arctic Ocean into the channels of the Canadian Arctic archipelago: the history of Hobson's Choice Ice Island. *Polar Record* **29**(**171**): 305-312.
Jeffries, M.O., H.R. Krouse, W.M. Sackinger and H.V. Serson, 1989. Stable-isotope ($^{18}O/^{16}O$) tracing of fresh, brackish, and sea ice in multi-year land-fast sea ice, Ellesmere Island, Canada. *J. Glaciol.* **35**: 9-16.
Johannesson, M. and A. Hendrien, 1978. Chemistry of snow meltwater: changes in concentration during melting. *Water Resour. Res.* **14**(**4**): 815-619.
Johansen, B.E. and H. Tømmervik, 1992. Finnmarksvidda, mapping of vegetation. NORUT Information Technology, Tromsø, Norway. NORUT Information Technology report 2020. (In Norwegian).
Johnson, L., 1975a. Physical and chemical characteristics of Great Bear Lake, Northwest Territories. *J. Fish. Res. Bd Can.* **32**(**11**): 1971-1987.
Johnson, L., 1975b. The Great Bear Lake: its place in history. *Arctic* **28**(**4**): 230-243.
Johnson, L., 1994a. Great Bear Lake. *In:* R.J. Allan, M. Dickman, C.B. Gray and V. Cromie (eds.). The book of Canadian lakes, pp. 549-559. The Canadian Association on Water Quality, Gloucester, Ontario, Canada. Monograph Series #33.
Jones, E.P. and L.G. Anderson, 1986. On the origin of the chemical properties of the Arctic Ocean halocline. *J. Geophys. Res.* **91**: 10759-10767.
Jones, E.P. and A.R. Coote, 1980. Nutrient distribution in the Canadian archipelago: indicators of summer water mass and flow characteristics. *Can. J. Fish. aquat. Sci.* **37**: 589-599.
Jónsson, S. and A. Foldvik, 1992. The transport and circulation in Fram Strait. ICES C.M. 1992. C: 10. International Council for the Exploration of the Sea, Copenhagen.
Jopling, A.V., 1960. An experimental study on the mechanics of bedding. PhD dissertation, Harvard University, Cambridge, Massachusetts.
Joussaume, S., 1990. Three-dimensional simulations of the atmospheric cycle of desert dust particles using a General Circulation Model. *J. Geophys. Res.* **95**: 1909-1941.
Joussaume, S., 1993. Paleoclimatic tracers: An investigation using an atmospheric general circulation model under ice age conditions 1. Desert dust. *J. Geophys. Res.* **98**: 2767-2805.
Jury, W.A., W.F. Spencer and W.J. Farmer, 1983. Behavior assessment model for trace organics in soil. I. Model description. *J. Environ. Qual.* **12**: 558-566.
Jury, W.A., W.F. Spencer and W.J. Farmer, 1984a. Behavior assessment model for trace organics in soil. II. Chemical classification and parameter sensitivity. *J. Environ. Qual.* **13**: 567-572.
Jury, W.A., W.F. Spencer and W.J. Farmer, 1984a. Behavior assessment model for trace organics in soil. IV. Review of experimental evidence. *J. Environ. Qual.* **13**: 580-586.
Jury, W.A., W.F. Spencer and W.J. Farmer, 1984c. Behaviour assessment model for trace organics in soil: III. Applications of screening model. *J. Environ. Qual.* **13**: 573-579.
Kane, D.L., 1994. Northern hydrology in Alaska. *In:* T.D. Prowse, C.S.L. Ommaney and L.E. Watson (eds.). Northern hydrology: International perspectives, pp. 5-20. Environment Canada, Saskatoon, Saskatchewan, NHRI Science Report No.3.
Kane, D.L., R.E. Gieck and L.D. Hinzman, 1990. Evaporation from a small Alaskan arctic watershed. *Nordic Hydrology* **12l**(**4/5**): 253-272.
Kane, D.L., L.D. Hinzman, C.S. Benson and G.E. Liston, 1991. Snow hydrology of a headwater Arctic Basin: I. Physical measurements and process studies. *Water Resour. Res.* **27**(**6**): 1099-1109.
Kane, D.L., R.E. Gieck, G. Wendler and L.D. Hinzman, 1993. Snowmelt at a small Alaskan watershed, 2. Energy related modeling results. *In:* T.D. Prowse, C.S.L. Ommaney and K.E. Ulmer (eds.). Proceedings of the Ninth International Northern Research Basins Symposium/Workshop, pp. 227-248, August 14-22, 1992. Whitehorse, Dawson city, Eagle Plains, Yukon and Inuvik, Northwest Territories. National Hydrology Research Institute, Environment Canada, Saskatoon, Saskatchewan, Canada.
Kautsky, H., 1987. Investigation on the Distribution of ^{137}Cs, ^{134}Cs and ^{90}Sr and the water mass transport times in the Northern North Atlantic and the North Sea. *Dt. Hydrogr. Z.* **40**: 49-69.
Kempema, E.W., E. Reimnitz and P.W. Barnes, 1989. Sea ice sediment entrainment and rafting in the Arctic. *J. Sed. Petrol.* **59**: 308-317.
Kidd, K.A., D.W. Schindler, D.C.G. Muir and R.H. Hesslein, 1996. The biomagnification of organochlorines through the food web of Lake Laberge and other Yukon Lakes. *In:* J.L. Murray, R.G. Shearer and S.L. Han (eds.). Synopsis of research conducted under the 1994/95 Northern Contaminants Program, pp. 209-214. Indian Affairs and Northern Development, Ottawa, Canada, Environmental Studies no. 73.
Killingtveit, Å., 1994. Northern hydrology in Norway. *In:* T.D. Prowse, C.S.L. Ommaney and L.E. Watson (eds.). Northern hydrology: International perspectives, pp. 81-107. Environment Canada, Saskatoon, Saskatchewan, NHRI Science Report No.3.
Killingtveit, Å. and A. Harby, 1994. Multi purpose planning with the "River System Simulator" – A decision support system for water resource planning and operation. Presented at Environmental modelling seminar, Trondheim 17-19 August 1994.
Killingtveit, Å. and K. Sand, 1991. On aerial distribution of snowcover in a mountainous area. *In:* T.D. Prowse and C.S.L. Ornmanney (eds.). Northern hydrology: Selected perspectives, pp. 189-203. Proceedings of the Northern Hydrology Symposium, 10-l2 July, 1990, Saskatoon, Saskatachewan. Environment Canada, Saskatoon, Saskatchewan, NHRI Symposium No. 6.
Killworth, P.D., 1979. On chimney formations in the oceans. *J. Phys.*

Oceanogr. **9**: 531-554.
Killworth, P.D., 1983. Deep convection in the world ocean. *Rev. Geophys. Space Phys.* **21**: 1-26.
Kinder, T.H. and J.H. Schumacher, 1981. Hydrographic structure over the continental shelf of the southeastern Bering Sea. *In:* D.W. Hood and J.A. Calder (eds.). The Eastern Bering Sea shelf: Oceanography and resources, pp. 31-52. Office of Marine Pollution Assessment, National Oceanic and Atmospheric Administration. University of Washington Press, Seattle.
Kinder, T.H., D.C. Chapman and J.A. Whitehead Jr., 1986. Westward intensification of the mean circulation on the Bering Sea shelf. *J. Phys. Oceanogr.* **16**: 1217-1229.
Kirkland, R.A. and C.B.J. Gray, 1986. Reconnaissance of the chemical and biological limnology in four large lakes of the Yukon River basin. Environment Canada, National Hydrology Research Institute, Saskatoon, Saskatchewan, Canada, Paper No. 33, 23p.
Kislalioglu, M. and F. Berkes, 1994. La Grande 2 (LG2 Reservoir). *In:* R.J. Allan, M. Dickman, C.B. Gray and V. Cromie (eds.). The book of Canadian lakes, pp. 188-208. The Canadian Association on Water Quality, Gloucester, Ontario, Canada. Monograph Series #33.
Klinck, J.M., J.J. O'Brien and H. Svendsen, 1981. A simple model of fjord and coastal circulation interaction. *J. Phys. Oceanogr.* **11**: 1612-1626.
Knezovich, J.P., F.L. Harrison and R.G. Wilhelm, 1987. The bioavailability of sediment-sorbed organic chemicals: A review. *Water Air Soil Pollut.* **32**: 233-245.
Kotchetov, S.V., I.Y. Kulakov, V.K. Kurajov, L.A. Timokhov and Y.A. Vanda, 1994. Hydrometeoroligical regime of the Laptev Sea. Federal Service of Russia for Hydrometeorology and Monitoring of the Environment, The Arctic and Antarctic Research Institute, St. Petersburg, Russia. manuscript, 85p.
Kovacs, A., 1972. Ice scoring marks floor of Arctic shelf. *The Oil and Gas Journal,* October 23, 1972, vol. 70, no. 43.
Krishnappan, B.G., R. Stephens, J.A. Kraft and B.H. Moore, 1995. Size distribution and transport of suspended particles, Athabasca River, February and September, 1993. Northern River Basins Study, Edmonton, Alberta, June, 1995, Project Report no. 51, 10p.
Kristmannsson, S.S., S.-A. Malmberg and J. Briem, 1989. Inflow of warm Atlantic water to the subarctic Iceland Sea. *Rapp. P.-v. Réun. Cons. int. Explor. Mer.* **188**: 74.
Krysell, M. and D.W.R. Wallace, 1988. Arctic ocean ventilation studied with a suite of anthropogenic halocarbon tracers. *Science* **242**: 746-748.
Ku, T.-L. and W.S. Broecker, 1967. Rates of sedimentation in the Arctic Ocean. *Prog. Oceanogr.* **4**: 95-104.
Kuusisto, E., 1994. North hydrology in Finland. *In:* T.D. Prowse, C.S.L. Ommaney and L.E. Watson (eds.). Northern hydrology: International perspectives, pp. 129-146. Environment Canada, Saskatoon, Saskatchewan, NHRI Science Report No.3.
Kuznetsov, I.M., 1983. About the ice exchange through Karskiye Vorota Strait. *Proc. AARI* **380**: 123-128. (In Russian).
Kvambekk, A.S. and T. Vinje, 1993. The ice transport through Fram Strait. Paper presented at the Nansen Centennial Symposium, Bergen, Norway, 21-25 June, 1993. (Unpublished).
LaChapelle, E.R., 1969. Field guide to snow crystals. University of Washington Press, Seattle.
Lamb, D. and R. Blumenstein, 1987. Measurement of the area of entrapment of sulphur dioxide by rimed ice. *Atmos. Environ.* **21**: 1765-1772.
Langner, J. and H. Rodhe, 1991. A global three-dimensional model of the tropospheric sulphur cycle. *J. Atmos. Chem.* **13**: 225-263.
Larson, L.W. and E.L. Peck, 1974. Accuracy of precipitation measurements for hydrologic modelling. *Water Resour. Res.* **10(4)**: 857-863.
Lauff, G.H. (ed.). 1967. Estuaries. American Association for the Advancement of Science, Washington D.C., 757p.
Laws, E.A., 1993. Aquatic pollution: An introductory text. John Wiley and Sons Inc., New York, 611p.
Lazier, J.R.N., 1973. The renewal of Labrador Sea water. *Deep-Sea Res.* **20**: 341-353.
Lazier, J.R.N., 1980. Oceanographic conditions at O.W.S. Bravo 1964-1974. *Atmosphere-Ocean* **18**: 227-238.
Lazier, J.R.N. and D.G. Wright, 1993. Annual velocity variations in the Labrador Current. *J. Phys. Oceanogr.* **23**: 659-678.
LeBlond, P.H., 1980. On the surface circulation in some channels of the Arctic archipelago. *Arctic* **33**: 189-197.
Lee, A. and D. Ellett, 1967. On the water masses of the Northwest Atlantic Ocean. *Deep-Sea Res.* **14**: 183-190.
Leister, D.L. and J.E. Baker, in press. Influence of non-filterable particles on the scavenging of organic contaminants by rain. *Environ. Sci. Technol.* **29**: (in press).
Lemke, P., 1987. A coupled one-dimensional sea ice-ocean model. *J. Geophys. Res.* **92**: 13164-13172.
Lesack, L.F.W., P. Marsh and R.E. Hecky, 1991. Ice-cover growth and freeze-out of solutes in a Mackenzie Delta lake. *In:* T.D. Prowse and C.S.L. Ommanney, (eds.). Northern hydrology: Selected perspectives, pp. 219-236. Canada Ministry of Supply and Services, Ottawa, NHRI Symposium No.6.
Leuenberger, C., J. Czuczwa, E. Heyerdahl and W. Giger, 1988. Aliphatic and polycyclic aromatic hydrocarbons in urban rain, snow and fog. *Atmos. Environ.* **22(4)**: 695-705.
Levitus, S., 1982. Climatological atlas of the world ocean. National Oceanic and Atmospheric Administration, U.S.Dept. of Commerce, Washington D.C., Publ. 13, 173p.
Levitus, S. and T.P. Boyer, 1994. World ocean atlas. Volume 4: Temperature. NOAA Atlas NESDIS 4. National Oceanic and Atmospheric Administration (NOAA), Washington D.C.
Levitus, S., R. Burgett and T.P. Boyer, 1994. World ocean atlas. Volume 3: Salinity. NOAA Atlas NESDIS 3. National Oceanic and Atmospheric Administration (NOAA), Washington D.C.
Lewis, E.L., 1982. The Arctic Ocean: water masses and energy exchanges. *In:* L. Rey and B. Stonehouse (eds.). The Arctic Ocean, pp. 43-68. Macmilan Press, London.
Lewis, P., 1991. Sedimentation in the Mackenzie Delta. *In:* P. Marsh and C.S.L. Ommanney (eds.). Mackenzie Delta: Environmental interactions and implications of development, pp. 37-38. Proceedings of the Workshop on the Mackenzie Delta 17-18 October, 1989, Saskatoon, Saskatchewan. Environment Canada, Saskatoon, Saskatchewan, National Hydrology Research Institute Symposium No.4.
Li, S.M., R.W. Talbot, L.A. Barrie, R.C. Harriss, C.I. Davidson and J.-L. Jaffrezo, 1993. Seasonal and geographical variations of methane sulphanic acid in the Arctic troposphere. *Atmos. Environ.* **27**A: 3011-3024.
Lindsey, G.C., K. Patalas, R.A. Bodaly and C.P. Archibald, 1981. Glaciation and physical, chemical and biological limnology of Yukon Lakes. Fisheries and Oceans Canada, Winnipeg, Manitoba, Canada, Can. Tech. Rep. Fisheries and Aquatic Sciences No. 966, 37p.
Lisitsin, A.P., 1988. Avalanche sedimentation and interuptions in sediment accumulation in seasonal oceans. Nauka, Moscow, 308p. (In Russian).
Liss, P.S. and P.G. Slater, 1974. Flux of gases across the air-sea interface. *Nature* **247**: 181-184.
Livingston, H.D., 1988. The use of Cs and Sr isotopes as tracers in the Arctic Mediterranean Seas. *Phil. Trans. R. Soc. London* **A325**: 161-176.
Livingston, H.D., S.L. Kupferman, V.T. Bowen and R.M. Moore, 1984. Vertical profile of artificial radionuclide concentrations in the central Arctic Ocean. *Geochim. Cosmochim. Acta* **48**: 2195-2203.
Lockhart, W.L., 1996. Depositional trends – Lake and marine sediments. *In:* J.L. Murray, R.G. Shearer and S.L. Han (eds.). Synopsis of research conducted under the 1994/95 Northern Contaminants Program, pp. 61-69. Indian Affairs and Northern Development, Ottawa, Canada, Environmental Studies no. 73.
Lockhart, W.L. and D. Muir, 1996. Food chain accumulation, biological effects and sediment contamination in Lake Laberge and other Yukon Lakes. *In:* J.L. Murray, R.G. Shearer and S.L. Han (eds.). Synopsis of research conducted under the 1994/95 Northern Contaminants Program, pp. 199-207. Indian Affairs and Northern Development, Ottawa, Canada, Environmental Studies no. 73.
Lockhart, W.L., R. Wagemann, B. Tracey, D. Sutherland and D.J. Thomas, 1992. Presence and implications of chemical contaminants in the freshwaters of the Canadian arctic. *Sci. Total Environ.* **122(1-2)**: 165-243.
Loeng, H., 1989. Ecological features of the Barents Sea. *In:* L. Rey and V. Alexander (eds.). Proceedings of the sixth Conference of the Comité Arctique International, 13-15 May 1985, Leiden. E.J. Brill, Leiden, The Netherlands.
Loeng, H., 1991. Features of the physical oceanographic conditions of the Barents Sea. *Polar Res.* **10**: 5-18.
Loeng, H. and T.E. Vinje, 1979. On the sea ice conditions in the Greenland and Barents seas. *In*: (Anon. ed.). Proceedings of the fifth International Conference on Port and Ocean Engineering under Arctic Conditions. POAC Vol. 1. NTH, Trondheim.
Loeng, H., V. Ozhigin, B. Ådlandsvik and H. Sagen, 1997: Water fluxes through the Barents Sea. *ICES J. Mar. Sci.* **54**: 310-317.
Lorenz, E.N., 1963. Deterministic non-periodic flow. *J. Atmos. Sci.* **20**: 130-141.
Macdonald, R.W. and J.M. Bewers, 1996. Contaminants in the arctic marine environment: priorities for protection. *ICES J. mar. Sci.* **53**: 537-563.
Macdonald, R.W. and E.C. Carmack, 1991. The role of large-scale under-ice topography in separating estuary and ocean on an Arctic shelf. *Atmosphere-Ocean* **29(1)**: 37-53.
Macdonald, R.W. and D.J. Thomas, 1991. Chemical interactions and sediments: The western Canadian Arctic shelf. *Cont. Shelf Res.* **11**: 843-864.
Macdonald, R.W., E.C. Carmack, F.A. McLaughlin, K. Iseki, D.M. Macdonald and M.C. Obrien, 1989. Composition and modification of water masses in the Mackenzie shelf estuary. *J. Geophys. Res.* **94**: 18057-18070.
Macdonald, R.W., E.C. Carmack and D.W.R. Wallace, 1993. Tritium and radiocarbon dating of Canada Basin deep waters. *Science* **259**: 103-104.
Macdonald, R.W., D.W. Paton, E.C. Carmack and A. Omstedt, 1995. The freshwater budget and under-ice spreading of Mackenzie River water in the Canadian Beaufort Sea based on salinity and $^{18}O/^{16}O$ measurements in water and ice. *J. Geophys. Res.* **100**: 895-919.
Macdonald, R.W., S.M. Solomon, R.E. Cranston, H.E. Welch, M.B. Yunker and C. Gobeil, 1995a. A sediment and organic carbon budget for the Canadian Beaufort shelf. *Mar. Geol.* (submitted)
Mackay, D., 1991. Multimedia environmental models: the Fugacity approach. Lewis Publishers, Chelsea, Michigan.
Mackay, D. and W. Stiver, 1991. Predictability and environmental chemistry. *In*: R. Grover and A.J. Cessna (eds.). Environmental chemistry of herbicides, Vol. II, pp. 281-297. CRC Press, Boca Raton, Florida.
Mackay, D. and F. Wania, 1995. Transport of contaminants to the Arctic: partitioning, processes and models. *Sci. Total Environ.* **160/161**: 25-38.
Mackay, D., S. Paterson and W.Y. Shiu, 1992. Generic models for evaluating the regional fate of chemicals. *Chemosphere* **24**: 695-717.

Malmberg, S.-A., 1984. Hydrographic conditions in the east Icelandic Current and sea ice in north Icelandic waters, 1970-1980. *Rapp. P.-v. Réun. Cons. int. Explor. Mer.* **185**: 170-178.
Malmberg, S.-A. and S. Jónsson, 1997. Timing of deep convection in the Greenland and Iceland Seas. *ICES J. Mar. Sci.* **54(3)**: 300-309.
Malmberg, S.-A. and S.S. Kristmannsson, 1992. Hydrographic conditions in Icelandic waters 1980-1989. *ICES mar. Sci. Symp.* **195**: 76-92.
Malmberg, S.-A., S.S. Kristmannsson and E. Buch, 1990. Greenland Sea Project in the western part of the Iceland Sea from Jan Mayen to Denmark Strait. ICES C.M. 1990 C: 27. International Council for the Exploration of the Sea, Copenhagen.
Manley, T.O., K.L. Hunkins and R.D. Meunch, 1987. Current regimes across the east Greenland polar front at 78° 40' north latitude during summer 1984. *J. Geophys. Res.* **92**: 6741-6753.
Mantyla, A.W. and J.L. Reid, 1983. Abyssal characteristics of the world ocean waters. *Deep-Sea Res.* **30**: 805-833.
Martin, J.J., P.K. Wang and H.R. Pruppacher, 1980. A theoretical determination of the efficiency with which aerosol particles are collected by simple ice crystal plates. *J. Atmos. Sci.* **37**: 1628-1638.
Martin, J.M., D.M. Guan, F. Elbaz-Poulichet, A.J. Thomas and V.V. Gordeev, 1993. Preliminary assessment of the distribution of some trace elements (As, Cd, Cu, Fe, Ni, Pb and Zn) in a pristine aquatic environment: the Lena River estuary (Russia). *Mar. Chem.* **43**: 185-199.
Martin, S., 1981. Frazil ice in rivers and oceans. *Ann. Rev. Fluid Mech.* **13**: 379-397.
Martinson, K., M. Sydor, N. Marcotte and S. Beltaos, 1993. RIVICE model update. *In:* T.D. Prowse (ed.). Proceedings of the Workshop on Environmental Aspects of River Ice, August 18-20, 1993, pp. 127-144. National Hydrology Research Institute, Saskatoon, Saskatchewan, Canada.
Mason, R.P. and W.E. Fitzgerald, 1991. Mercury speciation in open ocean waters. *Water Air Soil Pollut.* **56**: 779-789.
Maykut, G.A. and N. Untersteiner, 1971. Some results from a time-dependent thermodynamic model of sea ice. *J. Geophys. Res.* **76**: 1550-1575.
McCarthy, L.H., T.G. Williams, G.R. Stephens, J. Peddle, K. Robertson and D. Gregor, 1996. Baseline studies in the Slave River, NWT, 1990-1994: Part I. Evaluation of the chemical quality of water and suspended sediment from the Slave River (NWT). *Sci. Total Environ.* (in press).
McCartney, M.S. and L.D. Talley, 1984. Warm-to-cold water conversion in the northern North Atlantic Ocean. *J. Phys. Oceanogr.* **14**: 922-935.
McCrea, R.C. and J.D. Fischer, 1986. Heavy metal and organochlorine contaminants in the five major Ontario rivers of the Hudson Bay Lowland. *Water Pollut. Res. J. Can.* **21**: 225-234.
McCrea, R.C. and G.M. Wickare, 1986. Organochlorine contaminants in peatlands and selected estuary sites of the Moose River. *Water Pollut. Res. J. Can.* **21(2)**: 251.
McDougall, T.J., 1983. Greenland Sea bottom water formation: a balance between advection and double-diffusion. *Deep-Sea Res.* **30**: 1109-1117.
McLaren, I.A., 1964. Zooplankton of Lake Hazen, Ellesmere Island and a nearby pond with special reference to the copepod *Cyclops scutifer* Sars. *Can. J. Zool.* **42**: 613-629.
McLaughlin, F.A., E.C. Carmack, R.W. Macdonald and J.K.B. Bishop, 1996. Physical and geochemical properties across the Atlantic/Pacific water mass front in the southern Canadian Basin. *J. Geophys. Res.* **101**: 1183-1197.
McVetty, B.D. and R.A. Hites, 1988. Atmospheric deposition of polycyclic aromatic hydrocarbons to water surfaces: A mass balance approach. *Atmos. Environ.* **22**: 511-536.
Means, J.C., J.J. Hassett, S.G. Wood and W.L. Banwart, 1979. Sorption properties of energy related pollutants and sediments. *In:* P.W. Jones and P. Leber (eds.). Polynuclear aromatic hydrocarbons, pp. 327-340. Third international symposium on Chernisigy and biology. Carcinogenesis and miaagenesis. Ann Arbor Science Publishers Inc., Ann Arbor.
Meincke, J., 1983. The modern current regime across the Greenland-Scotland ridge. *In:* A. Bott *et al.* (eds.). Structure and development of the Greenland-Scotland Ridge, pp. 637-650. Plenum, New York.
Melling, H. and E.L. Lewis, 1982. Shelf drainage Beaufort Sea and their effect on the Arctic Ocean pycnocline. *Deep-Sea Res.* **29**: 967-986.
Melling, H. and R.M. Moore, 1995. Modification of halocline source waters during freezing on the Beaufort Sea shelf: evidence from oxygen isotopes and dissolved nutrients. *Cont. Shelf Res.* **15(1)**: 89-113.
Melling, H. and D.A. Riedel, 1996. Development of seasonal pack ice in the Beaufort Sea during the winter of 1991-92: A view from below. *J. Geophys. Res.* **101(C5)**: 11975-11991.
Melling, H., R.A. Lake, D.R. Topham and D.B. Fissel, 1984. Oceanic thermal structure in the western Canadian Arctic. *Cont. Shelf Res.* **3**: 233-258.
Mellor, G.L., 1973. Analytic prediction of the properties of stratified planetary surface layers. *J. Atmos. Sci.* **30**: 1061-1069.
Mellor, G.L., 1993. Users guide for a three-dimensional, primitive equation, numerical ocean model. AOS Program, Princeton University, Princeton Report NJ 08540.
Mellor, G.L. and L.H. Kantha, 1989. An ice-ocean coupled model. *J. Geophys. Res.* **94**: 10937-10954.
Mellor, G.L. and T. Yamada, 1974. A hierarchy of turbulence closure models for planetary boundary layers. *J. Atmos. Sci.* **31**: 1791-1806.
Mellor, G.L. and T. Yamada, 1982. Development of a turbulence closure model for geophysical fluid problems. *Rev. Geophys. Space Phys.* **20**: 851-875.
Melnikov, S.A., 1991. Report on heavy metals. University of Lapland, Arctic Centre, Rovaniemi, The State of the Arctic Environment Reports 2, pp. 82-153.
Melnikov, I.A. and G.L. Pavlov, 1978. Characteristics of organic carbon distribution in the waters and ice of the Arctic Basin. *Oceanology* **18(2)**: 163-167.
Meybeck, M., 1993. C, N, P and S in rivers: from sources to global inputs. *In:* R. Wollast, F.T. Mackenzie and L. Chou (eds.). Interactions of C, N, P and S. Biogeochemical Cycles and Global Change. NATO ASI Series, Volume 14, pp. 163-193. Springer-Verlag Berlin-Heidelberg.
Meybeck, M. and A. Ragu, 1995. GEMS/WATER contribution to the Global Register of River Inputs (GLORI). Provisional Final Report. UNEP/WHO/UNESCO.
Meybeck, M., D.V. Chapman and R. Helmer (eds.). 1989. Global environment monitoring system, global freshwater quality: A first assessment. World Health Organization and United Nations Environment Programme. Basil Balckwell Ltd., Oxford, United Kingdom, 306p.
Meybeck, M.G., G. Friedrich, R. Thornas and D. Chapman, 1992. Rivers *In:* D. Chapman (ed.). Water quality assessments, pp. 239-316. Chapman and Hall, London.
Midttun, L., 1985. Formation of dense bottom water in the Barents Sea. *Deep-Sea Res.* **32**: 1233-1241.
Midttun, L. and H. Loeng, 1987. Climatic variations in the Barents Sea. *In:* H. Loeng (ed.). The effect of oceanographic conditions on distribution and population dynamics of commercial fish stocks in the Barents Sea. Proc. 3rd Soviet-Norwegian Symp. Murmansk, 26-28 May 1986. Institute of Marine Research, Bergen, Norway.
Milburn, D. and T.D. Prowse, 1996. The effect of river-ice break-up on suspended sediment and selected trace-element fluxes. *Nordic Hydrology* **27**: 69-84.
Miller, N.L. and P.K. Wang, 1991. A theoretical determination of the collection rates of aerosol particles by falling ice crystal plates and columns. *Atmos. Environ.* **25A**: 2593-2606.
Milliman, J.D. and J.P.M. Syvitski, 1992. Geomorphic/tectonic control of sediment discharge to the ocean: the importance of small mountainous rivers. *J. Geol.* **100**: 525-544.
Mitchell. M., 1956. Early identification of Arctic haze – reference to the Alaskan Arctic. *J. Atmos. Terrestrial Phys.* Special Suppl.: 195-211.
Mitra, S.K., U. Barth and H.R. Pruppacher, 1990. A laboratory study of the efficiency with which aerosol particles are scavenged by snow flakes. *Atmos. Environ.* **24A**: 1247-1254.
Moore, R.M. and J.N. Smith, 1986. Disequilibria between Ra, ^{21}OPb and ^{210}Po in the Arctic Ocean and the implications for chemical modification of the Pacific water inflow. *Earth Planet. Sci. Lett.* **77**: 285-292.
Moss, A.J. and P.H. Walker, 1978. Particle transport by continental water flows in relation to erosion, deposition, soils and human activities. *Sedim. Geol.* **20**: 81-139.
Mudroch, A., R.J. Allan and S.R. Joshi, 1992. Geochemistry and organic contaminants in the sediments of Great Slave Lake, Northwest Territories, Canada. *Arctic* **45(1)**: 10-19.
Muench, R., 1983. Mesoscale oceanographic features associated with the central Bering Sea ice edge: February-March 1981. *J. Geophys. Res.* **88**: 2715-2722.
Muench, R.D., 1971. The physical oceanography of the northern Baffin Bay region. *In:* Baffin Bay north water project science, Report I. Arctic Institute of North America, Montreal, Canada.
Muench, R.D., 1990. Greenland Sea Project. *EOS* **71**: 750-755.
Müller, F., A. Ohmura and R. Braithwaite, 1976. On the climatic influence of North Water. *In:* International Geographical Congress: Symposium on the geography of polar countries (extended summaries), pp. 55-58. Gidrometeoizdat, Leningrad.
Munro, D.S., 1991. On modelling surface meltwater discharge from Arctic and Alpine glaciers. *In:* T.D. Prowse and C.S.L. Ommanney (eds.). Northern hydrology: Selected perspectives, pp. 253-262. Proceedings of the Northern Hydrology Symposium, July 10-12, 1990. Environment Canada, National Hydrology Research Institute, Saskatoon, Saskatchewan, Canada.
Murakami, M., T. Kimura, C. Magono and K. Kikuchi, 1983. Observations of precipitation scavenging for water-soluble particles. *J. Met. Soc. Japan* **61**: 346-357.
Murakami, M., C. Magono and K. Kikuchi, 1985. Experiments on aerosol scavenging by natural snow crystals Part III. The effect of snow crystal charge on collection efficiency. *J. Met. Soc. Japan* **63**: 1127-1137.
Murakami, M., K. Kikuchi and C. Magono, 1985. Experiments on aerosol scavenging by natural snow crystals Part II. Attachment rate of 0.1 μm Dia. particles to stationary snow crystals. *J. Met. Soc. Japan* **63**: 130-135.
Murphy, T.J., 1995. Comment on: "Seasonal variations in air-water exchange of PCBs in Lake Superior". *Environ. Sci. Technol.* **29**: 846-847.
Mysak, L.A. and D.K. Manak, 1989. Arctic sea-ice extent and anomalies, 1953-1984. *Atmosphere-Ocean* **27(2)**: 376-405.
Nakamura, N. and A.H. Oort, 1988. Atmospheric heat budgets of the polar regions. *J. Geophys. Res.* **93D**: 9510-9524.
Nansen, F., 1906. Northern waters: Captain Roald Amundsen's oceanographic observations in the Arctic seas in 1901. Videnskabs-Selskabets Skrifter. I. Mathematisk-Naturvitenskapelig Kalsee, 1906, Dybwad, Christiania, 1, 145p.
NEFCO, 1995. Proposals for environmentally sound investment projects in the Russian part of the Barents Region. V.1 Non-radioactive contamination. AMAP Report, AMAP Secretariat, Oslo, 147p.
Newbury, R.W., G.K. McCullough and R.E. Hecky, 1984. The Southern

Indian Lake impoundment and Churchill River diversion. *Can. J. Fish. Aquat. Sci.* **41(4)**: 548-557.
Newton, J.L. and L.K. Coachman, 1974. Atlantic water circulation in the Canada Basin. *Arctic* **21**: 297-303.
Nicholson, K.W., J.R. Branson and P. Geiss, 1991. Field measurements of the below-cloud scavenging of particulate material. *Atmos. Environ.* **25A**: 771-777.
Norton, S.A., 1986. A review of the chemical record in lake sediments of energy related air pollution and its effects on lakes. *Water Air Soil Pollut.* **39**: 331-345.
Nurnberg, D., D.K. Futterer, F. Niessen, N. Norgaard-Pedersen, C.J. Schubert, R.F. Spielhagen and M. Wahsner, 1995. The depositional environment of the Laptev Sea continental margin: Preliminary results from the R/V Polarstern ARK IX-4 cruise. *Polar Res.* **14**: 43-53.
O'Brien, M.C., K. Iseki, R.W. Macdonald, J.R. Forbes, Y. Liangfeng and D. McCullough, 1991. Sediment trap data collected in the Beaufort Sea, March 1987 - March 1988. *Can. Data Rep. Hydrogr. Ocean Sci.* **60(8)**: 237.
Oberhuber, J.M., 1993a. Simulation of the Atlantic circulation with a coupled sea ice-mixed layer-isopycnal general circulation model. Part I: Model description. *J. Phys. Oceanogr.* **23**: 808-829.
Oberhuber, J.M., 1993b. Simulation of the Atlantic circulation with a coupled sea ice-mixed layer-isopycnal general circulation model. Part II: Model experiment. *J. Phys. Oceanogr.* **23**: 830-845.
Oehme, M., 1991. Transport of polychlorinated aromatics and pesticides from North America and Eurasia to the Arctic. *In:* R. Shearer (ed.). Proc. 8th Int. Conf. on global significance of the transport and accumulation of polychlorinated hydrocarbons in the Arctic. Comite Arctique International, Oslo, Norway, Sept. 18-22, 1989.
Oehme, M., J.-E. Haugen and M. Schlabach, 1995. Ambient air levels of persistent organchlorines in spring 1992 at Spitsbergen and Norwegian mainland: comparison with 1984 result and quality control measures. *Sci. Total Environ.* **160/161**: 139-152.
Omstedt, A., E.C. Carmack and R.W. Macdonald, 1994. Modeling the seasonal cycle of salinity in the Mackenzie shelf/estuary. *J. Geophys. Res.* **99**: 10011-10021.
Östlund, H.G., 1982. The residence time of the freshwater component in the Arctic Ocean. *J. Geophys. Res.* **87**: 2035-2043.
Östlund, H.G., 1993. Transport patterns of Siberian river water in the Arctic Basin. *In:* P. Strand and E. Holm (eds.). Environmental radioactivity in the Arctic and Antarctic, pp. 151-155. Norwegian Radiation Protection Authority, Østerås, Norway.
Östlund, H.G. and G. Hut, 1984. Arctic Ocean water mass balance from isotope data. *J. Geophys. Res.* **89C**: 6373-6381.
Östlund, H.G., G. Possnert and J.H. Swift, 1987. Ventilation rate of the deep Arctic Ocean from carbon 14 data. *J. Geophys. Res.* **92C**: 3769-3777.
Ostromogil'skii, A.K., A.O. Kokorin and M.I. Afanas'ev., 1985. Modelling the global DDT cycle. *Met. Gidrologiya* **2**: 37-45.
Ottar, B., 1989. Arctic air pollution: a Norwegian perspective. *Atmos. Environ.* **23**: 2349-2356.
Overland, J.E., 1981. Marine climatology of the Bering Sea. *In:* D.W. Hood and J.A. Calder (eds.). The Eastern Bering Sea shelf: Oceanography and resources, pp. 15-27. Office of Marine Pollution Assessment, National Oceanic and Atmospheric Administration. University of Washington Press, Seattle.
Overland, J.E. and A.T. Roach, 1987. Northward flow in the Bering and Chukchi Seas. *J. Geophys. Res.* **92**: 7097-7105.
Pacyna, J.M., 1995. The origin of Arctic air pollutants: lessons learned and future research. *Sci. Total Environ.* **160/161**: 39-53.
Pacyna, J.M. and B. Ottar, 1988. Vertical distribution of aerosols in the Norwegian Arctic. *Atmos. Environ.* **22**: 2213-2222.
Paluskiewicz, T. and H.J. Niebauer, 1984. Satelitte observations of circulation in the eastern Bering Sea. *J. Geophys. Res.* **89**: 3663-3678.
Paquette, R.G. and R.H. Bourke, 1974. Observations on the coastal current of Arctic Alaska. *J. mar. Res.* **32**: 195-207.
Paquette, R.G. and R.H. Bourke, 1981. Ocean circulation and fronts as related to ice melt-back in the Chukchi Sea. *J. Geophys. Res.* **86**: 4215-4230.
Paquette, R.G., R.H. Bourke, J.F. Newton and W.F. Perdue, 1985. The east Greenland Polar Front in autumn. *J. Geophys. Res.* **90**: 4866-4882.
Parkinson, C.L. and W.M. Washington, 1979. A large-scale numerical model of sea ice. *J. Geophys. Res.* **84(C)**: 311-337.
Parkinson, C.L., J.C. Comiso, H.J. Zwally, D.J. Cavalieri, P. Gloersen and W.J. Campbell, 1987. Arctic Sea ice, 1973-1976: Satellite passive-microwave observations. NASA, Washington D.C., 296p.
Parungo, F., C. Nagamoto and R. Madel, 1987. A study of mechanisms of acid rain formation. *J. Atmos. Sci.* **44**: 3162-3174.
Pavlov, V.K., 1993. Formation features of the structure and variability of the hydrological processes of the Kara Sea area. Proceedings of the Conference on Radioactivity and Environmental Security in the Oceans: New research and policy priorities in the Arctic and North Atlantic, Woods Hole, Massachusetts, U.S.A., 7-9 June, 1993. Woods Hole Institute of Oceanography, Woods Hole, Mass., U.S.A.
Pavlov, V. and S.L. Pfirman, 1995. Hydrographic structure and variability of the Kara Sea: Implications for pollutant distribution. *Deep-Sea Res.* **42**: 1369-1390.
Pavlov, V.K. and V.A. Volkov, 1993. Numerical modeling of the oceanographic fields and transport of radioactive contaminants in the Kara seas. International Meeting on assessment of actual and potential consequences of dumping radioactive waste into Arctic Seas, Oslo, Norway, 1-5 February, 1993.
Pavlov, V.K., L.A. Timohov, G.A. Baskakov, M.Y. Kulakov, V.K. Kurazhov, P.V. Pavlov, S.V. Pivovarov and V.V. Stanovoy, 1994. Hydrometeorological regime of the Kara, Laptev and East Siberian Seas. Arctic and Arntarctic Research Institute, St. Petersburg, Russia. manuscript, 179p.
Pawlowicz, R.A., J.F. Lynch, W.B. Owens and P.F. Worcester, 1994. Deep water formation in the Greenland Sea. *Oceanus* **37:2**, 9-11.
Pearce, C.M., 1993. Overbank sedimentation patterns on the Mackenzie Delta, NWT. Report to the NWT Programs Branch, Environment Canada, Yellowknife, NWT.
Peulv, Ú.S., I. Broyelle, M.-A. Sicrer, I. Bouloubassi, A. Lorre, A. Saliot, J.W. de Leeuw and M. Baas, 1993. Characterization of the organic matter in an Arctic delta (Lena River) using biomarkers and macromolecular indicators. Organic Geochemistry, Stavanger, Falch Hurtigtrykk, pp. 393-397.
Pfirman, S., M.A. Lange, I. Wollenburg and P. Schlosser, 1990. Sea ice characteristics and the role of sediment inclusions in deep-sea deposition: Arctic-Antarctic comparisons. *In:* U. Bleil and J. Thiede (eds.). Geological history of the polar oceans: Arctic versus Antarctic, pp. 187-211. Kluwer Academic Publishers, Dordrecht, The Netherlands.
Pfirman, S.L., D. Bauch and T. Gammelsrød, 1994. The northwestern Barents Sea: summer water mass distribution and circulation. *In:* O.M. Johannessen, R.D. Muench and J. E. Overland (eds.). The role of the Polar Oceans in shaping the global environment. Geophysical Monograph Series, AGU 85, AGU, Washington D.C. 525p
Pfirman, S.L., H. Eicken, D. Bauch and W. Weeks, 1995a. The potential transport of pollutants by Arctic sea ice. *Sci. Total Environ.* **159**: 129-146.
Pfirman, S.L., J. Koegler and B. Anselme, 1995b. Coastal environments of the western Kara and eastern Barents Seas. *Deep-Sea Res.* **42**: 1391-1412.
Pham, M., J.-F. Muller, G.P. Brasseur, C. Granier and G. Megie, 1995. A three-dimensional study of the tropospheric sulfur cycle. *J. Geophys. Res.* **100**: 26061-26092.
Piacsek, S., R. Allard and A. Warn-Varnas, 1991. Studies of the Arctic ice cover and upper ocean with a coupled ice-ocean model. *J. Geophys. Res.* **96**: 4631-4650.
Pirazzoli, P.A., 1991. World atlas of Holocene sea-level changes. Elsevier Oceanography Series 58, Elsevier, New York, 300p.
Plumb, R.A. and J.D. Mahlman, 1987. The zonally averaged transport characteristics of the GFDL circulation/transport model. *J. Atmos. Sci.* **44**: 298-327.
Pomeroy, J.W. and D.M. Gray, 1995. Snowcover accumulation, relocation and management. National Hydrology Research Institute Saskatoon, Canada, Science Report no. 7, 144p.
Pomeroy, J. and H.G. Jones, 1996. Windblown snow: sublimation, transport and changes to polar snow. *In:* E. Wolff and R.C. Bales (eds.). Chemical exchange between the atmosphere and polar snow. Global Environmental Change. NATO ASI Series I, Volume 43, pp. 453-490. Springer-Verlag, Heidelberg, Germany.
Pomeroy, J.W., T.D. Davies and M. Tranter, 1991. The impact of blowing snow on snow chemistry. *In:* T.D. Davies, M. Tranter and H.G. Jones (eds.). Seasonal snowpacks – Processes of compositional change. NATO ASI Series G, pp. 71-113. Springer-Verlag, Berlin, Germany.
Potanin, V.A. and S.V. Korotov, 1988. Seasonal variability of the main currents in the southern Barents Sea and water exchange with the adjacent areas. Geological and geographical problems of natural resourses exploitation in the northern seas. Murmansk, 1988, pp. 81-90 (In Russian).
Preller, R.H. and R. Edson (eds.), 1995. Proceedings of the ONR/NRL Workshop on Modeling the Dispersion of Nuclear Contaminants in the Arctic Seas. October 18-19, 1994. Monterey, California. Naval Research Laboratory, Stennis Space Center, Monterey, California, U.S.A. Report no.: NRL/MR/7322—95-7584.
Price, J.F. and M. O'Neil Baringer, 1994. Outflows and deep water production by marginal seas. *Prog. Oceanogr.* **33**: 161-200.
Pritchard, D.W., 1967. Observations of circulation in coastal plain estuaries, *In:* G.H. Lauff (ed.). Estuaries. American Association for the Advancement of Science, Washington D.C., Publ. V. 83, pp. 37-44.
Prinsenberg, S.J., 1983. Time variability of physical oceanographic parameters in Hudson Bay. *Le Naturaliste Canadian* **109**: 685-700.
Prinsenberg, S.J., 1986a. On the physical oceanography of Foxe Basin. *In:* I.P. Martini (ed.). Canadian inland seas, pp. 217-236. Elsevier Science, New York.
Prinsenberg, S.J., 1986b. Salinity and temperature distributions of Hudson Bay and James Bay. *In:* I.P. Martini (ed.). Inland coastal seas, pp 163-186. Elsevier Press, New York.
Prinsenberg, S.J., 1986c. The circulation pattern and current structure of Hudson Bay. *In:* I.P. Martini (ed.). Canadian inland seas, pp. 187-204. Elsevier Science, New York.
Prinsenberg, S.J., 1991. Effects of hydro-electric projects on Hudson Bay's marine and ice environments. James Bay Publication Series, No. 2, 7p.
Proehl, J.A. and M. Rattray Jr., 1984. Low-frequency response of wide deep estuaries to non-local atmospheric forcing. *J. Phys. Oceanogr.* **14**: 904-921.
Prowse, T.D., 1994. Environmental significance of ice to stream flow in cold regions. *Freshw. Biol.* **32**: 241-259.
Prowse, T.D. and M. Conly, 1996. Inpacts of flow regulation on the aquatic ecosystem of the Peace and Slave Rivers. Northern River Basins Study, Edmonston, Alberta, Synthesis Report No. 1, 168p.

Prowse, T.D. and R.L. Stephenson, 1986. The relationship between winter lake cover, radiation receipts and the oxygen deficit in temperate lakes. *Atmosphere-Ocean* **24**(**4**): 386-403.
Pruppacher, H.R., 1981. The microstructure of atmospheric clouds and precipitation. *In:* P.V. Hobbs and A. Deepak (eds.). Clouds: Their formation, optical properties and effects, pp. 93-186. Academic Press Inc., New York.
Quadfasel, D. and J. Meincke, 1987. Note on the thermal structure of the Greenland Sea gyres. *Deep-Sea Res.* **34**: 1883-1888.
Quadfasel, D. and B. Rudels, 1990. Some new observational evidence for salt induced convection in the Greenland Sea. Inst. Meereskunde, Hamburg, Techn. Rep. 4-90, 30p.
Quadfasel, D., B. Rudels and K. Kurz, 1988. Outflow of dense water from a Svalbard fjord into the Fram Strait. *Deep-Sea Res.* **35**: 1143-1150.
Quadfasel, D., B. Rudels and S. Selchow, 1992. The Central Bank vortex in the Barents Sea: watermass transformation and circulation. *ICES mar. Sci. Symp.* **195**: 40-51.
Quadfasel, D., A. Sy and B. Rudels, 1993. A ship of opportunity section to the North Pole: upper ocean temperature observations. *Deep-Sea Res.* **40**: 777-789.
Radke, L.F., J.H. Lyons, D.A. Hegg, P.V. Hobbs and I.H. Bailey, 1984. Airborne observations of Arctic aerosols. 1. Characteristics of Arctic haze. *Geophys. Res. Lett.* **11**: 393-396.
Rahn, K.A. and G. Shaw, 1982. Sources and transport of Arctic air pollution aerosol: a chronicle of six years of ONR research. *Naval Res. Rev.* March (**3**): 3-26.
Rasch, M. and N. Nielsen, 1995. Coastal morpho-stratigraphy and Holocene relative sea level changes at Tuapaat, southeastern Disko Island, central West Greenland. *Polar Res.* **14**: 277-289.
Rawson, D.S, 1950. The physical limnology of Great Slave Lake. *J. Fish. Res. Bd Can.* **8**: 3-66.
Rawson, D.S., 1947. Northwest Canadian fisheries surveys in 1944-1945, Great Slave Lake *Bull. Fish. Res. Bd Can.* **LXXII**: 45-68.
Raynor, G.S. and J.V. Hayes, 1983. Differential rain and snow scavenging efficiency implied by ionic concentration differences in winter precipitation. *In:* H.R. Pruppacher, R.G. Semonin and W.G.N. Slinn (eds.). Precipitation scavenging, dry deposition and resuspension, pp. 249-264. Elsevier Science Publishing, New York.
Redkin, Y.N., 1973. Washout of atmospheric aerosols by snow in the surface layer. *In:* V.M. Voloshchuk and Y.S. Sedunov (eds.). Hydrodynamics and thermodynamics of aerosols. John Wiley and Sons, New York.
Reed, R.K., 1984. Flow of the Alaskan Stream and its variations. *Deep-Sea Res.* **31**: 369-386.
Reed, R.K., 1990. A year-long observation of water exchange between the North Pacific and the Bering Sea. *Limnol. Oceanogr.* **35**: 1604-1609.
Reed, R.K. and P.J. Stabeno, 1993. The recent return of the Alaskan Stream to Near Strait. *J. mar. Res.* **51**: 515-527.
Regnell, O., 1994. The effect of pH and dissolved oxygen levels on methylation and partitioning of mercury in freshwater model systems. *Environ. Pollut.* **84**: 7-13.
Regnell, O. and A. Tunlid, 1991. Laboratory study of chemical speciation of mercury in lake sediment and water under aerobic and anaerobic conditions. *Appl. Environ. Microbiol.* **57**: 789-795.
Rehkopf, J., M. Newiger and H. Grassl, 1984. A 2-D model of global aerosol transport. *Atmos. Environ.* **18**: 2745-1752.
Reimnitz, E. and K.F. Bruder, 1972. River discharge into an ice-covered ocean and related sediment dispersal, Beaufort Sea, coast of Alaska. *Geol. Soc. Am. Bull.* **83**: 861-866.
Reimnitz, E. and E.W. Kempema, 1987. Field observations of slush ice generated during freeze-up in arctic coastal waters. *Mar. Geol.* **77**: 219-231.
Reimnitz, E., S.M. Graves and P.W. Barnes, 1988. Map showing Beaufort Sea coastal erosion, sediment flux, shoreline evolution, and erosional shelf profile. U.S. Department of the Interior, U.S. Geological Survey, Miscellaneous Investigations Series, 22p. + map.
Reimnitz, E., E.W. Kempema, W.S. Wefer, J.R. Clayton and J.R. Payne, 1990. Suspended-matter scavenging by rising frazil ice. *In:* S.F. Ackley and W.F. Weeks (eds.). Sea ice properties and processes, pp. 97-100. Proceedings of the W.F. Weeks Sea Ice Symposium. Cold Regions Research and Engineering Laboratory, Hanover, New Hampshire, CRREL Monograph 90-1.
Reimnitz, E., L. Marincovich Jr., M. McCormick and W.M. Briggs, 1992. Suspension freezing of bottom sediment and biota in the Northwest Passage and implications for Arctic Ocean sedimentation. *Can. J. Earth Sci.* **29**: 693-703.
Reimnitz, E., M. McCormick, K. McDougall and B. Brouwers, 1993. Sediment export by ice rafting from a coastal polynya, Arctic Alaska, U.S.A. *Arct. alp. Res.* **23**: 83-98.
Riebesell, U., I. Schloss and V. Smetacek, 1991. Aggregation of algae released from melting sea ice: implications for seeding and sedimentation. *Polar Biol.* **11**: 239-248.
Riedlinger, S.H. and R.H. Preller, 1991. The development of a coupled ice-ocean model for forecasting ice conditions in the Arctic. *J. Geophys. Res.* **96**: 16955-16977.
Rigor, I., 1992. Arctic Ocean buoy program. *Argos Newsl.* **44**: 1-3.
Rigor, I. and R. Colony, 1997. Sea ice production and transport of pollutants in the Laptev Sea, 1979-1993. *Sci. Total Environ.* **202**: 89-110.
Roach, A.T., K. Aagaard, C.H. Pease, S.A. Salo, T. Weingartner, V. Pavlov and M. Kulakov, 1995. Direct measurements of transport and water properties through Bering Strait. *J. Geophys. Res.* **100**(**C9**): 18443-18457.
Robock, A., 1980. Ice and snow feedbacks and the latitudinal and seasonal distribution of climate sensitivity. *J. Atmos. Sci.* **40**: 986-997.
Roden, G.I., 1967. On river discharge into the northeastern Pacific Ocean and Bering Sea. *J. Geophys. Res.* **72**: 5613-5629.
Rognerud, S. and E. Fjeld, 1993. Regional survey of heavy metals in lake sediments in Norway. *Ambio* **22**(**4**): 206-212.
Rognerud, S., S.A. Norton and V. Duvalter, 1993. Heavy metal pollution in lake sediments in the border areas between Russia and Norway. SFT (Norwegian State Pollution Control Authority), Oslo, Norway. SFT Report 522/93, 18p.
Romanov, I.P., 1992. The ice cover of the Arctic Ocean. AARI, St. Petersburg, 211p.
Roots, E.F., 1982. The changing Arctic marine environment: Some basic considerations. *In*: L. Rey (ed.). The Arctic Ocean. The hydrographical environment and the fate of pollutants. Comite Arctique International, Macmillan Press, London.
Rosenberg, D.M., R.A. Bodaly, R.E. Hecky, R.W. Newbury and K. Patalas, 1985. Hydroelectric development in northern Manitoba: the Churchill-Nelson River diversion and flooding of southern Indian Lake. *Bull. Can. Soc. Environ. Biol.* **42**(**2**): 31-42.
Ross, C.K., 1978. Overflow variability in Denmark Strait. ICES C.M. 1978 C: 21. International Council for the Exploration of the Sea, Copenhagen.
Royer, T.C. and W.J. Emery, 1984. Circulation in the Bering Sea 1982-1983, based on satelitte tracked drifter observations. *J. Phys. Oceanogr.* **14**: 1914-1920.
Rozanski, K., 1979. Krypton-85 in the atmosphere 1950-1977. A data review. *Environ. Int.* **2**: 139-143.
Rudd, J.W.M., 1995. Sources of methyl mercury to freshwater ecosystems: A review. *Water Air Soil Pollut.* **80**: 697-713.
Rudels, B., 1986a. The tetha-S relations in the northern seas: Implications for the deep circulation. *Polar Res.* **4**: 133-159.
Rudels, B., 1986b. The outflow of polar water through the Arctic archipelago and the oceanographic conditions in Baffin Bay. *Polar Res.* **4**: 161-180.
Rudels, B., 1987a. On the exchange of water masses between the Polar Ocean and the North Atlantic. Ph.D. thesis, University of Gothenburg.
Rudels, B., 1987b. On the mass balance of the Polar Ocean with special emphasis on the Fram Strait. *Norsk Polarinst. Skr.* **188**: 1-53.
Rudels, B., 1990. Haline convection in the Greenland Sea. *Deep-Sea Res.* **37**: 1491-1511.
Rudels, B., 1993. High latitude ocean convection. *In:* D.B. Stone and S.K. Runcorn (eds.). Flow and creep in the solar system: Observations, modeling and theory, pp. 323-356. Kluwer Academic Publishers, The Netherlands.
Rudels, B. and D. Quadfasel, 1991. The Arctic Ocean component in the Greenland-Scotland overflow. ICES C.M. 1991 C: 30. International Council for the Exploration of the Sea, Copenhagen.
Rudels, B., D. Quadfasel, H. Friedrich and M.-N. Houssais, 1989. Greenland Sea convection in the winter of 1987-1988. *J. Geophys. Res.* **94**: 3223-3227.
Rudels, B., E.P. Jones and L.G. Anderson, 1994. On the intermediate depth waters of the Arctic Ocean. *In:* O.M. Johannessen, R.D. Muench and J.E. Overland, (eds.). The Polar Oceans and their role in shaping the global environment: the Nansen Centennial Volume, pp. 33-46. American Geophysical Union, Washington D.C. Geophysical Monograph 85.
Rudels, B., L.G. Anderson and E.P. Jones, 1996. Formation and evolution of the surface mixed layer and halocline of the Arctic Ocean. *J. Geophys. Res.* **101**(**C4**): 8807-8821.
Runnells, D.D., T.A. Shepherd and E.E. Angino. 1992. Metals in water, determining natural background concentrations in mineralized areas. *Environ. Sci. Technol.* **62**(**12**): 2316-2323.
Sackinger, W.M., W.M. Serson, M.O. Jeffries, H.D. Sohoemake and M.-H. Yan, 1985. Ice islands as hazards to arctic offshore production structures. Proceedings of the Offshore Technology Conference, pp. 399-408. May 6-9, 1985. Houston, Texas.
Sadler, H.E., 1976. Water, heat and salt transports through Nares Strait, Ellesmere Island. *J. Fish. Res. Bd Can.* **33**: 2286-2295.
Sadler, H.E., 1982. Water flow into Foxe Basin through Fury and Hecla Strait. *Le Naturaliste Canadian* **109**: 701-707.
Sælen, O.H., 1983. Exchange of bottom water between the Greenland and Norwegian Seas. Paper presented at 18th General Assembly. Int. Union of Geod. and Geophys., Hamburg, Germany.
Sarynina, R.N., 1969. Conditions of origin of cold deep-sea waters in the Bear Island channel. ICES C.M. 1969 Symp:28, 1-8. International Council for the Exploration of the Sea, Copenhagen.
Saunders, P.M., 1990. Cold outflow from the Fareo Bank Channel. *J. Phys. Oceanogr.* **20**: 29-43.
Sauter, D.P. and P.K. Wang, 1989. An experimental study of the scavenging of aerosol particles by natural snow crystals. *J. Atmos. Sci.* **46**: 1650-1655.
Schindler, D.W., H.E. Welch, J. Kalff, G.J. Brunskill and N. Kritsch, 1974. Physical and chemical limnology of Char Lake, Cornwallis Island, (75°N lat.). *J. Fish. Res. Bd Can.* **31**(**5**): 585-607.
Schlosser, P., G. Bönisch, B. Kromer, K.O. Münnich and K.P. Koltermann, 1990. Ventilation rates of the waters in the Nansen Basin of the Arctic Ocean derived by a multi-tracer approach. *J. Geophys. Res.* **95**: 3265-3272.

Schlosser, P., G. Bönisch, M. Rhein and R. Bayer, 1991. Reduction of deepwater formation in the Greenland Sea during the 1980s: Evidence from tracer data. *Science* **251**: 1054-1056.

Schlosser, P., D. Bauch, R. Fairbanks and G. Bönisch, 1994a. Arctic river-runoff: mean residence time on the shelves and in the halocline. *Deep Sea Res.* **41**(**7**): 1053-1068.

Schlosser, P., B. Kromer, G. Östlund, B. Ekwurzel, G. Bönisch, H.H. Loosli and R. Furtschert, 1994b. On the ^{14}C and ^{39}Ar distribution in the central Arctic Ocean: implications for the deep water formation. *Radiocarbon* **36**(**3**): 327-345.

Schlosser, P., J.H. Swift, D. Lewis and S.L. Pfirman, 1995a. The role of large-scale Arctic Ocean circulation in the transport of contaminants. *Deep-Sea Res.* **42**: 1341-1367.

Schlosser, P., G. Bönisch, B. Kromer, H.H. Loosli, B. Bühler, R. Bayer, G. Bonani and K.P. Koltermann, 1995b. Mid 1980s distribution of ^{3}H, ^{3}He, ^{14}C, and ^{39}Ar in the Greenland/Norwegian seas and the Nansen Basin of the Arctic Ocean. *Prog. Oceanogr.* **35**: 1-28.

Schnell, R.C. and W.E. Raatz, 1984. Vertical and horizontal characteristics of Arctic haze during AGASP: Alaskan Arctic. *Geophys. Res. Lett.* **11**: 369-372.

Scholton, J.C., M.M. Rutgers van der Loeff and A. Michel, 1995. Distribution of ^{230}Th and ^{231}Pa in the water column in relation to the ventilation of the deep Arctic basins. *Deep-Sea Res. II* **42**(**6**): 1519-1531.

Schöndorf, T. and R. Herrmann, 1987. Transport and chemodynamics of organic micropollutants and ions during snowmelt. *Nordic Hydrology* **18**: 259-278.

Schott, F., M. Visbeck and J. Fischer, 1993. Observations of vertical currents and convection in the central Greenland Sea during the winter of 1988-1989. *J. Geophys. Res.* **98**: 14401-14421.

Schreier, H., W. Erlebach and L. Albright, 1980. Variations in water quality during winter in two Yukon rivers with emphasis on dissolved oxygen concentration. *Water Res.* **14**(**9**): 1345-1351.

Schumacher, J.D. and T.H. Kinder, 1983. Low-frequency current regimes over the Bering Sea shelf. *J. Phys. Oceanogr.* **13**: 607-623.

Schumann, T., B. Zinder and A. Waldvogel, 1988. Aerosol and hydrometeor concentrations and their chemical composition during winter precipitation along a mountain slope-I: Temporal evolution of the aerosol, microphysical and meteorological conditions. *Atmos. Environ.* **22**: 1443-1459.

Scott, B.C., 1981. Sulphate washout ratios in winter storms. *J. appl. Met.* **20**: 619-625.

Scrimgeour, G.J., T.D. Prowse, J.M. Culp and P.A. Chambers, 1994. Ecological effects of river ice breakup: a review and perspective. *Freshw. Biol.* **32**: 261-275.

Semb, A., 1985. A circumpolar SO_2 emission survey. Norwegian Institute of Air Research, Kjeller, Norway, NILU OR 69/85.

Semkin, R., 1996. Processes and fluxes of contaminants in aquatic systems - 1994/95. *In:* J.L. Murray, R.G. Shearer and S.L. Han (eds.). Synopsis of research conducted under the 1994/95 Northern Contaminants Program, pp. 105-118. Indian Affairs and Northern Development, Ottawa, Canada, Environmental Studies no. 73.

Semtner, A.J., 1976a. Numerical simulation of the Arctic Ocean circulation. *J. Phys. Oceanogr.* **6**: 409-425.

Semtner, A.J., 1976b. A model for the thermodynamic growth of sea ice in numerical investigation of climate. *J. Phys. Oceanogr.* **6**: 379-389.

Semtner, A.J., 1987. A numerical study of sea ice and ocean circulation in the Arctic. *J. Phys. Oceanogr.* **17**: 1077-1099.

Semtner, A.J. and R.M. Chervin, 1992. Ocean general circulation from a global eddy-resolving model. *J. Geophys. Res.* **97**: 5493-5550.

Shaw, G.E., 1995. The arctic haze phenomenon. *Bull. Am. Met. Soc.* **76**: 2403-2413.

Shen, G., E.R. Sholkovitz and D.R. Mann, 1983. The P coagulation of dissolved $^{239,240}Pu$ in estuaries as determined from a mixing experiment. *Earth Planet. Sci. Lett.* **64**: 437-444.

Shen, H.T. and N.L. Ackermann, 1990. Wave-induced sediment enrichment in coastal ice covers. *In:* S.F. Ackley and W.F. Weeks (eds.). Sea ice properties and processes: Proceedings of the W.F. Weeks Sea Ice Symposium, pp. 100-102. Cold Regions Research and Engineering Laboratory, Hanover, New Hampshire, CRREL Monograph 90-1.

Shiklomanov, I.A. and B.G. Skakalsky, 1994. Studying water, sediment and contaminant runoff of Siberian Rivers. *In:* B. Molnia and K.B. Taylor (eds.). Proceedings of the Workshop on Arctic Contamination, Interagency Arctic Research Policy Committee, May 2-7, 1993, Anchorage, Alaska. *Arct. Res. U.S.* **8**: 295-306.

Sholkovitz, E.R., 1976. The flocculation of dissolved organic and inorganic matter during the mixing of river water and seawater. *Geochim. Cosmochim. Acta* **40**: 831-845.

Sholkovitz, E.R., 1983. The geochemistry of plutonium in fresh and marine water environments. *Earth-Sci. Rev.* **19**: 95-161.

Sholkovitz, E.R., E.A. Boyle and N.B. Price, 1978. Removal of dissolved humic acid and iron during estuarine mixing. *Earth Planet. Sci. Lett.* **40**: 130-136.

Shortreed, K.S. and J.G. Stockner, 1986. Trophic status of 19 sub-arctic lakes in the Yukon Territories. *Can. J. Fish. aquat. Sci.* **43**: 797-805.

Shpaikher, A.O. and Z.S. Yankina, 1971. Relationship of mean annual levels in the Arctic seas with hydrometeorological factors. *Probl. Arctic Antarctic* **38**: 29-42.

Siegenthaler, U. and F. Joos, 1992. Use of a simple model for studying oceanic tracer distribution and the global carbon cycle. *Tellus* **44B**: 186-207.

Slinn, W.G.N., 1983. Air-to-sea transfer of particles. *In:* P.S. Liss and W.G.N. Slinn (eds.). Air-sea exchanges of gases and particles, pp. 299-405. D. Reidel Publishing Co., Boston.

Smethie, W.M. Jr. and J.H. Swift, 1989. The tritium/krypton-85 age of Denmark Strait overflow water and Gibbs Fracture Zone water just south of Denmark Strait. *J. Geophys. Res.* **94**: 8265-8275.

Smethie, W.M. Jr., D.W. Chipman, J.H. Swift and K.P. Koltermann, 1988. Chlorofluoromethanes in the Arctic Mediterranean Seas: evidence for formation of bottom water in the Eurasian Basin and deep water exchange through Fram Strait. *Deep-Sea Res.* **35**: 347-369.

Smith, D.W. and T.D.W. James, 1979. Sump studies III - biological changes in permafrost terrain adjacent to high Arctic oil and gas wellsites. Indian and Northern Affairs Canada, Ottawa, Environmental Studies No. 16, 150p.

Smith, J.N., K.M. Ellis, S. Forman, L. Polyak, G. Ivanov, D. Matishov, L.Kilius and S. Dahle, 1995. Radionuclide sources in the Barents and Kara Seas. *In:* P. Strand and A. Cooke (eds.). Proceedings of international conference on environmental radioactivity in the Arctic, pp. 179-185. Oslo, Norway, Aug. 21-25, 1995. Norwegian Radiation Protection Authority, Østerås, Norway.

Solheim, A. and S.L. Pfirman, 1985. Sea-floor morphology outside a grounded, surging glacier: Bråsvellbreen, Svalbard. *Mar. Geol.* **65**: 127-143.

Sparmacher, H., K. Fülber and H. Bonka, 1993. Below-cloud scavenging of aerosol particles: particle bound radionuclides-experimental. *Atmos. Environ.* **24A**: 1247-1254.

Stabeno, P.J. and R.K. Reed, 1991. Recent Lagrangian measurements along the Alaskan Stream. *Deep-Sea Res.* **38**: 289-296.

Stabeno, P.J. and R.K. Reed, 1992. A major circulation anomaly in the western Bering Sea. *Geophys. Res. Lett.* **19**: 1671-1674.

Stabeno, P.J. and R.K. Reed, 1994. Circulation in the Bering Sea Basin observed by satellite-tracked drifters: 1986-1993. *J. Phys. Oceanogr.* **24**: 848-854.

Staehelin, J., A. Waldvogel, J.L. Collett Jr., R. Dixon, R. Heimgartner, W. Henrich, C. Hsu, L. Li, L. Mosimann, B. Oberholzer, A.S.H. Prevot, W. Schmid, T. Schumann, M. Steiner, M. Volken and B. Zinder, 1993. Scientific goals and experiments of the project "Winter precipitation at Mt. Rigi": an overview. *Water Air Soil Pollut.* **68**: 1-14.

Stefánsson, U., 1962. North Icelandic waters. *Rit Fiskideildar* **3**: 1-269.

Stein, M. and G. Wegner, 1990. Thermohaline observation on waters off west Greenland. *Nafo-Sci. Counc. Stud.* **14**: 29-37.

Stein, R., H. Grobe and M. Wahsner, 1994. Organic carbon, carbonate, and clay mineral distributions in eastern central Arctic Ocean surface sediments. *Mar. Geol.* **119**: 269-285.

Stigebrandt, A., 1981. A model of the thickness and salinity of the upper layer in the Arctic Ocean and the relationship between the ice thickness and some external parameters. *J. Phys. Oceanogr.* **11**: 1407-1422.

Stigebrandt, A., 1984. The North Pacific: A global-scale estuary. *J. Phys. Oceanogr.* **14**: 464-470.

Stigebrandt, A., 1990. On the response of the horizontal mean vertical density distribution in a fjord to low-frequency density fluctuations in the coastal water. *Tellus* **42A**: 605-614.

Stirling, I.S. and H. Cleator, 1981. Polynyas in the Canadian Arctic. Canadian Wildlife Service.

Strand, A. and Ø. Hov, 1993. A two dimensional zonally averaged transport model including convection motions and a new strategy for the numerical solution. *J. Geophys. Res.* **98**: 9023-9037.

Strand, A. and Ø. Hov, 1996. A model strategy for the simulation of chlorinated hydrocarbon distribution in the global environment. *Water Soil Air Pollut.* **86**: 283-316.

Stumm, W. and J.J. Morgan, 1981. Aquatic chemistry. John Wiley and Sons, New York.

Sturgess, D.L., 1986. Precipitation measured by dual gauges, Wyoming-shielded gauges, and in a forested opening. *In:* D.L. Kane (ed.). Proceedings of the Symposium: Cold regions hydrology, pp. 387-396. 22-25 July, 1986, Fairbanks, Alaska. American Water Resources Association, Bethesda, Maryland, AWRA Technical Publication Series No. TPS-86-l.

Subba Rao, D.V. and T. Platt, 1984. Primary production of Arctic waters. *Polar Biol.* **3**: 191-201.

Sugden, D., 1982. Arctic and Antarctic – A modern geographical synthesis. Blackwell, Oxford, 472p.

Svendsen, H., 1977. A study of the circulation in a sill fjord on the west coast of Norway. *Mar. Sci. Comm.* **3**: 151-209.

Svendsen, H., 1981. A study of circulation and exchange processes in the Ryfylkefjords. Ph.D. Thesis, University of Bergen, Geophysical Institute, Report No 55..

Svendsen, H., 1995. Physical oceanography of coupled fjord-coast systems in northern Norway with special focus on frontal dynamics and tides. *In:* H.R. Skjoldal, C. Hopkins, K.E. Erikstad and H.P. Leinaas (eds.). Ecology of fjords and coastal waters. Elsevier Science B.V., Amsterdam, The Netherlands.

Swift, J.H., 1984. The circulation of the Denmark Strait and Iceland-Scotland overflow waters in the north Atlantic. *Deep-Sea Res.* **31**: 1339-1355.

Swift, J.H., 1986. The Arctic waters. *In:* B.G. Hurdle (ed.). The Nordic Seas, pp. 129-154. Springer-Verlag, New York.

Swift, J.H. and K. Aagaard, 1981. Seasonal transitions and water mass formation in the Iceland and Greenland Seas. *Deep Sea Res.* **28**: 1107-1129.

Swift, J.H. and K.P. Koltermann, 1988. The origin of Norwegian Sea deep water. *J. Geophys. Res.* **93**: 3563-3569.
Swift, J.H., K. Aagard and S.-A. Malmberg, 1980. The contribution of the Denmark Strait overflow to the deep North Atlantic. *Deep-Sea Res.* **27**: 29-42.
Swift, J.H., T. Takahashi and H.D. Livingston, 1983. The contribution of the Greenland and Barents Seas to the deep water of the Arctic Ocean. *J. Geophys. Res.* **88**: 5981-5986.
Tait, J.B., 1957. Hydrography of the Faroe Shetland Channel 1927-1952. *Mar. Res. Scot.* 1957, No.2, 309p.
Takahashi, T., 1963. Chemical composition of snow in relation to their crystal shapes. *J. Met. Soc. Japan* **41**: 327-336.
Takenouti, A.Y. and K. Ohtani, 1974. Currents and water masses in the Bering Sea: A review of Japanese work. *In:* D.W. Hood and E.J. Kelly (eds.). Oceanograpy of the Bering Sea with emphasis on renewable resources, pp. 39-57. University of Alaska, Institute of Marine Science, Fairbanks.
Talley, L.D. and M.S. McCartney, 1982. Distribution and circulation of Labrador Sea water. *J. Phys. Oceanogr.* **12**: 1189-1205.
Tarrason, L. and T. Iversen, 1992. The influence of North American sulphur emissions over western Europe. *Tellus* **44B**: 114-132.
Tarrason, L. and T. Iversen, 1996. Sulphur dispersion in the northern hemisphere, simulations with a 3-dimensional time-resolved model. *Tellus*. (submitted)
Taylor, K.E. and J.E. Penner, 1994. Response of the climate system to atmospheric aerosols and greenhouse gases. *Nature* **369**: 734-737.
Tchernia, P., 1980. Descriptive regional oceanography. Pergammon Marine Series Volume 3, New York, 253p.
Thomas, D.J., R.W. Macdonald and A.B. Cornford, 1986. Geochemical mass-balance calculations for the coastal Beaufort Sea, NWT, Canada. *Rapp. P.-v. Réun. Cons. int. Explor. Mer* **186**: 165-184.
Thomas, D.J., F. Noone, A. Blyth and B.D. Smiley, 1990. Arctic data compilation and appraisal, vol.20, Beaufort Sea: Chemical oceanography - hydrocarbons, metals, pigments, nutrients, oxygen and others. *Can. Data Rep. Hydrogr. Ocean Sci.* **5(20)**: 51.
Thomas, D.J., B. Tracey, H. Marshall and R.J. Norstrom, 1991. Arctic terrestrial ecosystem contamination. *Sci. Total Environ.* **122**: 135-164.
Thomas, R. and M. Meybeck, 1992. The use of particulate material. *In:* D. Chapman (ed.). Water quality management, pp. 121-170. Chapman and Hall, London.
Thomsen, T., 1994. Northern hydrology in Greenland. *In:* T.D. Prowse, C.S.L. Ommaney and L.E. Watson (eds.). Northern hydrology: International perspectives, pp. 21-39. Environment Canada, Saskatoon, Saskatchewan, NHRI Science Report No.3.
Thorndike, A.F., 1986. Kinematics of sea ice. *In:* N. Untersteiner (ed.). Geophysics of sea ice. NATO ASI Series B, Physics, 146, pp. 489-550. Plenum Press, New York.
Timofeyev, V.T., 1961. The movement of Atlantic water and heat into the Arctic Basin. *Okeanologiya* **1**: 407-411.
Timofeyev, V.T., 1963. Interaction of the Arctic ocean waters with Atlantic and Pacific waters. *Okeanologiya* **3**: 569-578.
Timokhov, L.A., 1994. Regional characteristics of the Laptev and the east Siberian Seas: Climate, topography, ice phases, thermohaline regime, circulation. *Ber. Polarforsch.* **144**: 15-31.
Top, Z., W.B. Clarke, W.C. Eismont and E.P. Jones, 1980. Radiogenic helium in the Baffin Bay bottom water. *J. mar. Res.* **38**: 435-455.
Topham, D.R., R.G. Perkin, S.D. Smith, R.J. Anderson and G. den Hartog, 1983. An investigation of a polynya in the Canadian archipelago: 1. Introduction and oceanography. *J. Geophys. Res.* **88C**: 2888-2916.
Tranter, M., P. Brimblecombe, T.D. Davies, C.E. Vincent, P.W. Abrahams and I. Blackwood, 1986. The composition of snowfall, snowpack and meltwater in the Scottish Highlands – evidence for preferential elution. *Atmos. Environ.* **20**: 517-525.
Tsiouris, S., C.E. Vincent, T.D. Davies and P. Brimblecombe, 1985. The elution of ions through field and laboratory snowpacks. *Ann. Glaciol.* **7**: 196-201.
Tsunogai, S., M. Kusakabe, H. Iizumi, I. Koike and A. Hattori, 1979. Hydrographic feature of the deep water of the Bering Sea - The Sea of Silica. *Deep-Sea Res.* **26**: 641- 659.
Uhlmann, D.R., B.Chalmers and K.A. Jackson, 1964. Interaction between particles and a solid-liquid interface. *J. appl. Phys.* **35**: 298-299.
Uralov, N.S., 1960. On the advective component of heat balance in the southern Barents Sea. *Trudy Gos. Oceanogr. Inst.* **55**: 3-20. (In Russian).
van Everdingen, R.O., 1990. Ground-water hydrology. *In:* T.D. Prowse and C.S.L. Ommanney (eds.). Northern hydrology, Canadian perspectives, pp. 77-101. National Hydrology Research Institute, Environment Canada, Saskatoon, NHRI Science Report No. 1.
Verkhunov, A.V. and Y.Y. Tkachenko, 1992. Recent observations of variability in the western Bering Sea current system. *J. Geophys. Res.* **97**: 14369-14376.
Vinje, T., 1985. Physical environment western Barents Sea: Drift, composition, morphology and distribution of the sea ice field in the Barents Sea. *Norsk Polarinst. Skr.* **179C**: 1-26.
Vinje, T., 1987. Morphology and dynamics of the Barents Sea ice field. POAC 77, University of Alaska, Fairbanks.
Vinje, T. and O. Finnekåsa, 1986. The ice transport through Fram Strait. *Norsk Polarinst. Skr.* **186**: 4-39.
Voldner, E.C., L.A. Barrie and A. Sirois, 1986. A literature review of dry deposition of oxides of sulphur and nitrogen with emphasis on long range transport modelling in North America. *Atmos. Environ.* **20**: 2101-2123.
Volken, M. and T. Schulmann, 1993. A critical review of below-cloud aerosol scavenging results on Mt. Rigi. *Water Air Soil Pollut.* **68**: 15-28.
Wadhams, P., 1986a. The seasonal sea ice zone. *In:* N. Untersteiner (ed.). Geophysics of sea ice. NATO ASI Series B, Physics, 146, pp. 825-991. Plenum Press, New York.
Wadhams, P., 1986b. The ice cover. *In:* B.G. Hurdle (ed.). The Nordic Seas, pp. 21-85. Springer-Verlag, New York.
Wadhams, P. and R.J. Horne, 1980. An analysis of ice profiles obtained by submarine sonar in the Beaufort Sea. *J. Glaciol.* **25**: 401-423.
Wallace, D.W.R. and R.M. Moore, 1985. Vertical profiles of CCl3F (F-11) and CCl2F2 (F-12) in the central Arctic Ocean basin. *J. Geophys. Res.* **90(C1)**: 1155-1166.
Wallace, D.W.R., R.M. Moore and E.P. Jones, 1987. Ventilation of the Arctic Ocean cold halocline: rates of diapycnal and isopycrial transport, oxygen utilization and primary production inferred using chlorofluormethane distributions. *Deep Sea Res.* **34**: 1957-1979.
Walsh, J.E. and C.M. Johnson, 1979. An analysis of arctic sea ice fluctuations, 1953-77. *J. Phys. Oceanogr.* **9**: 580-591.
Wania, F., 1994. Temperate and chemical behavior in the environment – towards an understanding of the global fate of persistent organic chemicals. Ph.D. Thesis, University of Toronto.
Wania, F. and D. Mackay, 1993. Modeling the global distribution of toxaphene: a discussion of feasibility and desirability. *Chemosphere* **27**: 2079-2094.
Wania, F. and D. Mackay, 1995. A global distribution model for persistent organic chemicals. *Sci. Total Environ.* **160/161**: 211-232.
Wania, F. and A. Strand, 1998. Introducing atmospheric layering in a global distribution model for persistent organic pollutants based on the fugacity approach. Submitted to *Environ. Toxicol. Chem.* February 1998.
Weeks, W., 1994. Possible roles of sea ice in the transport of hazardous material. *In:* B. Molnia and K.B. Taylor (eds.). Proceedings of the Workshop on Arctic Contamination, Interagency Arctic Research Policy Committee, May 2-7, 1993, Anchorage, Alaska. *Arct. Res. U.S.* **8**: 34-52.
Weeks, W.F. and S.F. Ackley, 1986. The growth, structure, and properties of sea ice. *In:* N. Untersteiner (ed.). Geophysics of sea ice. NATO ASI Series B, Physics, 146, pp. 9-164. Plenum Press, New York.
Wefer, G., 1989. Particle flux in the ocean: effects of episodic production. *In:* W. H. Berger, V.S. Smetacek and G. Wefer (eds.). Productivity of the ocean: Present and past, pp. 139-153. John Wiley and Sons, New York.
Wefer, G., G. Fischer, D. Fuetterer and R. Gersonde, 1988. Seasonal particle flux in the Bransfield Strait, Antarctica. *Deep-Sea Res.* **35(6)**: 891-898.
Welch, H.E., 1974. Metabolic rates of arctic lakes. *Limnol. Oceanogr.* **19(1)**: 65-73
Welch, H.E., 1985. Introduction to limnology research at Sagvagjuac, northern Hudson Bay. *Can. J. Fish. aquat. Sci.* **42(3)**: 494-505.
Welch, H.E., 1994. Char Lake. *In:* R.J. Allan, M. Dickman, C.B. Gray and V. Cromie (eds.). The book of Canadian lakes, pp. 563-570. The Canadian Association on Water Quality, Gloucester, Ontario, Canada. Monograph Series #33.
Welch, H.E. and M.A. Bergmann, 1985a. Water circulation in small arctic lakes in winter. *Can. J. Fish. aquat. Sci.* **42(3)**: 506-520.
Welch, H.E. and M.A. Bergmann, 1985b. Winter respiration of lakes at Sagvagjuac, N.W.T. *Can J. Fish. aquat. Sci.* **42(3)**: 521-528.
Welch, H.E. and J.A. Legault, 1986. Precipitation chemistry and chemical limnology of fertilized and natural lakes at Sagvagjuac, N.W.T. *Can. J. Fish. aquat. Sci.* **43(6)**: 1104-1134.
Welch, H.E., D.C.G. Muir, B.N. Billeck, W.L. Lockhart, G.J. Brunskill, H.J. Kling, M.P. Olson and R.M. Lemoine, 1991. Brown snow: a long-range transport event in the Canadian Arctic. *Environ. Sci. Technol.* **25**: 280-286.
Wendland, W.M. and R.A. Bryson, 1981. Northern hemispheris airstream regions. *Monthly Weather Rev.* **109**: 255-270.
Weschler, C.J., 1981. Identification of selected organics in the arctic aerosol. *Atmos. Environ.* **15**: 1365-1369.
Wheeler, P.A., M. Gosselin, E. Sherr, D. Thibault, D.L. Kirchman, R. Benner and T.E. Whitledge, 1996. Active cycling of organic carbon in the central Arctic Ocean. *Nature* **380**: 697-699.
Whitfield, P.H. and B. McNaughton, 1986. Dissolved oxygen depressions under ice cover in two Yukon rivers. *Water Resour. Res.* **22**: 1675-1679.
WHO/UNEP, in press. Regional former Soviet Union water quality assessment. Ed. by V. Kimstach and M. Meybeck.
Wiens, L.H., 1991. The effect of Peace River flow regulation on inflows to the Mackenzie Delta. *In:* P. Marsh and C.S.L. Ommanney (eds.). Mackenzie Delta: Environmental interactions and implications of development, pp. 189-191. Proceedings of the Workshop on the Mackenzie Delta. 17-18 October, 1989, Saskatoon, Sask. National Hydrology Research Institute, Environment Canada, Saskatoon, Saskatchewan, Symposium No.4.
Williams, J., 1979. Introduction to marine pollution control. John Wiley & Sons, New York, 173p.
Williams, M.W. and J.M. Melack, 1991. Solute chemistry of snowmelt and runoff in an alpine basin, Sierra Nevada. *Water Resour. Res.* **27**: 1575-1588.
Wollast, R. and J.C. Duincer, 1982. General methodology and sampling

strategy for studies on behaviour of chemicals in estuaries. *Thalassis Jugoslavia* **18**: 471-491.
Woo, M-k., 1992. Arctic streamflow. *In:* M-k. Woo and D. J. Gregor (eds.). Arctic environment: Past, present and future. pp. 105-111. Proceedings of a Symposium held at McMaster Universty, Nov. 14-15, 1991. McMaster University, Department of Geography, Hamilton, Ontario.
Woo, M-k. and P. Marsh, 1977. Determination of snow storage for small eastern high Arctic basins. *In:* Proceedings of the Thirty-Fourth Annual Eastern Snow Conference, Belleville, Ontario, Feb. 3-4, 1977. pp. 147-162.
Woo, M-k. and J. Sauriol, 1980. Channel development in snow filled valleys, Resolute, N.W.T., Canada. *Geografiska Annaler* **62A**: 37-56.
Woo, M-k., R. Heron, P. Marsh and P. Steer, 1983. Comparison of weather station snowfall with winter snow accumulation in High Arctic basins. *Atmosphere-Ocean* **21**(**3**): 312-325.
Worthington, L.V., 1976. On the North Atlantic circulation. The Johns Hopkins Oceangr. Stud. No. 6, 110p.
Yablokov, A.V., V.K. Karasev, V.M. Rumyantsev, M. Kokeyev, O.I. Petrov, V.N. Lystov and A.F. Melyanenkov, 1993a. Russian Federation state report on burial of radioactive wastes. Admin. Press. Russ. Fed., Moscow, 108p.
Yablokov, A.V., V.K. Karasev, V.M. Rumyantsev, M.Y. Kokeyev, O.I. Petrov, V.N. Lytsov, A.F. Yemelyanenkov and P.M. Rubtsov, 1993b. Facts and problems related to radioactive waste disposal in seas adjacent to the territory of the Russian federation. Office of the President of the Russian Federation, Moscow *(also known as "The Yablokov Report")*, 72p.
Yunker, M.B., W.J. Cretney, B.R. Fowler, R.W. Macdonald, F.A McLaughlin and B.G. Whitehouse, 1991a. On the distribution of dissolver hydrocarbons in natural water. *Org. Geochem.* **17**(**3**): 301-307.
Yunker, M.B., R.W. Macdonald, B.R. Fowler, W.J. Cretney, S.R. Dallimore and F.A. McLaughlin. 1991b. Geochemistry and fluxes of hydrocarbons to the Beaufort Sea shelf: A multivariate comparison of fluvial inputs and coastal erosion of peat using principal components analysis. *Geochim. Cosmochim. Acta* **55**: 255-273.
Yunker, M.B., R.W. Macdonald, W.J. Cretney, B.R. Fowler and F.A. McLaughlin, 1993. Alkane, terpene, and polycyclic aromatic hydrocarbon geochemistry of the Mackenzie River and Mackenzie shelf: Riverine contributions to Beaufort Sea coastal sediment. *Geochim. Cosmochim. Acta* **57**: 3041-3061.
Zakharov, V.F., 1976. Cooling of the arctic and ice cover of the Arctic seas. *Trudy Trans.* **337**: 96.
Zakharov, V.F., 1994. On the character of cause and effect relationships between sea ice and thermal conditions of the atmosphere. *Ber. Polarforsch.* **144**: 33-43.
Zenkovitch, V.P., 1985. Arctic USSR. *In:* E.C.F. Bird and M.L. Schwarz (eds.). The world's coastline, pp. 863-871. Van Nostrand Reinhold Company, New York.
Zhulidov, A.V., J.V. Headley, R.D. Robarts, A.M. Nikanorov and A.A. Ischenko, 1977. Atlas of Russian wetlands: biogeography and metal concentrations. National Hydrology Research Institute, Environment Canada, Saskatoon, SA., Canada. 312p.
Zinder, B., T. Schumann and A. Waldvogel, 1988. Aerosol and hydrometeor concentrations and their chemical composition during winter precipitation along a mountain slope-II. Enhancement of below cloud scavenging in a stably stratified atmosphere. *Atmos. Environ.* **22**: 2742-2750.
Zubakin, G.K., 1987. About the ice exchange in the Barents Sea. Arctic and Antarctic Research Institute, St. Petersburg, Proceedings Vol. 410, pp. 133-117. (In Russian).
Zubov, N.N., 1943. Arctic ice. Translation No.103, The U.S. Navy Oceanographic Office and the American Meteorological Society. U.S. Navy Elect. Lab., San Diego, California, U.S.A.